THÈSE

En vue de l'obtention du
DOCTORAT DE L'UNIVERSITÉ DE TOULOUSE

Délivré par l'Université Toulouse 3 - Paul Sabatier

Présentée et soutenue par

Paty NAKHLE

Le 13 décembre 2021

Dissémination des bactéries indicatrices de contamination fécale dans les hydrosystèmes tropicaux : transport et devenir d'*Escherichia coli* dans le bassin versant du Mékong au Laos

---

Ecole doctorale : **SDU2E - Sciences de l'Univers, de l'Environnement et de l'Espace**

Spécialité : **Surfaces et interfaces continentales, Hydrologie**

Unité de recherche :
GET - Géosciences Environnement Toulouse

Thèse dirigée par
Olivier RIBOLZI et Laurie BOITHIAS

Jury

M. Jean MARTINS, Rapporteur
M. Kyunghwa CHO, Rapporteur
Mme Michèle GOURMELON, Examinatrice
Mme Emilie JARDE, Examinatrice
Mme Emma ROCHELLE-NEWALL, Examinatrice
M. Olivier RIBOLZI, Directeur de thèse
Mme Laurie BOITHIAS, Co-directrice de thèse
M. Bruno LARTIGES, Président

Résumé

La contamination fécale des eaux de surface demeure une menace majeure pour la santé publique, en particulier dans les zones rurales des pays en développement. Les maladies diarrhéiques sont l'une des principales causes de décès notamment chez les enfants de moins de cinq ans, en raison de manque d'infrastructures sanitaires, et du faible accès aux ressources en eau salubre et aux soins médicaux. Plus de 70 millions de personnes dépendent de ressources en eau non améliorées dans le bassin inférieur du Mékong. Les progrès significatifs réalisés pour mieux comprendre la dynamique de la contamination fécale en milieu tempéré, de nombreuses lacunes subsistent en milieu tropical. Pour réduire la morbidité, il est nécessaire de mieux comprendre la dynamique des pathogènes fécaux surtout dans le contexte de changements globaux (croissance démographique, changements d'usage des terres, barrages hydroélectriques, et changement climatique).

L'utilisation d'une approche multidisciplinaire est essentielle pour évaluer les risques contamination fécale à l'interface animal-homme-écosystème. L'objectif principal de la thèse est d'identifier les facteurs clés contrôlant le devenir et transport de la bactérie fécale indicatrice (FBI), *Escherichia coli* (*E. coli*), à différentes échelles spatiales des tributaires du Mekong au Laos. Cette thèse présente les résultats basés sur (i) les données *in situ* collectées dans les principaux tributaires du Mékong au Laos, afin d'identifier les facteurs (hydrologie et utilisation des terres) contrôlant les concentrations d'*E. coli* à l'échelle du bassin versant ; (ii) une approche expérimentale pour évaluer deux facteurs clés (rayonnement solaire et dépôt de particules en suspension) contrôlant la mortalié/survie d'*E. coli* dans une zone humide tropicale montagneuse; et (iii) des approches statistiques et de modélisation pour évaluer l'impact d'un barrage hydroélectrique sur la dynamique hydro-sédimentaire et d'*E. coli* dans un tributaire majeur du Mékong, la Nam Khan, au Laos.

Les résultats des campagnes de mesures *in situ* ont révélé des variabilités saisonnières des concentrations d'*E. coli* dans les cours d'eau, plus élevées pendant la saison humide, et fortement corrélées aux concentrations en matières en suspension (MES) et aux pourcentages de forêts exploitées à l'échelle du bassin versant. Ces résultats soulignent le rôle des MES en tant que vecteurs pour le transport bactérien, ainsi que l'importance de des usages des terres comme l'un des facteurs clés ayant un impact sur la dissémination d'*E. coli* à l'échelle du bassin versant dans un contexte tropical érosif. La majorité des tributaires échantillonnés présentaient des concentrations

d'*E. coli* pendant la saison des pluies, dépassant 500 colonies par 100 ml, seuil au-delà duquel l'OMS considère que le risque de maladie gastro-intestinale après une seule exposition est de 10 %. Le rôle des MES a été mis en évidence dans l'approche expérimentale, où les bactéries attachées à des particules étaient prédominantes (91%) et présentaient des taux de mortalité plus faibles que ceux des bactéries sous forme libre. Alors que le processus de dépôt était le principal facteur de réduction du stock d'*E. coli* dans la colonne d'eau, comparé aux radiations solaires, nous avons constaté que la remise en suspension temporaire des sédiments déposés suggérait un potentiel de survie ou même de croissance d'*E. coli* dans les sédiments en milieu tropical. Enfin, étant donné l'importance de la dynamique hydro-sédimentaire sur la dissémination bactérienne, nous avons évalué l'impact du barrage, reflété par des diminutions brutales en termes de débit (en moyenne de 42%), et les concentrations en MES et *E. coli* (en moyenne de 89%) mesurées en aval du barrage. Cette approche fournit de nouvelles preuves de l'atténuation de la contamination bactérienne induite par le barrage. Dans l'ensemble, ces résultats de thèse fournissent de nouvelles informations sur la dynamique des FBI dans le bassin inférieur du Mékong, qui pourraient être utiles dans l'établissement des stratégies efficaces de gestion des ressources en eau.

Abstract

Fecal contamination of surface water remains a major threat to public health especially in the rural areas of developing countries. Diarrheal diseases are a leading cause of death especially among children under age five, due to inadequate sanitation infrastructure, low access to safe water resources, and poor medical care in developing countries. Over 70 million people depend on unimproved water resources in the lower Mekong basin stretching from southern Chinese border to the delta in southern Vietnam. Despite the significant advances made towards a better understanding of the fecal contamination dynamics in temperate regions, yet many knowledge gaps exist in tropical conditions. Reducing the disease burden, requires a better understanding of fecal pathogens dynamics in the context of rapid global changes, e.g. population growth, land use changes, hydropower dam constructions, and climate change.

Therefore, the use of a multi-disciplinary approach is essential to adress existing and potential risks of fecal contamination at the animal-human-ecosystems interface. The main objective here was to identify key factors controlling the fate and transport of the fecal indicator bacteria (FIB), *Escherichia coli* (*E. coli*), at different spatial scales of major Mekong tributaries in Lao PDR. This research work presents the results from (i) *in-situ* data collected from major Mekong tributaries from northern to southern Lao PDR aiming to identify main factors (hydrology and land use) controlling the in-stream *E. coli* concentrations at watershed-scale; (ii) experimental approach to assess two key factors (solar radiation exposition and suspended particles deposition) controlling *E. coli* decay/survival in a mountainous tropical headwater wetland; and (iii) statistical and modeling approaches to assess the impact of hydropower dam on hydro-sedimentary and *E. coli* dynamics in a major Mekong tributary, the Nam Khan in northern Lao PDR.

Our spatial and temporal monitoring results reported seasonal variabilities of in-stream *E. coli* concentrations, significantly higher during the wet season, and strongly correlated to total suspended sediment (TSS) concentration, and unstocked forests percentage areas at watershed-scale. These results point out the role of TSS as an important vector for bacterial transport, as well as the importance of land use management as one of major factors affecting *E. coli* dissemination at watershed-scale in a tropical context prone to soil erosion. The majority of sampled tributaries had *E. coli* concentrations during the rainy season, exceeding 500 colonies per 100 mL, the threshold above which the WHO considers a 10% risk of gastrointestinal illness after one single

exposure. The role of TSS in *E. coli* dynamics was further highlighted in the experimental approach, where particle-attached *E. coli* were predominant (91%) and showed lower decay rates as opposed to those of free-living *E. coli*. While deposition process was the main factor for *E. coli* stock reduction in the water column as opposed to solar radiation, we found that temporary resuspension of deposited sediments suggested a potential *E. coli* survival or even a regrowth in the sediment under tropical conditions. At last, given the importance of the hydro-sedimentary dynamics on bacterial dissemination, we assessed the dam impact reflected by abrupt decreases in terms of discharge (by an average of 42%), as well as TSS and *E. coli* concentrations (by an average of 89% for both) measured downstream of the dam. These statistical and modeling approaches provide new evidence of the attenuation of the bacterial contamination by the dam reservoir. Overall, this thesis work provides new insights on FIB dynamics in a tropical context that could be helpful in establishing effective strategies for water resource management.

Contents

List of figures

List of tables

List of abbreviations

WHO: World Health Organization

UNICEF:

UN: United Nations

USEPA: United States Environmental Protection Agency

UNICEF: United Nations Children's Fund

UNEP: United Nations Environment Program

GEMS: Global Environment Monitoring System

EC: European Commission

LMB: Lower Mekong basin

UMB: Upper Mekong basin

FIB: Fecal Indicator Bacteria

E. coli: Escherichia coli

ENT: Enteroccocus

TSS: Total Suspended Sediments

MST: Microbial Source Tracking

qPCR: quantitative Polymerase Chain Reaction

Acknowledgements

Et voilà, le moment tant attendu est arrivé! Cette aventure de 3 ans m'a tant apporté au niveau professionnel qu'au niveau personnel. Et ça n'aurait pas été possible sans toutes les personnes qui ont croisé mon chemin et qui ont fait de cette expérience un très bon souvenir.

Tout d'abord, j'aimerais remercier infiniment mes deux directeurs de thèse, Olivier Ribolzi et Laurie Boithias pour leur grande disponibilité et leurs conseils avisés tout le long de ce chemin. Je tiens à exprimer ma gratitude pour votre soutien et bonne humeur, ainsi que vos idées scientifiques enrichissantes et la confiance qua vous m'avez accordé. La mission terrain au Laos avec vous restera gravée dans ma mémoire pour la vie, et je profite pour dire merci à toute l'équipe laotienne, Phabvilay, Bounsamay, Mr. Kee, Chanthamousone, sans laquelle, ce travail de thèse ne serait pas possible. Thank you all for your help, I highly appreciate it and this thesis would not have been possible without you ! Je remercie également Norbert Silvera, Emma Rochelle-Newall, et Anne Pando pour votre aide sur les préparations des manips et pendant le séjour au Laos ainsi que pour toutes les données fournies et essentielles à l'avancement de mes travaux.

Je voudrais remercier aussi l'équipe coréenne, qui nous ont accueilli chaleureusement dans leur laboratoire à Ulsan, et surtout je tiens à remercier Professor Cho et Minjeong Kim. Thank you for the enriching scientific exchange and for your time and help in the modelisation. And of course a big thank you for all the good memories I have from Korea!

Merci aux membres de mon comité de suivi de thèse et aux jury de thèse pour les conseils et discussions enrichissantes. And thank you Jean MARTINS et Kyunghwa CHO for accepting to be the reviewers of this research work, it's a big honor.

Cette thèse n'aurait pas été possible sans tout le support moral autour du travail scientifique. Il faut savoir que cette partie de la thèse, les remerciements, était l'une parmi les plus difficiles à écrire, par peur d'oublier quelqu'un. Je ne sais pas par où commencer, je suis chanceuse dans la vie d'avoir rencontré autant de belles personnes autour de moi.

Un énorme merci à tous mes collègues de bureaux, doctorants et post-doctorants, qui sont devenus très cher amis, et avec qui j'ai passé des super moments depuis 2018. Thank you for

being a huge part of my PhD adventure, for all the parties, all the breakdowns, the trips and adventures, all the support and tips, I would not have made it without you. And from you my dear international friends, I learned a lot and still am learning from every meal we share and every conversation we have and every perspective we shift. You were always there for me and you believed in me, and I am forever grateful!

To my friends from Lebanon I say, no matter the distances, no words are enough to express my admiration and love for you. It is not easy to go through life with constant worry about home and loved ones, but I did learn a life lesson: “l’espoir fait vivre”. I am proud to have learned so much from you, and having your support from far away means the world to me. You are my chosen family and forever will be.

Et enfin, les mots ne suffiront pas pour remercier ma famille qui m’a soutenu de près et de loin, sans vous je serais pas arrivée au bout. Merci de m’avoir encouragé à faire cette thèse au début, et puis tout au long de ces trois années. La distance a été difficile à supporter et j’aurais aimé vous voir plus souvent, mais votre amour m’a donné plein de force et de courage. Tous les appels vidéos et les messages reçus ont été un carburant essentiel pour mon progrés. Merci à toi Papa de m’avoir donné le goût du travail, le courage de faire face aux problèmes, et ton optimisme malgré toutes les circonstances parfois sombres. Merci à toi Maman de m’avoir poussé à aller toujours plus loin et de m’avoir soutenu dans la vie avec un amour inconditionnel. Merci à ma grande-mère Teta Tamar, tu es symbole de force et de générosité, et je te remercie pour tous les conseils de vie, ta joie, ta bonne humeur, ton amour, et tes bons plats. Merci à mes tantes qui gardent l’esprit joyeux et qui m’ont appris que ce qui comptait c’est d’être heureux dans la vie. Et finalement Merci à mes frères et sœurs Jessy, Maguy, et Joseph, et ma cousine Estelle, mes piliers dans la vie et pour toujours, bhebkon ktir.

Mes sincères remerciemenets, choukran ktir, huge thanks, muchas gracias, muito obrigada!

Introduction générale

Contexte général et problématique

La pénurie en eau propre et potable est un concept abstrait pour certains et une dure réalité quotidienne pour d'autres. Dans bien des cas, il ne s'agit pas que d'un problème de quantité suffisante, il peut s'agir aussi d'un problème de qualité et d'accès à de l'eau salubre (UN, 2021). Pourtant, l'eau est une ressource naturelle primordiale à la vie humaine. Bien que 70% de la surface de notre planète soit couverte d'eau, seul 2,5% de celle-ci est douce (Shiklomanov, 1993). Une majorité de cette eau douce est difficile voire impossible à atteindre en raison de sa localisation dans les glaciers (69%) et les aquifères profonds (30%) (Shiklomanov, 1993). Il en résulte que les sources d'eau douce facilement accessibles, telles que les rivières et les lacs, ne représentent que 0,3% (UNEP, 2002). Ces dernières sont pourtant les principales sources d'eau utilisées par les 7,8 milliards d'habitants de la planète Terre (ONU, 2021). Si la quantité d'eau douce sur la planète est restée relativement constante au fil du temps, la population mondiale a presque triplé en moins de 70 ans, passant de 2,6 milliards en 1950 à 7,8 milliards en 2019 (UN, 2019). La consommation mondiale d'eau douce a été multipliée par six entre 1960 et 1995, soit plus de deux fois le taux de croissance démographique (ONU, 2021). De nos jours, le nombre de régions touchées par le stress hydrique ne fait qu'augmenter. Mesuré par le rapport entre l'utilisation d'eau et les réserves disponibles, le stress hydrique affecte plus de 1.7 milliards de personnes mondialement (UN-Water, 2018). Avec la demande en eau grandissante, cette ressource fondamentale, inégalement répartie, et inégalement accessible, est devenue l'un des enjeux les plus préoccupants du développement socioéconomique et humain au sens large (WHO/UNICEF, 2019).

L'accès à l'eau potable et salubre est un droit humain fondamental, reconnu en 2010 par l'Assemblée générale des Nations unies (ONU, 2021). Garantir l'accès universel et équitable à l'eau potable à un coût abordable d'ici 2030 est le sixième objectif de développement durable de l'ONU (ONU, 2020). En dépit d'un progrès notable depuis 2017, 2,2 milliards de personnes dans le monde ne bénéficient toujours pas d'un accès à l'eau potable gérée en sécurité, i.e. provenant d'une source d'eau améliorée locale, disponible, et exempte de contamination chimique et fécale (WHO/UNICEF, 2020).

En 2015, près de 2% de la population mondiale puisait son eau de consommation courante directement dans les eaux de surface, s'exposant régulièrement aux agents pathogènes présents dans l'eau (OMS/UNICEF, 2017). Les ressources en eau de surface font l'objet de multiples usages : irrigation, aquaculture, domestiques, récréatifs, hydroélectriques etc. Dans les zones

rurales des pays en développement, où l'accès aux infrastructures sanitaires adéquates est limité (Edokpayi et al., 2017), les eaux superficielles sont également utilisées pour les rejets d'effluents domestiques, industriels et agricoles. Ces rejets, dont la plupart ne sont pas traités, engendrent une pollution chimique et microbiologique des eaux douces et, par voie de conséquence, amenuisent les réserves d'eau potable (WWAP, 2017).

Encore aujourd'hui, la présence de bactéries pathogènes d'origine fécale dans les eaux de surface représentent la contamination la plus courante dans les pays en voie de développement (UNEP, 2016). Les sources de pollutions fécales varient entre sources ponctuelles, comme les rejets d'eau usée non traitée dans les rivières, et sources diffuses comme les débordements des dispositifs d'assainissement ou le lessivage de sols contaminés par la faune sauvage, les animaux d'élevage, et la défécation à l'air libre des humains (WHO, 2011a). Ces matières fécales sont depuis longtemps reconnues comme une source des bactéries pathogènes pour l'humain. Parmi ces pathogènes, on peut par exemple citer *Salmonella spp*., *Campylobacter spp., Listeria spp*., et *Escherichia coli* O157:H7 (WHO, 2003). L'exposition à ces pathogènes est responsable de nombreuses épidémies de maladies hydriques, telles que le choléra, la diarrhée, la dysenterie et les fièvres entériques, comme l'ont démontré de nombreuses études dans le monde entier et surtout dans les pays en voie de développement (Pandey et al., 2014; WHO, 2011b). En 2016, le nombre total de décès dus à la diarrhée était de 1,4 million, dont environ 60% du total des décès est attribuable à une eau, un assainissement, et une hygiène inadéquats (Prüss-Ustün et al., 2019).

Afin de permettre la détection rapide de la contamination fécale de l'eau, l'Organisation Mondiale de la Santé (OMS) recommande l'utilisation des Bactéries Indicatrices de contamination Fécales (*Fecal Indicator Bacteria* ou FIB en anglais), tels que les coliformes fécaux et *Escherichia coli* (*E. coli*) (WHO, 1993). Ces derniers sont couramment utilisés en raison de leurs multiples avantages :

(i) présence en grand nombre dans les matières fécales des humains et des animaux ;
(ii) comportement similaire à la plupart des bactéries pathogènes fécales ;
(iii) faible potentiel pathogène ;
(iv) méthodes de détection abordables, rapides, et sensibles (WHO, 2011b).

C'est dans ce contexte que divers textes réglementaires au niveau mondial ont fixé des objectifs pour limiter, diminuer et même supprimer les pathogènes fécaux dans l'eau consommée (EC, 2006; EPA, 2012). Les normes de qualité de l'eau publiées par l'OMS exigent l'absence des FIB dans l'eau potable, et considèrent par exemple un risque de 10 % de maladie

gastro-intestinale après seulement une exposition avec une eau contenant *E. coli* à une concentration dépassant les 500 colonies par 100 mL (WHO, 1993).

Entre 1990 et 2010, les concentrations de coliformes fécaux dans les cours d'eau ont respectivement augmenté d'environ 59 %, 63 % et 69 % dans les grands fleuves en Amérique latine, en Afrique, et en Asie (UNEP, 2016). On estime au moins 1,8 milliard de personnes dans le monde dont plus de 50% sur les continents africain et asiatique, qui utilisent une eau de boisson contaminée par des matières fécales (Bain et al., 2014). Une revue systématique récente issue de 345 études à l'échelle mondiale, a trouvé que l'eau de boisson est plus souvent contaminée dans les zones rurales (41%) que dans les zones urbaines (12%), et que la contamination de l'eau est la plus présente en Afrique (53%) et en Asie du Sud-Est (35%). L'accès à l'eau potable est donc un problème auquel sont confrontées les populations urbaines et rurales des pays en développement, surtout en milieu tropical.

La réduction de la morbidité dans les pays en développement ne nécessiterait pas de grandes avancées technologiques, mais plutôt d'une meilleure compréhension de la dynamique des pathogènes fécaux, et un plan de gestion bien établi pour détecter, prévenir, et minimiser l'exposition aux sources d'eau contaminées. Toutefois, souvent en raison de contraintes économiques, ces pays souffrent de l'absence d'un système adéquat de surveillance de la qualité de l'eau, et d'un manque de connaissances sur la dynamique de ces pathogènes (Rochelle-Newall et al., 2015). Il est essentiel d'identifier les facteurs qui contrôlent la persistance et la dissémination de ces pathogènes dans les pays en développement qui font, par ailleurs, face à des changements globaux rapides.

Cette problématique est très prégnante dans les régions tropicales, dont fait partie le bassin du Mékong en Asie du Sud-est où plus que 70 millions de personnes dépendent directement de cette ressource en eau (Piman and Shrestha, 2017a). Le Mékong, appelé « Mère de tous les fleuves » par l'ethnie Taï, dont le débit annuel moyen est d'environ 14,500 $m^3 s^{-1}$, est le 12ème plus long fleuve du monde (4,900 km). Il traverse 6 pays (i.e. Chine, Laos, Myanmar, Thaïlande, Cambodge et Vietnam) et draine une superficie totale de 795,000 km^2, ce qui en fait le 10ème plus grand bassin du monde (MRC, 2005). De juin à octobre, le régime hydrologique du Mékong est sous l'influence de la mousson qui entraine une forte augmentation du débit et déclenche un cycle annuel de crue (MRC, 2005). Cette caractéristique hydrologique est déterminante pour la richesse biologique de ce bassin, qui est le deuxième fleuve le plus riche en biodiversité au monde après l'Amazone (WWF, 2013). Le cycle annuel de crue est le

déclencheur dominant du cycle annuel des flux de sédiments et de la forte productivité des écosystèmes en particulier dans la plaine d'inondation de Tonle Sap et le delta du Mékong (Lamberts and Koponen, 2008; Piman and Shrestha, 2008; Suif et al., 2016).

Le Mékong et la population dense qui en dépend sont actuellement confrontés à de profondes transformations (MRC, 2021; Piman et al., 2013) qui entraînent plusieurs problèmes de pollution des écosystèmes, dont la contamination fécale (Le Meur et al., 2021). Diverses activités anthropiques et des changements globaux ont profondément affecté la région au cours des dernières décennies, tels que les changements d'utilisation des terres, la construction d'infrastructures hydro-électriques, et les changements climatiques régionaux (Piman and Shrestha, 2017a). L'impact propre à ces diverses activités anthropiques sur l'hydrologie, les flux sédimentaires, les dynamiques de la contamination fécale, et les écosystèmes du Mékong n'est toujours pas clairement établie (Pokhrel et al., 2018). Comparé aux bassins versants tempérés, le réseau de surveillance hydrométéorologique du bassin du Mékong est très limité, ce qui rend difficile l'étude des perturbations d'origine humaine susceptibles de modifier les réponses hydrologiques, sédimentaires et la qualité microbiologique des ressources en eau à l'échelle du bassin versant (Le Meur et al., 2021).

Dans ce contexte de changements rapides, il semble important d'adopter une approche collaborative, multisectorielle et transdisciplinaire, et qui considère différents niveaux d'organisation spatiale (i.e. local, régional, national et transfrontalier), et qui reconnaisse l'interconnexion entre les personnes, les animaux, les plantes et leur environnement commun (Mackenzie and Jeggo, 2019). La santé humaine, animale, végétale, environnementale et écosystémique sont inter-liées comme le décrit le concept de l'initiative "Une seule santé" (Lerner and Berg, 2015). Ce dernier a été reconnu comme une stratégie importante pour examiner et traiter les questions complexes de santé mondiale tels que la résistance aux antibiotiques, les maladies hydriques, l'insécurité alimentaire (Destoumieux-Garzón et al., 2018). L'identification et la compréhension de ces inter-relations sont essentielles pour atteindre un grand nombre des objectifs de développement durable des Nations unies (Mackenzie and Jeggo, 2019). Il est donc nécessaire de faire face à ces enjeux en étudiant la dynamique des pathogènes fécales sous l'impact des activités anthropiques, afin de réduire les risques sur la santé humaine, mais également de garantir la durabilité des bassins fluviaux en particulier dans les pays tropicaux en développement où l'accès à l'eau potable, à l'assainissement, et à l'hygiène, reste précaire.

Ce travail de thèse vise à répondre aux questions suivantes :

(i) Quels sont les différents facteurs qui contrôlent *E. coli* à l'échelle des grands tributaires du Mékong au Lao PDR ?

(ii) Comment deux facteurs clés environnementaux, exposition au rayonnement solaire et dépôt de particules en suspension, impactent-ils la mort ou la survie d'*E. coli* dans une zone humide montagneuse tropicale ?

(iii) Quelles sont les conséquences de la construction d'un barrage hydroélectrique sur le régime hydrologique, la continuité des flux sédimentaires, et la dynamique bactérienne à l'échelle du bassin versant ?

Structure de la thèse

A la suite de cette brève introduction, le second chapitre s'appuie sur une revue de l'état de l'art, et décrit le contexte général de cette étude, la problématique, ainsi que les questions scientifiques auxquelles cette thèse répond.

Le chapitre 2 décrit le site d'étude et le contexte global du bassin du Mékong ainsi que les défis majeurs exercés sur cet écosystème. Les processus mis en équation dans le modèle numérique, dont le choix a été préalablement justifié, sont détaillés.

Le chapitre 3 se concentre sur les déterminants environnementaux à l'échelle régionale, en particulier le régime hydrologique et les usages de terre, sur les concentrations en *Escherichia coli* dans les tributaires du Mékong du Laos. En premier lieu, les principaux objectifs de ce travail étaient d'examiner la saisonnalité des concentrations d'*E. coli* en réponse à des événements hydrologiques contrastés. En deuxième lieu, ce chapitre vise à identifier les facteurs de contrôle de la concentration d'*E. coli* dans les cours d'eau à l'échelle d'un grand bassin versant, pendant les saisons sèches et humide, et de quantifier l'importance relative de plusieurs facteurs tels que les concentrations matières en suspension, l'usage des terres, les caractéristiques des événements pluvieux, et la densité de la population humaine et du bétail.

Le chapitre 4 s'intéresse aux facteurs contrôlant le devenir des bactéries fécales (*E. coli*) à l'échelle spatiale d'une zone humide tropicale de montagne. Ainsi, ce chapitre présente les résultats d'une approche expérimentale que j'ai effectué dans une zone humide située dans le bassin versant de Houay Pano au nord du Laos. Les objectifs principaux étaient (i) d'évaluer les taux de mortalité des *E. coli* totaux, libres et attachés aux particules, (ii) de quantifier l'importance relative de l'exposition au rayonnement solaire et du dépôt de particules en

suspension sur les taux de mortalité, et (iii) d'étudier la survie des *E. coli* dans les sédiments déposés au fond.

Le chapitre 5 tente d'analyser la dynamique hydro-sédimentaire et bactérienne (*E. coli*) à l'échelle du bassin versant de la Nam Khan (7500 km²), au nord du Laos, soumis à l'impact du développement rapide des projets de barrages hydroélectriques en cascade. Dans ce contexte, l'objectif est d'abord de détecter statistiquement les tendances et les points de rupture dans les séries temporelles des variables mesurées à l'exutoire du bassin versant au cours d'une décennie, avant et après la construction du barrage. Dans un deuxième temps, ce chapitre décrit l'approche de modélisation (SWAT) visant à simuler le débit, les concentrations en sédiments en suspension et les concentrations d'*E. coli* en excluant la présence d'un barrage dans le modèle, afin de comparer les variables simulées aux variables observées, et de quantifier l'impact du barrage sur ces variables.

Le chapitre 6 présente la conclusion générale de ce travail de thèse ainsi que des orientations futures nécessaires pour minimiser les aléas et les risques auxquels sont exposés les populations vulnérables dans le bassin du Mékong.

Chapter 1. General introduction

1.1 General context and problematic

The scarcity of clean, safe water is an abstract concept for some and a harsh daily reality for others. In many cases, it is not only a problem of sufficient quantity, but also a problem of quality and access to safe water (UN, 2021). Yet water is a natural resource that is essential to human life. Although 70% of our planet's surface is covered by water, only 2.5% of it is fresh (Shiklomanov, 1993). A majority of this fresh water is difficult or impossible to reach due to its location in glaciers (69%) and deep aquifers (30%). (Shiklomanov, 1993). As a result, easily accessible freshwater sources, such as rivers and lakes, account for only 0.3% (UNEP, 2002). Yet these are the main sources of water used by the 7.8 billion people on the planet Earth (ONU, 2021). While the amount of freshwater on the planet has remained relatively constant over time, the world's population has nearly tripled in less than 70 years, from 2.6 billion in 1950 to 7.8 billion in 2019 (UN, 2019). Global freshwater consumption increased sixfold between 1960 and 1995, more than twice the rate of population growth (ONU, 2021). Today, the number of regions affected by water stress is only increasing. Measured by the ratio of water use to available supplies, water stress affects over 1.7 billion people globally (UN-Water, 2018). With the growing demand for water, this fundamental, unevenly distributed, and unequally accessible resource has become one of the most concerning issues in broader socioeconomic and human development(WHO/UNICEF, 2019).

Access to safe drinking water is a basic human right, recognized in 2010 by the United Nations General Assembly (ONU, 2021) . Ensuring universal and equitable access to affordable drinking water by 2030 is the UN's sixth sustainable development goal (ONU, 2020). Despite significant progress since 2017, 2.2 billion people worldwide still lack access to safely managed drinking water, i.e., from a locally available, improved water source free of chemical and fecal contamination (WHO/UNICEF, 2020). In 2015, nearly 2% of the world's population drew their drinking water directly from surface water, regularly exposing themselves to pathogens in the water (OMS/UNICEF, 2017) . The presence of fecal pathogenic bacteria in surface waters is one of the most common water contamination in developing countries (UNEP, 2016).

1.2 Fecal contamination and water quality

1.2.1 Water quality standards and fecal indicator bacteria

Over the course of the years, there was an increasing need for an efficient water quality

monitoring system, aiming to minimize the risk of waterborne diseases on public health. Because it is expensive and technically complicated to directly measure all the diversity of pathogens present in the environment, it was essential to establish fecal indicator bacteria (FIB) allowing a fast reliable and accessibly cheap water quality monitoring (WHO, 1993). Legislative framework over water quality monitoring is based on standards defined by thresholds of FIB concentrations, e.g. Enterococci (ENT) and *Escherichia coli* (*E. coli*) (Geldreich, 1970). Nowadays the classification of water microbiological quality relies on international censuses adopted from guidelines for drinking-water quality regularly published by WHO (Table 1). These water quality guidelines are respected in Europe (Directive 2006/7/CE) (EC, 2006), Canada (HC), United States (USEPA) (EPA, 2012) and the developed countries across the world.

Table 1: European directives for drinking water and recreational water (2006/7/EC) microbiological standards

Parameter	**Enterococci (ENT) (CFU 100 mL^{-1})**	***Escherichia coli* (*E coli*) (CFU 100 mL^{-1})**
Drinking water	0	0
Recreational inland water		
Excellent	200 (*)	500 (*)
Good	400 (*)	1,000 (*)
Sufficient	330 (**)	900 (**)
Recreational coastal water		
Excellent	100 (*)	250 (*)
Good	200 (*)	500 (*)
Sufficient	185 (**)	500 (**)
Reference method of analysis	ISO 7899-1 or ISO 7899-2	ISO 9308-3 or ISO 9308-1

(*) based upon a 95-percentile evaluation; (**) based upon a 90-percentile evaluation.

Since early 20th century, *E. coli* has been traditionally used for water-quality surveillance and monitoring of a possible fecal and pathogenic contamination (Dufour and Ballentine, 1986). The water quality monitoring approach recommended by WHO, uses the detection and enumeration of *E. coli* and/or ENT meeting the following criteria: (i) universally present in feces of humans and animals in high numbers; (ii) behave in a similar manner to most fecal pathogenic bacteria; (iii) have low pathogenic potential; and (iv) be easily detected by standardized inexpensive culture-based methods (WHO, 2018; WHO and OECD, 2003). The use of *E. coli* has been the most widely accepted approach for decades by the international community: American Public Health Association, the European Union (Odonkor and Ampofo,

2013).

Over the last four decades, many studies have investigated the efficiency of using FIB as a proxy for the pathogens presence (e.g. *Salmonella* sp, *Shigella* sp, *E. coli* O157:H7, *Giardia lamblia*…) in aquatic ecosystems. Total coliforms and enterococci were significantly correlated in deep aquifer waters in France (Charriere et al., 1994), and in 108 sites along the California coastline, USA (Noble et al., 2004b). Furthermore, in the Febros river in Portugal, total and fecal coliforms, ENT, and fecal streptococci were found all significantly inter-correlated (Cabral and Marques, 2006). A study done in freshwater in Canada identified *E. coli* as the preferred indicator to detect the presence of a pathogen in surface water, when compared with *C. perfringens*, ENT, and total coliforms (Wilkes et al., 2009). In addition, several studies carried out in sub-tropical and tropical regions have arrived to similar conclusions in terms of correlations among FIB and fecal pathogens. For instance, in Georges River in Australia, fecal coliforms, fecal streptococci, and *C. perfringens* spores were all positively inter-correlated (Ferguson et al., 1996). Moreover, a long term study in Nakivubo channel in Uganda, stated significant correlations among all microbiological variables including total and fecal coliforms, *E. coli* (Byamukama et al., 2005).

Overall, results suggest that correlations and usefulness of FIB remain specific to each study area, water type, pathogen sources, sample size, and detection methods. However, detected FIB can indicate the hygienic status of an aquatic environment (Odonkor and Ampofo, 2013; Pachepsky et al., 2016). A literature review based on numerous studies investigating FIB-pathogen correlations between 1970 and 2009, have concluded that although no single FIB was identified as the most correlated with all pathogens, high numbers of *E. coli* and ENT generally indicated an increased risk to human health (Wu et al., 2011). A recent review stated that both high and low correlations between FIB and pathogens were reported in previous studies, therefore, water quality standards are not only established based on correlations but rather on epidemiological studies using probabilities of enteric illnesses as function of *E. coli* concentrations in recreational waters (Pachepsky et al., 2018),

1.2.2 Waterborne diseases

Outbreaks of waterborne diseases due to waterborne pathogens in surface water remain a major burden on public health (Table 2). Several epidemiological studies have found infectious diseases episodes positively correlated to *E. coli* in freshwater (Vidon et al., 2008)

and to ENT in both fresh and marine water (Cabelli, 1989; Wade et al., 2006).

Table 2: Examples of fecal pathogens found in aquatic environments, associated diseases, probable sources and transmission mode (modified from WHO, 2003).

Agent	Diseases	Probable source	Transmission mode
Bacteria			
Salmonella sp.	Salmonellosis, gastroenteritis fever, pain	Human and animals	Ingestion
Shigella sp.	Shigellosis, bacillary dysentery, abdominal pain	Human	Ingestion
E. coli O157:H7	Diarrhea, hemorrhagic colitis, hemolytic uremic syndrome	Human and animals	Ingestion
Enterotoxigenic E. coli (ETEC)	Diarrhea, gastroenteritis	Humans and animals	Ingestion
Enteropathogenic *E. coli (EPEC)*	Diarrhea, gastroenteritis	Humans and animals	Ingestion
Campylobacter sp.	Diarrhea, gastroenteritis	Human and animals	Ingestion
Faecal streptococci	Diarrhea, gastroenteritis	Human and animals	Ingestion
Viruses			
Rotaviruses	Gastroenteritis	Human	Ingestion
Adenoviruses	Respiratory disease, gastroenteritis	Human	Ingestion, inhalation
Norovirus	Gastroenteritis	Human	Ingestion, inhalation
Hepatitis A	Liver disease	Human	Ingestion
Parasitic protozoa			
Cryptosporidium parvum oocysts	Diarrhea, fever	Human and animals	Ingestion
Entamoeba histolytica	Amoebic dysentery	Human	Ingestion
Giardia lamblia	Diarrhea, abdominal cramp	Human	Ingestion

Outbreaks of waterborne diseases like cholera, diarrhea, dysenteries, and enteric fevers, still occur across the world but are highly context-specific, often due to contaminated water used for drinking, recreation, irrigation, and aquaculture (Pandey et al., 2014; WHO, 2011b). As a consequence of the progress in the legislative framework and water quality management plans, waterborne diseases outbreaks are significantly less frequent than previously in developing countries (WHO/UNICEF, 2013). Occasionally, gastroenteritis episodes associated to waterborne pathogens can occur due to the intrusion of wastewater following heavy rainfall events, but also due to the malfunctioning of disinfection systems or contamination of the distribution network (Moreira and Bondelind, 2017). In the United States for instance, 36

outbreaks associated to drinking-water, and 134 outbreaks associated to recreational-waters were documented between 2007 and 2008 (Hlavsa et al., 2011). Canada, Finland, France and Greece have reported at least one contamination event resulting in more than 1000 cases of gastroenteritis between 2000 and 2014 (Moreira and Bondelind, 2017).

On the other hand, incidence of waterborne diseases outbreaks is the highest in low-income countries. In Bangladesh, Cyanobacteria and *V. cholerae* are found abundant in the aquatic environments, causing seasonal cholera epidemics (Sagir Ahmed et al., 2007). Some of the major pathogens reported in aquatic systems of tropical and subtropical climates, are *Salmonella, V. cholerae, C. perfringens, Shigella sp.,* Cyanobacteria, Rotavirus, *Entamoeba,* and *Giardia* (Islam et al., 2021). Diarrhea remains one of the leading causes of childhood death in low-income countries (Fig. 1) (WHO, 2020). We estimate around 1.8 billion people globally using drinking water fecally contaminated, and 1.1 billion of which, consume water classified as at least 'moderate' risk (>10 *E. coli* 100 mL^{-1}) (WHO/UNICEF, 2019). In a recent analysis on diseases burden in low and middle-income countries, a total of 1.4 million diarrheal deaths were reported in 2016, out of which, 60 % were attributed to inadequate water, sanitation and hygiene behaviors (WASH) (Troeger et al., 2017).

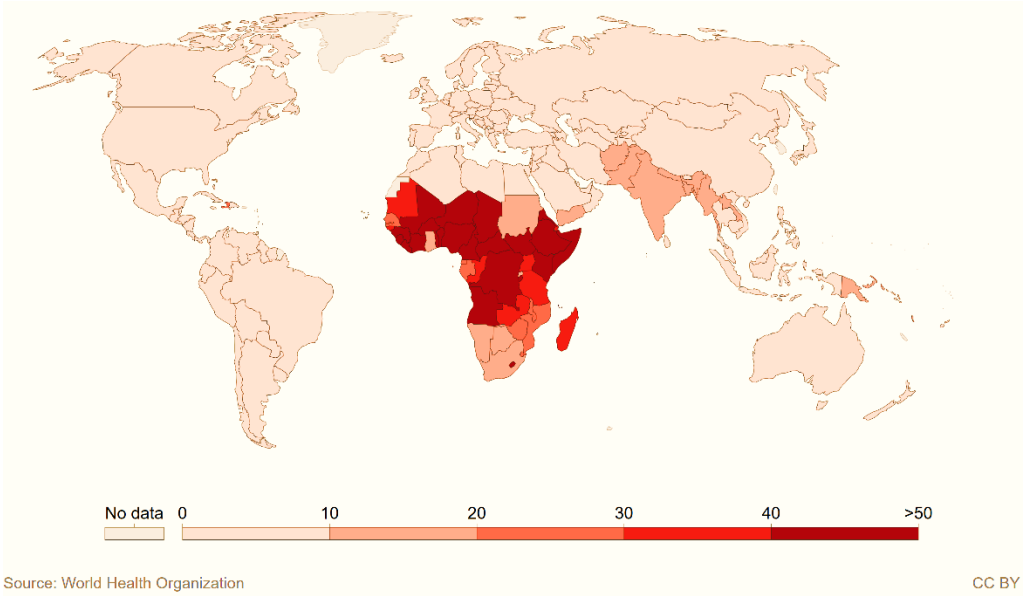

Figure 1: Mortality rate attributable to unsafe water, sanitation, and hygiene (WASH), measured as the number of deaths per 100,000 people of a given population. Source: WHO, 2016a .

By improving drinking water infrastructure, adequate sanitation and hygiene practices, an important fraction of overall deaths would have been preventable in low and middle-income countries. Progress towards decreasing the global burden of diseases in developing countries, does not require major technological advances, but rather a better understanding of the fecal pathogens dynamics, and a well-established management plan to detect, prevent and

minimize the exposure to contaminated water sources.

1.2.3 Water quality assessment

According to a global water quality assessment report (UNEP, 2016), a significant improvement of the surface water microbiological quality has been noted in most of the developed countries. However, major problems still persist and further intensify in aquatic environments of developing countries, mostly in rivers of Latin America, Africa and Asia (UNEP, 2016). The UNEP report relies on the Global Environment Monitoring System (GEMS), which uses aggregated global water quality data. The latter reported median concentrations of fecal coliforms around 1,500 CFU 100 mL^{-1} from sparse measurements in African rivers (n=215), which is considered significantly higher than the severe pollution level (>1,000 CFU 100 mL^{-1}). GEMS observations in rivers in Latin America (n=1,725) and in Asia (n=4,131), as compared to African rivers, had lower FIB concentrations by factor 10, thus classified as low pollution (UNEP, 2016). Between 1990 and 2010, in-stream fecal coliform bacteria concentrations have increased of around 59%, 63%, and 69% in Latin America, Africa, and Asia respectively (UNEP, 2016). These global assessments give an overview of the surface water quality status, but cannot provide reliable conclusions on the status of river pollution and the associated health risks. These large ranges of estimations reflect the uncertainties and stress the need to closely investigate and to expand monitoring efforts on smaller spatio-temporal scales, of the surface water pollution in developing countries. The FIB concentrations vary widely across the regions. A systematic review based on 345 studies worldwide, estimated the exposure to fecal contamination of water resources by region (Bain et al., 2014). They reported that drinking water is found to be more often contaminated in rural areas (41%, CI: 31%–51%) than in urban areas (12%, CI: 8–18%), and that the water contamination is the most present in Africa (53%, CI: 42%–63%) and Southeast Asia (35%, CI: 24%–45%).

Most of the water quality studies have been conducted in developed countries, and are very limited in developing countries, particularly in tropical and subtropical regions (Islam et al., 2021). Developed countries successfully developed a well-established framework including management plans to achieve defined targets with the aim of improving not only drinking water resources, but also rivers, lakes, and groundwater (Loucks and Beek, 2017). Despite efforts being invested in improving the access to clean drinking water supplies in developing countries, another major underexplored facet of the problem is the proximity between rural communities and their often polluted surface water on which they directly depend (WHO, 2016b). The focus of water quality research should include water resources used for agriculture, aquaculture,

bathing, and recreational activities. The use of informal water resources expose vulnerable societies especially children and women, to pathogens putting human health at risk. Implementing a cost-effective and sustainable surveillance system in the developing countries remains challenging and complex due to the lack of adequate structures for long term water quality monitoring systems, and to economic constraints (Howard, 2021). Moreover, in order to establish a management plan to reduce the pathogen pollution and mitigate associated health risks, it is necessary to define the pollution sources and factors influencing pathogen dynamics and persistence in aquatic bodies, especially of tropical context.

1.3 FIB sources

1.3.1 Primary sources

Primary sources of fecal pathogens in surface water are of human and animal origin (Table 3), but their main pathways vary greatly across the regions, and can arise from both point sources and diffuse sources (WHO, 2011a). Point source pollution originates from a single, identifiable and direct point of pollution discharge. Non-point source or diffuse source often come from many different sources with no specific point of discharge, on an extensive area of land, and can be transported to water systems via different hydrological pathways (overland flow, lateral and groundwater flow). .

Table 3: E. coli *production per day and per capita for human and domestic animals. Source Causse et al., 2015.*

Type	***E. coli* load** (*E. coli* day^{-1} animal $^{-1}$)
Cattle	1.3×10^{10}
Buffalo	2.5×10^{10}
Sheep	9.7×10^{9}
Goat	1.9×10^{9}
Pig	1.3×10^{10}
Poultry	1.2×10^{9}
Human	1.6×10^{11}

Identifying pollution sources can be a very useful approach in order to monitor and to control the contamination and to minimize the risks on humans. Several techniques are available nowadays to allow tracking the source of the contamination. A molecular technique method known as microbial source tracking (MST), is used to determine the presence or absence and relative abundance of species-specific microbial biomarkers like *Bacteroides* sp. (HF183)

(Harwood et al., 2014). Methods based on quantitative polymerase chain reaction (qPCR) allow to detect and quantify fecal source-associated genetic markers, and was evaluated in tropical river in Thailand (Kongprajug et al., 2019). Other specific biomarkers can be used, like fecal sterols and stanols which are molecules found in animal faces, and have been suggested as good indicator to determine the origin of fecal contamination source (Gourmelon et al., 2010). It is also possible to trace the source of the contamination using chemical indicators specific to humans often found in sewage network, like caffeine or acetaminophen (Ekklesia et al., 2015a; Jeanneau et al., 2012). Although no single chemical indicator has emerged as proxy for the presence of fecal pathogens, it is suggested to be best used as a confirmatory approach. Overall, these previously described tracking methods are culture independent, yet they need relatively high level analytical capacities, which can be limiting factor in developing countries (Rochelle-Newall et al., 2015).

1.3.2 Point sources

In developed countries, the main pollution sources are point sources, originating from discharges of wastewater from the sewer system into the surface water. Wastewater is broadly defined as "used" water that has been contaminated as a result of human activities, and combines domestic effluents (black and grey waters), industrial effluents, and agricultural effluents (intensive livestock feedlots) (Mateo-Sagasta et al., 2015). While the aim of wastewater collection and treatment is to reduce pollutant loadings to the environment, these facilities can occasionally act as point sources of pollution (Jones et al., 2021). For instance, during periods of heavy rainfall, combined sewer network designed to simultaneously collect rainwater and wastewater, can overflow and discharge directly into aquatic systems.

A study conducted in the Seine river in France, revealed that sewer overflow resulted in an increase of FIB concentrations up to 2.9×10^5 MPN 100 mL^{-1} of *E. coli* and 7.6×10^4 MPN 100 mL^{-1} of ENT, which exceeds by two orders of magnitude the usual dry weather concentrations (Passerat et al., 2011). Moreover, several epidemiological studies conducted in developed countries between 2000 and 2014, identified sewer overflow as point sources causing waterborne diseases outbreaks (Arias et al., 2006; Larsson et al., 2014; Røstum et al., 2009; Scarcella et al., 2009). These outfall events are expected to increase in rural areas, with the climate change intensification (e.g. frequent extreme rainfall episodes) and the population growth. Therefore, further measures are still needed to be taken, to increase wastewater network capacities, and reduce the contamination risks.

Unlike the developed countries, sanitation infrastructures in developing countries are poorly managed (UN, 2021). Wastewater production, collection and treatment vary with the level of economic development (Fig. 2) (WHO, 2020). It is estimated that 48 % of global wastewater production is released untreated into the environment, particularly in South and Southeast Asia (Jones et al., 2021). Main point sources in developing countries include direct release from wastewater drains into nearby aquatic environments (Edokpayi et al., 2016), and direct deposit by grazing livestock and wildlife that have access to water bodies (Soupir et al., 2006).

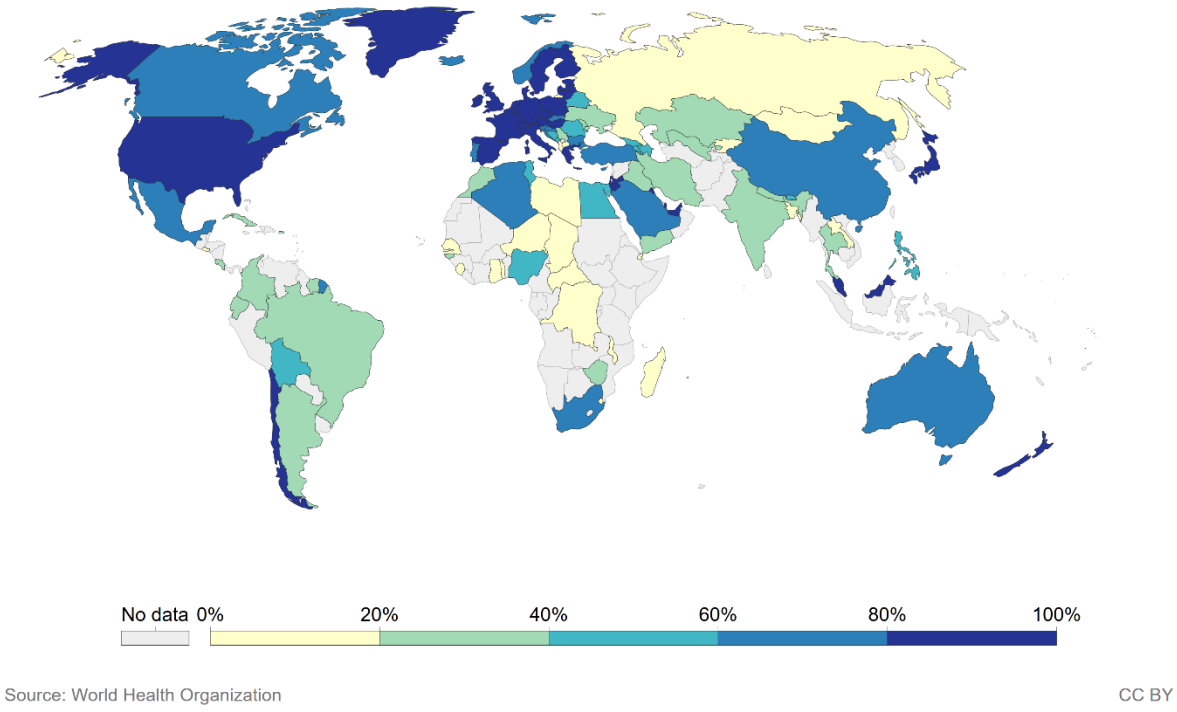

Figure 2: Proportion (%) of safely treated domestic wastewater flows in 2020. Source: WHO, 2020 .

1.3.3 Diffuse sources

In developed countries, one of the major diffuse sources is urban runoff from domestic and industrial effluents, and feces of wild animals, birds and domestic pets (Müller et al., 2020). Urbanized watersheds are prone to the loss of permeable surfaces (e.g. forests, wetlands, grasslands, etc...), and an increased overland flow transporting sediment and pathogens into hydrographic networks. Significant relationships have been found in developed countries, between heavy rainfall events and fecal pathogen contaminations of rivers and groundwater (Moreira and Bondelind, 2017). High numbers of *E. coli* and ENT were observed in the overland flow during storm events in six urban catchments across Australia, most likely due to

the presence of fecal contamination from sewage leakage and animal sources (Sidhu et al., 2013). Another main diffuse source in developed countries with farming practices is agricultural runoff. A study in a rural catchment in Canada, have reported a higher *E. coli* load from an agricultural sub-catchment (average 8.92 × 1010 CFU ha^{-1}) than a residential sub-catchment (average 8.43 × 109 CFU ha^{-1}) (Sinclair et al., 2009). High *E. coli* concentrations up to 104 to 106 MPN 100 mL^{-1} were measured in surface runoff from lands receiving animal manures (Meals and Braun, 2006). Historically, animal manure which is solid and liquid waste generated by livestock, has been used as soil amendment for crop production (Szogi et al., 2015). However when manure is not properly composted, it may contain pollutants pathogens, heavy metals, antimicrobials, and hormones, which can contaminate the crops, and nearby soil and water through surface leaching and surface runoff (USEPA, 2013).

In developing countries, diffuse sources are mostly predominant (OECD, 2017), directly through livestock grazing, and raw animal excreta is still widely used as organic fertilizer on agricultural lands (Islam et al., 2021). Wildlife is also accounted among diffuse sources of fecal pathogens in developing countries, especially in rural areas. Significant positive correlations between the number of livestock owned by a household and the risk of fecal contamination of drinking-water were demonstrated in a study conducted in Ghana, Bangladesh, and Nepal (Wardrop et al., 2018). The close proximity of animals to the households, is a critical contamination pathway to take into account to reduce the burden of disease in humans (Delahoy et al., 2018). In a study across 60 rural Indian villages, public tube wells and ponds used for multi-purposes (bathing, swimming, brushing teeth, washing utensils, laundry) were exposed to human and domestic animal fecal contamination through sub-surface leaching and latrines inundation (Odagiri et al., 2016). The occurrence of high number of child diarrhea was associated with the proportion of contaminated groundwater drinking sources within 6 weeks after contamination detection (Odagiri et al., 2016). Although the rates of open defecation by humans have been decreasing worldwide, yet up to now, more than 5% of the population still practices open defecation in 55 countries, mainly in Central and Southern Asia, and Saharan Africa (Fig. 3) (WHO/UNICEF, 2019). For example, in a small rural catchment in Lao PDR in 2015, about 60% of the population practices open defecation, and non-point pollution sources are predominant, while only 5% of *E. coli* production were associated to point sources (Causse et al., 2015). The latter reported high *E. coli* concentrations in the river exceeded 5,000 MPN 100 mL^{-1} during high discharge periods, due to latrines overflow, while in dry season, soils acted as contamination filter (Causse et al., 2015).

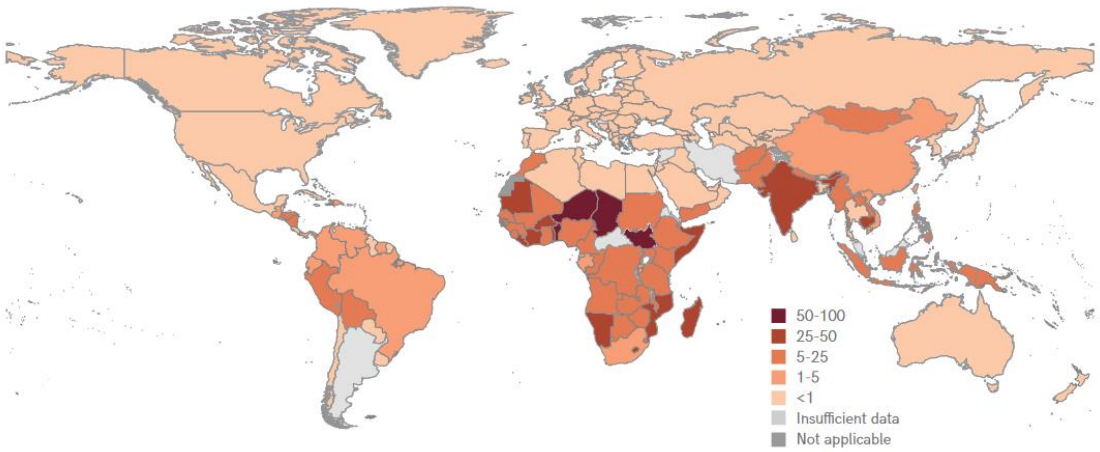

Figure 3: Proportion of population practicing open defecation in 2017 (%). Source: UNICEF and WHO, 2019.

1.4 FIB fate at watershed-scale

A watershed is a topographically delimited area drained by water system, and is composed of inter-connected aquatic and terrestrial ecosystems (Flotemersch et al., 2016). Rivers are dynamic systems characterized by hydrological connectivity, which refers to water-mediated transfer of matter, energy, and organisms within or between elements of hydrological cycles (Pringle, 2003). The hydrological pathways can be: (i) longitudinal (upstream-downstream), (ii) vertical (river- aquifer through hyporheic exchange), (iii) horizontal (major bed-minor bed). The transport capacity is highly variable in time and space depending on the topography, the climate, and the geology of the watershed (Ward et al., 2002). The in-stream processes of dispersion, dilution, horizontal and vertical and longitudinal transport, determine the distribution of pathogen at watershed-scale (Fig. 4) (Zhang et al., 2021). Humans, livestock and wildlife are primary sources of pathogens, responsible for the direct contamination of nearby soils and water bodies. Upon release in the environment, FIB can be disseminated via soil erosion and overland flow, thereby contaminating off-site soils and water downstream (Fig. 4).

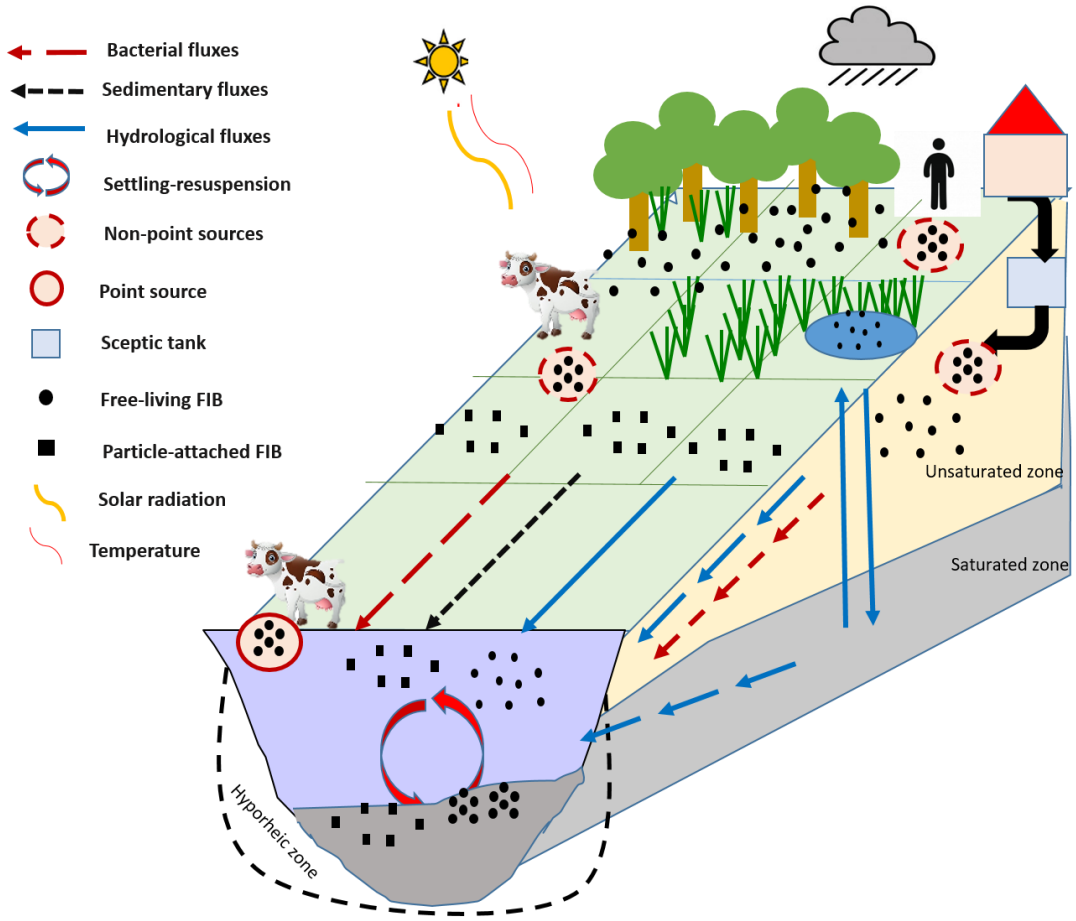

Figure 4: Conceptual diagram of FIB sources and transport at watershed-scale.

Until relatively recently, *E. coli* was believed not to survive well outside of the host, nor to replicate in the environments (Winfield and Groisman, 2003). However, studies have revealed that some specific strains of FIB were found able to survive outside of the host, adapt and potentially reproduce on soil of tropical environments (Byappanahalli et al., 2012b), and temperate environments (Byappanahalli and Fujioka, 1998; Pachepsky and Shelton, 2011). Due to the potential natural growth and persistence of FIB in soil, these habitats contaminated by primary sources can become potential reservoirs or "secondary sources" of FIB (Rochelle-Newall et al., 2015). During rainfall events of high intensity especially in humid tropical areas, contaminated soils are washed off and eroded in overland flow often highly turbid (Ferguson et al., 2003; Gourdin et al., 2014). Consequently, FIB are introduced into the downstream aquatic ecosystem where depending on the conditions, they can die-off, deposit in streambeds of rivers, be re-suspended during high discharge events or by hyporheic exchange. Previous studies have found variable FIB concentrations in streambed sediments depending on the study locations (Table 4) (Pachepsky and Shelton, 2011). The latter suggests the FIB ability to persist in the

sediments where conditions might be favorable for FIB survival and potential growth, increase the risk of adding significant potential FIB reservoirs or "tertiary sources" that contribute to releasing bacterial load into the environment (Fig. 4) (Rochelle-Newall et al., 2015). Few studies have investigated the FIB survival/decay under various conditions (Table 4).

Table 4: Bacterial decay rates under different conditions.

Organism	**Conditions**	**Decay rate k (day^{-1})**	**Reference**
Fecal coliform	Laboratory conditions	0.047 at 4 °C ; 0.097 at 25 °C ; 0.139 at 35 °C 0.104 in sand and loam ; 0.043 in clay	Howell et al., 1996
E. coli	Dark control chamber Sunlight-exposed chamber	0.0171 in dark ; 0.277 in light	Sinton et al., 2002
E. coli	Flow-through chambers	0.161 < k < 0.346 at 24 °C (water)	Garzio-Hadzick et al., 2010
E. coli	Dialysis bags placed in the water column	1.41 at dark 2 < k < 6 under high light conditions	Maraccini et al., 2016
E. coli and enterococci	Flow-through chambers	Growth from day 0 to 2 k in sandy sediment > k in clayey sediment	Smith et al., 2019

Pathogens are expected to behave differently in temperate and tropical ecosystems due to distinct ecological differences between the two ecosystems. In fact, relatively high concentrations of nutrients, organic matter and suspended sediments, stable and warm temperatures, as well as dense riparian vegetation, are conditions met in subtropical and tropical region likely to favor FIB extra-host survival (Rochelle-Newall et al., 2015). Overall, FIB fate is governed by a number of factors, including environmental factors and anthropic factors, which are discussed in detail in the following section.

1.5 FIB occurrence in the environment

1.5.1 Environmental factors

When present in the environment, FIB is exposed to various environmental stressors, considerably different than their primary habitats. A significant number of studies have been exploring the relationships between the FIB concentrations in surface water and environmental factors such as temperature, pH, salinity, nutrients and organic matter, sunlight, microbiota, association to suspended sediment, etc. (Van Elsas et al., 2011). While most of the published

studies were conducted in temperate regions have provided an overview of the major factors involved in FIB survival (Ferguson and Signoretto, 2011; Pachepsky and Shelton, 2011; Philipsborn et al., 2016), major knowledge gaps remain in tropical ecosystems (Rochelle-Newall et al., 2015).

1.4.1.1 Hydrology

During rainfall events, secondary and tertiary FIB sources are mobilized, and disseminated in the environment in both temperate and tropical regions. However, in temperate regions, higher rainfall occur during the cold winter season thereby tending to reduce FIB number (Mitch et al., 2010), whereas in humid tropical regions, heavy and erosive rainfall occur during the warm wet season which can affect both survival and the transport of FIB (Pandey et al., 2012). FIB number is expected to show a seasonal variability, yet its behavior may vary considerably across different climates.

Researchers in temperate regions investigated FIB seasonality in a small catchment in Canada, where FIB loading were higher in stormflow when compared to baseflow (Sinclair et al., 2009). This result is further confirmed in another study conducted in North Carolina by Stumpf et al., 2010. The latter reported an average total stormflow loading of *E. coli* and *Enterococcus sp.* higher by 30 and 37 times respectively than baseflow loading. Similar trends were noted in a highly urbanized watershed in Republic of Korea where greater FIB concentrations occurred at higher rainfall intensity (Cho et al., 2010a, 2010b). Epidemiological study in the UK showed significant relationship between diarrhea and climate variables (Nichols et al., 2009). Several authors linked the deterioration of surface water quality by increasing FIB concentrations, to streambed sediments resuspension and to an increased runoff washing-off contaminated soils (Henry et al., 2016; Hrdinka et al., 2012; L et al., 2019; Stumpf et al., 2010; Vermeulen and Hofstra, 2014).

These processes are further exacerbated in tropical ecosystems due to erosive frequent rainfall events (Lal, 1983) that generate strong overland flow and soil erosion as well as sediment and bacteria transport to downstream environment (Gourdin et al., 2014; Olivier; Ribolzi et al., 2011). Therefore, it is not surprising to find an increasing number of studies identifying the significant relationship between FIB concentrations and rainfall (Staley et al., 2012; Walters et al., 2011). A recent study done in a subtropical catchment in Australia, have reported a tenfold increase of *E. coli* and *Enterococcus sp.* in wet compared to dry weather samples (Ahmed et al., 2018). A one year monitoring of three small catchments in Lao PDR,

Vietnam and Thailand reported continuous FIB in-stream concentrations, with the highest occurring in wet season (Rochelle-Newall et al., 2016). The latter attributed the smaller *E. coli* peaks during dry season to the intense farming and the small episodic rainfall events. Thereby the latter highlighted the importance of an adequate sampling protocol during stormflow, in order to capture the FIB variability and peaks.

In addition to the increased overland flow during tropical rainfall events, the importance of groundwater during storm events (Kirchner, 2003) contributions to FIB dissemination was highlighted in few studies (Ribolzi et al., 2016; Rochelle-Newall et al., 2016). Based on a method using fallout radionuclides (^{7}Be and $^{210}Pb_{xs}$) and hydrograph separations, applied in a tropical mountain catchment, authors found that overland flow contributed just over one tenth of total flood volume, but was responsible for more than two-third of the *E. coli* transferred downstream. On the other hand, groundwater flow typically comprising low *E. coli* concentrations, contributed up to 89 % of the flood volume. While groundwater can control the FIB dilution magnitude in the stream flow, it can also increase the streambed sediments and FIB resuspension. In a recent study on a small tropical mountain headwater catchment, showed that overland flow contributed of about 41% to overland flow and an average of 89% to the in-stream *E. coli* concentrations (Boithias et al., 2021b). The latter reported that while sub-surface flow was dominating, mean *E. coli* was lower yet still exceeding 1,000 MPN 100 mL^{-1}, which suggests that streambeds can be a considerable source and sink of *E. coli* (Pachepsky et al., 2017; Smith et al., 2008).

Contrary to the widely reported positive association between rainfall events and FIB concentrations in surface water, contradictory findings of epidemiological studies highlight the complex relationship between hydro-meteorological factors and the seasonality of waterborne diseases outbreaks (Guzman et al., 2015; Jagai et al., 2009). As stated by Boithias et al., 2016, diarrhea epidemics in the Luang Prabang area started during dry season triggered by water shortage and ended during the wet season due to aquifer refill. These findings suggest that anthropogenic drivers, like type of water supply, and human behavior, were at least as important as environmental factors in predicting diarrheal risks.

The risk of waterborne disease transmission is likely to increase with the increase with future shifts in climate, and extreme events related to climate change, such as floods and drought, especially in vulnerable regions of the tropical belt (Hofstra, 2011; UNESCO and UN-Water, 2020). Therefore, in addition to hydrology, other important interactive factors are to be

taken into consideration when investigating major FIB controlling factors in surface water, like attachment to suspended sediments, rapid land use and climate changes, hygiene practices, etc. This stresses the need to further investigate FIB fate, which up to now, still has not been sufficiently explored in developing tropical countries.

1.4.1.2 Temperature

Temperature is often cited as the most important environmental factor influencing FIB survival. Temperature in natural temperate environment is generally lower than the stable optimal temperature for *E. coli* growth found in the intestinal tract of the hosts (36–40 °C). Negative correlations between FIB and water temperature, were reported by a number of studies conducted in the temperate region (e.g. (Christian et al., 2020; Herrig et al., 2019; Walters et al., 2011). On the other hand, opposite trends were noted in most of the tropical studies identifying positive correlations between water temperature and FIB concentrations (Derose et al., 2020; Islam et al., 2017; Kelly-Hope et al., 2007; Koirala et al., 2008).

In addition to their ability to persist in surface water, *E. coli* was also found in temperate soils of the Lake Superior watersheds (Ishii et al., 2006), where the highest concentrations were measured during the summer and the lowest during the winter (3×10^3 and <1 CFU g^{-1} respectively). In laboratory conditions, *E. coli* incubated in non-sterile and non-amended soils, was able to grow and replicate at 30-37 °C, and was able to survive longer than 1 month without replicating, when incubated at 25 °C (Ishii et al., 2006). Another study showed that *E. coli* remained viable for up to 33 days after incubation at low nutrient and temperature levels (Boaretti et al., 2003).

Moreover, most of the studies were conducted in temperate environments, and much less is known about the FIB occurrence in tropical soils and water at natural *in-situ* conditions. It is necessary to further investigate in different tropical environments while taking into account other environmental factors like erosive rainfall events during wet season.

1.4.1.3 Sunlight

It has been demonstrated that sunlight and more specifically, ultraviolet wavelengths, have bactericidal effect susceptible to cause direct DNA damage of a wide range of micro-organisms including FIB (Jozić et al., 2014; Nelson et al., 2018). Sunlight is considered an important determinant of the FIB persistence in surface waters (Chan et al., 2015; Sinton et al., 2002). When exposed to solar radiation, bacteria can get inactivated by entering a “viable but

non-culturable" (VBNC) state (Pienaar et al., 2016). Therefore, exposure to sunlight is an important inactivation mechanism used in certain circumstances when no alternative water treatment process is available (Nelson et al., 2018).

A study in temperate waters of a South Korean creek, showed that FIB concentrations during the dry season, were mainly controlled by sunlight during daylight, but quickly recovered at night due to continuous point-sources (Cho et al., 2010a, 2010b). Likewise, transparent mesocosms experiment in Lake Michigan, showed that sunlight was the predominant abiotic factor decreasing exponentially *E. coli* numbers (Whitman et al., 2004). In tropical regions characterized with high solar radiation intensity and duration, sunlight is a major driving factor reducing bacterial number in surface waters (Conan et al., 2008). These findings were contrasted in a tropical urban catchment in Singapore, where FIB concentrations were significantly higher during daytime than nighttime, due to the diurnal pattern of the sewer flow (Ekklesia et al., 2015b).

While solar inactivation levels are important in tropical regions, freshwater systems are often turbid during the wet season, thus limiting the sunlight penetration in the water column (Maraccini et al., 2016; Walters et al., 2014). Furthermore, in relatively shallow tropical aquatic ecosystems like wetlands, solar radiation can be attenuated as well by the presence of dense riparian vegetation and aquatic macrophytes. Therefore, it is important to shed the light on the complexity of bacterial decay due to sunlight and its dependence on numerous factors like turbidity, total suspended solids concentrations, temperature, location and land use in the catchment. Major knowledge gaps in this field remain underestimated in tropical systems, yet essential in order to provide adequate FIB decay rates in the wide range of tropical aquatic conditions.

1.4.1.4 Nutrients and dissolved organic matter

Once released in the environment, FIB show different metabolic capacities to adapt and survive or decay in various environments often colder, more oxygenated and diluted compared to their hosts (Anderson et al., 2005; Byappanahalli and Fujioka, 1998; Ishii et al., 2006; Winfield and Groisman, 2003). Studies investigated the bacterial decay rates under natural physico-chemistry conditions, like the availability and abundance of dissolved organic matter (DOM) and nutrients (Wu 1976; Milne 1991). A previous study by Garzio-Hadzick et al., 2010, reporting higher *E. coli* concentrations in soils rich in organic matter as opposed to sandy soils poor in nutrients, and (Topp et al., 2003) reported higher survival in loamy soils which further

increased with the addition of manure. Moreover, laboratory studies reported limited *E. coli* growth to less than one log increase in CFU, on medium lacking carbon and nitrogen (Ishii 2010). On the other hand, adding dissolved nutrients, namely glucose and peptone, have helped increased *E. coli* survival in aquatic environment (Milne et al., 1991).

Research has found that FIB have developed the capacity to degrade carbon sources found in soil (Fujioka and Byappanahalli, 2001), and that FIB persistence depended mainly on substrate concentration rather than temperature of coastal soil in Senegal (Bouvy et al., 2008). Therefore, adequate carbon and nutrient availability can modify the response of *E. coli* to other stressors and increase its ability to survive and possibly even proliferate. This is particularly probable in tropical developing countries where nutrient-rich environments and frequent fresh manure applications might favor FIB persistence (Trevisan et al., 2002; Yajima and Kurokura, 2008). Research have highlighted the ability for *E. coli* to be naturalized, and found genetically distinct *E. coli* strains in soil than those in the hosts intestinal tract (Byappanahalli et al., 2012b; De Wit and Bouvier, 2006).

These findings underline the importance of assessing the use of *E. coli* for example, as an indicator bacteria in tropical humid environments where its adaptation and proliferation capacities remain largely underexplored and underestimated. Overall, *E. coli* growth or decay is indeed affected by the physico-chemical status of the system, e.g. available nutrient and organic matter, but also conditioned by other factors like microbial community structure, soil moisture and attachment to suspended particles (Byappanahalli and Fujioka, 2004).

1.4.1.5 Microbiota

Many studies have suggested that FIB interactions with the microbiota have important implications on FIB abundance and persistence in the environment (Brettar and Hoflet, 1992; Davies and Bavor, 2000; Gonzalez et al., 1992, 1990; Korajkic et al., 2013). Under natural conditions, the influence of diverse microbial community on FIB varies with FIB species, location, and natural conditions. For example, in Mississippi river, it was found that protozoan predation and viral lysis resulted in decrease of enterococci numbers but not of *E. coli* (Korajkic et al., 2013; Wanjugi and Harwood, 2013). Thereby, the susceptibility to predation can differ between bacteria and may be attenuated in highly turbid environments like humid tropical ecosystems (Iriberri et al., 1994).

1.4.1.6 Association to suspended particles, and aquatic organisms

The ability of bacteria to attach to surfaces and particles has been of considerable interest to many researchers in various fields. In fact, bacterial cells generally have a net negative charge on their cell walls that varies depending on the species, ionic strength, pH, etc. The attachment of bacteria including FIB to particles, is mediated by a complex range of physical, chemical and electrostatic bindings (Olsen et al., 1982; Palmer et al., 2007).

In soil and sediments, bacteria is likely to be found attached to particles rather than free-living (Oliver et al., 2007). However, in aquatic ecosystems, the particle-attached bacterial proportion is highly variable across study areas, ranging from 10% in clear water to over 70% in highly turbid estuaries (Crump et al., 1998; Lemée et al., 2002). Turbidity tend to be higher in tropical systems during the wet season following heavy erosive rainfall events (Milliman and Syvitski, 1991; Milliman et al., 1983). A study conducted in a high altitude tropical catchment in Uganda, showed strong positive correlations between the presence of FIB in aquatic systems and suspended sediments concentrations (Byamukama et al., 2005). Another study in the Hudson River in USA, stated a significant positive correlation between turbidity and FIB. The same study showed that over half of the *Enterococci* was attached to particles in the water column (Suter et al., 2011). Furthermore, previous investigations identified significant negative correlations between particle size and bacterial association, which raises concerns on the bacterial transport further downstream and its consequences on water quality (Oliver et al., 2007; Petersen and Hubbart, 2020a).

In addition to the attachment to suspended particles, many bacteria are known capable of producing and proliferating in biofilms, enhancing their access to nutrients and organic matter (September et al., 2007; Wingender and Flemming, 2011). Moreover, few studies in temperate and sub-tropical systems, found FIB associated with macrophytes and filamentous cyanobacteria (Byappanahalli et al., 2003; Vijayavel et al., 2013), which increased the FIB persistence in the water column of a constructed wetland in Arizona (Karim et al., 2004). However, limited information is available on bacterial associations to macrophytes, biofilms or cyanobacteria in tropical humid climate.

Given current understanding, all these bacterial associations may reflect favorable conditions for bacterial survival, such as providing access to nutrients, and protection from stressors like predation and sunlight (Amalfitano et al., 2017; Walters et al., 2014). Much is still unknown on the partition of particle-attached and free-living bacteria in tropical systems and

on the attachment impact on FIB and pathogens survival, decay and transport in a wide range of tropical systems. Overall, the impact of land use changes subject to more erosive processes, on the FIB transport and persistence has important health risk implications and remains to be evaluated.

1.5.2 Anthropic factors

Human-induced disturbances are likely to have impact at watershed-scale, and cause damage to ecosystems and their functionality (Ducharne, 2007; Palmer et al., 2008). For instance, changes in land management may alter hydrological responses and sediment yield, and dam construction can as well alter the hydrological and sedimentary connectivity (Zhang et al., 2021).Therefore, it is important to investigate the direct and indirect impact of such anthropic factors on sedimentary and bacterial fluxes at watershed-scale to reduce the risks on public health.

1.4.2.1 Land management

It is well known that land management like urbanization, deforestation, agriculture, etc. have a wide range of impact on the ecosystems. Agriculture intensification on the expense of forests for example, contribute to FIB inoculation and, directly through livestock grazing, and fresh manure application, and to FIB dissemination through increasing soil erosion and decreasing soil infiltration (Zhang et al., 2012).

In most of the temperate regions, agriculture has been shifting towards industrial large-scale production practices. Previous studies have linked the high livestock density and manure production, to higher probability of soil and water contamination (Brown et al., 2014; Kloot, 2007; Pandey et al., 2014). A study found higher FIB numbers during baseflow periods due to direct cattle access to the river (Vidon et al., 2008). it is important to have adequate management practices like maintaining a riparian buffer zone, that provide ecosystem services, e.g. trapping pathogens, pesticides, and sediments, as well as stabilizing eroding river banks in both temperate and tropical areas (Gannon et al., 2005; Monaghan et al., 2009; Ziegler et al., 2006).

On the other hand, agriculture in tropical regions is mostly based on extensive production practices at smallholder scales located in the upstream of the catchment. In addition to the wide use of untreated manure, tropical rural communities (humans and livestock) usually live nearby the rivers and humid zones on which they depend for water supply, bathing, washing

and for untreated wastewater release. As stated by study on a rural steep catchment in Lao PDR, a high spatial variability of water quality was noted along the river. The highest FIB concentrations mostly occurred along the urbanized river banks, within the riparian zone where livestock roamed freely, downstream of the villages and of small industrial plants, and during flood events (O. Ribolzi et al., 2011). Therefore, it is important to note that soil erosion and export to downstream rivers, not only depend on the slope, but also on the land cover, and the rainfall intensity (Janeau et al., 2014; Magdoff and Weil, 2004; Podwojewski et al., 2008).

However, some tropical areas are witnessing rapid land use changes. For example, authors found that the conversion of native forests to agriculture and urbanized development contributed to FIB increase in a tropical Hawaian river (Derose et al., 2020; Hathaway et al., 2010; Strauch et al., 2014). Furthermore, rapid land use changes are increasingly reported in the mountainous catchments in Southeast Asia (Huong et al., 2018; Ribolzi et al., 2017; Sidle et al., 2006; Turkelboom et al., 2008), like shifting from annual crops to commercial tree plantations (e.g. teak) with limited understorey. Unlike fallow, land covers like maize and teak tree plantations result in high soil crusting rates, thus increased overland flow and potentially increased FIB concentrations (Lacombe et al., 2018; Song et al., 2020; Ziegler et al., 2006). Recent studies highlighted the splash effect of the rain droplets falling from teak tree canopy with higher kinetic energy, accelerating soil detachment and erosion (Mügler et al., 2021). A study comparing three small rural catchments highlighted the important role of land use as a controlling FIB factor besides hydrological regime (Fig. 5) (Rochelle-Newall et al., 2016). The impact on FIB dynamics remain to be evaluated in large-scale tropical catchments.

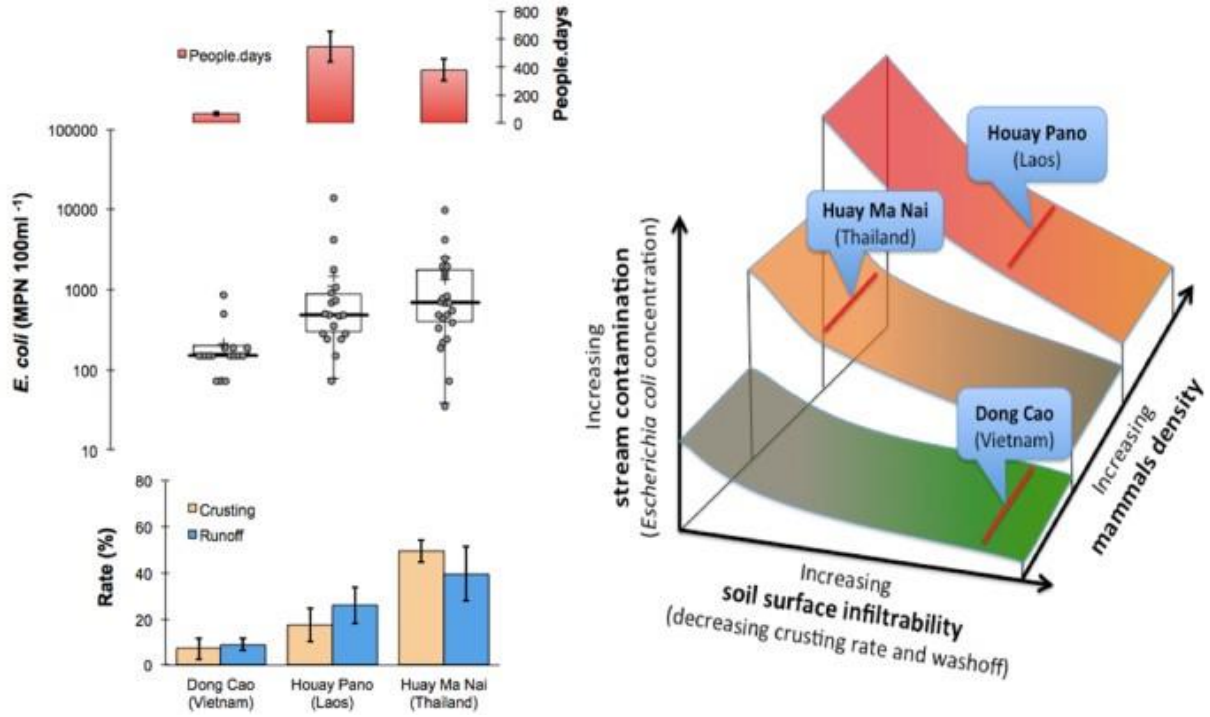

Figure 5: Escherichia coli (E. coli), soil surface infiltrability and mammalian presence in the studied catchments. Concentrations of E. coli in streamwater during baseflow (Dong Cao ≠ Houay Pano = Huay Ma Nai; $p < 0.05$), soil surface crusting rate (Dong Cao < Houay Pano < Huay Ma Nai; $p < 0.05$), runoff (Dong Cao < Houay Pano < Huay Ma Nai; $p < 0.05$), and people.days (Dong Cao < Huay Ma Nai < Houay Pano; $p < 0.05$) as a proxy of mammalian density (left side panel). Conceptual diagram showing the relationship between mammalian density, soil surface infiltrability and in-stream E. coli loads (right side panel). Each of the three studied catchments is placed on the graph as indicated by a red line. A change in either soil infiltrability or mammalian density would result in a change in the position along and across the different zones. Source: Rochelle-Newall et al., 2016 .

In many areas as well, riparian zones are used for cultivation, which may lead to higher suspended sediments and FIB levels in surface waters (Soupir and Mostaghimi, 2011; Vigiak et al., 2008). Conservation of wetlands and riparian zones may significantly allow sediment and FIB retentions, thus improve water quality downstream (Pachepsky et al., 2008; Ribolzi et al., 2011). To our knowledge, very little work has been done on the role of wetlands in tropical systems where environmental conditions in streambed sediments (temperature, nutrients, sunlight), might favor FIB persistence, and thus transform the FIB sink into FIB source.

1.4.2.2 Water management

Nearly half of the world's greatest rivers are regulated with at least one large dam (Nilsson et al., 2005). Many countries rely upon hydropower dams to have access to electricity, but dams reservoirs also serve for flood protection, aquaculture, and drinking or irrigation water purposes. Hydropower is expected to grow by over 70% in developing countries in the coming decades, mainly in emerging economies of Southeast Asia, South America, and Africa (Fig. 6) (EIA, 2016; Zarfl et al., 2015).

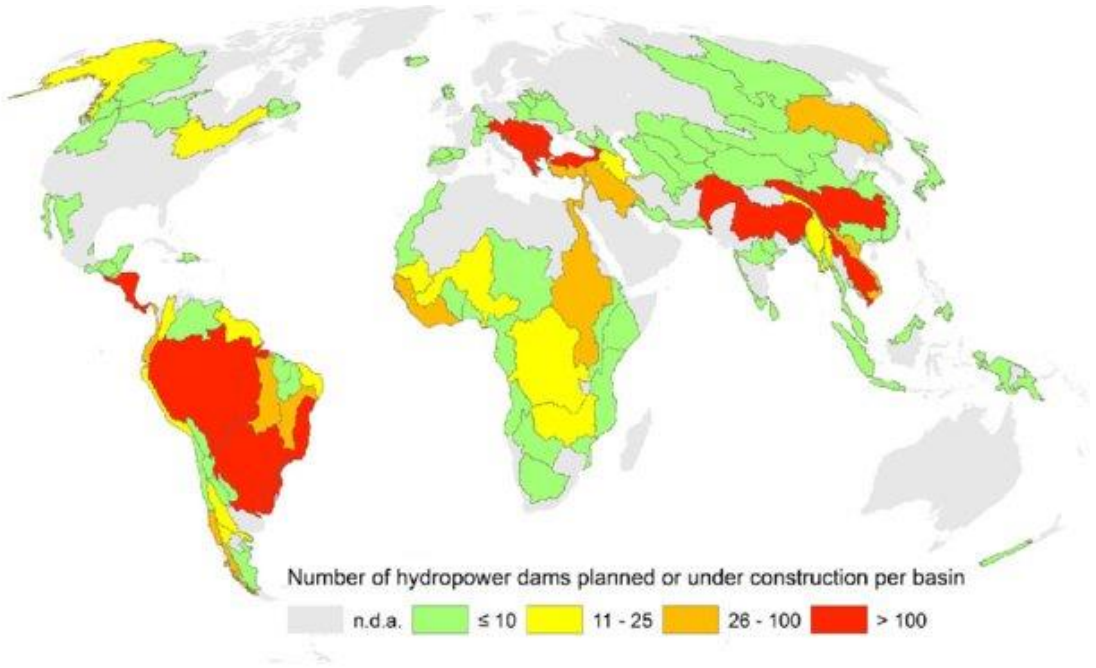

Figure 6: Number of future hydropower dams per major river basin. Source : Zarfl et al., 2015.

However, hydropower dams not only disturb the hydrological connectivity, but also sediment transport and might affect water quality, upstream and downstream of constructed dams. There is increasing evidence showing direct significant hydrological and ecological repercussions of dam construction, threatening some of the richest freshwater ecosystems in the world including the Amazon, Congo and Mekong (Poff and Zimmerman, 2010; Winemiller et al., 2016). A number of studies emphasized sediment retention upstream of the dam (Gao et al., 2010; Vörösmarty et al., 2010). Due to large reservoirs and to reduced water velocity, sediment transport to the river downstream decreases and creates sediment-starved or "hungry" water with an increased erosive potential (Fig. 7) (Kondolf, 1997; Manh et al., 2015; Wei et al., 2019).

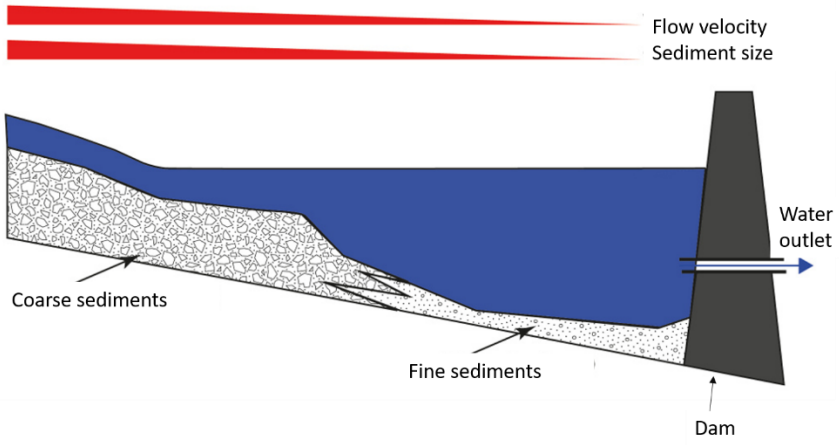

Figure 7: Dam influence on sediment grain size sorting upstream of the structure. Adapted from Frémion et al., 2016 .

Sediment particles and sediment transport processes in turn affect transport of particle-attached bacteria, including fecal pathogens released by humans and animals in the environment. Hence, retention of sediment and bacteria can attenuate the contamination downstream, but can also lead to serious consequences on the FIB persistence in the reservoir and in consequence, on the activities implemented upstream of the dam directly relying on untreated surface waters (fishing, irrigation or daily domestic uses). Therefore, understanding the impact of tributaries hydropower dams on water quality is crucial for the sustainability of river basins and for public health safety especially in tropical developing countries where access to clean water, sanitation and hygiene remains challenging. Up to now, investigations about the relationship between water resource infrastructure like dams, and water quality are still lacking in developing countries, especially in transboundary basins involving several stakeholders.

1.6 Modelling studies for FIB fate and transport

There is a need for studies providing new insights on mechanistic understanding of diverse global changes like climate change impacting surface water quality. More particularly, tropical regions are expected to face significant climate change consequences (frequency and intensity of extreme rainfall and/or drought events) (Vörösmarty et al., 2010; Vorosmarty and Sahagian, 2000). The latter, combined with the population growth, and with rapid changes in land and water management practices, is likely to result in significant changes in overland flow, soil erosion, sediment and bacterial transport across the watershed. In order to address these challenges, modeling tools can be useful to (i) understand FIB sources, fate and transport, (ii) help watershed stakeholders to establish adequate strategies to reduce the exposure risk on public health, (iii) analyze various future global changes scenarios, and (iv) develop early warning predictive tools for vulnerable communities affected by water contaminations. Three main types of mathematical approach are widely used to investigate and model the complex hydrological sedimentary and bacterial responses to changes in land use and climate (Miller et al., 2013).

The first approach is based on statistical models like empirical regression such as multiple regressions (Chu et al., 2011; Mahloch, 1974) and double mass curves (Tang et al., 2013; Wang et al., 2012) as well as artificial neural networks (Thoe et al., 2012). These approaches usually use environmental variables as input data, and provide FIB concentrations as an output.

The second approach uses mechanistic or physical process-based models. These models can simulate FIB transport through processes like advection dispersion equations (Wilkinson et al., 1995), streambed resuspension (Cho et al., 2010b). Unlike the first approach, this one allows considering and ranking underlying mechanisms responsible for the mobilization, transfer and concentration of FIB in the system.

The third approach is based on spatially distributed and semi-distributed models at watershed scale, e.g. ECOMSED (Blumberg and Mellor, 2012), SWAT (Arnold et al., 1998), SENEQUE/Riverstrahler (Billen et al., 1994), MIKE (DHI, 2011), and HSPF (Abbas et al., 2021). These models consider watershed morphology, soil properties, hydrology, land use, and pollution point sources. They can also take into account processes like streambed bacteria resuspension (Kim et al., 2010), FIB die-off rates, and, FIB transport model (Chin et al., 2009; Dorner et al., 2006). This approach allows to test complex scenarios and simulate the impact of future changes in the system and their potential impacts on public health on the catchment (Cho et al., 2012; Kashefipour et al., 2002).

However, these models require comprehensive knowledge of (i) the drainage basin morphology, and hydro-meteorology data for model parametrization (ii) long-term water quality data for calibration (iii) FIB die-off, deposition, runoff and resuspension rates, and (iv) FIB sources. Access to these data can be challenging and limited in some tropical and developing countries with sparse water quality monitoring networks. Nonetheless, this research area is expanding and some of the existing models have been adapted to tropical systems (Le et al., 2005; Luu et al., 2010). Few, to our knowledge, were successfully capable of simulating the transport and fate of FIB in these systems (Causse et al., 2015; Coffey et al., 2013; Kim et al., 2017; Thoe et al., 2012), which provides new opportunities to explore this research area.

Each model presents some advantages and limitations. For instance, MIKE model is good for small river basins or water bodies, and can generate hourly output data. On the other hand, the simulation time is longer which makes it difficult to apply it for climate change scenario analysis (Islam et al., 2021). SWAT (i) has a large user community, (ii) covers a large range of processes at watershed-scale, (iii) can be used for various applications, and (iv) simulates from sub-daily time step to inter-annual time step. Another advantage of SWAT over other models like hydrological simulation program fortran (HSPF) is that it allows the simulation of persistent and less-persistent bacteria populations in the same model run (Niazi et al., 2015; Qiu et al., 2018).

Progress has been made towards improving SWAT performance in simulating FIB fate and transport at watershed-scale. SWAT is able to estimate FIB sources and loading in watershed (Coffey et al., 2010), and to assess the magnitude of FIB sources within the watershed (Coffey et al., 2013). SWAT was further improved by including in-stream processes to estimate the impact of the streambed sediment re-suspension or deposition on FIB number (Kim et al., 2010; Pandey et al., 2012). Furthermore, SWAT was able to better reproduce the seasonal variability of bacteria after including bacterial growth/die-off adjustable by changing temperature (Cho et al., 2016). Recent advances showed better simulation of low concentrations of bacteria during the dry season with associated base flow, after taking into account additional bacteria in-stream processes like hyporheic exchange process (Kim et al., 2017).

1.7 Specific objectives and scientific approach

Surface water contamination by fecal pathogens remains a major threat to public health in developing countries of the tropical region. Despite the significant advances made towards a better understanding of the FIB dynamics in temperate regions, many knowledge gaps exist on the underlying mechanisms of fecal contamination in tropical conditions. There is a need for studies to provide new insights regarding FIB transport and survival in tropical conditions at watershed-scale, in order to mitigate health risks associated to the use of contaminated water.

In the Mekong basin, over 70 million people rely on unimproved surface water for their domestic requirements. Communities living in these areas are not only exposed to continuous fecal contamination from point and diffuse sources, but are also facing rapid global changes (land use, climate change, hydropower dams) with various consequences on FIB fate and public health. These anthropic activities are likely to have consequences on water contamination at various scales.

Therefore, the main objective of this research was to characterize the dissemination of FIB and its dynamics at different spatio-temporal scales in the lower Mekong basin. This thesis work aims to answer the following questions:

(i) What are the different factors that control *E. coli* at the scale of large Mekong River tributaries in Lao PDR?

(ii) How do two key environmental factors (solar radiation exposition and suspended particles deposition) affect the decay or survival of *E. coli* in a tropical mountainous wetland?

(iii) What are the consequences of hydroelectric dam construction on the hydrological regime, sediment flow continuity, and bacterial dynamics at the watershed scale?

To this end, this research was based on a multidisciplinary approach described in the following chapters.

Chapter 2 describes the study site and the global context of the Mekong River basin as well as the major challenges facing this ecosystem. The processes equated in the numerical model, whose choice has been previously justified.

Chapter 3 provides an overview of the key factors, in particular the hydrological regime and land uses, controlling the spatio-temporal dynamics of *E. coli* as a FIB in the lower Mekong basin. First, we investigated the seasonality of *E. coli* at large watersheds-scale. Second, we aimed to identify the effects of seasonal hydrology and of land use on *E. coli* concentration in the main Mekong tributaries of Lao PDR.

Chapter 4 investigates the environmental factors, solar radiation exposure and suspended sediment deposition, effecting in-stream *E. coli* survival/decay, at the spatial scale of a tropical headwater mountain wetland, which are likely to play a key role in stream water purification of fecal pollutants. To this end, I went to the field in Lao PDR in order to conduct a mesocosm experiment in the headwater wetland in Houay Pano in August 2019. The main objectives of this experimental approach were (i) to quantify decay rates of total, free-living, and particle-attached *E. coli*, (ii) to quantify the relative importance of solar radiation exposure and suspended sediment deposition on decay rates, and (iii) to investigate the survival of *E. coli* in the sediment deposited in the streambed. These findings may contribute to parameterize hydrological and water quality models in a tropical context.

Chapter 5 attempts to analyze the hydro-sedimentary and bacterial (*E. coli*) dynamics at the scale of the Nam Khan River watershed (7,500 km²), in northern Lao PDR, subject to the impact of the rapid development of cascade hydroelectric dam projects. In this context, the objective is first to statistically detect trends and breakpoints in the time series of variables measured at the watershed outlet over a decade, before and after the dam construction. Second, this chapter describes the modeling approach (SWAT) to simulate flow, suspended sediment concentrations, and *E. coli* concentrations excluding the presence of a dam in the model, in order to compare simulated variables to observed variables, and to quantify the impact of the dam on these variables.

Chapter 6 presents the overall conclusion of this thesis work as well as future directions needed to minimize the hazards and risks to vulnerable populations in the Mekong River Basin.

Chapter 2. Material and methods

This chapter is not intended to be a repetition of the material and methods specific section of the following scientific chapters. The objective here is to bring complementary elements helping to better understand the overall context of this research work. Therefore, a general description of the Mekong basin are given in the first section along with the main issues and challenges facing the ecosystem and the population. Moreover, a detailed description of SWAT model is described with further details to better understand the underlying processes of the model.

2.1 Study site

2.1.1 General description of the Mekong basin

The Mekong river is approximately 4,900 km long, listed as the 12th longest river in the world, and the longest in Southeast Asia (MRC, 2005). It originates from the Tibetan plateau at more than 4,500 m above sea level, flows through China, Myanmar, Lao PDR, Thailand and Cambodia, and eventually creates the world's third largest delta in Vietnam, before finally debouching into the South China Sea. The Mekong basin is commonly divided into two parts: the Upper Mekong Basin (UMB) covering China and Myanmar, and the Lower Mekong Basin (LMB) covering Thailand, Lao PDR, Cambodia and Vietnam. The Mekong transboundary river drains a total area of 795,000 km^2, making it the 10th largest basin in the world, with a mean annual discharge of about 14,500 $m^3 s^{-1,}$ unevenly distributed among the countries (Table 5).

Table 5: Country share of the Mekong basin territory and water discharge. Source: MRC, 2003a.

Country	Drainage area (km^2)	% of Mekong basin	% of area country	% of Mekong discharge
China	165,000	21	2	16
Cambodia	155,000	20	86	18
Lao PDR	202,000	25	85	35
Myanmar	24,000	3	4	2
Thailand	184,000	23	23	18
Vietnam	65,000	8	20	11

2.1.1.1 Climate

The climate of the Mekong river basin ranges from high-altitude continental and temperate in the UMB to tropical monsoonal in the LMB (MRC, 2003b). Temperatures in the UMB range between an average of 25 °C and 14 °C, and exhibit more seasonal variation than those in the LMB. In the LMB, there is little seasonal variation in temperatures in the lowlands and river valleys, ranging on average between 32°C in April and 23°C in December. However, further north in the highlands of Lao PDR, average temperatures can fall as low as 15 °C and below during December and January (MRC, 2010a).

The tropical monsoonal climate is dominated by the Southwest Monsoon, generating a bi-seasonal pattern. The wet season starts at the onset of the monsoon rainfall, usually from June until October, and is followed by the dry season from November until May (MRC, 2005). Heavy rainfall occurs in most of the basin from June to October, with a distinct east-to-west distribution gradient of mean annual rainfall over the basin. The highest annual rainfall (up to 3,000 mm) occurs in the uplands in Lao PDR and Cambodia and the lowest annual rainfall (1,000-1,600 mm) in northeastern Thailand (Fig. 8).

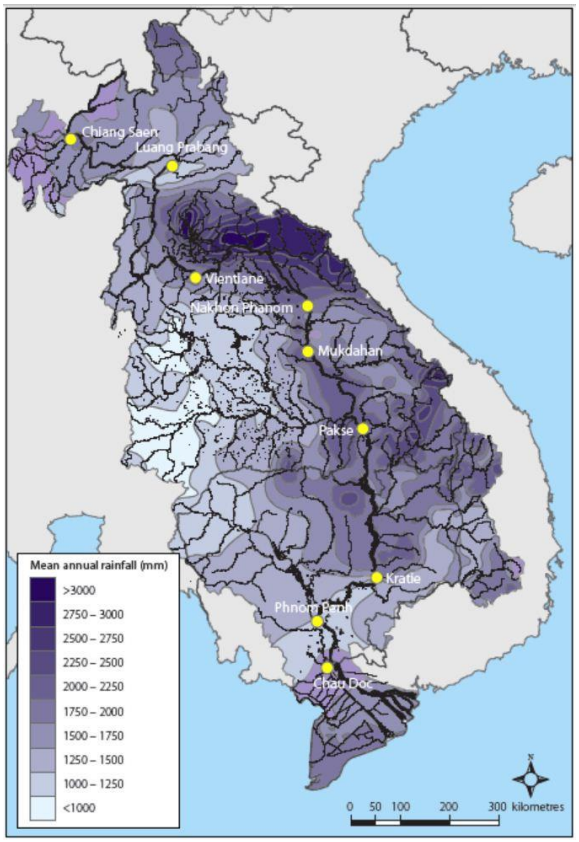

Figure 8: Mean annual rainfall in the lower Mekong basin; Source: MRC, 2010a.

2.1.1.2 Hydrology

The hydrology of the Mekong river is characterized by high intra-annual variability, where discharge during the wet season is on average 5 to 10 times higher than during the dry season (MRC, 2021). The snowmelt in the Tibetan Plateau upstream of the Mekong, contributes the most during the dry season to the Mekong discharge north of Vientiane, Lao PDR (MRC, 2021). During the wet season, the natural hydrological regime of the Mekong river is mainly determined by the southwest monsoon between June and October, which is the main driver of the Mekong annual flood pulse. This results in a distinct seasonal annual hydrological cycle between a flood season and a low-flow season. Moreover, tropical cyclones incursions into the basin from the South China Sea are responsible for intense rainfall and extensive flooding in part of Lao PDR, and in the Mekong delta in Cambodia and Vietnam (MRC, 2021). These tropical storms can generate distinct individual peaks to the wet season flows, generally occurring during September and October when the seasonal discharge is already high. Historically, these events have been responsible for many of the most extreme flood discharges that have been observed, but also cause the large flow reversal up the Tonle Sap River to the Great Lake in Cambodia. This annual flooding cycle triggers fish movement and delivers a pulse of sediment and nutrients to the floodplain, which supports fish and other biodiversity, and allows rice agriculture around the lake (MRC, 2021).

The Mekong river basin is characterized by a large network of tributaries, forming as many sub-basins. Tributaries located on the left bank drain the high-rainfall areas of Lao PDR tributaries and contribute to the major wet season flow. Tributaries on the right bank drain a large part of northeast Thailand and low relief regions of lower rainfall (MRC, 2005). Overall, the geographical rainfall distribution pattern determines the greatest contributions to Mekong river flow during the wet season, mostly from the Se Kong, Se San and Sre Pok (3S) river system, and from the large left-bank tributaries in Lao PDR between Vientiane and Nakhon Phanom, and between Pakse and Stung Treng (Fig. 9).

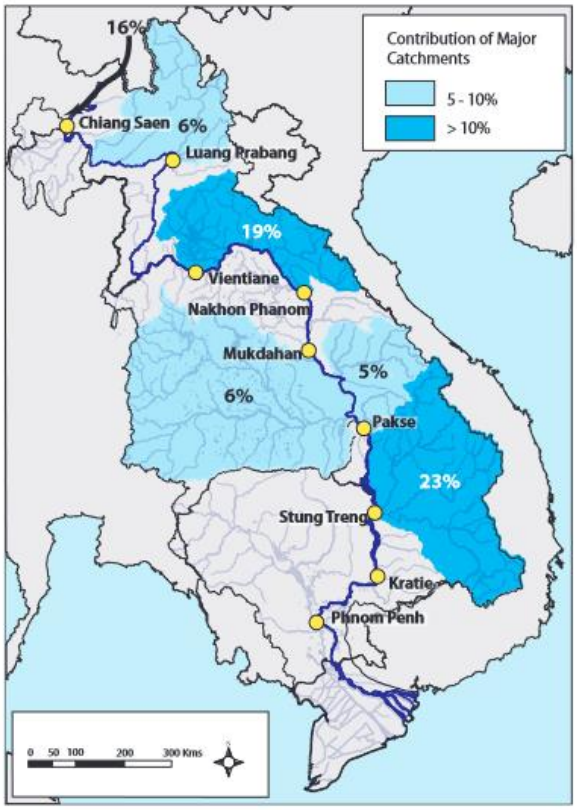

Figure 9: Major contributions of the LMB to the Mekong discharge. Source: MRC, 2009.

2.1.1.3 Biodiersity and livelihoods

Mekong annual flooding is an important hydrological characteristic of the Mekong basin and an important part of the ecology of the region. The Mekong annual flood pulse is the dominant trigger of the annual cycle of sediment fluxes and ecological processes within the fluvial system (Piman et al., 2013). The annual flood pulse and the associated flooding and drying periods, create a rich ecology (e.g. seasonal wetlands and flooded forests) and support much of the region's biodiversity (MRC, 2003b). Consequently, the Mekong flood pulse drives the high productivity of aquatic ecosystems and biodiversity (Lamberts and Koponen, 2008), particularly the Tonle Sap floodplain and the Mekong delta (Hortle, 2007; Kummu et al., 2006; Lamberts, 2006). These important hydrological characteristics of the Mekong basin make it the second most biodiverse river in the world, after the Amazon river.

The water resources and productivity of the Mekong basin play a vital role in the Mekong basin. About 65 million people live in the LMB and depend on the Mekong River and its tributaries for transportation, drinking, bathing, fishing, and agricultural irrigation. Population living in the Mekong basin work in harmony with the annual flooding cycle of the river (MRC, 2021). Their

livelihoods are strongly related to the river system through abundant fisheries and fertile floodplains (MRC, 2010b). The Mekong basin is considered the largest inland fishery in the world, with more than 2.1 million tons of fish harvested each year, representing about 18% of the world's freshwater fish yield. On the other hand, about 70% of the population relies on agriculture, which is the most important economic activity of the basin (MRC, 2014). Total irrigated agricultural land is estimated around 4.3 million ha, 98% of which is irrigated by surface water, and the other 2% by groundwater (FAO, 2011). Rice cultivations are the foundation of Southeast Asia livelihoods. More particularly, the Mekong delta in Vietnam is the world's second most important rice exporter. The high productivity of this land is due to the annual floods enriching the delta soils with fish and sediments transported from far upstream (MRC, 2010b). Although fish and rice are the main livelihoods of the basin population, other agricultural activities exist and include a wide range of tropical fruits, vegetables, forestry products, and livestock.

2.1.2 Main challenges on the Mekong basin

The Mekong river is facing several major challenges. In addition to the growing food and energy needs due to population growth, the region is undergoing rapid economic development, placing additional pressure on the land and water resources to meet the growing needs (Le Meur et al., 2021; Pokhrel et al., 2018).

2.1.2.1 Land use

About 60% of the basin is covered by clay-rich soils of high acidity and low fertility, therefore, these areas are commonly forested (evergreen deciduous, coniferous, bamboo, and plantation forests) (MRC, 2011a). Most of the forests are found in the mountain ranges of Lao PDR and Cambodia (Fig. 10). The central to southern parts of Lao PDR, and further south till the Mekong delta, are areas characterized by large areas of plains and fertile soils, suitable for permanent agriculture, mainly dominated by paddy field areas (MRC, 2010a).

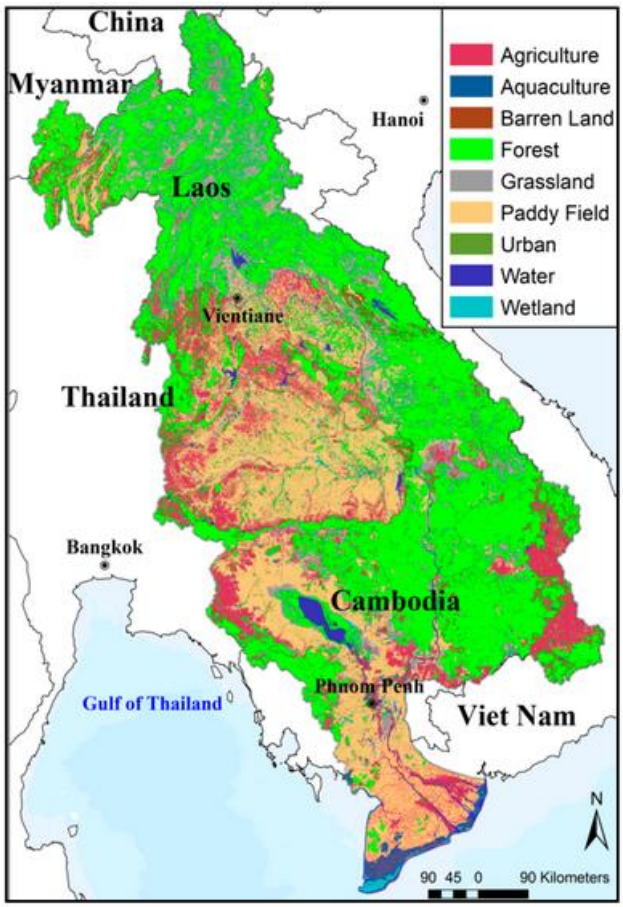

Figure 10: The 2010 MRC land use/land cover (LULC) map of the LMB. Source: Ly et al., 2020.

Over the past few decades, land use has been shifting towards intensified annual cash-crops cultivations on the expense of fallow and forested lands (MRC, 2011b). Mekong basin, excluding China, have lost, between 1973 and 2009, under a third of its forest cover (WWF, 2013). For instance, in Lao PDR, forests have rapidly shrunk from 73% in the 1960s to 40% in the 1990s, while annual crop production with reduced fallow period and suppressed understory cover have increased (Huong et al., 2018; Thongmanivong and Fujita, 2006; Valentin et al., 2008b). In the past 20 years, we observed an increase in the surface area covered with commercial perennial monocultures such as teak tree plantations at the expense of traditional slash-and-burn cultivation systems in steep montane environments of Lao PDR (Ribolzi et al., 2017). The transition from forests and crop cultivation to large-scale monoculture cultivations leads to a decrease in water infiltration and an increase in overland flow, sediment yield and bacterial loads from the soil surface to downstream aquatic ecosystems (Homdee et al., 2011; Kim et al., 2018; Ly et al., 2020; Ribolzi et al., 2017).

Hydropower development

As a consequence of agricultural expansion and population growth, the water resources exploitation started slowly in the 1950s from the basin downstream, but accelerated during the last decades (Fig. 11).

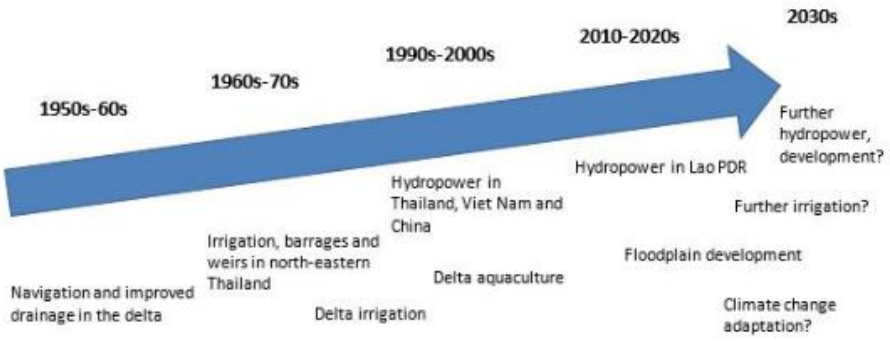

Figure 11: Illustration of basin development trajectory since the 1950-1960 to 2030 and beyond. Source: MRC, 2021.

Water resources infrastructures like hydropower dams, are rapidly developing on the Mekong river and its tributaries. Historically, Mekong basin was one of the least regulated large river basins worldwide (i.e., the fraction of the annual water discharge stored in reservoirs), but now it is undergoing unprecedented extensive hydroelectric dam construction throughout its basin (Grumbine et al., 2012). In the last ten years, more than 100 large dams have been built on the Mekong river (Fig. 12). In 2008, the total active reservoir storage capacity of the Mekong (8.6 km^3) represented only 2% of its mean annual discharge (Kummu and Sarkkula, 2008), but it is expected to increase up to 19% (86.8 km^3) in 2025 (Kummu et al., 2010). In addition to displacing hundreds of people living along the river banks, the various degrees of dam impact on the river hydrology, sediment and nutrient transport, biodiversity and productivity, have been investigated (Soukhaphon et al., 2021).

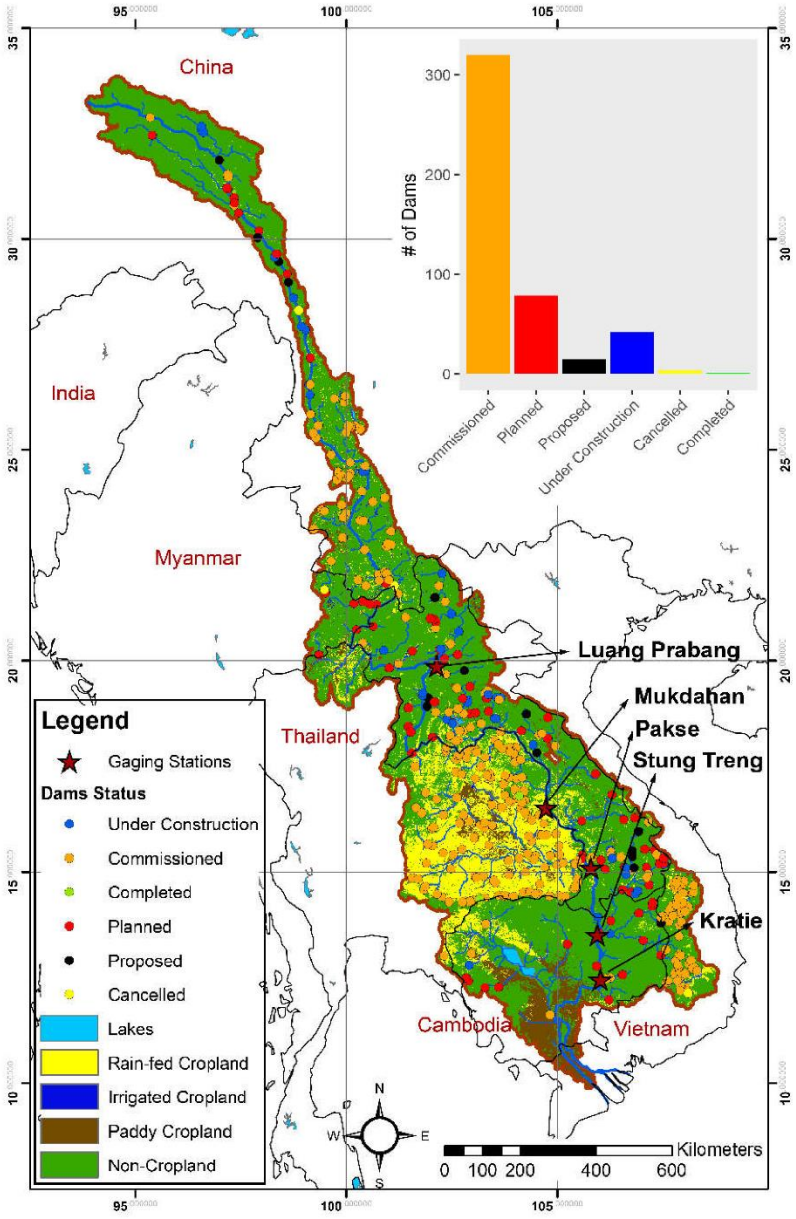

Figure 12: Dams in the Mekong river basin. The background shows land use types and irrigated croplands obtained from (Salmon et al., 2015). The dam database was provided by the Research Program on Water, Land, and Ecosystems (WLE), Greater Mekong (WLE, 2020). Source : Pokhrel et al., 2018.

Climate change

In parallel to the previously mentioned issues reported in the Mekong basin, climate change is likely to further exacerbate the pressures on the ecosystems, along with the water resources and the livelihoods (MRC, 2011b). Studies have stated changes in the wet season Mekong discharge, as well as more frequent floods and droughts, in recent years, which have led to aquatic ecosystems and rural livelihoods disruptions (MRC, 2010b; Pokhrel et al., 2018). Projections based on climate model results suggest a significant increase in basin-wide temperatures and changes in rainfall

events and intensities (MRC, 2021). It is still unclear of how the combined impacts of climate change and dam expansions will manifest on the hydrology, agriculture, aquatic systems, and livelihoods of the Mekong basin (Pokhrel et al., 2018). Therefore, it is crucial to improve our knowledge on potential changes of the ecosystem and water quality, in order to be able to mitigate negative consequences.

Water quality

In the context of rapid global changes, e.g. population growth, land use, hydropower development, and climate change, it is highly likely to observe water quality degradation in the Mekong river and its tributaries. Water Quality Monitoring Network Program by the Mekong River Commission (MRC), began in Lao PDR, Thailand, and Vietnam in 1985, and in Cambodia in 1995. Since 2010, MRC conducts routine monthly monitoring of water quality in the LMB by measuring 19 water quality parameters at 48 stations, 17 of which are located in the Mekong river, and 26 in the Mekong tributaries. A recently published study evaluated the spatial-temporal water quality of the Lower Mekong Basin (LMB) using biological and physical-chemical data collected over the last two decades (Sor et al., 2021). The latter authors revealed a water quality degradation during the last decade, particularly near Vientiane City, within the Sekong, Sesan, and Srepok (3S) river system, within the Tonle Sap Lake system and in the Mekong Delta. Water quality degradation is likely associated to hydrological alteration, sediment trapping, and point source and non-point source wastewater releases, resulting from rapid hydropower development, deforestation, intensive agriculture, and urbanization. Another study aiming to understand the spatial variability of water quality in LMB, used the Self-Organizing Map (SOM) to classify 117 monitoring sites and hotspots of pollution within the basin (Chea et al., 2016). They found that the Mekong river was less polluted than its tributaries and that the main water quality issues were eutrophication and salinity increase in many tributaries.

Other studies have shed the light on the fecal pollution exceeding the safe water quality thresholds, in several Mekong tributaries (Boithias et al., 2016; O. Ribolzi et al., 2011; Rochelle-Newall et al., 2016). Nevertheless, very few long term monitoring stations of waterborne pathogens in the environment exist in the Mekong tributaries, therefore major knowledge gaps persist on the distribution of these pathogens in tropical environments. Given the high spatio-temporal variability of FIB and the associated risks on human health, regular and extensive water quality monitoring

within the Mekong basin and particularly in Mekong tributaries, is needed to maintain the ecosystem function as well as the livelihoods in the LMB.

For all these reasons listed previously, the LMB is an adequate study area that allows to answer the scientific questions of this research work aiming to improve our overall understanding of fecal pollution in tropical hydrosystems. Given the important hydrological contributions of left-bank tributaries to the Mekong discharge, we focused on Mekong tributaries located in Lao PDR to investigate the controlling factors of fecal pollution at various spatial scales going from the major Mekong tributaries at regional-scale of Lao PDR (between 239 km^2 and 25,946 km^2; Chapter 3), to a small headwater wetland (0.6 km^2; Chapter 4), and a large-scale Nam Khan watershed regulated by cascade hydropower dams (7,500 km^2 Chapter 5). To do so, we used various approaches which are described in the following section.

2.2 Methods

Three complementary approaches were adopted in the current research work, including *in-situ* observations at various spatio-temporal scales, experimental approach using mesocosms, and modeling approach using SWAT (Fig. 13).

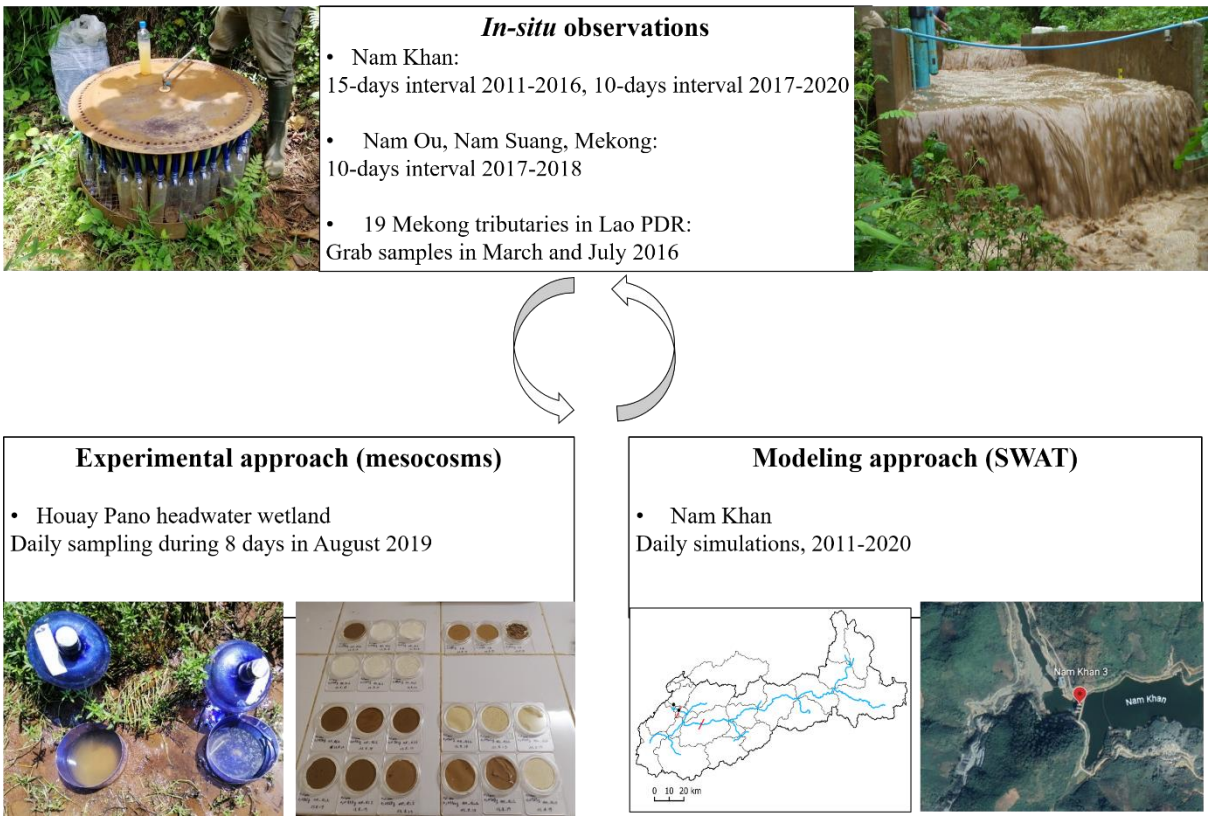

Figure 13: Overview of the main approaches used in this research work.

2.2.1 *In-situ* observations

In-situ observations include two types of variables: (i) hydro-meteorological variables (water level, rainfall, air temperature, wind speed, solar radiations, relative humidity), and (ii) water physico-chemical and microbiological quality variables (turbidity, pH, electrical conductivity, dissolved oxygen, water temperature, and concentrations of TSS and *E. coli*).

Hydro-meteorological data is gathered from various sources:

(i) Rainfall is measured daily at four stations operated by the Lao PDR Government, Department of Meteorology and Hydrology (DMH), in Ban Somsanook Pakou near Nam Ou river (20.081972, 102.264139), in Ban Sibounhome near Nam Suang river (19.967111, 102.272444), and in Luang Prabang airport near Mekong river (19.898472, 102.16525).

(ii) Water level is recorded twice per day at four gauging stations in Nam Ou river (20.245556, 102.348806), Nam Suang river (19.967111, 102.272444), Nam Khan river (19.78602, 102.18336), and Mekong river (19.89225, 102.13417).

(iii) Meteorological data (air temperature, wind speed, solar radiations, and relative humidity) is obtained from an automatic weather station located in Houay Pano watershed (Boithias et al., 2021a). Houay Pano is an experimental site, part of the Multiscale TROPIcal CatchmentS (M-TROPICS) critical zone observatory (Gaillardet et al., 2018), which operates under the umbrella of the Observatoires de la Zone Critique: Applications et Recherche (OZCAR).

Water physico-chemical and microbiological quality variables are measured *in-situ* in various locations:

(i) Nam Khan river (19.786015, 102.183356) at 15-days interval from 2011 to 2016 and at 10-days interval from 2017 to 2020.
(ii) Nam Ou (20.08642, 102.26406), Nam Suang (19.97931, 102.24728), and Mekong (19.892246, 102.13465), at 10-days interval from July 2017 to December 2018.
(iii) Mekong river at six sampling sites, and 19 Mekong tributaries at 22 sampling sites, located between 15 and 20°N, sampled once in March 2016 and once in July 2016.

The measurement methods are described in the material and methods section of each of the following chapters.

2.2.2 Experimental approach

The experimental approach in this thesis aimed to investigate two key environmental factors (solar radiation exposition and suspended particles deposition) effecting in-stream E. coli survival/decay in a tropical headwater mountain wetland. The detailed description of this approach is provided in Chapter 4. Hereby we present a general description of the approach. The experiment was conducted using semi-controlled environments mesocosms. 15 mesocosms (51 cm high and 27 cm in diameter transparent plastic buckets) were filled with contaminated water collected from the Houay Pano river and installed in the water column of the wetland of Houay Pano for a monitoring period of 8 days.

Mesocosms were divided into four treatments with triplicates: (i) sediment deposition-light (DL); (ii) sediment deposition-dark (DD); (iii) sediment resuspension-light (RL); and (iv) sediment resuspension-dark (RD). An additional set of three mesocosms (control) were used to verify the

absence of external contamination during the experiment (raindrops splash, dry atmospheric deposits, etc.). Open top mesocosms (covered in case of rainfall event) were used for DL, RL, and control. Covered top mesocosms using two layers of plastic covers wrapped in aluminum foil with ventilation holes to ensure the aeration inside the mesocosm were used for DD and RD. Mesocosms were randomly distributed by series of replicates, and installed in the center of the wetland, spaced one meter apart, held straight with bamboo rods, and driven 10 cm deep into the streambed sediment (Fig. 14).

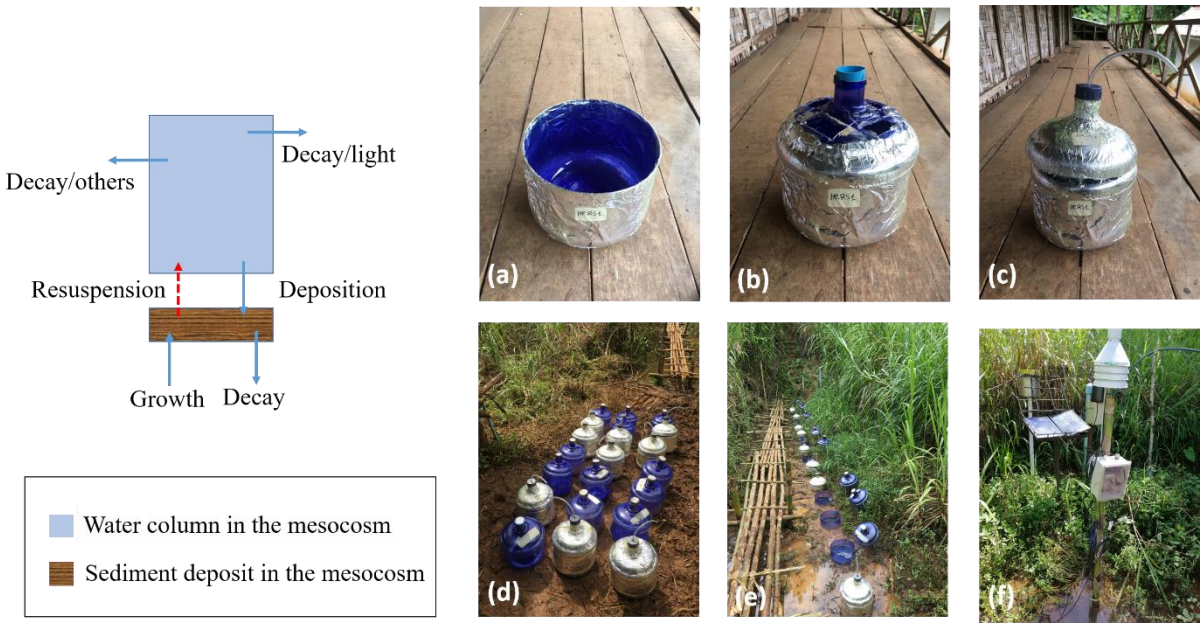

Figure 14: Conceptual diagram of the main processes occurring in mesocosms, and photos taken on the field: (a, b, c) preparation steps of the covered top mesocosms, (d) 15 mesocosms before installation in wetland, 15 mesocosms randomly distributed by series of replicates, (f) meteorological station installed in the wetland.

2.2.3 Modelling approach

In this research work, the Soil and Water Assessment Tool (SWAT) was used in Chapter 5 to study the dam impact on river discharge, and TSS and *E. coli* concentrations in the Nam Khan watershed, in Lao PDR. SWAT is a physically based watershed-scale agro-hydrological model developed in Texas by Arnold et al., (1998). SWAT model was initially developed to study the impact of agricultural practices on hydrology, sediment and water quality at watershed-scale. Details of the creation of this model were published by Arnold et al., (2012).

SWAT is a well-known reliable, among the widely used models for multidisciplinary

studies in various regions of the world. Over the years, the model has expanded to include the study of climate change, land use change, pollutants and sediments monitoring, anthropogenic impacts like hydropower dams (Tan et al., 2019). It covers a wide range of processes related to hydrological balance, water quality and erosion elements (Mannschatz et al., 2016). Therefore, the number of studies using SWAT has rapidly increased since 1998 on the global scale, and specially since 2009 in Southeast Asia countries, particularly around the Mekong basin (Fig. 15) (Tan et al., 2019).

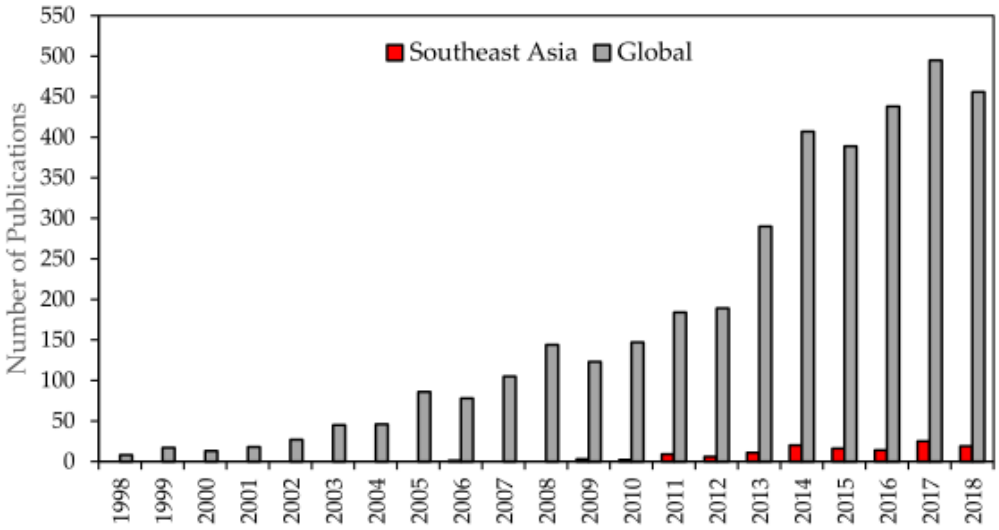

Figure 15: Number of SWAT publications on the global scale and in Southeast Asia. Source: Tan et al., 2019.

The watershed is divided into sub-basins based on the Digital Elevation Model (DEM), and the sub-basins into Hydrological Response Units (HRU) based on unique combinations of homogeneous soil, land use and slope. HRUs represent percentages of the sub-basin area but are not identified spatially within the sub-basins. Subdividing the watershed into sub-basins allows the model to reflect the differences in hydrology according to diverse land uses and soils properties (Neitsch et al., 2011). SWAT is a complex model that consists in several modules linked together by the hydrological cycle. Modules are built on the basis of equations representing the physical reality applicable to different time scales (annual, daily, and sub-daily). In the present study, SWAT operates on a daily time step.

2.2.3.1 Hydrology module

The hydrological cycle in SWAT can be separated into two major phases. The land phase (HRU) controls the loading of water, sediment, nutrients and pesticides to the main channel per sub-basin, and the water or routing phase that controls the amount of water, sediment, nutrients and

pesticides loading through the stream network. The runoff is simulated for each HRU and then summed together to get the total runoff from the sub-basin. The output of one sub-basin is the input of the following sub-basin. These two phases are detailed in the SWAT document (Neitsch et al., 2011). Different compartments of the hydrological cycle of the SWAT model are presented in (Fig. 16).

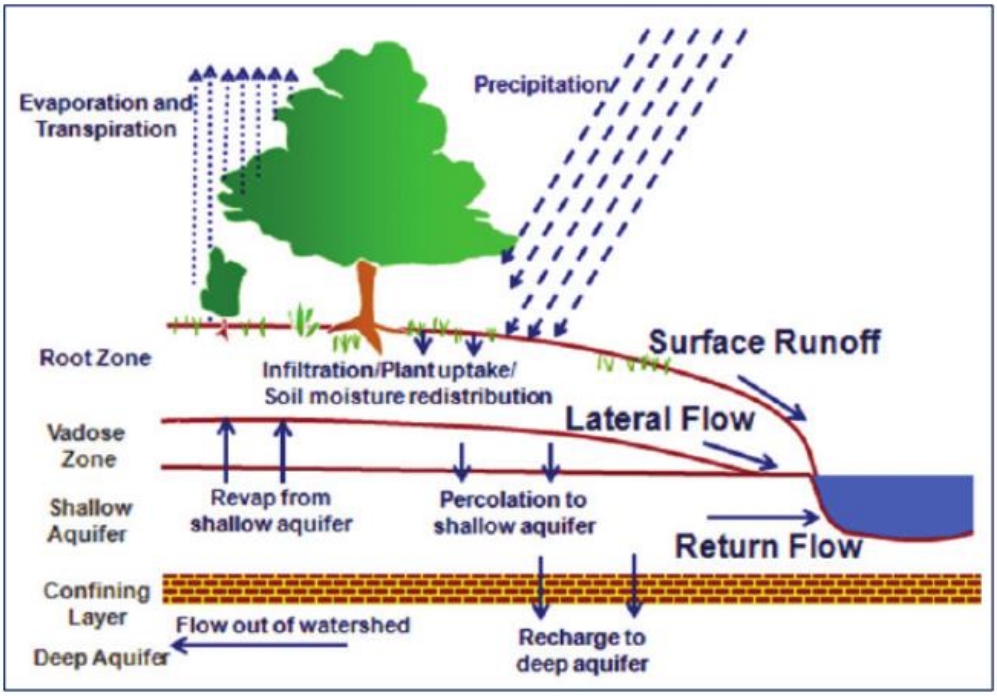

Figure 16: Schematic representation of the hydrologic cycle in SWAT model. Source: Neitsch et al., 2011.

A. *Land phase (HRU)*

For each HRU, SWAT returns a simulated hydrological response based on the following land water balance equation:

$$SW_t = SW_0 + \sum_{i=1}^{t} (R_{day} - Q_{surf} - E_A - W_{seep} - Q_{gw}) \quad (2.1)$$

where SW_t is the final soil water content (mm H2O), SW_0 is the initial soil water content (mm H2O), t is the time (days), R_{day} is the amount of precipitation on day i (mm H2O), Q_{surf} is the amount of surface water flow on day i (mm H2O), E_A is the amount of evaporation on day i (mm H2O), w_{seep} is the amount of percolation and bypass flow exiting the soil profile bottom on day i (mm H2O), Q_{gw} is the amount of return flow on day i (mm H2O).

This equation represents the initial stock of water and integrates the incoming and outgoing water flows. A fraction of the water integrating an HRU at a time t, is directly in contact with the soil. Therefore other processes will be modeled, such as infiltration in the soil, redistribution in the soil, surface runoff, lateral flow, contribution to the water table. The quantity of water intercepted per day by the canopy is a function of the size of the canopy also called Leaf Area Index (LAI):

$$can_{day} = can_{mx} \times \frac{LAI_{day}}{LAI_{mx}} \quad (2.2)$$

where can_{day} is the maximum amount of water that can be stored in the canopy on the day (mm H20), can_{mx} is the maximum amount of water that can be stored when the canopy is most developed (LAI_{day}=LAI_{mx}), and LAI_{day} is the maximum leaf area index for the plant.

The SWAT model uses an estimate of potential evapotranspiration (PET) to determine actual evapotranspiration (AET). PET is calculated based on the Penman-Monteith method (Monteith, 1965) which depends on input meteorological variables: air temperature, solar radiation, wind speed, and air relative humidity. Two other methods to calculate PET, the Priestley-Taylor method and the Hargreaves method, are included in the model (Neitsch et al., 2011) but where not used in this PhD thesis. PET is the maximum potential evapotranspiration in a given system, but it is the value of the AET that will determine the actual amount of water evaporated. This AET depends in part on the water stock available to meet the PET. First, water will be intercepted by the canopy and then soil water from different horizons will be mobilized for evapotranspiration by plants and sublimated/evaporated from the soil. The amount of water evaporated from the soil depends on the maximum sublimation/evaporation potential of the soil, which depends on the soil biomass and residues.

The determination of the amount of water runoff and infiltration from precipitation can be estimated in SWAT from the runoff coefficient method, SCS curve number (USDA-SCS, 1972). The SCS curve number equation is:

$$Q_{surf} = \frac{R_{day} - 0.2.S}{R_{day} - 0.8.S} \quad (2.3)$$

where Q_{surf} is the accumulated runoff or rainfall excess (mm), R_{day} is the rainfall depth for the day

(mm), and S is the retention parameter (mm).

SCS defines three antecedent moisture conditions CN: (i) CN_1 in dry condition at wilting point, (ii) CN_2 in average humidity condition, and (iii) CN_3 under wet conditions (field capacity). The CN varies in time according to the water content of the soil and in space depending on the soil type, land cover and topography. Details of SCS equations can be found in (Neitsch et al., 2011).

Finally, the amount of water infiltrating the soil is calculated by the difference between the total precipitation reaching the ground and the amount of water runoff.

The volume of water infiltrated into the soil will feed the lateral flow or percolate to the shallow or deep aquifers. The lateral flow is a result of the saturated zone of the soil and can be significant in certain impermeable environments with high hydraulic conductivity. The lateral flow is simulated in SWAT using the kinematic storage model developed by Sloan et al. (1983). This model is based on water volume and slopes. More details on the operation of this module can be found in Sloan and Moore (1984) and in Neitsch et al. (2011).

The difference between the infiltrated volume and the lateral flow indicates the volume infiltrating into aquifers. The volume of groundwater recharge is estimated by the model of Venetis (1969) and Sangrey et al (1984) as follows:

$$Q_{gw,i} = w_{rchrg,sh} \times \left(1 - \exp\left[-\partial_g \times \Delta t\right]\right) + Q_{gw,i-1} \times \left(1 - \exp\left[-\partial_g \times \Delta t\right]\right), \quad if\ aq_{sh} > aq_{shtr,q} \tag{2.4}$$

$$Q_{gw,i} = 0\ if\ aq_{sh} < aq_{shtr,q} \tag{2.5}$$

where $Q_{gw,i}$ is the groundwater flow into the main channel on day i (mm H2O), $Q_{gw,i-1}$ is the groundwater flow into the main channel on day i-1 (mm H2O), ∂gw is the base flow recession constant, Δt is the time step (1 day), $w_{rchrg,sh}$ is the amount of recharge entering the shallow aquifer on day i (mm H2O), a_{qsh} is the amount of water stored in the shallow aquifer at the beginning of day i (mm H2O), and $a_{qshthr,q}$ is the threshold water level in the shallow aquifer for groundwater contribution to the main channel to occur (mm H2O).

B. Routing phase (river)

The water depth in the channel is calculated as follows:

$$ch_{dep} = \sqrt{\frac{A_{ch}}{z_{ch}} + (\frac{W_{btm}}{2 \times z_{ch}})^2} - \frac{W_{btm}}{2 \times z_{ch}} \quad (2.6)$$

where ch_{dep} is the depth of water in the channel (m), A_{ch} is the cross sectional area of flow in the channel (m^2), W_{btm} is the bottom width of the channel (m), z_{ch} is the inverse of the channel side slope.

The water balance in the channel is as follows:

$$V_{stored,2} = V_{stored,1} + V_{in} - V_{out} - \text{tloss} - E_{ch} + \text{div} + V_{bnk} \quad (2.7)$$

where $V_{stored,2}$ is the volume of water in the reach at the end of the day (m^3 H2O), $V_{stored,1}$ is the volume of water in the reach at the beginning of the day (m^3 H2O), V_{in} is the volume of water flowing into the channel during the day (m^3 H2O), V_{out} is the volume of water flowing out of the channel during the day (m^3 H2O), $tloss$ is the volume of water lost from the reach via transmission through the bed (m^3 H2O), E_{ch} is the evaporation form the reach for the day (m^3 H2O), div is the volume of water added or removed from the reach for the day through diversion (m^3 H2O), and V_{bnk} is the volume of water added to the reach via return flow from bank storage (m^3 H2O).

Manning's equation was used to define the rate and velocity of flow. Two methods are incorporated in the SWAT model to calculate the water flow process in the channel, in this thesis we used the variable storage routing method. The detailed description of the two methods can be found in Neitsch et al. (2009). Flood is also simulated in SWAT model, when the volume of water in the channel exceeds the maximum amount that can be held by the channel. During flooding, the bottom width of the floodplain is considered to be five times of the channel bank full width.

2.2.3.2 Sediment module

A. Land phase (HRU)

SWAT uses the Modified Universal Soil Losses Equation (MUSLE) to calculate the daily sediment yield (Williams 1975), as follows:

$$\text{Sed} = 11.8 \times \left(Q_{surf} \cdot q_{peak} \cdot area_{HRU}\right)^{0.56} \times USLE.K \times USLE.C \times USLE.P \times LS_{USLE} \times CFRG \quad (2.8)$$

where Sed is the sediment yield on a given day (tons), Q_{surf} is the surface runoff volume (mm ha^{-1}), q_{peak} is the peak runoff rate ($m^3\ s^{-1}$), $area_{hru}$ is the HRU area (ha); USLE_K is the USLE soil erodibility factor, USLE_C is the USLE cover and management factor, USLE_P is the USLE support practice factor, LS_{USLE} is the USLE topographic factor, and CFRG is the coarse fragment factor. More details of the processes are described in SWAT theoretical documentation (Neitsch et al. 2009).

B. Routing phase (river)

In the main channel, erosion occurs when (i) the stream power (transport capacity) of the water is high and the sediment load from the upstream regions is lower than this capacity and (ii) when the shear stress exerted by the water on the bed and bank is higher than the critical shear stress to dislodge the sediment particle. The daily potential bank and bed erosion (in tons) are calculated as a function of the daily potential bank and bed erosion rates predicted with the excess shear stress equation (Hanson and Simon 2001):

$$\xi = K_d \,.\, (\tau_e - \tau_c) \times 10^{-6} \tag{2.9}$$

where ξ is the erosion rates of the bank and bed ($m\ s^{-1}$), K_d is te erodibility coefficient of bank and bed ($cm^3/(N^{-s})$), and τ_e and τ_c respectively are the effective and the critical shear stresses acting on the bank and bed ($N\ m^{-2}$). The effective shear stress τ_e acting on the bank and bed is calculated based on the dimensions and the configuration of the channel using the equation of Eaton and Millar (2004).

The simplified version of Bagnold (1977) stream power equation (CH_EQN=0) was used to calculate the maximum sediment transport capacity of the channel, which depends on the peak channel velocity $v_{ch,pk}$ ($m\ s^{-1}$):

$$v_{ch,pk} = \frac{q_{ch,pk}}{A_{ch}} \tag{2.10}$$

where $q_{ch,pk}$ is the peak flow rate ($m^3\ s^{-1}$) and Ach is the cross-sectional area of flow in the channel (m^2). The peak flow rate is defined as:

$$q_{ch,pk} = PRF_{BSN} . q_{ch} \tag{2.11}$$

where PRF_{BSN} is the peak rate adjustment factor and q_{ch} is the average rate of flow ($m_3\ s^{-1}$). The maximum amount of sediment that can be transported from a reach segment is calculated as:

$$conc_{sed,ch,mx} = SPCON.v_{ch,pk}{}^{SPEX} \quad (2.12)$$

where $conc_{sed,ch,mx}$ is the maximum concentration of sediment that can be transported by the water (tons m^{-3}), SPCON is a coefficient defined by the user, $v_{ch,pk}$ the peak channel velocity ($m\ s^{-1}$) and SPEX is an exponent defined by the user.

If the peak channel velocity is bigger than the concentration of sediment in the reach at the beginning of the time step, the dominant process in the reach segment will be deposition. Detailed description of all the equations can be found in (Neitsch 2011).
Finally, the mass balance equation for sediment routing is

$$sed_{ch} = sed_{ch,i} - sed_{dep} + sed_{res} \quad (2.13)$$

where sed_{ch} is the amount of suspended sediment in the reach (tons), $sed_{ch,i}$ is the amount of suspended sediment entering the reach at the beginning of the time-step (tons), sed_{dep} is the amount of sediment deposited in the reach segment (tons), and sed_{res} is the amount of sediment resuspended from bank and bed in the reach segment (tons).

2.2.3.3 Bacteria module

In the current version of the SWAT model, bacteria fate processes are described for both the land and the routing phase. Bacteria is introduced into the environment through manure application, where they can be applied on soil surface or intercepted by foliage. SWAT model partitions bacteria on the soil surface into free-living bacteria in soil solution and particle-attached bacteria. Depending on the hydrology, and on the free-living/particle-attached bacteria partition, bacteria can be transferred to the river network with surface runoff during rain events:

$$bact_{surf} = \frac{bact_{sol} \times Q_{surf}}{\rho_b \times depth_{surf} \times k_{bact,surf}} \quad (2.14)$$

where $bact_{surf}$ is the bacteria number transported in surface runoff (MPN m^{-2}), $k_{bact,surf}$ is the parameter of bacteria soil partitioning ($m^3\ Mg^{-1}$), and Q_{surf} is the amount of surface runoff (mm).

$$bact_{sed} = 0.0001 \times conc_{sedbact} \times \left(\frac{sed}{area_{hru}}\right) \times \varepsilon_{bact,sed} \quad (2.15)$$

where $bact_{sed}$ is the bacteria number transported with suspended sediments in surface runoff (MPN

m^{-2}), $conc_{sed,bact}$ is the amount of bacteria attached to soil particles in the top soil (MPN ton^{-1}), sed is the yield of suspended solids (ton), $area_{hru}$ is the HRU area (ha), and $\varepsilon_{bact,sed}$ is the ratio of bacteria enrichment.

Bacteria can be leached along the soil profile and assumed to die in deeper soil layers. The decay/regrowth of both free-living and particle-attached bacteria is modeled on foliage, and on surface soil. Chick's Law first order equation determines the quantity of removed bacteria by decay or the quantity of added bacteria by regrowth:

$$N = N_0 \exp(-\mu t) \tag{2.16}$$

where N is the number of bacteria in a given time t (CFU 100 mL^{-1}), N_0 is the original number of bacteria indicator (CFU), μ is the bacterial decay rate constant (h^{-1}), and t represents time (h). In SWAT model, temperature is one of the variables that determines the decay rate which can be obtained as:

$$\mu = \mu_{20^{\theta T-20}} \tag{2.17}$$

where μ_{20} refers to the decay rate at 20°(h^{-1}), θ is the temperature correction parameter for the first-order decay, and T shows the temperature in °C..

In addition to the simulation using the original bacteria module of SWAT, we have tested the modified version of SWAT bacteria module developed by Kim et al., (2017), which takes into account additional bacteria in-stream processes (Fig. 17). In order to simulate low concentrations of bacteria during the dry season with associated base flow, the hyporheic exchange process was implemented in the model. The amount of the bacteria released through the sediment pore fluid by hyporheic exchange into the stream was estimated by Grant et al., (2011). Once in the river, bacteria can either die off or regrow. Moreover, depending on the hydrological conditions of the reach, bacteria can settle with sediments or be released during sediment resuspension events.

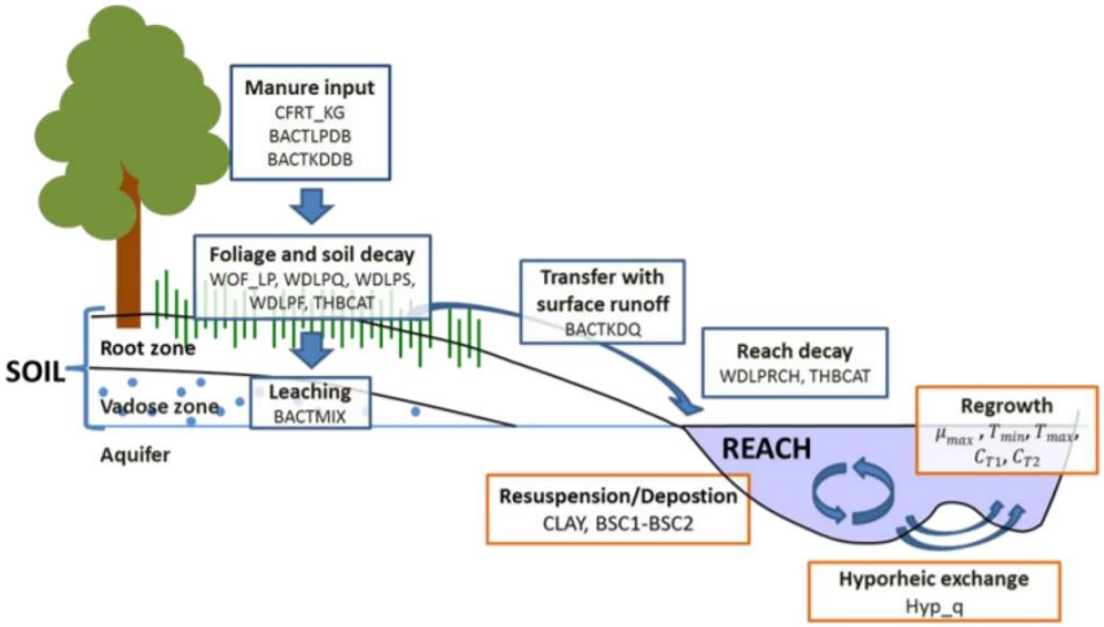

Figure 17: Main processes affecting the fate of fecal bacteria in the environment included in the current SWAT model (Blue boxes) and model improvements described in (Kim et al., 2017) (Orange boxes). Source: Kim et al., 2017.

A. Resuspension

The resuspension and deposition processes were tested in SWAT by Kim et al., (2010) to improve the module. The bacteria concentration in the streambed $conc_{bact,sed}$ (MPN per ton sediment) is calculated based on the empirical regression equation with new defined parameters, as follows:

$$\log(conc_{bact,sed}) = BSC_1 \times \sin\left(BSC_2 \times \frac{day - BSC_3}{366} \times \pi\right) + BSC_4 \quad (2.18)$$

where day is the day of year, and BSC_1, BSC_2, BSC_3 and BSC_4 are the regression coefficients in streambed bacteria concentration equation (Kim et al., 2010).

The amount of bacteria released from streambed with the sediment resuspension ($bact_{res}$, MPN), and bacteria settled from water with sediment deposition ($bact_{dep}$, MPN) is determined as follows:

$$bact_{res} = sed_{res} \times conc_{bact,sed} \quad (2.19)$$

$$bact_{dep} = bact_{ch} \times \frac{K_p \times sed_{dep}}{V_{ch} + conc_{sed,ch} \times V_{ch}} \quad (2.20)$$

where sed_{res} is the amount of resuspended sediment (ton sediment), sed_{dep} is the amount of

deposited sediment (ton sediment), $conc_{bact,sed}$ is the concentration of bacteria in the streambed (MPN per ton sediment), $bact_{ch}$ is the total amount of bacteria in water (MPN), K_p is the linear partitioning coefficient of bacteria between sediment and water (m^3 water per ton sediment) calculated as a function of the percentage of clay (CLAY) in suspended sediment, $conc_{sed,ch}$ is the sum of the concentration of suspended and deposited sediment (ton sediment m^{-3}), and V_{ch} is the volume of water in the reach segment (m^3 water). Detailed description of the equations can be found in (Kim et al., 2010).

B. Bacterial regrowth

Bacterial in-stream regrowth processes was implemented in this modified bacteria module by Kim 2017, based on a temperature dependent bacterial regrowth rate which varies between the minimum and maximum growth temperatures (Hipsey et al., 2008; Pandey et al., 2016) . The bacterial regrowth model is expressed as follows:

$$g = \mu_{max}[C_{T1}(T - T_{min}) \times (1 - exp(C_{T2}(T - T_{max})))]^2 \quad (2.21)$$

where g is the regrowth rate (day^{-1}), μ_{max} is the maximum growth rate (day^{-1}), C_{T1} and C_{T2} are coefficients that determine the shape of the regrowth trend, T_{min} and T_{max} are the minimum and maximum growth temperatures (°C), respectively, and T is the air temperature (°C). More details can be found in (Hipsey et al., 2008).

C. Hyporheic exchange

Hyporheic exchange processes were implemented in this modified module in order to study the importance of the streambed bacteria release and deposition in simulating bacteria flux from sediment to water column at low flow. Before partitioning the bacteria attached to the deposited sediment in (Eq. 2.20), the amount of the bacteria released by hyporheic exchange into the stream ($bact_{hyp}$) was added (Grant et al., 2011). The amount of bacteria $bact_{hyp}$ released through the sediment pore fluid is calculated as follows:

$$conc_{pore} = conc_{bact,sed} \times \frac{\rho_b}{\emptyset} \quad (2.22)$$

$$bact_{hyp} = conc_{pore} \times Q_h \quad (2.23)$$

where $conc_{pore}$ is the concentration of bacteria in the pore fluid (MPN m^{-3}), $conc_{bact,sed}$ is the

concentration of bacteria in the streambed (MPN per ton sediment), ρb is the bulk density of channel bed sediment (g cm^{-3}), Ø is the porosity, and Qh is the amount of water moving through the pore to the stream by hyporheic exchange. Hyporheic exchange was assumed to take place only on the sediment bed and not on the sediment bank, and the flow is constant over the years.

Chapter 3. Effects of hydrological regime and land use on in-stream *Escherichia coli* concentration in the Mekong basin, Lao PDR

Introduction to chapter 3

This chapter provides an overview of the spatio-temporal dynamics of *E. coli* in major Mekong tributaries of Lao PDR located between 15°N and 20°N. The sampling was designed to encompass a broad range of catchment sizes (239 km^2 to 25,946 km^2), as well as a large range of geographical, topographical, and land use features. This dataset was coupled with a two years monitoring at 10-day interval of water quality in the Mekong river and two of its major tributaries in northern Lao PDR. The main findings in this study point out the seasonal variability of *E. coli* and its strong correlation to TSS, and to areas prone to higher TSS export via soil erosions during tropical rainfall events. Moreover, this study brings new evidence on the continuous in-stream presence of *E. coli* in all of the three regularly monitored sites and in the majority of sampled tributaries across Lao PDR during rainy season. Given the low access to improved water resources, these results suggest a high risk on population relying directly on these water resources for their domestic needs. This work was published in Scientific Reports:

Nakhle, P., Ribolzi, O., Boithias, L., Rattanavong, S., Auda, Y., Sayavong, S., Zimmermann, R., Soulileuth, B., Pando, A., Thammahacksa, C., Rochelle-Newall, E.J., Santini, W., Martinez, J.M., Gratiot, N., Pierret, A., 2021c. Effects of hydrological regime and land use on in-stream Escherichia coli concentration in the Mekong basin, Lao PDR. Sci. Rep. 11, 3460. https://doi.org/10.1038/s41598-021-82891-0

Abstract

In the basin of Mekong, over 70 million people rely on unimproved surface water for their domestic requirements. Surface water is often contaminated with fecal matter and yet little information exists on the underlying mechanisms of fecal contamination in tropical conditions at large watershed scales. Our objectives were to (1) investigate the seasonality of fecal contamination using *Escherichia coli* as fecal indicator bacteria (FIB), and (2) establish links between the fecal contamination in stream water and its controlling factors (hydrology and land use). We present the results of (1) a sampling campaign at the outlet of 19 catchments across Lao PDR, in both the dry and the rainy seasons of 2016, and (2) a 10-day interval monitoring conducted in 2017 and 2018 at three point locations of three rivers (Nam Ou, Nam Suang, and Mekong) in northern Lao PDR. Our results show the presence of fecal contamination at most of the sampled sites, with a seasonality characterized by higher and extreme *E. coli* concentrations occurring during the rainy season. The highest *E. coli* concentrations, strongly correlated with total suspended sediment concentrations, were measured in catchments dominated by unstocked forest areas, especially in mountainous northern Lao PDR and in Vientiane province.

3.1 Introduction

Emerging water quality issues resulting from various anthropogenic pressures and rapid global change are a topic of worldwide concern (Schwarzenbach et al., 2010; Vörösmarty et al., 2010). While the goal of improving surface water quality is being achieved in developed countries, an opposite trend towards increased organic and biological water pollution is observed in developing countries (UNEP, 2016). Fecal pollution of water resources is one of the major health issues in low-income tropical countries in Africa and Asia (UNEP, 2016), due to inadequate sanitation facilities, low access to safe water resources, and poor medical care. In 2015, diarrheal diseases caused more than 1.3 million deaths globally (GBD LRI Collaborators, 2017). The World Health Organization recommends measuring fecal indicator bacteria (FIB), such as *Escherichia coli* (*E. coli*), as a low-cost proxy for the presence of fecal pathogens in water bodies (WHO, 2011b). According to the 2016 UNEP report, about a third to one half of Asian rivers are estimated to be severely polluted, with monthly in-stream concentrations of fecal coliform bacteria, like *E. coli*, higher than 1,000 cfu 100 mL^{-1}. These large ranges of estimations reflect the uncertainties

(UNEP, 2016) and stress the need to better assess at various space and time scales, the actual risks for public health in tropical areas associated with such pollutants.

During the last three decades, Southeast Asia has experienced rapid economic development and population growth, strongly impacting water quality in many parts of the Mekong basin (Chea et al., 2016). Commonly identified water quality issues in Mekong basin include microbiological pollution from human and animal waste, as well as chemical pollution from intensive agricultural activities leading to salinity and eutrophication increase (Chea et al., 2016). In addition, the rapid hydropower development impacts the hydrological regime, sediment fluxes, and ecosystem services (Arias et al., 2014a; Pokhrel et al., 2018). The Mekong is the third largest river in terms of water discharge in Southeast Asia (Thi Ha et al., 2018) and one of the most diverse aquatic ecosystems, making it the source of one of the largest inland fishery and aquaculture production system in the world (Food and Agricutlure Organization of the United Nations, 2011). In the lower Mekong basin stretching from southern Chinese border to the delta in southern Vietnam, over 70 million people depend on valuable ecosystem services provided by the transboundary Mekong river and its tributaries (Food and Agricutlure Organization of the United Nations, 2011). The livelihood and food security of rural populations are, as a consequence, highly vulnerable to changes in water quality.

Watersheds in Lao PDR contribute to approximately 35% of the overall Mekong river flow (Food and Agricutlure Organization of the United Nations, 2011). Like many developing countries, the population in Lao PDR is mostly rural (Lao Statistics Bureau Ministry of Planning and Investment, 2015), and relies directly on untreated water via natural canal systems and small tributaries for domestic water use (Olivier Ribolzi et al., 2011). Diarrheal diseases are a leading cause of death nationwide, especially among children under age five (GBD LRI Collaborators, 2017; WHO, 2015). However, no comprehensive survey of the fecal contamination of the Mekong, including main stream as well as tributaries and spanning successive seasons, has yet been published. Similarly, the underlying mechanisms of water fecal contamination has not been yet documented, although their understanding is needed to achieve an improved integrated management of water resources and to reduce associated diseases.

FIB dynamics in tropical waterbodies are subject to various interactive factors controlling

their fate in the environment (Rochelle-Newall et al., 2015, 2016). When FIB are released from hosts into secondary habitats (aquatic system and sediment), their persistence is function of abiotic factors including temperature, solar radiation, pH, salinity, nutrients, and suspended particles, and biotic factors like the presence of other microorganisms, biofilms and predators (Byappanahalli et al., 2012a; Korajkic et al., 2013; Rochelle-Newall et al., 2015). These factors can be strong drivers of microbial activity and stability in tropical context, potentially favorable for slower bacterial decay rates (Nguyen et al., 2016). It has been shown that FIB tend to be associated with particles in soils and water columns (Byamukama et al., 2005; Oliver et al., 2007), which can provide benefits to microorganisms like access to nutrients, as well as protection from various stressors such as predation and sunlight (Farrell et al., 2018; Walters et al., 2014). In tropical regions, FIB is likely to be found correlated to total suspended sediment concentrations in rivers with high particle loads due to erosive tropical rainfall (Byamukama et al., 2005).

Furthermore, several studies have documented FIB transport in the environment and shed light on the complex linkages between hydrometeorology and fecal contamination dynamics, both in urban and rural areas. During the rainy season, strong and frequent tropical rainfall and overland flow can induce declining surface water quality (Boithias et al., 2016), increased water turbidity, total suspended sediment and contaminant concentrations (Causse et al., 2015; Ekklesia et al., 2015b; Olivier Ribolzi et al., 2011; Olivier; Ribolzi et al., 2011). Deterioration of surface water microbial quality was highlighted by a study carried out in three tropical rural catchments in Lao PDR, Thailand and Vietnam, where the highest concentrations of *E. coli* in streams were found to occur during the rainy season (Rochelle-Newall et al., 2016). Responses to tropical erosive rainfall are influenced by watershed topography and soil hydrodynamic properties (e.g., drainage area, slope gradient, and infiltration rate), which are in turn strongly modulated by land use (Lacombe et al., 2018; Olivier; Ribolzi et al., 2011; Valentin et al., 2008a). The scientific community has shown a growing interest in evaluating the impacts of the rapid land use change, including dam construction, that are affecting many parts of Southeastern Asia, with particular focus on the hydrological and sedimentary responses, at plot and hillslope scales (Ding et al., 2016; Huon et al., 2013; Ntajal et al., 2020; Valentin et al., 2008a). Land use is considered to be one of the key factors controlling soil erosion (Janeau et al., 2014; Valentin et al., 2008a) over gentle to moderate terrain slope, and microbial community export, including *E. coli*, from the soil surface into the hydrographic networks in tropical environments (Causse et al., 2015; Huong et al., 2018; Lacombe

et al., 2018; Ribolzi et al., 2017).

Although the main factors controlling the dynamics of *E. coli* are well evaluated in temperate and subtropical aquatic ecosystems (Ferguson and Signoretto, 2011; Ishii and Sadowsky, 2008; Liang et al., 2013; Pachepsky et al., 2011), only few studies have investigated the fate and transport of *E. coli* in tropical ecosystems. Key processes as well as environmental and anthropogenic drivers of *E. coli* dynamics were identified in small watersheds in tropical montane environments of Lao PDR (Boithias et al., 2016; Kim et al., 2018, 2017; Olivier Ribolzi et al., 2011; Olivier; Ribolzi et al., 2011; Ribolzi et al., 2016; Rochelle-Newall et al., 2016), of Singapore (Ekklesia et al., 2015b), as well as in larger catchments, in northern Lao PDR (Boithias et al., 2016; Ekklesia et al., 2015b) and in the Mekong delta in Vietnam (Isobe et al., 2004; Nguyen et al., 2016).

While these studies have significantly improved our understanding on the behavior of FIB in tropical ecosystems on relatively local scales, the relevance of these findings on a regional-scale remains uncertain. Moreover, due to limited data in tropical developing countries, little information exists on long-term seasonal variations of FIB in large-scale watersheds, and none exists on the spatial distribution of FIB at the country scale in Lao PDR**.**

Our study is based on two sets of physico-chemical, microbiological, and environmental data. The first dataset was collected in 2016 during both the rainy and the dry seasons, in the Mekong river and 19 tributaries, in order to capture the spatial heterogeneity in terms of *E. coli* concentrations in the hydrographic network across Lao PDR. This approach was completed by a second dataset, a close-up investigation at 10-day interval between July 2017 and December 2018, of water quality in three watersheds at three point locations of three rivers (Nam Ou, Nam Suang, and Mekong) in northern Lao PDR, to provide better understanding of the FIB seasonal variations. The main objectives of this work were to (i) examine the seasonality of FIB (*E. coli*) concentrations and its response to contrasted hydrological events and (ii) identify the relative importance of several parameters such as total suspended sediment concentrations, land use, rainfall event characteristics, human and livestock population density, as controlling factors of *E. coli* in-stream concentration at large-catchment scale, during both the dry and the rainy seasons.

3.2 Material and methods

3.2.1 Study site

Sampling sites were located in Lao PDR, a landlocked country in Southeast Asia, sharing borders with Myanmar, Cambodia, China, Thailand, and Vietnam. Lao PDR is mainly covered with mountains and forested hills, plateaus and plains along the Mekong river, where approximately 6.5 million people live on a 236,800 square kilometers land (Lao Statistics Bureau Ministry of Planning and Investment, 2015). About 70% of its population lives in rural areas and have a resource-based economy, relying mainly on agriculture and forestry for their livelihood. The tropical wet and dry climate (Aw climate) is under the influence of monsoon regime, dividing the year into 2 seasons: a dry season from October to April, and a rainy season from May to October. The average annual rainfall in Lao PDR varies from 1,300 mm to 2,500 mm and exceeds 3,500 mm in central and Southwestern Lao PDR (Fig. S1). The air temperature ranges from a minimum 15 °C in December-January to a maximum temperatures of 25 ± 30 °C from May to September (Boithias et al., 2016). The Mekong river runs about 4,350 km through China, Lao PDR, Myanmar, Thailand, Cambodia and Vietnam, draining a 795,000 km^2 surface area (MRC, 2005). The river flows from North to South of Lao PDR, forming a natural border with Thailand over 800 km.

3.2.2 Sampling design and watersheds characteristics

Our study investigates seasonal dynamics of fecal contamination, based on field monitoring at multiple space and time scales. We used two different datasets (Fig. 18; Table 6):

i. A field campaign conducted in 2016 that sampled the Mekong river at 6 sampling sites, and 19 Mekong tributaries at 22 sampling sites including 4 sites along the Nam Ngum river (Fig. 18) located on mountains, hills and plains (Fig. 19a). The sampling was conducted once in March 2016 (dry season) and once in July 2016 (rainy season). The choice of sampling sites was based on a broad geographical coverage of Lao PDR between 15°N and 20°N, and to encompass a broad range of catchment sizes (239 km^2 to 25,946 km^2), and a large range of geographical, topographical, and land use features. The sampling sites were also chosen to allow a large spatial sampling, covering the majority of the Mekong tributaries, in a relatively short time and logistically accessible from the road (Table 6, Appendix I: Table 14).

ii. Regular water quality monitoring of three rivers in northern Lao PDR, conducted at 10-day intervals from July 2017 to December 2018, including two rainy seasons from April to October 2017 and 2018: two sampling points on the Nam Ou (Nou) and Nam Suang (Nsu), both located on the left bank of the Mekong river, and one sampling point in the Mekong river in Luang Prabang (MK_17).

*Table 6: Description of sampling sites in Lao PDR: names of river, geographical coordinates of sampling sites (i.e., latitude and longitude in degrees, WGS 1984), sampling dates during field surveys in March and July 2016, and regular monitoring from July 2017 to December 2018, and catchment drainage area in km^2. * sampling frequency of 10-days interval.[1] Geographical coordinates in degrees (WGS 1984).*

Sampling sites	River	Geographical coordinates[1]		Sampling dates	Catchment area (km^2)
		Latitude (°)	Longitude (°)		
Nou	Nam Ou	20.08642	102.26406	2016 2017-2018*	25,946
Nsu	Nam Suang	19.97931	102.24728	2016 2017-2018*	6,577
Npa	Nam Pa	19.96049	102.28289	2016	758
MK_17	Mekong	19.89224	102.13416	2016 2017-2018*	27,215
Nk20	Nam Khan	19.78601	102.18335	2016	7,236
A6	Houay Khan	19.76009	102.18112	2016	239
Nmi	Nam Mi	17.91917	101.68856	2016	1,021
Nsa	Nam Sang	18.22284	102.14222	2016	1,210
Ntho	Nam Thôn	18.09152	102.28159	2016	582
Nlik	Nam Lik	18.63280	102.28104	2016	3,022
Nng_3	Nam Ngum	18.52502	102.52631	2016	8,366
Nng_4	Nam Ngum	18.35581	102.57204	2016	14,318
Nng_2	Nam Ngum	18.20269	102.58588	2016	14,985
Nng_1	Nam Ngum	18.17879	103.05593	2016	16,841
Nma	Nam Mang	18.37017	103.19838	2016	1,793
Ngn	Nam Gniep	18.41756	103.60217	2016	4,564
Nxa	Nam Xan	18.39523	103.65408	2016	2,223
Nka	Nam Kadin	18.32517	103.99924	2016	14,820
Nhi	Nam Hin Boun	17.72699	104.56798	2016	2,152
Xbi	Xe Bang Fai	17.07782	104.98496	2016	9,433
Xbg	Xe Bang Hieng	16.09804	105.37625	2016	19,817

Xbn	Xe Bang Nouan	16.00290	105.47937	2016	1,351
SR	Nam Sedon	15.12390	105.80748	2016	7,225
MK_1	Mekong	19.95601	102.24113	2016	263,880
MK_7	Mekong	17.89870	101.62397	2016	295,246
MK_2	Mekong	17.97276	102.50410	2016	301,826
MK_3	Mekong	17.39714	104.79999	2016	373,368
MK_4	Mekong	16.00503	105.42449	2016	417,09,4
MK_5	Mekong	15.10721	105.79878	2016	549,055

The surface area of the catchments of the Mekong tributaries ranges from 239 km^2 (A6) to 25,946 km^2 (Nou) (Table 6). A range of eight different land use classes, grouped in eight main categories, is found across Lao PDR (Fig. 19b; Appendix I: Table 14). The highest percentage of unstocked forest areas and the lowest percentage of forest areas were found in catchments of northern Lao PDR (Nou, Nsu, Npa, Nk20 and A6), and Vientiane Province (Nmi, Nsa, Ntho), whereas forest areas dominated the catchments in southern Lao PDR (Nka, Nhi, Xbi, Xbg, Xbn, SR). The highest percentages of paddy rice and other agriculture areas were found in the southern catchment near Pakse (SR) followed by catchments in Vientiane Province (Nmi, Nsa, Ntho). The highest percentages of grassland and water areas were found in Vientiane Province (Nlik, Nng_3, Nng_4, Nng_2, and Nng_1). The livestock population is mostly present in catchments near Vientiane Capital followed by southern provinces of Savannakhet and Pakse (Fig. 19c; Appendix I: Table 14). Human population density is variable across Lao PDR. The densest catchments are mostly found in the southern province of Pakse, followed by Savannakhet and Vientiane Capital (Fig. 19d, Appendix I: Table 14). Catchments are also highly variable in terms of rainfall (Appendix I: Table 14). During March 2016 (dry season), the rainfall was low (Fig. 19e). During July 2016 (rainy season), the highest rainfall was recorded in catchments located on steep terrain (Nlik, Nng_3, Nng_4, Nng_2, and Nng_1) and plains (Nmi, Nsa, Ntho) of Vientiane Province (Fig. 19f; Appendix I: Table 14).

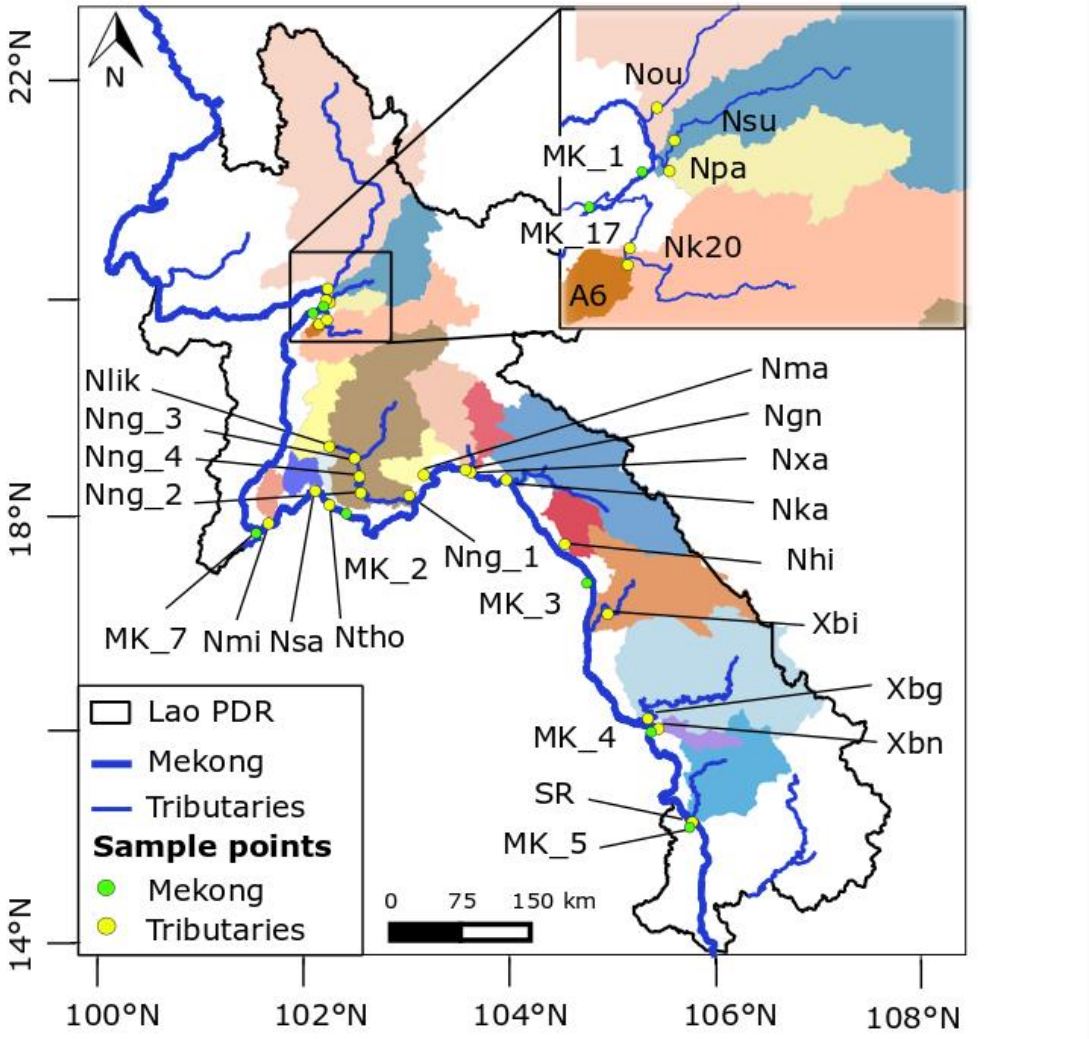

Figure 18: Mekong river and watersheds of Mekong tributaries (colored areas) sampled in March and July 2016 in Lao PDR. Geographic coordinate system: WGS 1984, latitude and longitude in degrees.

3.2.3 Geographical analyses

The SRTM 90-m resolution digital elevation model (DEM) was used to draw the elevation map in the QGIS 2.6.1 software (https://www.qgis.org/en/site/forusers/). Based on this DEM and the geographical location of the sampling points, the catchment areas were then determined using the QGIS 2.6.1 software. We also computed surface area, perimeter, median slope, and median elevation of each of the catchment areas upstream of the sampling points from the DEM (Fig. 19a).

3.2.4 Land use

We used information from the land use map provided by the Department of Agriculture Land Management (DALaM) of Lao PDR in 2013 (Fig. 19b). Technically, this land use map included land cover classes, namely: rock, water, grassland, and forest, as well as land use classes, namely: unstocked forest, paddy rice, other agriculture, and urban areas, making up a total of eight classes expressed in percentage of surface area. According to Lao Forestry Administration (Lestrelin et al., 2013) and the Food and Agriculture Organization of the United Nations (FAO) (Forestry Department Food and Agriculture Organization of the United Nations, 2010), forests refer to areas of more than 0.5 ha with a canopy cover of more than 10 % and trees higher than 5 meters. Unstocked forests are forests with a crown density lower than 20% resulting from exploitation for logging or shifting cultivation cycles. Unfertile or degraded areas covered by grass are attributed to grassland category. Other agriculture refers to agricultural lands used for non-crop purposes like livestock grazing. Water class includes rivers and water reservoirs exceeding 10 meters of width and 0.5 ha of surface area. Urban areas include permanent settlements like villages, towns, and roads having a width of more than 5 m. Data on regional dams in Lao PDR represent maximum reservoir area (ha) of dams located upstream of our sampling sites. These data were taken from the dataset on the dams of the greater Mekong by Mekong Region Futures Institute (WLE, 2020).

3.2.5 Data on livestock and local populations

We obtained data on local populations and livestock per district from the Lao PDR Population and Housing Census 2015 conducted by Lao PDR Statistics Bureau (Lao Statistics Bureau Ministry of Planning and Investment, 2015). Based on the percentage of area occupied by each district present in each catchment, we calculated the density of the human population and of livestock in each basin's catchment area (Fig. 19c,d). The data on livestock densities (cattle, buffaloes, pigs, goats, ducks, local and commercial chickens) were obtained from the Lao agricultural census 2010/11 (Department of Planning, Ministry of Agriculture and Forestry, 2012).

3.2.6 In-situ measurements and laboratory analyses

We measured a set of physico-chemical parameters *in situ*, at approximately 5 cm under water surface, including stream water temperature (T), pH, electrical conductivity normalized to 25 °C (EC), dissolved oxygen saturation (DO), using a Multi Probe System with a data logger (YSI 556 MPS). Concentrations of DO were transformed to oxygen saturations (%), using the Hua formula (Hua, 1990). We collected 500-mL water samples 10 cm beneath the water surface in sterile plastic containers, and conserved them at a low temperature in the dark until laboratory analysis. A subsample of the collected water was analyzed within 24 hours, for *E. coli* counts, using the standardized microplate method (ISO 9308-3). The latter consists of a 48-hour incubation at 44°C of each sample, at four dilution rates (1:2, 1:20, 1:200 and 1:2000), in a culture medium specific for *E. coli* on a 96-well microplate (MUG/EC, Biokar Diagnostics). By counting the number of positive wells for each microplate, and applying the Poisson distribution, the index of viable bacteria called most probable number (MPN) can be determined. The concentration of *E. coli* ([*E. coli*]) is expressed in MPN 100 mL^{-1} and used as an indicator of the fecal contamination (Lebaron et al., 2005). This method has already been used successfully in a tropical context (Causse et al., 2015; Rochelle-Newall et al., 2016). Another subsample was analyzed for total suspended sediment concentration ([TSS]): [TSS] was determined for each sample after filtration on 0.2 µm porosity cellulose acetate filters (Sartorius) and evaporation in an oven at 105°C for 48 h. The concentrations of total particulate carbon ([TPC]) and of total nitrogen ([TN]) in river water (mg L^{-1}), were determined by isotope ratio mass spectrometry coupled with elemental analyzer (Integra 2 Stable Isotope Analyser, Sercon).

3.2.7 Rainfall and water level

We used the Multi-Source Weighted-Ensemble Precipitation (MSWEP V2) 2016 rainfall data in order to have accurate, spatially distributed precipitation over the watersheds of interest. MSWEP is a global precipitation product merged from gauge, satellite, and reanalysis data (Beck et al., 2019). It has a high temporal (3-hourly) and spatial (0.1°) resolution, which was evaluated and assessed on a global scale (Beck et al., 2017) and in Eastern Asia (Xu et al., 2019)-(Wu et al., 2018). In our study, we used MSWEP cumulative rainfall data over a one-week period (corresponding to the sampling campaign duration) before the sampling during the 2016 campaign,

averaged per sampled watershed area.

The daily rainfall measurements for 2017 and 2018 associated with the Mekong, Nam Ou, and Nam Suang sampling sites, were taken from three stations of the Lao PDR Government (Department of Natural Resources and Environment of Luang Prabang). The rainfall station in Nam Ou (20.081972, 102.264139) is located at the outlet of the catchment, at a 530 m distance from the stream sampling point, in Nam Suang (19.967111, 102.272444) at 3 km upstream to the sampling point, and in Mekong (19.898472, 102.16525) at 3 km distance from MK_17 sampling point. Water level data were measured at three gauging stations situated in Nam Ou (20.245556, 102.348806) at 21 km upstream the outlet, in Nam Suang (19.967111, 102.272444) at 3 km upstream the sampling point, and in Mekong (19.892361, 102.134167) near MK_17.

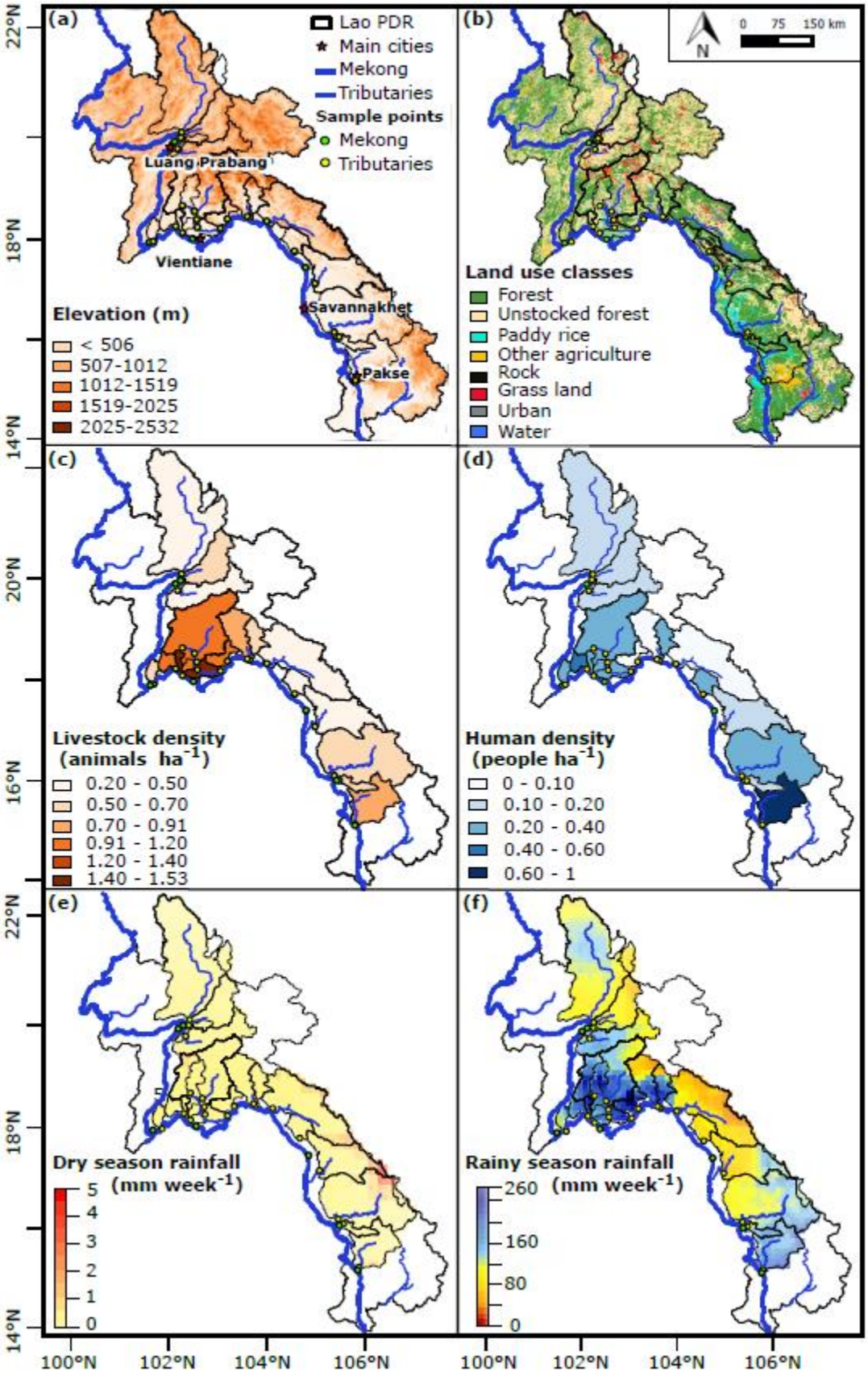
(a)
Lao PDR
Main cities
Mekong
Tributaries
Sample points
Mekong
Tributaries
Luang Prabang
Vientiane
Savannakhet
Pakse
Elevation (m)
< 506
507-1012
1012-1519
1519-2025
2025-2532
(b)
N
0 75 150 km
Land use classes
Forest
Unstocked forest
Paddy rice
Other agriculture
Rock
Grass land
Urban
Water
(c)
Livestock density
(animals ha-1)
0.20 - 0.50
0.50 - 0.70
0.70 - 0.91
0.91 - 1.20
1.20 - 1.40
1.40 - 1.53
(d)
Human density
(people ha-1)
0 - 0.10
0.10 - 0.20
0.20 - 0.40
0.40 - 0.60
0.60 - 1
(e)
Dry season rainfall
(mm week-1)
5
4
3
2
1
0
(f)
Rainy season rainfall
(mm week-1)
260
160
80
0
22°N
18°N
14°N
20°N
16°N
100°N
102°N
104°N
106°N

Figure 19: Geographical and meteorological characteristics of the sampled watersheds in Lao PDR: (a) geomorphological features (Digital Elevation Model); (b) land use classes; (c) livestock density; (d) human density; (e) total rainfall recorded one week pre-sampling in March 2016 (mm week^{-1}); (f) total rainfall recorded one week pre-sampling in July 2016 (mm week^{-1}). Geographic coordinated system: WGS 1984, latitude and longitude in degrees. Altitudes of highest and lowest points in meters above mean sea level, from SRTM 90 m. Local populations and livestock per district were taken from the Lao PDR Population and Housing Census 2015. Rainfall data were obtained from the Multi-Source Weighted-Ensemble Precipitation (MSWEP V2); spatially distributed rainfall data was averaged per sampled watershed area. The land use map included land cover classes, namely: rock, water, grassland, and forest, and land use classes, namely: unstocked forest, paddy rice, other agriculture, and urban areas, making up a total of eight classes. According to FAO 2010, forests refer to areas of more than 0.5 ha with a canopy cover of more than 10 % and trees higher than 5 meters. Unstocked forests are forests with crown density lower than 20% resulting from exploitation for logging or shifting cultivation. Unfertile or degraded areas covered by grass are attributed to grassland category. Other agriculture refers to agricultural lands used for non-crop purposes like livestock grazing. Water class includes rivers and water reservoirs exceeding 10 meters of width and 0.5 ha of surface area. Urban areas include permanent settlements like villages, towns, and roads having a width of more than 5 m:

3.2.8 Statistical analysis

In this study, we first focused on identifying links between [*E. coli*] and discriminating variables like hydro-meteorological factors, land use, and geomorphological characteristics of 19 Mekong tributaries in Lao PDR. Therefore, we used an exploratory data analysis, namely the Partial Least Square (PLS) regression, which is a multivariate approach (Geladi and Kowalski, 1986). It is the most adapted to our dataset, as it is able to handle (1) a large database with more variables than observations, (2) nonlinear relationships between response and independent variables, and (3) possibly collinear variables (Pirouz, 2010). Before applying the PLS algorithm, we centered and normalized the data, since the dataset included variables with different scales and measurement units. Moreover, turbidity, [TSS], and [*E. coli*], were log-transformed because the measured data were positively skewed. The variable importance in the projection number (VIP; between 0 and 2) was computed to determine the importance of variables. VIP greater than 1 are considered to be important in the analysis. To test the significant difference between measured variables in Mekong and Mekong tributaries during dry and rainy seasons, we divided the 2017-2018 monitoring dataset into two datasets: a dry season from November to May, and a rainy season from June to October. We used the paired Wilcoxon-test, to test the significant difference of measured variables in 19 tributaries between dry and rainy seasons of the 2016 campaign, and of the 2017-2018 monitoring datasets, with statistical significance set at p-value < 0.05.

We calculated Spearman correlation coefficients to investigate relationships between measured variables and [*E. coli*] measured in 19 tributaries during the 2016 campaign, as well as during the water quality monitoring 2017/2018 at the outlet of three watersheds in northern Lao

PDR (Nam Ou, Nam Suang, Mekong). In the statistical analyses on Mekong tributaries (PLS analysis, Spearman correlation and Wilcoxon test), only the Nam Ngum outlet (Nng_1) among the Nam Ngum sampling sites, was taken into account, to avoid the overrepresentation of the Nam Ngum tributary among the data.

3.3 Results

3.3.1 Spatial surveys conducted during the 2016 dry and rainy seasons

3.3.1.1 Descriptive analysis of the datasets

During the March 2016 (dry season) and July 2016 (rainy season) sampling campaigns, we measured *E. coli* concentration ([*E. coli*]) and a set of physico-chemical parameters: turbidity, temperature (T); dissolved oxygen saturation (DO); pH, electrical conductivity (EC); total suspended sediment concentration ([TSS]); total nitrogen concentration ([TN]); total particulate carbon concentration ([TPC]) in 19 Mekong tributaries (Fig. 18). The sampling sites were chosen to ensure a broad geographical coverage of Lao PDR, and to represent a large range of geographical, topographical, and land use features. The sampling sites were also chosen for being logistically accessible from the road, in order to cover the majority of Mekong tributaries in a relatively short time (Table 6, Appendix I: Table 14).

[*E. coli*] were found to be highly spatially variable across Lao PDR (Fig. 20), and 71% of the sampling sites displayed [*E. coli*] equal or greater to the lower detection limit of 38 MPN 100 mL^{-1} during both seasons. [*E. coli*] were below the detection limit in central and southern catchments (Nka, Ngn, Xbn) during the dry season and in central catchments (Nka, Xbi, Nhi) during the rainy season.

In March 2016, [*E. coli*] varied between 38 and 11,000 MPN 100 mL^{-1} at the outlet of the sampled Mekong tributaries (Fig. 20a). The highest [*E. coli*] were measured in four northern catchments (Nk20, A6, Npa, Nsu) and Vientiane plain (Nmi, Ntho), while the lowest [*E. coli*] were found in the mountainous parts of Vientiane Province (Nng_1), in central Lao PDR (Ngn), and in southern Lao PDR (Nka, Nhi, SR).

In July 2016, [*E. coli*] varied between 38 and 80,000 MPN 100 mL^{-1} at the outlet of the sampled Mekong tributaries (Fig. 20a). The highest [*E. coli*] were measured in the three catchments

of the Vientiane plain (Nsa, Ntho, Nmi), and in catchments of northern Lao PDR (Npa, Nsu, A6). Multiple sampling along the Nam Ngum river (Nng_3, Nng_4, Nng_2, and Nng_1), as well as along the Mekong river (MK_1, MK_7, MK_2, MK_3, MK_4, and MK_5), pointed out the spatial variability of *E. coli* contamination along rivers (Fig. 20b,c). In March 2016, [*E. coli*] ranged between 38 and 200 MPN 100 mL^{-1} along the Nam Ngum river, decreasing in the downstream direction (Nng_1). In July 2016, [*E. coli*] ranged between 38 and 300 MPN 100 mL^{-1} along the Nam Ngum river, increasing in the downstream direction (Fig. 20b).

Moreover, [*E. coli*] were highly variable along the Mekong river mainstream (Fig. 20c). In the dry season, [*E. coli*] in the Mekong river ranged between 0 and 520 MPN 100 mL^{-1}, while it varied between 0 and 57,000 MPN 100 mL^{-1} in the rainy season. The highest [*E. coli*] were found at the sampling sites located near urbanized areas around Vientiane (MK_7 and MK_2), and to a lesser extent in the southern station near Pakse (MK_5). The lowest [*E. coli*] were found in the highlands of northern Lao PDR (MK_1) and in southern Lao PDR (MK_3, MK_4) (Fig. 20c).

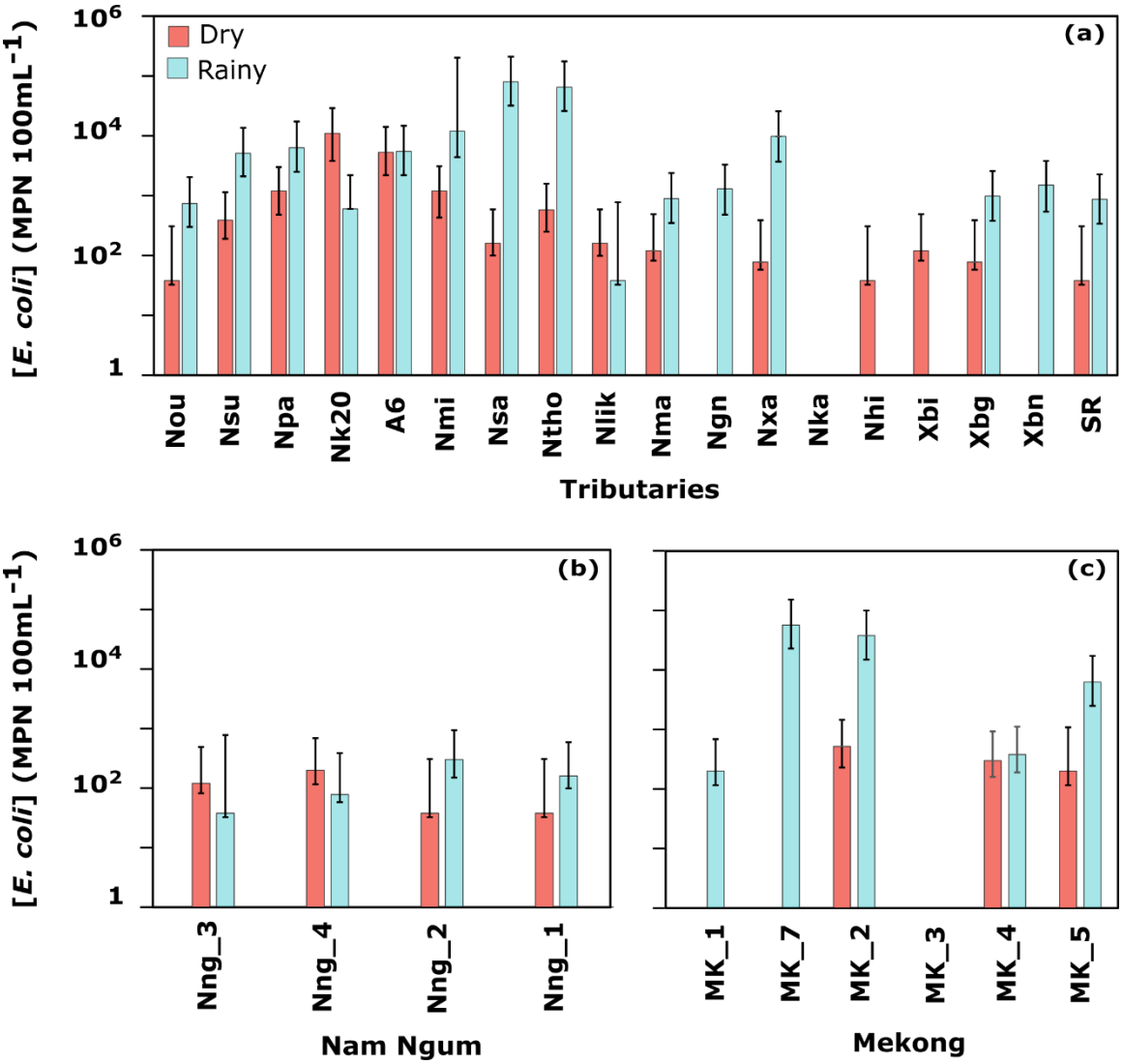

Figure 20: E. coli concentration with lower and upper 95% confidence limits ([E. coli], MPN 100 mL-1) in sampled watersheds of (a) Mekong tributaries, (b) Nam Ngum river, and (c) Mekong river across Lao PDR. Bars filled with orange represent concentrations during during March 2016 (dry season) and bars filled with blue represent concentrations during July 2016 (rainy season). Sampling stations are classified from northern to southern Lao PDR.

In the following statistical analyses on Mekong tributaries, only the Nam Ngum outlet (Nng_1) among the Nam Ngum sampling sites, was taken into account, to avoid the overrepresentation of the Nam Ngum tributary among the data.

Overall, seasonal variations of in-stream [*E. coli*] in Mekong tributaries were observed at the majority of the sampled sites. [*E. coli*] were different between the dry and the rainy seasons ($p < 0.05$), and followed a lognormal distribution during both seasons, yet more stretched towards upper extreme values during the rainy season (Fig. 21a).

Contrasted seasons also showed contrasted dynamics of physicochemical properties in the Mekong tributaries. [TSS], turbidity, [TPC], [TN], and T were significantly different between seasons ($p < 0.05$) (Fig. 21b,c,d,e,f). These variables followed the same trend as [*E. coli*], showing higher values during the rainy season compared to the dry season. DO, pH, and EC showed the opposite dynamics and were significantly higher during the dry season as compared to the rainy season ($p < 0.05$), with the exception of EC (Fig. 21g,h,i).

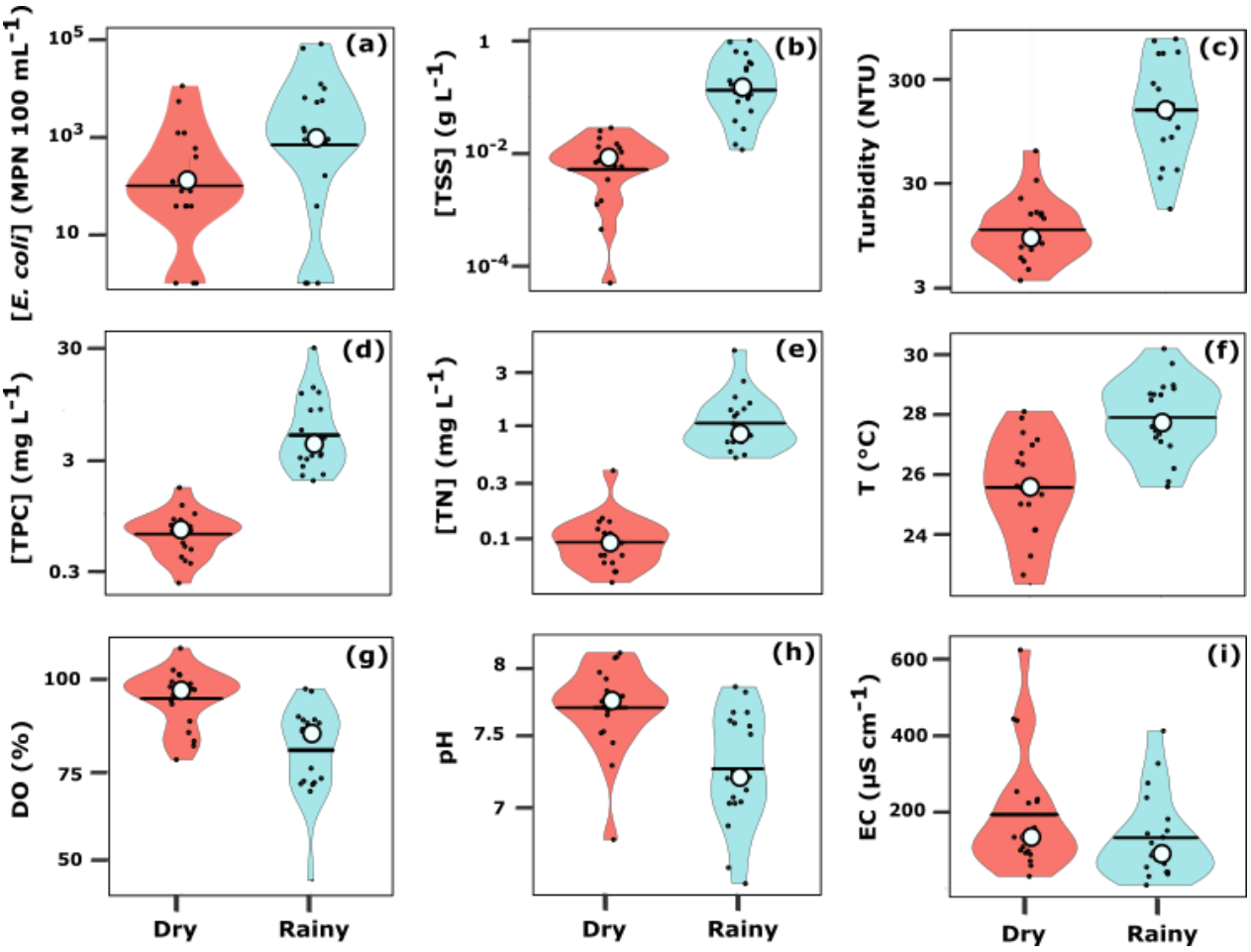

Figure 21: Violin plots of measured variables across sampling sites in Mekong tributaries of Lao PDR in March 2016 (dry season) and in July 2016 (rainy season): (a) E. coli concentrations ([E. coli], MPN 100 mL^{-1}); (b) total suspended sediment concentrations ([TSS], g L^{-1}); (c) turbidity (NTU); (d) total nitrogen concentration ([TN], mg L^{-1}); (e) total particulate carbon concentration ([TPC], mg L^{-1}); (f) temperature (T, °C); (g) dissolved oxygen saturation (DO, %); (h) pH; (i) electrical conductivity (EC, µS cm^{-1}). Black circle represents the mean, the black line is the median, and black dots are the variable observations.

3.3.1.2 PLS analysis

We conducted two separate PLS analyses aiming to identify the relative importance of the

main controlling factors of [*E. coli*] at large-catchment scale, during each of the dry and the rainy seasons, in 19 Mekong tributaries. We considered the samples taken during the dry and the rainy season separately in order to discriminate the seasonal effect from the other factors (geomorphology, land use, population densities). We used constant parameters during 2016 such as altitude, slope, and catchment area to describe the geomorphological features of these catchments (Fig. 19a). To describe the land use within the watershed, we used dams' reservoir areas (Appendix I: Table 14), and areal percentages of unstocked forest, forest, paddy rice, grassland, urban, water and other agriculture areas in each catchment (Fig. 19b, Appendix I: Table 14),, as well as human and livestock population densities per catchment (Fig. 19c,d, Appendix I: Table 14). Furthermore, we used seasonally variable parameters measured during both seasons in 2016, including [TSS], turbidity, [TN], [TPC], T, DO, pH, and EC; as well as the rainfall accumulated over one week before sampling (Fig. 19e,f).

During the dry season, [*E. coli*] was mainly explained in the PLS model by the first component (57%) and to a lesser extent by the second component (21.5%) (Fig. 22; Appendix I: Table 15). The VIPs (Variable Importance in the Projection) for each explanatory variable of both components showed that areal percentages of forest and unstocked forest, [TN], and EC, contributed the most to the model (VIP > 1.5). During the rainy season, [*E. coli*] was mainly explained by the first component (66%) and to a lesser extent by the second component (19%) (Appendix I: Table 15). Areal percentages of unstocked forest, turbidity, and [TSS], were highly influential on the model (VIP > 1.5).

During both seasons, the first component associated [*E. coli*] with common factors like watershed characteristics including areal percentages of land use classes, population density, catchment area and physico-chemical parameters ([TSS], [TN], [TPC], and turbidity). However, their relative importance changed with the season (Fig. 22).

During both seasons, [*E. coli*] was positively correlated to unstocked forest percentage area ($r = 0.65$ in dry season, $r = 0.62$ in rainy season, $p < 0.05$) and negatively correlated to catchment area ($r = -0.49$ in dry season, $r = -0.70$ in rainy season, $p < 0.05$) (Fig. 22). During the dry season, [*E. coli*] was positively correlated with EC ($r = 0.59$, $p < 0.05$) and T ($r = 0.47$, $p < 0.05$), and negatively correlated with forest percentage area ($r = -0.55$, $p < 0.05$) and DO ($r = -0.45$, $p = 0.054$).

During the rainy season, [*E. coli*] was positively correlated to [TN] (r = 0.48, p < 0.05), [TSS] (r = 0.44; p = 0.055), turbidity (r = 0.44, p = 0.060), [TPC] (r = 0.44; p = 0.061), and livestock density (r = 0.48, p = 0.054). Negative correlations were noted between [*E. coli*] and grassland percentage area (r = -0.53, p < 0.05), and between [*E.* coli] and water percentage area (r = -0.48, p < 0.05).

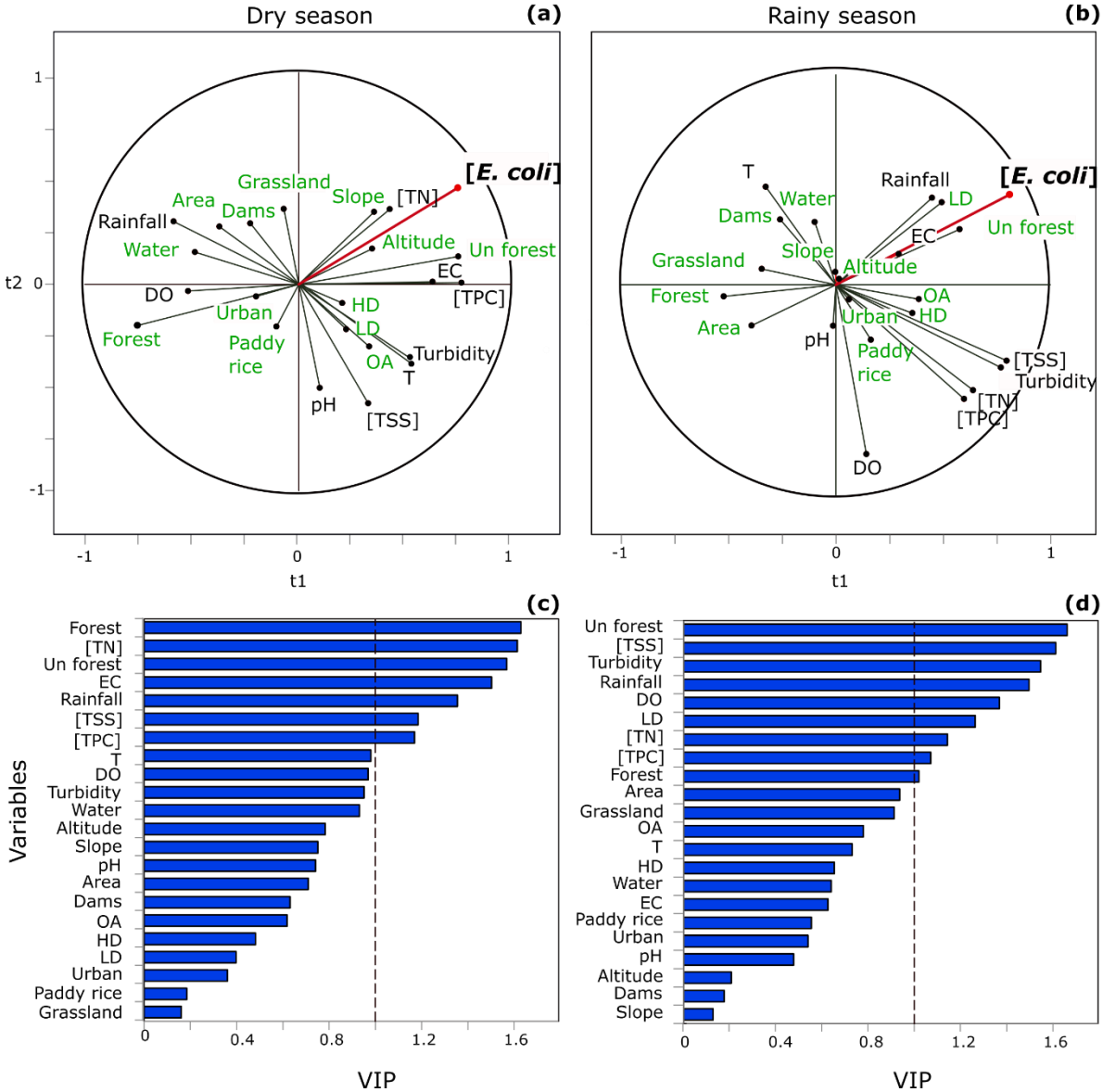

Figure 22: Correlation circles and Variable Importance in the Projection (VIP) scores of the PLS regression analysis of variables measured in Mekong tributaries during the 2016 campaign: (a) correlation circle from PLS of dry season; (b) correlation circle from PLS of rainy season; (c) VIP plot from PLS of dry season; (d) VIP plot from PLS of rainy season. Variables in green are those that remain constant during 2016: catchment median altitude (Altitude, m), catchment median slope (Slope, %), catchment area (Area, ha), dams reservoir area (Dams, ha); human density (HD, people ha^{-1}), livestock density (LD, animal ha^{-1}), and percentage areas of unstocked forest (Un forest, %), forest (Forest, %), paddy rice (Paddy rice, %), grassland (Grassland, %), water (Water, %) and other agriculture (OA, %).Variables in black are those that were measured during both the dry and the rainy seasons: E. coli concentrations ([E. coli], MPN 100 mL^{-1}); total suspended sediment concentration ([TSS], g L^{-1}); turbidity (NTU); total nitrogen

concentration ([TN], mg L^{-1}); total particulate carbon concentration ([TPC], mg L^{-1}); temperature (T, °C); dissolved oxygen saturation (DO, %); pH; electrical conductivity (EC, µS cm^{-1}) and total rainfall recorded one week pre-sampling (Rainfall, mm $week^{-1}$).

3.3.2 Water quality monitoring of three northern watersheds during 2017 and 2018

We conducted a closer investigation on *E. coli* dynamics through a two-year water quality monitoring at 10-day intervals, at three point locations of three rivers in the vicinity of the city of Luang Prabang, northern Lao PDR: Nam Ou (Nou; 25,946 km^2), Nam Suang (Nsu; 6,577 km^2), and Mekong (MK_17; 273,732 km^2). The study period extended from July 2017 to December 2018, and spanned two rainy seasons, from May to October in 2017 and 2018 (Fig. 23). The periodic water sampling showed a continuous in-stream presence of *E. coli* in all of the three catchments over the 2017-2018 period. The highest range of [*E. coli*] was measured at the MK_17 sampling site on the Mekong river (250-350,000 MPN 100 mL^{-1}), followed by the Nsu site at the outlet of Nam Suang (78-39,000 MPN 100 mL^{-1}) and the Nou site at the outlet of Nam Ou (0-7,100 MPN 100 mL^{-1}). The [*E. coli*] was marked by a seasonal variability, characterized by higher concentrations during the rainy season in all three watersheds ($p < 0.05$). [*E. coli*] was over two orders of magnitude and one order of magnitude higher during the rainy season compared to the dry season in both Nsu and Nou, and at MK_17, respectively.

Likewise, the seasonal variability of [TSS] in all sampled watersheds is marked by higher values during rainy season ($p < 0.05$). [TSS] followed the same seasonal pattern as [*E. coli*], increasing over three orders of magnitude in Nsu, over two orders of magnitude in Nou, and over one order of magnitude at MK_17 during the rainy season. The opposite trend was noted for EC dynamics that showed higher values during dry season ($p < 0.05$). The lowest peaks of EC occurred during rainfall events and the highest values of EC were recorded during the dry season (Fig. 23). In Nou, Nsu, and MK_17, water level was positively correlated to [TSS] and [*E. coli*], and negatively correlated to EC ($p < 0.05$) (Appendix I: Table 17). Likewise, [*E. coli*] in all three watersheds was positively correlated to [TSS] and negatively correlated to EC (Appendix I: Table 17).

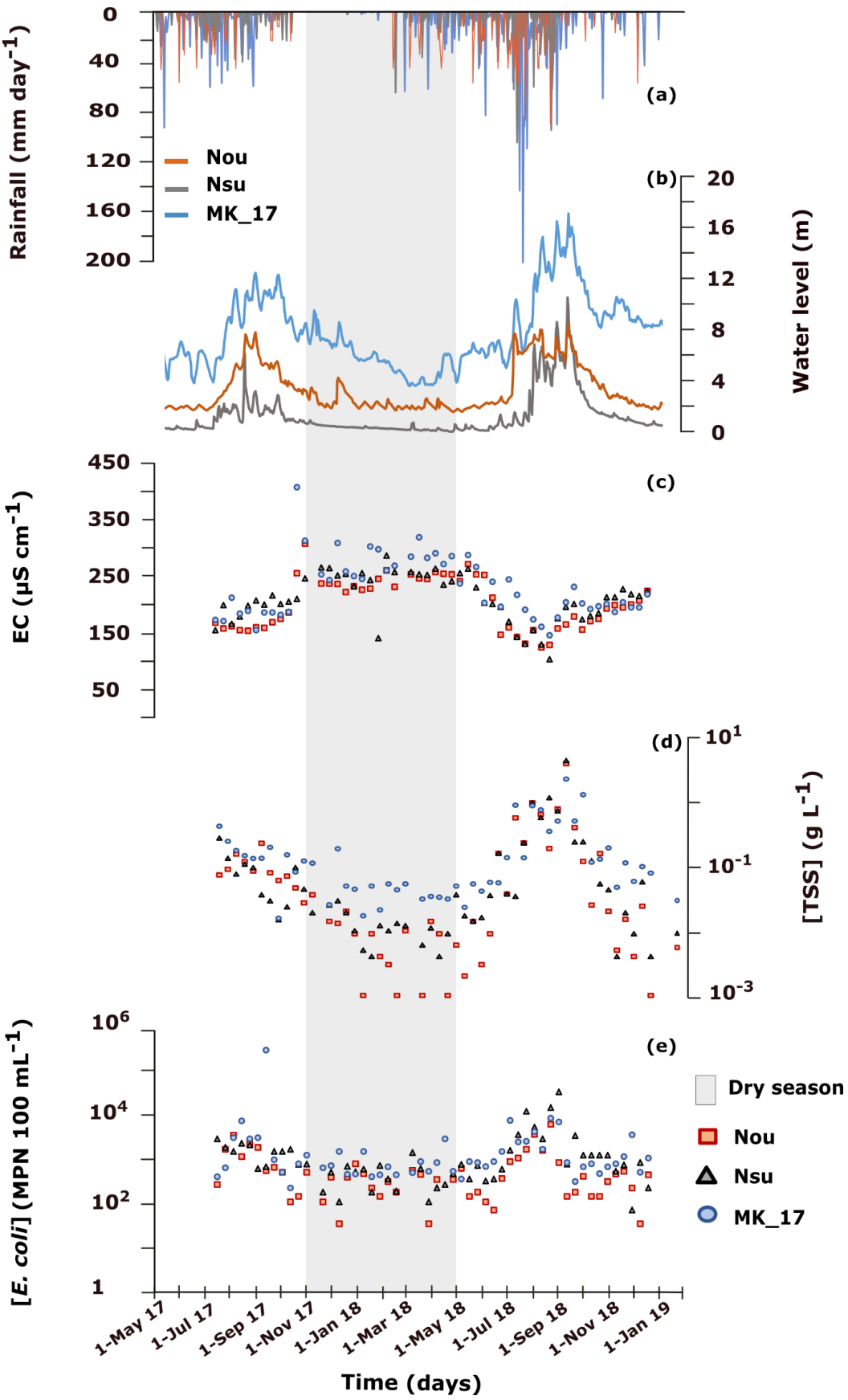
Rainfall (mm day-1)
0
40
80
120
160
200
(a)
Nou
Nsu
MK_17
(b)
20
16
12
8
4
0
Water level (m)
EC (µS cm-1)
450
350
250
150
50
(c)
(d)
10^1
10^-1
10^-3
[TSS] (g L-1)
[E. coli] (MPN 100 mL-1)
10^6
10^4
10^2
1
(e)
Dry season
Nou
Nsu
MK_17
1-May 17
1-Jul 17
1-Sep 17
1-Nov 17
1-Jan 18
1-Mar 18
1-May 18
1-Jul 18
1-Sep 18
1-Nov 18
1-Jan 19
Time (days)

Figure 23: 2017-2018 time series of variables measured at the outlet of three watersheds in northern Lao PDR, Nam Ou (Nou), Nam Suang (Nsu), and Mekong (MK_17): (a) daily rainfall (mm day^{-1}) taken from meteorological stations of the Department of Natural Resources and Environment of Luang Prabang; (b) daily water level (m); (c) electrical conductivity (EC, µS cm^{-1}); (d) total suspended sediment concentration ([TSS], g L^{-1}); (e) E. coli concentration ([E. coli], MPN 100 mL^{-1}). The highlighted area in grey represents the dry season (November-May).

3.4 Discussion

In this study, we investigated correlations between various environmental and water physico-chemical parameters and the occurrence of *E. coli*, as well as the seasonal variability of [*E. coli*] in the Mekong river and some of its major tributaries in Lao PDR.

Overall, our results show seasonal variabilities of [*E. coli*] and strong correlations between [*E. coli*] and [TSS] in the Mekong river and its tributaries. A seasonal comparison over two sampling years (2017-2018) have revealed contrasting hydrological, sedimental and microbiological responses that were driven by several factors. Higher water level, [TSS], and [*E. coli*], occurred in response to heavy rainfall. Similar distinctive seasonal fluctuations have been also observed in other tropical regions (Isobe et al., 2004; Nguyen et al., 2016). During the rainy season, surface runoff is a major factor controlling solid particles and *E. coli* transfer from top soil to the hydrographic network (Boithias et al., 2020; Causse et al., 2015; Mügler, C., Ribolzi, O., Janeau, J.-L., Rochelle-Newall, E., Latsachack, K., Thammahacksa, C., Viguier, M., Jardé, E., Henri-Des-Tureaux, T., Sengtaheuanghoung, O., Valentin, C., 2020; Ribolzi et al., 2018). This is consistent with our time series observations showing strong positive correlations between [*E. coli*] and [TSS] during rainy seasons, and negative correlations with EC values. The dynamics of EC can be used as an indicator of the relative contribution of overland flow to the streamflow (Cano-Paoli et al., 2019; Pellerin et al., 2008). A decreasing EC is characteristic of an increasing overland flow contribution, whereas an increasing EC indicates a higher contribution of groundwater (Ribolzi et al., 2018, 2016). During the 2017 and 2018 rainy seasons, EC decreased, suggesting an increase in overland flow contribution to streamflow, further contributing to the dispersion of suspended sediment and of microbial contaminants such as *E. coli* along hillslopes and downstream. Suspended sediment and washed-off free-living and particle-attached *E. coli* can deposit in streambeds of rivers before being re-suspended during high discharge events (Le et al., 2020; Navratil et al., 2010; Patin et al., 2012; Ribolzi et al., 2016). During the dry season, [*E. coli*] can be associated to other in-stream processes such as hyporheic exchange. In fact, during the dry

season at baseflow, the stream-groundwater interactions through lateral flow and advective groundwater movement in the hyporheic zone may be responsible for remobilizing bacteria trapped in the porous space of streambed sediments (Kim et al., 2017; Rochelle-Newall et al., 2016). Thus, the seasonal difference in terms of [TSS] and [*E. coli*] may be partly explained by seasonal streamflow regimes in response to meteorological patterns.

We noted similar trends in terms of positive correlations between [*E. coli*] and [TSS] during the rainy season of 2016 as compared to the rainy seasons of 2017 and 2018. Sources and dynamics of suspended particles were found to vary highly within a catchment (e.g., eroded sediments, re-suspended streambed sediments (Nguyen et al., 2016; Ribolzi et al., 2016)). Suspended particles are known to be carriers of adsorbed pollutants, nutrients, and microorganisms like *E. coli*, partly controlling their transport and fate (Craig et al., 2004; Nguyen et al., 2016; Oliver et al., 2007). Furthermore, suspended particles are not only vectors for bacterial transport, they could also provide optimal conditions for the survival of adsorbed coliform bacteria by protecting them from ultraviolet radiation and predators (Isobe et al., 2004). As suggested by several authors (Mügler, C., Ribolzi, O., Janeau, J.-L., Rochelle-Newall, E., Latsachack, K., Thammahacksa, C., Viguier, M., Jardé, E., Henri-Des-Tureaux, T., Sengtaheuanghoung, O., Valentin, C., 2020), bacterial decay rates can be influenced by the physico-chemistry of the stream water (e.g., pH, dissolved oxygen saturation, turbidity, EC and salinity (Burton et al., 1987; Flint, 1987; Nguyen et al., 2016; Petersen and Hubbart, 2020b)). Water physico-chemical properties could be key drivers explaining the higher *E. coli* concentrations in the majority of the sampled tributaries during the rainy season.

In the present work, PLS analysis also helped to identify various correlations between land use classes and [*E. coli*] in stream water. During both dry and rainy seasons, [*E. coli*] was positively associated with the percentage of unstocked forest area and negatively associated with the percentage of forest and grassland areas, especially during the rainy seasons. Such correlations are consistent with reports from previous studies in similar tropical watersheds (Brendel and Soupir, 2017; Ekklesia et al., 2015b; Ribolzi et al., 2017; Rochelle-Newall et al., 2015). Higher FIB concentrations were measured in watersheds located in steep mountainous areas of northern Lao PDR as well as in the Vientiane plain, where the dominant land use is unstocked forest, and to a lesser extent, paddy rice and other agricultural land. The unstocked forest percentage areas are largely present in Southeast Asian upland catchments, due to the general pressure towards clearing

forests for intensified annual crop production with reduced fallow period and suppressed understory cover (Huong et al., 2018; Patin et al., 2012; Thongmanivong and Fujita, 2006; Valentin et al., 2008a). Forest areas in Lao PDR have shrunk from about 73% in the 1960s to 40% in the 1990s (Forestry Department Food and Agriculture Organization of the United Nations, 2010; Ribolzi et al., 2017; Ziegler et al., 2006). These land use changes can affect soil erosion, water infiltration and overland flow (Gardner and Gerrard, 2003; Ribolzi et al., 2017; Sidle et al., 2006; Song et al., 2020), due to reduced topsoil cover and reduced soil binding by roots (Miura et al., 2003; Ribolzi et al., 2017). In steep regions, deforestation may also lead to landslides due to the absence of stabilizing roots network and loss of soil stability (Sidle et al., 2006; Ziegler et al., 2006). Unstocked forest areas are thereby more vulnerable to soil erosion and landslides processes (Huon et al., 2013; Turkelboom et al., 2008), especially during the rainy season, increasing overland flow loaded with soil particles and attached FIB that end up in the downstream river.

In contrast, southern Lao PDR watersheds (Nka, Nhi, Xbi), characterized by high percentages of forest areas, had the lowest contamination during both seasons. Areas dominated by forested watersheds with understory cover have been shown to have high infiltration rates, low soil erosion, and high contaminant trapping efficiencies (Yong and Chen, 2002; Zuazo and Pleguezuelo, 2008). Land cover and management practices can be key factors controlling runoff production and surface soil erosion, and thus FIB contamination levels of rivers (Petersen and Hubbart, 2020b, 2020a).

In our PLS analyses, negative associations between [*E. coli*] and dams' reservoir area were noted during both seasons, yet they were not significant at the 0.05 level in our study case. The impact of dams on FIB could be different in each catchment, depending on dams' reservoir area, as well as on the distance between dams and sampling sites and on potential FIB sources in-between. Many studies focused on the potential hydrological effects of dams in the Mekong basin (Hecht et al., 2019a). An important decrease in suspended sediment loads was noted in many tributaries following the construction of dams, for instance a 50% reduction at Pakse where the average suspended loads decreased from 120 to 60 Mt yr^{-1} (Piman and Shrestha, 2008). Along with flow alteration and sediment trapping, dams could also impact FIB fate and transport.

E. coli sources vary greatly across Lao PDR, depending on human and animal density, as

well as on the presence or absence of an operational wastewater collection system. It has been shown that mammalian presence closely influences the river's microbiological quality, particularly in rural areas of developing countries lacking sanitary infrastructure (Causse et al., 2015; Rochelle-Newall et al., 2016). However, our study did not show any significant correlation between human densities and measured downstream [*E. coli*] in either the dry or the rainy seasons. Livestock densities were weakly correlated with [*E. coli*] during the rainy season ($r = 0.45$, $p = 0.054$). This can tentatively be ascribed to several reasons.

On the one hand, the population of Lao PDR is unevenly distributed across the country. About 70% of the population lives in rural areas. Additionally, there are significant urban-rural disparities in terms of access to improved sanitation facilities. Thus, some rural watersheds, although less densely populated, are more exposed to fecal contamination through point sources (direct release of untreated wastewater into river stream), as compared to other populated urban watersheds equipped with wastewater treatment systems. However, despite incremental improvements of the sanitation system in Lao PDR, open defecation remains a major issue, estimated to concern 32% and 45% of the overall and rural populations, respectively (WHO/UNICEF, 2013). Along with the presence of wild animals or livestock, open defecation is a diffuse source of microbial pathogens, transferred to the stream with surface runoff, and contributing to the fecal pollution of rivers. Moreover, unstocked exploited forests in watersheds with low mammalian presence can be highly frequented by workers during specific periods and by villagers for their domestic needs, adding to the complexity of determining diffuse source inputs. On the other hand, the absence of strong correlations between human and livestock densities and FIB concentrations may also be due to the distance between primary sources (human and livestock) and water streams. This distance, in turn, affects survival rates of transferred FIB, which get increasingly exposed to environmental conditions as primary sources and streams are more distant from one another. During hot and dry periods, less favorable conditions for microbial development (e.g. more sunlight, less nutrients) might increase opportunities for their die-off (Cho et al., 2010a; Nguyen et al., 2016; Rochelle-Newall et al., 2015). In addition, longer transfer times from hillslopes to rivers due to disconnected flow paths might result in lower [*E. coli*] in downstream rivers due to the sedimentation of FIB-bound particles and FIB decay (Brendel and Soupir, 2017; Evrard et al., 2010). However, *E. coli* might be able to survive in streambed sediment reservoirs, explaining a continuous presence of *E. coli* in streams, even during the dry season. Several laboratory

experiments and field studies have shown that streambed sediments, under favorable conditions, are important bacterial reservoirs, both in temperate regions (Chahinian et al., 2012; Cho et al., 2010b; Walters et al., 2014), and tropical conditions (Pachepsky et al., 2017; Ribolzi et al., 2016).

PLS analyses helped identifying the relative importance of variables explaining [*E. coli*] in 19 tributaries across Lao PDR in dry and rainy season. While this study provides useful insights on relationships between various factors and FIB, we were limited by the available data, especially the land use data. In future studies, when updated land use data will be available, it will be necessary to differentiate between planted and natural forests within the forest category at watersheds scale. The impacts of commercial tree plantations (e.g., teak trees, rubber trees) on hydrological response and associated increase in soil erosion, were pointed out by a few studies (Lacombe et al., 2018; Neyret et al., 2020; Ribolzi et al., 2017). More accurate, complete, and higher land use data resolution would allow a closer understanding of the factors controlling bacterial contaminations and should be taken into account when addressing land management issues.

3.5 Conclusion

This study is the first to assess seasonal dynamics of fecal contamination in Lao PDR, based on a large physico-chemical, microbiological, and geomorphological dataset, with the aim of identifying the relative importance of different controlling factors of in-stream *E. coli* concentrations during both the dry and the rainy seasons. Our study consisting of (1) a spatial survey in 2016 during both the dry and the rainy seasons, and (2) a 10-day sampling monitoring from July 2017 to December 2018 at 3 stations, pointed out the following main findings:

- The seasonal variability of *E. coli* concentrations marked by higher and extreme values occurring during the rainy season, is noted in the majority of sampled Mekong tributaries. This is consistent with the increase in surface water turbidity during rainy season.
- *E. coli* concentrations are positively correlated to total suspended sediment concentrations in both of the datasets, highlighting the potential role of suspended sediment dynamics in FIB transport, more particularly in catchments prone to soil erosion in a tropical setting.

- *E. coli* concentrations are positively correlated with unstocked forest percentage areas, and negatively correlated to forest percentage areas, which points out the importance of land use / land cover as one of key factors impacting FIB dynamics at catchment-scale.

Our data provide new evidence that populations relying on untreated surface water resources of three northern watersheds in Lao PDR (Nam Ou, Nam Suang, and Mekong) are exposed to continuous fecal contamination all year round. Despite the World Health Organization (WHO) guidelines of 0 MPN 100 mL^{-1} of *E. coli* in drinking water, this remains an urgent public health issue in Lao PDR, putting lives at risk. The majority of sampled tributaries across Lao PDR in 2016 presented very high *E. coli* concentrations during the rainy season, exceeding 500 colonies per 100 mL, the threshold above which the WHO considers a 10% risk of gastrointestinal illness after one single exposure. This stresses the need for a better water quality assessment of the Mekong river and its tributaries, as well as a detailed evaluation of the risks posed by fecal waterborne diseases to rural populations directly depending on untreated water resources. In addition, given the rapid growth of hydropower plants in the Mekong basin (Arias et al., 2014a; Pokhrel et al., 2018), it will be necessary to investigate its impact on hydrology, sediment fluxes, and associated health issues like fecal contamination at watershed-scale in Lao PDR. It is also necessary to further investigate and quantify the factors controlling FIB survival and mortality in water and sediments under tropical conditions to understand the dynamics of these bacteria in this system.

Chapter 4. Apparent decay rate of *Escherichia coli* in a mountainous tropical headwater wetland

Introduction to chapter 4

This chapter focuses on the poorly documented FIB behavior in ecosystems like headwater tropical wetlands. In the humid tropical regions like the lower Mekong basin driven by annual flood pulse, wetlands are widespread and strongly contribute to the ecosystem biodiversity and productivity. Wetlands in tropical context generally characterized by high and stable temperatures, dense riparian vegetation, high ecological diversity, and long water residence time, can act as a natural sanitation system reducing waterborne pollutant loading to downstream environments. These reasons motivated the experimental approach presented in this chapter. We conducted a semi-controlled mesocosms experiments for 8 days to investigate the FIB decay/survival rates under solar radiation exposition and suspended particles deposition conditions. These findings underline the important role of TSS in providing *E. coli* protection from stressors like sunlight, as well as vertical migration from the water column to the bottom sediments potentially favorable for their survival. It is crucial to improve our understanding of the FIB behavior in tropical humid context, in the perspective of effective conservation of the valuable ecosystem services that they deliver. This work was published in Water:

Nakhle, P., Boithias, L., Pando-Bahuon, A., Thammahacksa, C., Gallion, N., Sounyafong, P., Silvera, N., Latsachack, K., Soulileuth, B., Rochelle-Newall, E.J., Marcangeli, Y., Pierret, A., Ribolzi, O., 2021b. Decay Rate of Escherichia coli in a Mountainous Tropical Headwater Wetland. Water 2021, Vol. 13, Page 2068 13, 2068. https://doi.org/10.3390/W13152068

Abstract

Surface water contamination by pathogen bacteria remains a threat to public health in rural areas of developing countries. Fecal indicator bacteria (FIB) like *Escherichia coli* (*E. coli*) are widely used to assess water contamination, but their behavior in tropical ecosystems is poorly documented. Our study focused on headwater wetlands, which are likely to play a key role in stream water purification of fecal pollutants. Our main objectives were to: (i) evaluate apparent decay rates (k) of the total, particle-attached and free-living *E. coli*; (ii) quantify the relative importance of sunlight exposition and suspended particles sedimentation on k; and (iii) investigate *E. coli* survival in the deposited sediment. We installed and monitored 12 mesocosms, 4,500 mL each, across the main headwater wetland of the Houay Pano catchment, northern Lao PDR, during 8 days. The four treatments with triplicates were sediment deposition-light (DL); sediment deposition-dark (DD); sediment resuspension-light (RL); and sediment resuspension-dark (RD). Particle-attached bacteria predominated in all mesocosms (97 ± 6%). Decay rates ranged from 1.43 ± 0.15 to 1.17 ± 0.13 day^{-1} for treatments DL and DD, and from 0.50 ± 0.15 to -0.14 ± 0.37 day^{-1} for treatments RL and RD. Sedimentation processes accounted for 99% of *E. coli* stock reduction. Sampling of *E coli* by temporary resuspension of the deposited sediment showed k values close to zero, suggesting potential survival or even growth of bacteria in the sediment.

Keywords: Fecal indicator bacteria; Lao PDR; Mekong basin; water purification; survival rates; mesocosms; solar radiation; sedimentation; resuspension.

4.1 Introduction

One in four people globally drink water contaminated with fecal matter (WHO, 2017). Surface water contamination by fecal pathogenic microorganisms is indeed a threat for public health worldwide (UNEP, 2016). Diarrheal diseases including gastroenteritis, mostly caused by water-borne pathogens, were responsible for the deaths of 1.6 million people in 2017 (Prüss-Ustün et al., 2019). This major public health issue especially affects developing countries in the intertropical band, where populations rely directly on local resources and have poor access to clean water, sanitation, and hygiene (WHO/UNICEF, 2015). For instance, rural communities in the Mekong basin depend directly on small tributaries and natural canal systems to fulfil their domestic water needs (O. Ribolzi et al., 2011). In Lao People's Democratic Republic (Lao PDR), temporary

camps, gardens, and fishponds can be found in the riparian zones where contamination levels were found to be high [6,7]. Moreover, riparian zones in tropical systems are often characterized by wetlands and swampy areas (Ribolzi et al., 2016).

Ecosystems such as wetlands have multiple ecological functions, like reducing flow velocity and filtering pollutants and fecal pathogens from surface water, resulting in the reduction of suspended particles and pollutant loading to downstream environments, and thereby improving water quality (Johnston, 1991; Mander and Mitsch, 2009). Wetlands, widespread in the humid tropics, are common landscape features in the Mekong basin (Arias et al., 2019; MacAlister and Mahaxay, 2009), and provide multiple ecosystem services including food production (Berg et al., 2017; Grundy-Warr et al., 2012), flood control (Zedler and Kercher, 2005), habitat biodiversity (Millennium Ecosystem Assessment, 2005), and water purification (Brauman et al., 2007). If large wetlands of fluvial plains are quite well studied (Lane et al., 2018; USEPA (U.S. Environmental Protection Agency), 2015), the functioning of those located along or nearby mountainous headwater streams are little studied, hence still poorly understood. Headwater wetlands, although representing a limited proportion of the drainage area of catchments, are likely to strongly affect the hydrological behavior (Krecek and Haigh, 2006) and biogeochemical characteristics of mountain streams (Alexander et al., 2007; Colvin et al., 2019). In a study based on a large data set consisting of 35 developing countries, it has been shown that upstream watershed conditions including wetlands can significantly influence downstream water quality (Herrera et al., 2017). To be able to effectively reduce the risk on human health (Ishii and Sadowsky, 2008), it is imperative to improve our understanding of environmental factors controlling fecal pathogens in tropical aquatic systems like headwater wetlands.

There is a growing scientific community interested in the main mechanisms involved in pathogens reduction within wetlands, mainly documented in temperate regions (Knox et al., 2008; Mander and Mitsch, 2009; Quin et al., 2015). The fecal contamination of water bodies is typically assessed by measuring levels of fecal indicator bacteria (FIB), e.g., *Escherichia coli* (*E. coli*) (Pachepsky and Shelton, 2011; WHO, 2011b). To our knowledge, little information exists on the survival of FIB in tropical headwater wetlands, which are generally characterized by high and stable temperatures, dense riparian vegetation, high ecological diversity, and long water residence time (Rochelle-Newall et al., 2015). All these characteristics can influence the *E. coli* decay rates.

Several studies pointed out the potential of *E. coli* to survive and possibly even proliferate in secondary and tertiary habitats such as soils and streambed sediments under tropical conditions (Anderson et al., 2005; Isobe et al., 2004; Naganandhini et al., 2015; Petersen and Hubbart, 2020c; Solo-Gabriele et al., 2000). Given the potential persistence of *E. coli* in the environment and its frequent use as a FIB, a further understanding of its decay mechanisms is needed to evaluate the environmental microbial contamination to which the rural population may be exposed.

Several studies have identified solar radiation as one of the most important factors controlling and reducing *E. coli* concentration in surface water bodies (Chan et al., 2015; Fujiokal and Narikawa, 1982; Sinton et al., 2002). It has been demonstrated that bacteria are susceptible to ultraviolet wavelengths within the solar spectrum wavelengths causing direct DNA damage (Jozić et al., 2014; Nelson et al., 2018; Sinton et al., 2002). When exposed to solar radiation, FIB can get inactivated by entering a state in which they maintain some metabolic activity but lose their culturability (Jozić et al., 2014). The "viable non-culturable state" is a state of dormancy of bacteria characterized by a very low metabolic activity (Pienaar et al., 2016). In relatively shallow aquatic ecosystems like wetlands, solar radiation can have a direct impact on bacterial decay rates within water column (Maraccini et al., 2016; Whitman et al., 2004). However, dense vegetation cover may dampen the net impact of radiations. Furthermore, bacterial attachment to suspended particles can also play a key role in protecting bacteria from the photo-inactivation (Walters et al., 2014). Bacteria attached to suspended particles at the top of the water column can access nutrients (Perkins et al., 2016) and be subject to settle in the bottom of a wetland. This deposition process is thought to be one of the major mechanisms of bacterial removal (Karim et al., 2004) and is therefore widely used to decontaminate water in constructed wetlands (O'Geen and Bianchi, 2015). However, some studies in freshwater ecosystems (Boutilier et al., 2009; Howell et al., 1996) and marine ecosystems (Anderson et al., 2005) showed the ability of *E. coli* to survive longer in sediments than in the water column. Thus, the bottom sediments of wetlands could potentially serve as a reservoir of FIB, which could be released into the water column during erosive stormflow events (Boithias et al., 2021b; Ribolzi et al., 2016). Various other environmental factors were also shown to impact *E. coli* decay rate in water, such as temperature (Blaustein et al., 2013; Craig et al., 2004), nutrients availability (Shelton et al., 2014), dissolved organic carbon availability (Gregory et al., 2017), salinity (Bordalo et al., 2002), and predation (Korajkic et al., 2013).

In this study, our first hypothesis is that if most *E. coli* in the water column are present in the attached form, the settling down of suspended particles should be a major process for reducing the bacterial load in the stream water. Our second hypothesis is that in humid tropical conditions, the effect of light should be strongly attenuated by the dense vegetation cover typical of humid environments. Hence, considering a mountainous headwater wetland located within the Houay Pano catchment (northern Lao PDR), whose land use is representative of humid tropical agroecosystems of Southeast Asia (Boithias et al., 2021a), the objectives of this study were: (i) to evaluate decay rates of the total, particle-attached, and free-living *E. coli*, (ii) to quantify the relative importance of solar radiation exposition and suspended particles deposition on decay rates, and (iii) to investigate the survival of *E. coli* in the deposited bottom sediment.

The majority of FIB decay experiments were conducted under laboratory-controlled conditions (Haller et al., 2009; Maraccini et al., 2016; Walters et al., 2014; Wang et al., 2018), which take into account a selected range of physical, chemical, and biological factors found in natural environments. In this study, in order to obtain decay rates estimates as realistic as possible, we adopted an experimental approach based on measurements and using *in situ* mesocosms. The latter were filled with contaminated water collected from the Houay Pano stream and were installed in the water column of the wetland, hence exposed to natural diurnal cycle variations.

4.2 Material and methods

4.2.1 Study area

The experiment was carried out in the Houay Pano catchment (19°51′ N–102°10′ E), located 10 km south of Luang Prabang, northern Lao PDR (Fig. 24a). The 60-ha Houay Pano catchment is a sub-catchment of the Houay Xon, a tributary of the Mekong River. Slopes in the catchment range from 0% to 171% with an average of 54% (Ribolzi et al., 2016). This experimental site is part of the Multiscale TROPIcal CatchmentS (M-TROPICS) critical zone observatory (Boithias et al., 2021a) which operates under the umbrella of the *Observatoires de la Zone Critique: Applications et Recherche* (OZCAR) (Gaillardet et al., 2018). This catchment is representative of the mountainous agroecosystems of Southeast Asia. The climate is tropical wet and dry climate, abbreviated “Aw climate” in the Köppen-Geiger-Pohl system, and characterized by a monsoon regime, with two contrasted seasons: a dry season from November to May and a rainy season from

June to October. The mean annual temperature is 23.4 °C. The mean annual rainfall is 1366 mm (CV = 0.23), about 71% (CV = 0.09) of which, falls during the rainy season (Boithias et al., 2021a). The headwater wetland (0.19 ha) is located in the central part of the Houay Pano catchment (Fig. 24b). The wetland drains 32.5 ha and is permanently fed by groundwater (Ribolzi et al., 2018). It is a typical upland headwater wetland, colonized by 2–4 m high Napier grass (*Pennisetum purpureum* Schumach.), and surrounded with teak tree plantations, fallow land, and secondary forest (Ribolzi et al., 2018).

In spite of the relatively small suspended particles size (median is between 6 and 24 µm) measured in the upstream inflow (Huon et al., 2017), this wetland is known to have a high sediment trapping efficiency (Huon et al., 2013), due to hydro-morphological conditions that favor particles settling (Hjulstrom, 1935): low water line slope gradient (3.5%), limited hydraulic radius of the wetted area (0.02–0.2 m), low to very low apparent stream flow velocity (close to 0.001 m s^{-1}), and high vegetation cover (Napier grass). It should be noted that, if Napier grass cover is high year round, it is sometimes cut to be used as fodder, or occasionally replaced by vegetable plants such as watercress (Huon et al., 2008). At the end of the dry season, the Napier grass cover is also sometimes accidentally or deliberately burnt by farmers. As a result, the global solar radiation reaching the water surface is likely to vary according to agricultural practices and land use. During this study, the canopy density of Napier grass (i.e., the percentage of the vertical projection area of vegetation on the ground) along the wetland was between 45 and 100%.

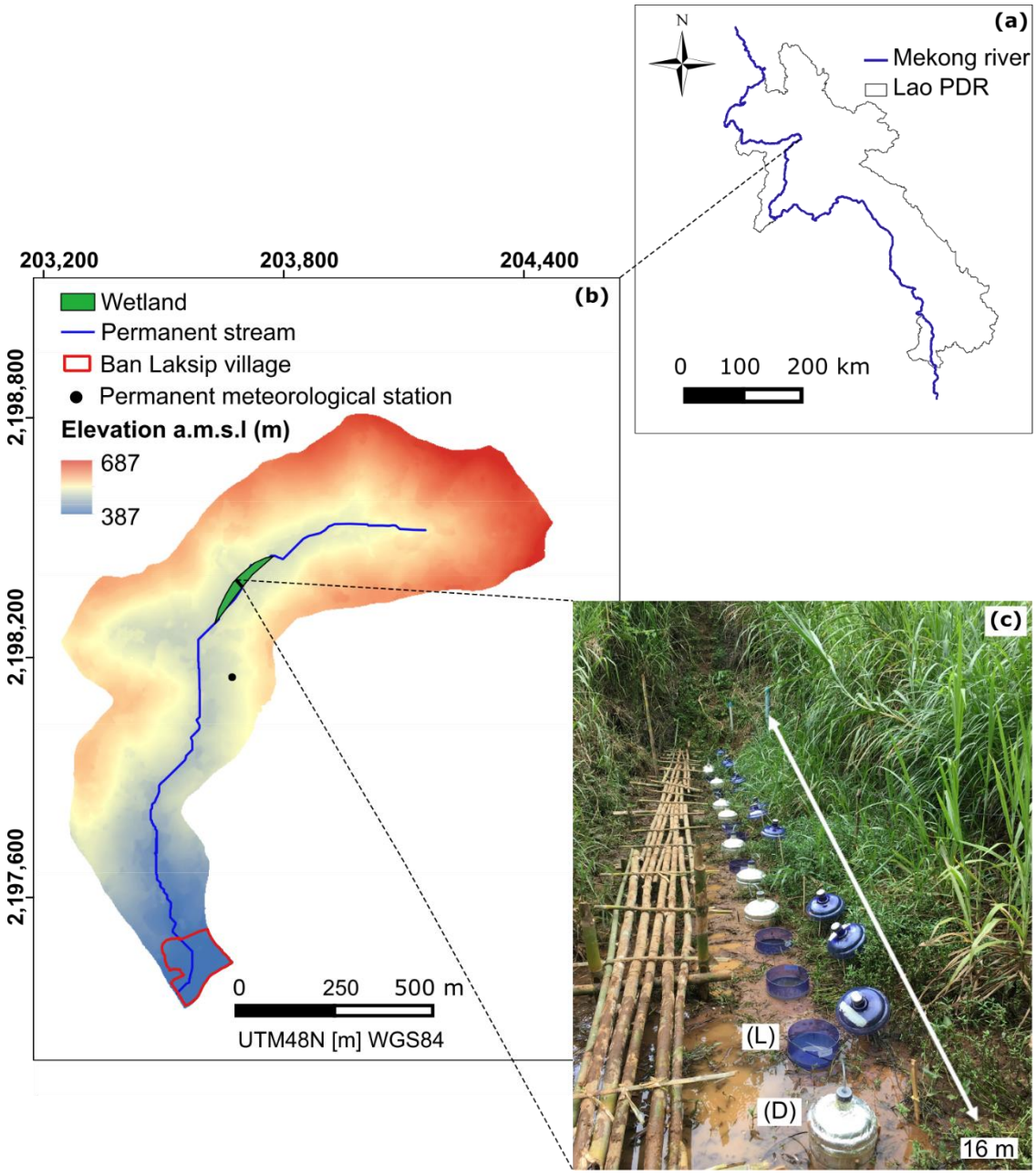

*Figure 24: Geographical location of (**a**) the Houay Pano catchment in northern Lao PDR, and (**b**) location of the study site in the headwater wetland; (**c**) photo of the transect within the wetland where the mesocosms exposed to natural light (L), the mesocosms kept in the dark (D), and the bamboo bridge, were installed 9–16 August 2019.*

4.2.2 Experimental design

Fifteen mesocosms (51 cm high and 27 cm in diameter transparent plastic buckets) were installed across the main headwater wetland of the Houay Pano catchment for a monitoring period of 8 days (Fig. 24c).

Mesocosms were divided into 4 treatments (3 replicates per treatment):

•Two of these treatments, i.e., suspended particles deposition in the light (DL) and suspended particles deposition in the dark (DD), were designed to quantify the decay rate of E. coli under wetland-like hydrodynamic conditions enabling the fall of suspended particles (i.e., absence or very low turbulence in the water column), with and without daylight (DL and DD respectively), to simulate the strong attenuation of the transmitted luminous flux to the water surface by dense vegetation cover (Fig. 25).

•Two other treatments, i.e., sediment resuspension in the light (RL) and sediment resuspension in the dark (RD), were aimed to evaluate the possible survival or even growth of E. coli in the deposited sediment. To this end, bacteria that had been deposited at the bottom of the mesocosm with the solid particles were resuspended by a daily 1-min manual stirring of the water column using sterile gloves, preceding each sampling. Here the cases with and without daylight (RL and RD respectively) were also tested.

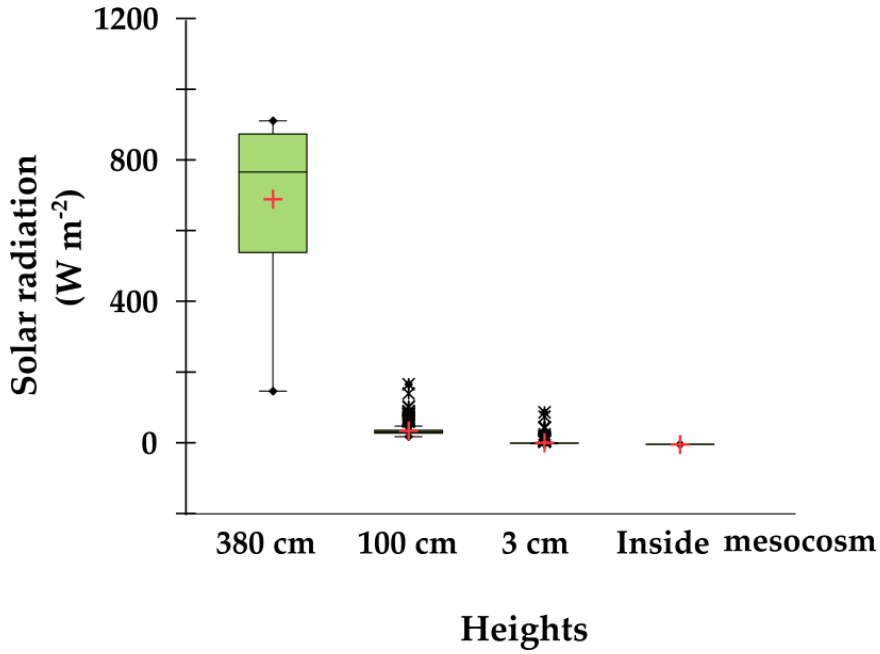

Figure 25: Boxplots of solar intensity (W m^{-2}) measured between 11 am and 3 pm for two days (24 and 25 October 2020) within the headwater wetland in Houay Pano catchment, northern Lao PDR, characterized with high Napier grass (Pennisetum purpureum Schumach.) cover (i.e., 100% at the measurement site) at 4 different heights: 380 cm, 100 cm, 3 cm, and inside of a covered top mesocosm. The red crosses indicate the means. The central horizontal bars are the medians. The lower and upper limits of the box are the 25th and 75th percentiles, respectively. The lower and upper lines of the boxes are the 10th and 90th percentiles. Points above or below the upper and lower limits are considered as outliers.

We used an additional set of three mesocosms (control) to verify the absence of external

contamination during the experiment (raindrops splash, dry atmospheric deposits, etc.).

Open top mesocosms (covered in case of rainfall event to avoid external contamination and concentration dilution) were used for the treatments with natural sunlight cycle exposure (DL, RL, and control). Covered top mesocosms using two layers of plastic covers wrapped in aluminum foil with ventilation holes to ensure the aeration inside the mesocosm were used for the treatments in the dark (DD and RD).

Mesocosms were randomly distributed by series of replicates, along a transect perpendicular to the stream flowing within the headwater wetland (Fig. 24c). The mesocosms were installed in the center of the wetland, spaced one meter apart, held straight with bamboo rods, and driven 10 cm deep into the streambed sediment (Fig. 24c).

A field worker was permanently present on the study site throughout the experiment duration, in order to ensure that no external source would contaminate the mesocosms (e.g., wild animals), and to avoid any change in mesocosm water balance by closing all the mesocosms during rainfall events. Before the start of the experiment, a bamboo bridge was built to facilitate the setup of the experiment and to access the mesocosms without contaminating them (Fig. 24c).

4.2.3 Mesocosms preparation

We used stream water to ensure the presence of nutrients, particles, and predators found in natural aquatic environment. We collected Houay Pano stream water in the Ban Laksip village (Fig. 24) approximately 10 cm below the water surface, 6 h before the installation of mesocosms. Approximately 70 L of water were collected into 4 sterilized 20 L buckets. The water from the 4 buckets was then mixed in a single large barrel in the vicinity of the experiment site, and vigorously stirred to ensure a homogenized distribution of the bacteria and of the suspended particles concentration in water before being distributed using a sterile 1000 mL test tube in the 12 mesocosms used for the four treatments. Each mesocosm was filled with 4500 mL of water.

For the three control mesocosms, we used groundwater collected within the Houay Pano catchment. We pumped groundwater from 6 piezometers located inside and on the edge of the wetland and characterized by low *E. coli* concentration (436 ± 102 MPN 100 mL^{-1}) when compared to water collected from Houay Pano stream (435,506 ± 215,275 MPN 100 mL^{-1}). The

biogeochemical background of the groundwater was comparable to that of the water collected in Houay Pano stream. The water was homogenized in a second barrel and 4500 mL were distributed in each of to three control mesocosms.

4.2.4 Analytical methods

We collected 30 mL water samples from each mesocosm, daily over 8 days (D0, D1, D2, D3, D4, D5, and D7), 1 cm beneath the water surface using 50-mL sterile plastic syringes. We stored the samples at ambient temperature and in the dark until measurement. We analyzed these samples within 6 h, by taking a subsample of 10 mL to determine the turbidity using a turbidity meter (EUTECH Instruments TN-100). We took another subsample of 10 mL to determine total *E. coli* concentration [*E. coli*]$_{total}$ (=particle-attached + free-living *E. coli*), and free-living *E. coli* concentration [*E. coli*]$_{free}$. We calculated particle-attached *E. coli* concentration ([*E. coli*]$_{att}$) from the difference between [*E. coli*]$_{total}$ and [*E. coli*]$_{free}$. To determine [*E. coli*]$_{total}$ and [*E. coli*]$_{free}$, we used 5 mL of raw water for total *E. coli* counts, and we filtered 5 mL of raw water through cellulose esters filters (Millipore, 3 µm, 47 mm) to separate the free-living *E. coli* in the collected filtrate from the particle-attached *E. coli* remaining on the filter (Nguyen et al., 2016). The method used for measuring [*E. coli*]$_{total}$ and [*E. coli*]$_{free}$ is the standardized microplate method (ISO 9308-3). This technique is based on a 48-h incubation at 44 °C of each sample, at four dilution rates (1:2, 1:20, 1:200, 1:2000 for treatments; and 1, 1:2, 1:20, 1:200 for control), in a culture medium specific for *E. coli* on a 96-well microplate (MUG/EC, Biokar Diagnostics). We determined [*E. coli*]$_{total}$ and [*E. coli*]$_{free}$ expressed in terms of most probable number per 100 mL (MPN 100 mL^{-1}), by counting the number of positive wells for each microplate, and by applying a statistical analysis based on Poisson's law (Lebaron et al., 2005).

We collected 80 mL water samples every other day (D0, D2, D4, and D7), 1 cm beneath the water surface using 50-mL sterile plastic syringes, and we stored them at ambient temperature and in the dark until measurement within 6 h after sampling. We filtered the water sample through a pre-weighted cellulose acetate filter (Whatman, 0.2 µm, 47 mm). To measure the total suspended sediment concentration ([TSS]), we used 20 mL of the collected filtrate. Then, we dried the retained matter on the filter at 105° during 24 h, and we calculated [TSS] by dividing the difference in weights of the filter before and after filtration, by the filtered volume (APHA, 1998). To determine the concentration of dissolved organic carbon ([DOC]) in water samples, we used a duplicate of a

30 mL of the collected filtrate. 30-mL [DOC] samples were stored in pre-combusted (450 °C, overnight) glass tubes, sealed with a Teflon lined cap, after preservation with 36 µL 85% phosphoric acid (H_3PO_4). [DOC] was then measured with a Shimadzu TOC-V CSH analyzer, using potassium phthalate calibration standards over the measurement range (0–450 µmol C L^{-1}).

4.2.5 Environmental variables

A permanent meteorological station, Campbell BWS200 with ARG100—0.2 mm capacity tipping-bucket (Campbell Scientific, Logan, Utah, USA), set up downstream of the swamp recorded rainfall at 1-min intervals. A meteorological station installed in the wetland recorded sediment temperature (°C) at 6-min intervals, using Campbell T108s probes inserted 7.5 cm deep in the wetland sediment (T1). The air temperature (°C) was also recorded at 6-min intervals using a Campbell CS215 probe. The water column temperature (°C) in the wetland was recorded at 6-min intervals with an AquiStar CT2X probe. The global solar radiation (W m^{-2}) averaged at 6 min intervals was recorded using a pyranometer Campbell CS300.

In order to evaluate the solar intensity attenuation by the Napier grass cover (i.e., 100% at the center of the wetland where the experiment was conducted) and to check the dark conditions inside the mesocosms, we measured the solar radiation intensities at 3 different heights above the wetland bottom sediments (380 cm, 100 cm and 3 cm) and inside the mesocosm (Appendix II: Fig. 37). The global solar radiation (W m^{-2}) averaged at 6-min intervals were recorded during two days using 4 pyranometers: SP110 (Campbell CS300) at 380 cm height; RG100 Solems at 100 cm height; Li200X (LI-COR PY34392) at 3 cm height; and RG100 Solems inside the mesocosm.

4.2.6 Apparent Decay Rates, T_{50} and T_{90} values

In this study, what we refer to as ‘apparent’ decay rate (k) accounts for the net equilibrium between the increase and the decrease in *E. coli* concentration due to possible bacteria growth, bacteria mortality, and suspended particles attachment and settlement, i.e., deposition process. The apparent decay rates of *E. coli* for each of the four treatments were estimated by fitting an exponential equation to the bacterial concentration measured over time. The equation has been expressed as a first order kinetic decay proposed by Chick, (1908):

$$C_t = C_i \cdot e^{-kt} \quad (1)$$

$$\ln C_t = \ln C_i - kt \quad (2)$$

where C_t is the measured concentration of *E. coli* at time t in MPN 100 mL^{-1}, C_i is the measured initial concentration of *E. coli* in MPN 100 mL^{-1}, k is the decay rate in day^{-1}, and t is the elapsed time in days. The k value was determined for both the free-living and particle-attached fractions of *E. coli* concentration and for the total *E. coli* concentration. Average k and standard errors were calculated for the triplicates of each treatment. When outliers due to external contaminations were detected, values of k were obtained after excluding the outliers in order to reduce the variance due to external contamination following the possible submersion of a mesocosm.

The time (hours) required for initial bacterial concentration to decrease by 50% and 90% is T_{50} (*E. coli* population half-life) and T_{90}, respectively. The previous equation can be written as:

$$T_{50} = \frac{-\ln(0.5)}{k * 24} \quad (3)$$

$$T_{90} = \frac{-\ln(0.1)}{k * 24} \quad (4)$$

4.2.7 *E. coli* stock variations

In order to estimate the respective contributions of solar radiation and particle deposition to bacterial apparent decay during the experiment, we applied a simple balance method. In this approach, only solar radiation-related decay and suspended particles deposition were assumed to be involved. Therefore, *E. coli* stocks at the start of the experiment (S_o) and after a period of time Δt (S_t) in the water column were compared between the DL and DD treatments. S_0 was obtained by multiplying a normalized initial concentration (C_o = 500,000 MPN 100 mL^{-1}) by the initial volume of water (V_o = 4500 mL). S_t was calculated by multiplying the final volume of water (V_t) by the final *E. coli* concentration (C_f) in DL and DD treatments. C_f was obtained using Equation (1) considering the fitted value of the apparent decay rates (Table 6). The number of decayed *E. coli* in the water column was deduced from the difference between S_0 and S_t at each sampling date Δt. The total number of decayed *E. coli* in the water column (N_t) was calculated considering that DL treatment cumulates the decay effects of both solar radiation and particle deposition. The

number of decayed *E. coli* due to deposition (n_t^D) only was obtained from the DD treatment. Finally, the number of decayed *E. coli* due to solar radiation (n_t^L) was deduced from the difference between N_t and n_t^D. A Monte Carlo approach was then used to quantify the uncertainties in n_t^D and n_t^L calculations (e.g., (Ribolzi et al., 2000)). The details of the equations that describe the *E. coli* stock variations, and their associated uncertainties, are given in the Appendix II.

4.3 Results

The results are presented by first describing the environmental context in the headwater wetland of the Houay Pano catchment during the experiment duration, followed by our main findings as we monitor the temporal variations of physico-chemical and microbiological variables in the mesocosms (Nakhle et al., 2021a). Based on the observations, we calculated the *E. coli* decay rates, T_{50} and T_{90} values, as well as *E. coli* stock variations.

4.3.1 Environmental variables

We measured the solar radiation intensities at 3 different heights above the wetland bottom sediments and inside the mesocosms to evaluate the solar intensity attenuation by the Napier grass cover and to check the dark conditions inside the mesocosms (Appendix II: Fig. 37). Solar radiation measured at 380 cm height, which is above the vegetation height (Appendix II: Fig. 37), ranged between 40 and 1068 W m^{-2} while at 100 cm, which is inside the vegetation, it ranged between 3 and 170 W m^{-2} (Fig. 25). At 3 cm height (under the vegetation), the solar radiation varied between 0 and 91 W m^{-2} (Fig. 25). Solar radiations were highly attenuated inside the wetland vegetation, which blocks an important part of the radiation from reaching the water column and bottom sediment. Inside the mesocosm, the solar radiation were almost completely blocked and dark conditions prevailed (Fig. 25).

We monitored, during the experiment duration, three main environmental variables including rainfall, global solar radiation, and the temperature of the air, swamp water, and swamp sediment (Fig. 26). Three rainfall events over the experiment duration were observed on 9, 10, and 12 August 2019, with a daily cumulative rainfall of 12.2, 12.6, and 8.4 mm, respectively (Fig. 26a). The temperatures measured during the experiment followed diurnal cycles. Air temperature varied between 24 and 36 °C. Likewise, diurnal temperature variations were also observed in wetland

sediment with highest temperatures up to 29 °C recorded during the daytime. Wetland water temperature remained stable around 25 °C (Fig. 26b). The global solar radiation followed diurnal cycles with peaks recorded in the middle of the day with a maximum value of 1160 W m^{-2} (Fig. 26c).

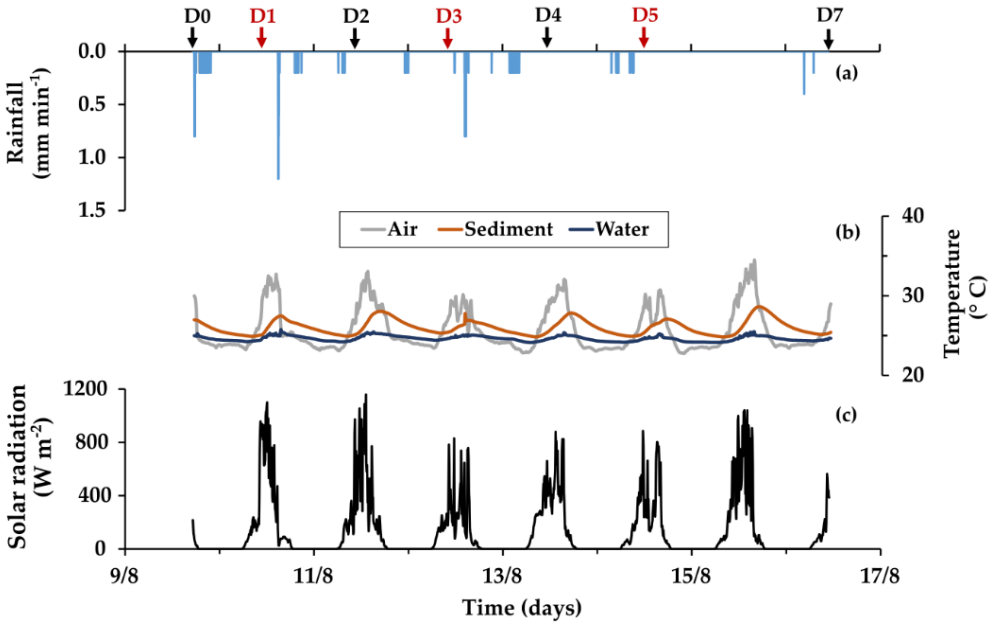

*Figure 26: Temporal variations of environmental variables in the headwater wetland of the Houay Pano catchment, northern Lao PDR, 9–16 August 2019: (**a**) Rainfall (mm min^{-1}); (**b**) Temperatures (° C) recorded in the swamp sediment, in the swamp water, and in the air; (**c**) solar radiation (W m^{-2}). The vertical black arrows above the upper y axis represent the days of sampling to measure turbidity and [E. coli] and the red arrows represent the days of sampling to measure [DOC] and [TSS] in addition to turbidity and [E. coli].*

4.3.2 Physico-chemical and microbiological variables

[TSS] and turbidity decreased over time (Fig. 27a–d). Two different trends are noted. In both light and dark conditions, RD and RL showed stable [TSS] the first 4 days of an average around 0.39 ± 0.20 g L^{-1} and 0.43 ± 0.23 g L^{-1}, respectively, and a slight decrease during the rest of the experiment to reach 0.27 ± 0.04 g L^{-1} and 0.22 ± 0.07 g L^{-1}, respectively. The mesocosms left to deposition processes in DD and DL showed a rapid decrease of [TSS] from the first day of experiment until the end of the experiment, reaching values around 0.02 g L^{-1}. [DOC] increased between the first and the third day of the experiment in the four treatments (Fig. 27e,f). [DOC] increased the most in light conditions, with values ranging from 0.08 to 0.12 mg L^{-1} in RL and 0.08 to 0.19 mg L^{-1} in DL and decreased during the rest of the experiment.

On the first day, [*E. coli*]$_{free}$ in the four treatments ranged from 9,700 to 51,600 MPN 100

mL^{-1} (Fig. 27g,h). [*E. coli*]$_{free}$ decreased over the course of the experiment to reach 0 MPN 100 mL^{-1} on the fourth day in DD and DL, and on the last day in RL. However, the decrease of [*E. coli*]$_{free}$ in RD was slower over time and reached 66 ± 88 MPN 100 mL^{-1} on day 6 but increased again to 2,470 ± 975 MPN 100 mL^{-1} on the last day of the experiment.

On the first day, [*E. coli*]$_{total}$ in the four treatments ranged from 330,000 to 505,000 MPN 100 mL^{-1} (Fig. 27i,j). The changes over time varied from one treatment to another. We can dissociate two distinct trends. The first group corresponds to DD and DL, showing an important [*E. coli*]$_{total}$ decrease during the experiment. The [*E. coli*]$_{total}$ at the end of the experiment was 226 ± 25 MPN 100 mL^{-1} for DD and 50 ± 58 MPN 100 mL^{-1} for DL. Within these two treatments, we also dissociated the faster [*E. coli*]$_{total}$ decrease in the mesocosm exposed to solar radiation (DL) as compared to the mesocosm left in the dark (DD). The second group corresponds to RD and RL, showing a more stable dynamic when compared with DD and DL. Within these two treatments, the mesocosm exposed to light (RL) showed a stable [*E. coli*]$_{total}$ and a slight decrease at the last day of the experiment, while the mesocosm in dark (RD) showed a slight [*E. coli*]$_{total}$ increase. At the end of the experiment, [*E. coli*]$_{total}$ was 38,763 ± 44,890 MPN 100 mL^{-1} for RD and 24,221 ± 33,238 MPN 100 mL^{-1} for RL.

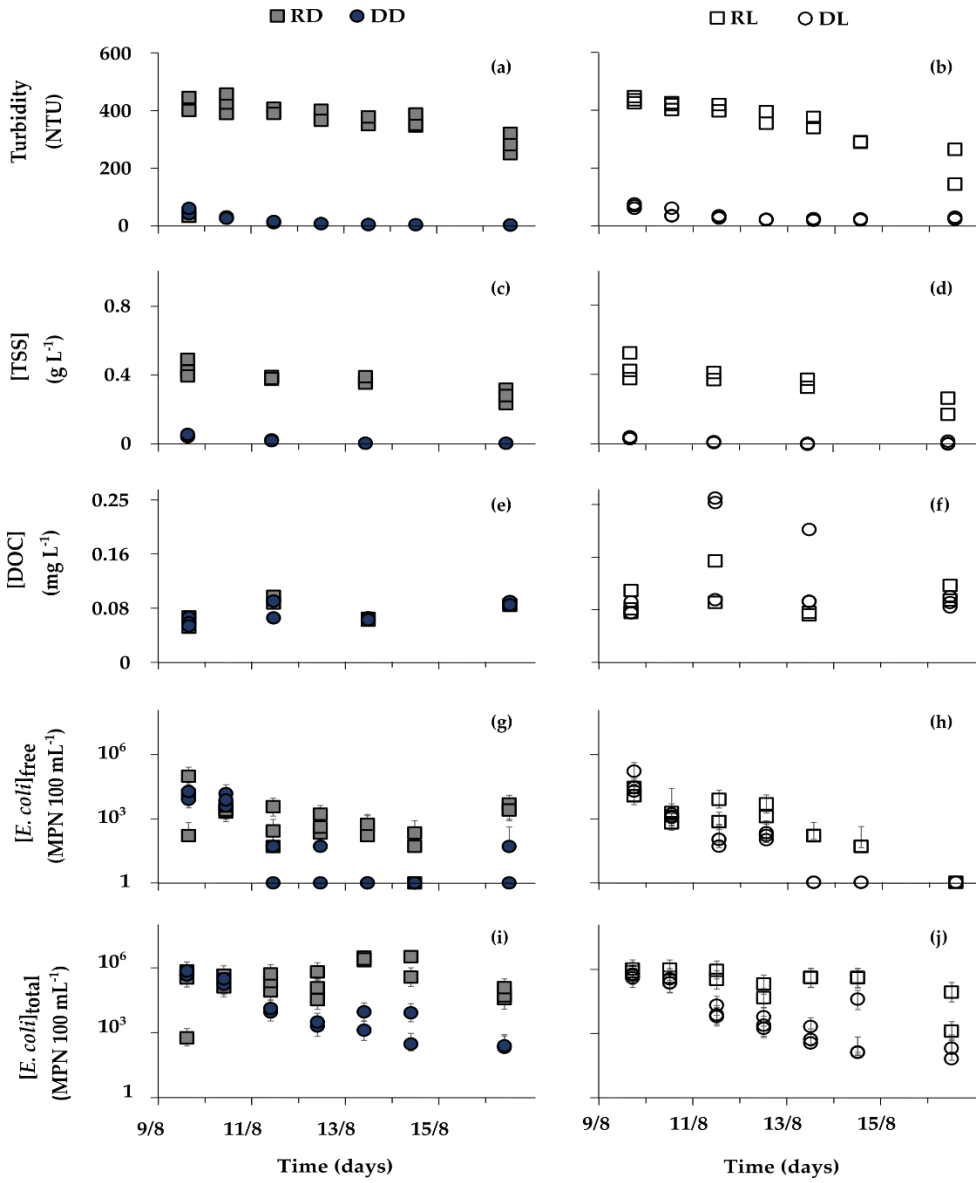

*Figure 27: Temporal variations of physico-chemical and microbiological variables in the mesocosm installed in the headwater wetland of the Houay Pano catchment, northern Lao PDR, from August 9 to August 16, 2019. Left side panels are for Resuspension—Dark (RD) and Deposition—Dark (DD), whereas right panels are for Resuspension—Light (RL) and Deposition—Light (DL). (**a**,**b**) Turbidity: turbidity (NTU); (**c**,**d**) [TSS]: total suspended sediment concentration (g L^{-1}); (**e**,**f**) [DOC]: dissolved organic carbon concentration (mg L^{-1}); (**g**,**h**) [E. coli]$_{free}$: free-living E. coli concentration (MPN 100 mL^{-1}); (**i**,**j**) [E. coli]$_{total}$: total E. coli concentration (MPN 100 mL^{-1}).*

4.3.3 Apparent decay rates and T_{50} and T_{90} values

The apparent decay rates of total *E. coli* concentration for mesocosms left to deposit (k = 1.43 day^{-1} in DL and 1.17 day^{-1} in DD) were higher than in mesocosms subject to resuspension (k = 0.50 day^{-1} in RL and −0.14 day^{-1} in RD). Likewise, the apparent decay rates for mesocosms exposed to solar radiation (RL and DL) were higher than mesocosms left in the dark (RD and DD).

However, in contrast to the majority of treatments, it is important to note the specific behavior of *E. coli* concentration tending to be stable and slightly increasing in RD mesocosms (Table 7).

Similarly, the particle-attached fraction of *E. coli* showed the same dynamics in terms of apparent decay rates in all four treatments. However, more accentuated apparent decay rates of free-living *E. coli* were noted in DL ($k = 1.53\ day^{-1}$), DD ($k = 1.36\ day^{-1}$), RL ($k = 1.20\ day^{-1}$), and RD ($k = 0.28\ day^{-1}$) in a decreasing order. Contrarily to the particle-attached fraction, dynamics of free-living *E. coli* in RD mesocosms tended to decrease over the incubation period ($k = 0.28\ day^{-1}$) (Table 7).

Table 7: Average apparent decay rates k (day−1) ± standard error (day−1) of replicates per treatment for total E. coli and for the free-living and particle-attached fractions of E. coli measured in mesocosms installed in the headwater wetland of the Houay Pano

Treatments	RL	DL	RD	DD
Total	0.50 ± 0.15	1.43 ± 0.15	−0.14 ± 0.37	1.17 ± 0.13
Attached	0.49 ± 0.15	1.41 ± 0.15	−0.15 ± 0.38	1.18 ± 0.13
Free	1.20 ± 0.13	1.53 ± 0.19	0.28 ± 0.35	1.36 ± 0.32

The time required to achieve T_{50}, i.e. 50% reduction of $[E.\ coli]_{total}$, was the longest in RD followed by RL ranging respectively between 117.8 and 33.4 hours, and the shortest for DL followed by DD ranging respectively between 11.6 and 14.2 hours. The particle-attached fraction of *E. coli* showed similar T_{50} values in all four treatments. The T_{50} in RD and RL is divided by two for $[E.\ coli]_{free}$, ranging respectively between 59.4 and 13.9 hours. As for the DL and DD, the T_{50} is similar to the $[E.\ coli]_{total}$, ranging respectively between 10.9 and 12.2 hours (Table 8).

The same dynamics were noted for the time required to achieve T_{90}, i.e. 90% reduction of $[E.\ coli]_{total}$, which was the longest in RD followed by RL, varying respectively between 3,91.2 and 111 hours, and the shortest for DL followed by DD, varying respectively between 38.6 and 47.2 hours. The particle-attached fraction of *E. coli* showed similar T_{90} values in all four treatments. The T_{90} in RL and RD is divided by two for $[E.\ coli]_{free}$, varying respectively between 197.4 and 46 hours. As for the DL and DD, the T_{90} is similar to the $[E.\ coli]_{total}$, varying respectively between 40.6 and 36.1 hours (Table 8).

Table 8: T50 (h) and T90 (h) values for total E. coli and for the free-living and particle-attached fractions of E. coli measured in mesocosms installed in the headwater wetland of the Houay Pano catchment, northern Lao PDR, from August 9 to August 16, 2019:

Treatments	**RL**		**DL**		**RD**		**DD**	
	T_{50}	**T_{90}**	**T_{50}**	**T_{90}**	**T_{50}**	**T_{90}**	**T_{50}**	**T_{90}**
Total	33.4	111	11.6	38.6	117.8	391.2	14.2	47.2
Attached	33.9	112.8	11.8	39.2	110.9	368.4	14.1	46.8
Free	13.9	46	10.9	36.1	59.4	197.4	12.2	40.6

4.3.4 *E. coli* stock variations

The *E. coli* stock variations approach allowed us to estimate the respective contribution of each factor separately, deposition and solar radiation, to bacterial apparent decay over the duration of the experiment (Fig. 28). The deposition accounted for the decrease in initial *E. coli* number by an average of 64% at day 1 of the experiment, by 89% at day 2, and by more than 96% from day 3 till the end of the experiment. Solar radiation accounted for the decrease in initial *E. coli* number of around 7% at day 1, 4% at day 2, and the contribution continuously decreased till the end of the experiment (Fig. 28). The deposition process accounted for an average of 92% of the decayed *E. coli* number over the experiment duration, while solar radiation accounted for around 2%. The remaining 6% is the residual fraction of decayed *E. coli* in the experiment (Appendix II: Fig. 40).

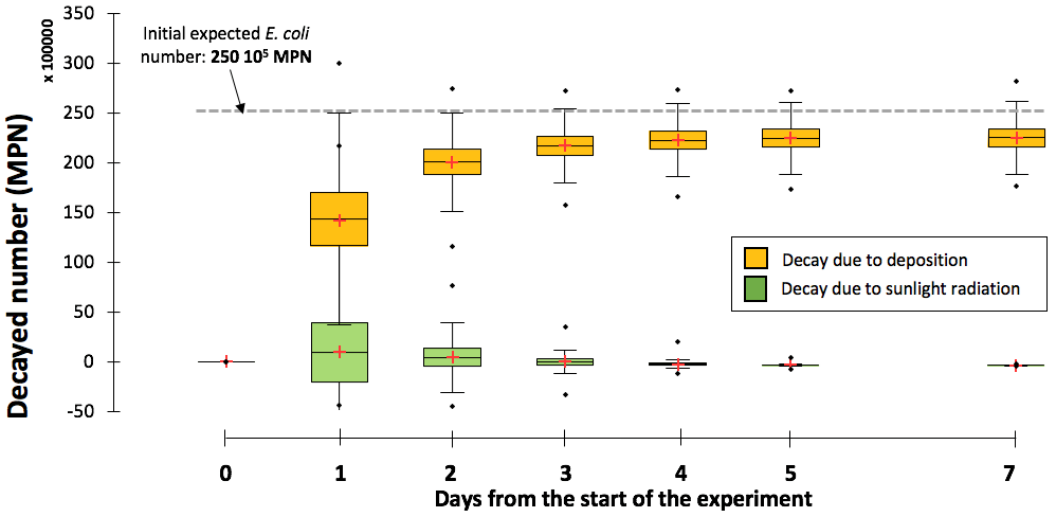

Figure 28: Temporal variations of estimated decayed E. coli number (MPN) due to particle deposition (yellow boxplots) and to solar radiation (green boxplots). The red crosses indicate the means, and the central horizontal bars are the medians. The lower and upper limits of the box are the first and third quartiles, respectively. The lower and upper lines of the boxes are the 10th and 90th percentiles, respectively.

4.4 Discussion

Most studies on factors impacting *E. coli* in the environment have been carried out in laboratory conditions (Haller et al., 2009; Maraccini et al., 2016; Walters et al., 2014; Wang et al., 2018). No comparable *in situ* studies for wetland ecosystems in a tropical humid context, such as that of the montane northern Lao PDR presented in this paper, were found in the scientific literature. This experiment provided an opportunity to study the factors controlling the apparent decay rates of *E. coli* in a tropical headwater wetland: (i) *E. coli* concentrations in the Houay Pano stream were usually high (mean initial concentration in this study > 400,000 MPN 100 mL^{-1}) and changes in concentration along the incubation period could therefore be easily observed; (ii) the wetland configuration allowed installing 15 mesocosms to study the effect of both the natural solar radiation, and the suspended particles deposition; (iii) the artificial resuspension process, prior to each sample collection allowed us to access the dynamics of deposited bacteria in the bottom sediment. Even though the multiple processes are more complex and interactive under natural conditions, the outcomes from the semi-controlled environmental conditions of our study are important for determining the effect and the relative importance of the two factors tested here, particle deposition and solar radiation, on the apparent decay rates.

4.4.1 Particle attachment effect on *E. coli* apparent decay rates

In our work, particle-attached bacteria predominated in all mesocosms during the experiment, with a mean of 97% ± 6% in RD; 99% ± 3% in RL; 91% ± 22% in DL; and 98% ± 4% in DD. It is interesting to note that both [TSS] and turbidity were strongly correlated (Spearman correlation, $p < 0.05$) with $[E.\ coli]_{total}$ in RL ($r = 0.87$; $r = 0.79$, respectively), DL ($r = 0.67$; $r = 0.72$, respectively), and DD ($r = 0.88$; $r = 0.93$, respectively). On the contrary, [TSS] and turbidity were not significantly correlated with $[E.\ coli]_{total}$ in RD. It is well documented that bacteria, including *E. coli*, tend to be attached to particles within the water column (Malham et al., 2014; Oliver et al., 2007; Petersen and Hubbart, 2020a), and several studies have identified positive correlations between TSS and *E. coli* concentration in tropical aquatic systems (Byamukama et al., 2005; Nakhle et al., 2021c; Nguyen et al., 2016). We observed that k values for free-living *E. coli* (k = 1.53 day^{-1} in DL; 1.36 day^{-1} in DD; 0.49 day^{-1} in RL; 0.28 day^{-1} in RD) were higher for the particle-attached *E. coli* (k = 1.41 day^{-1} in DL; 1.18 day^{-1} in DD; 1.20 day^{-1} in RL; −0.15 day^{-1} in RD). Yet, our [DOC]

measurements in the water column, over the incubation period, show that organic matter was not a factor limiting the survival of bacteria inside the mesocosms (Fig. 27e,f). The rapid reduction of free-living *E. coli* concentration from the water column in the mesocosms (Fig. 27g,h) can be partly attributed to predation-related mortality (Davies and Bavor, 2000; Korajkic et al., 2013; Wanjugi and Harwood, 2013), as also stated in a study on lake water mesocosms in Germany (Brettar and Hoflet, 1992). Our results are in alignment with previous studies that reported significantly lower decay rates for bacteria associated with particles as opposed to free-living *E. coli* (Craig et al., 2004; Davies et al., 1995). The association of FIB with particles in water can improve their survival by providing protection against the bactericidal effects of light (Davies-Colley et al., 1999; Farrell et al., 2018; Fujioka et al., 1981; Kapuscinski and Mitchell, 1983; Madge and Jensen, 2006; Perkins et al., 2016; Sinton et al., 2002). A study investigating the effect of particle size on *E. coli* solar inactivation (Walters et al., 2014), showed that 91% of *E. coli* were associated with particle sizes < 12 μm, and that they were inactivated on average two times faster than those associated with the larger particle fraction between 12 and 63 μm. In Houay Pano catchment, during low intensity floods, the median size of suspended particles ranged between 6 and 24 μm due to the particle sorting process and reduced water velocity within the wetland (Huon et al., 2017). The wetland hydrodynamic configuration, given the limited hydraulic radius of the wetted area, low flow velocity, and low slope, can significantly favor particle deposition processes. Therefore, suspended particles, not only provide benefits to bacteria, but also are vectors for bacterial transport settling in bottom sediment (Droppo et al., 2009) thereby providing a new environment for the cells.

4.4.2 Deposition effect on *E. coli* apparent decay rates

E. coli concentration in mesocosms left to deposition (DL and DD) decreased faster than in mesocosms exposed to daily resuspension (RL and RD) (Fig. 27i,j). The decrease in total *E. coli* concentration in the water column in the absence of resuspension (DD and DL) might be due to the process of bacterial trapping by sediment deposition, along with the process of bacterial mortality. Under deposition conditions, there was a 96% decrease in the total initial *E. coli* concentration in the first 24 h following the incubation, emphasizing the importance of the deposition process on the reduction of *E. coli* concentration within the water column. These findings are consistent with a previous study conducted in the Houay Pano catchment (O. Ribolzi et al., 2011), which reported a rapid drop in the concentrations [TSS] and particle-attached *E. coli*

within a short distance (100 m) downstream from the wetland. These observations (O. Ribolzi et al., 2011) along with other reports (Thornton et al., 2007) have also pointed out the filtering effect of wetlands, where aquatic plants can trap 30 to 70% of the suspended sediments. Therefore, it is likely that the headwater wetland represents a long-term sediment accumulation zone within the Houay Pano catchment (Huon et al., 2013).

In re-suspension treatments (RL and RD), the observed slight increase of *E. coli* concentration (Fig. 27i,j) reflects the balance between bacterial mortality and bacterial survival and/or growth in deposited sediments. Another study found that FIB decay rates were much lower in sediments than in the water column, indicating a potentially important role of sediments in harboring FIB populations (Craig et al., 2004; Nguyen et al., 2016). Recent studies have demonstrated that bottom sediments can act as a major reservoir of FIB harboring much more concentrated populations of microorganisms than the overlying water column (Buckley et al., 1998; Crabill et al., 1999; Jamieson et al., 2005; Smith et al., 2008). Further, bottom sediments can be mobilized by resuspension events, contributing to the bacterial input to surface waters (Boithias et al., 2021b; Fries et al., 2008; Pachepsky and Shelton, 2011). In a recent microcosm study (Smith et al., 2019), *E. coli* concentration increased in clayey sediment during the first 8 days of incubation before starting to decrease until the end of the experiment which lasted for 57 days. Our results are also comparable to that of a 50-day microcosm study of Geneva lake water contaminated with freshwater sediments (Haller et al., 2009) that found a growth phase between the 5th and 12th days of incubation and low decay rates of 0.29 day^{-1} in fine-textured sediments containing higher levels of organic matter. In the present study, the results of the RD treatment allowed to access *E. coli* in bottom sediments, suggesting that *E. coli* can survive, explaining the stable *E. coli* concentration observed during the first 5 days in RL and RD. These results must be qualified given the higher uncertainty compared to the other treatments (Appendix II: Fig. 41). In future studies, a longer period of observation of at least 30 days should be privileged, to allow a better understanding of the potential *E. coli* survival in secondary habitats, in order to better mitigate their potential impact on public health. Moreover, the utility of *E. coli* as an environmental FIB might be challenged given its likely ability to persist and grow under certain conditions likely to be found in tropical contexts (Nowicki et al., 2021; Rochelle-Newall et al., 2015).

4.4.3 Solar radiation effect on *E. coli* apparent decay rates

The total *E. coli* apparent decay rates k obtained in the mesocosms exposed to solar radiation ranged between 0.49 day^{-1} (RL) and 1.43 day^{-1} (DL), whereas in covered mesocosms, it ranged between −0.14 day^{-1} (RD) and 1.19 day^{-1} (DD) (Table 8). These results can be compared to the values of k obtained in a study carried out by Nguyen et al., (2016) in the Red River in northern Vietnam, where the total *E. coli* decay rates under dark conditions ranged from 0.01 to 1.13 day^{-1}. Hence, in the present work, a higher k was noted in RL when compared to RD, and it was also noted in DL when compared to DD. Several studies showed that solar radiation causes inactivation of a wide range of microorganisms present in water (Davies-Colley et al., 1999; Noble et al., 2004a). In particular, the U.V.-B part of the spectrum causes direct photo-biological damages degrading the nucleic acids within bacteria (Eisenstark, 1971; Sinton et al., 2002; Ziegelhoffer and Donohue, 2009). Both previous field observations and laboratory experiments have pointed out the importance of solar radiation in reducing FIB concentrations in surface waters. Research focusing on the impacts of solar radiation on FIB like *E. coli* have been mainly conducted in marine aquatic environments (Fujioka et al., 1981; Kay et al., 2005; Sinton et al., 2002). In a study carried out in subtropical coastal ecosystems (Chan et al., 2015), light intensity was identified as the most significant factor affecting *E. coli* decay rate as compared to dark conditions. In fact, the *in situ* bacterial decay rates found in (Chan et al., 2015), ranged between 1.3 and 5.1 day^{-1} and increased significantly with light intensity. Few studies only deal with freshwater ecosystems (Maraccini et al., 2016; Sinton et al., 2002). For instance, in a study conducted in Lake Michigan, USA (Whitman et al., 2004), an exponential decrease in *E. coli* counts was noted in the upper 90 cm of the lake during sunny days, contrasting with the much weaker *E. coli* inactivation noted during cloudy days.

In shallow aquatic ecosystems, sunlight penetration into the water column can be considered among the most important factors in bacterial inactivation and decline (Maraccini et al., 2016). However, tropical wetlands are often characterized by dense vegetation thereby limiting sunlight penetration (Milliman, 1995). Our study showed the attenuation of solar radiations by dense vegetation within the wetland, preventing most of the light from reaching the water column (Fig. 2; Appendix II: Fig. 39). Moreover, it seems important to take into account the impact of vegetation type and density on flow reduction within wetlands, which further impacts bacterial transport and fate.

While solar radiation can significantly affect *E. coli* survival, UV radiation can be scattered by TSS (Madge and Jensen, 2006; Walters et al., 2014) in highly turbid water following a resuspension event or surface runoff, especially during the rainy season in tropical environments. In a study conducted in estuarine and coastal waters in the UK (Kay et al., 2005), the bacterial decay in highly turbid water (> 200 NTU) exposed to solar radiation did not differ from their decay rates observed under dark conditions. When assessing the effect of solar radiation on *E. coli* reduction, it is therefore imperative to take into account the effect of TSS in the water column.

4.4.4 Relative effects of light and sedimentation on *E. coli* apparent decay rates

In order to identify the relative importance of the two studied factors, namely solar radiation and deposition process, in the apparent bacterial decay, we compared the percentages of *E. coli* stock variations attributed to each factor at each sampling date. A comparison of DL with DD indicates that the deposition process accounts for an average of 92% of the decayed bacterial number over the experiment duration, while 2% corresponds to the effect of solar radiation (Fig. 28 and Appendix II: Fig. 40). In DL and DD mesocosms, the T_{90} value was similar when exposed to solar radiation (DL, 38 h) and when in dark (DD, 47 h), whereas in RL and RD mesocosms, the T_{90} value was 111 h and 391 h respectively (Table 7). A study in the UK (Kay et al., 2005) showed lower T_{90} values of 24.8 h in low-turbidity estuarine waters in dark conditions, and 6 h when exposed to solar radiation. Although a large number of studies have been highlighting the solar radiation effect on *E. coli* T_{90} (Jozić et al., 2014; Tavares Carneiro et al., 2018), it is also imperative to consider other predominant factors like TSS dynamics as well as deposition and resuspension processes when investigating bacterial decay rates in aquatic ecosystems such as tropical wetlands, which are common landscape features especially in the mountainous area of northern Lao PDR and in the tropical Southeast Asia in general (MacAlister and Mahaxay, 2009). Deposition processes occurring in aquatic ecosystems are rather complex, influenced by multiple factors such as TSS concentrations, size, and settling velocity (Le et al., 2020), presence of dense vegetation (Chao et al., 2015), as well as hydrodynamic conditions (stream flow velocity, slope gradient, and turbulence in water column) (Teeter et al., 2001). The importance of *E. coli* reduction due to deposition depends largely on whether the bacteria are associated to particles which are vectors for vertical migration of bacteria within the water column (Droppo et al., 2009). In our study, more than 91% of total *E. coli* were attached to particles in all mesocosms over the incubation period. Our findings

are consistent with the studies that found that deposition process is identified as a key process involved in bacterial reduction and is widely used to decontaminate water in constructed wetlands. At local scales, wetlands have been shown to contribute to the regulating ecosystem service of reducing waterborne pollutant loading to downstream environments.

Wetlands act as a natural sanitation system (Morgan et al., 2008), providing a nature-based solution for water quality improvement. Over the last century, constructed wetlands have been designed to include physical, biological, and chemical processes similar to those occurring in natural wetlands. Today, constructed wetlands are recognized as a suitable alternative wastewater treatment technology in many countries (Almuktar et al., 2018; Mthembu et al., 2013; Paing et al., 2015; Sani et al., 2013; Scholz, 2010). An accurate understanding of FIB controlling factors in lentic systems like wetlands is fundamental for a better management of natural as well as constructed wetlands, in the perspective of the effective conservation of the valuable ecosystem services that they deliver. Such an improved understanding is especially critical in rural areas of developing tropical countries whose populations directly rely on untreated surface waters (Boithias et al., 2016).

4.5 Conclusion

This study aimed to determine *E. coli* apparent decay rates, i.e., the net equilibrium between the increase and the decrease in *E. coli* concentration due to possible bacteria growth, bacteria mortality, and deposition process, in a tropical headwater wetland. The environmental variables assessed were solar radiation and suspended particles deposition.

- Particle-attached bacteria prevailed in all mesocosms over the incubation period: over 91% of total *E. coli* were attached to particles.
- Apparent decay rates of free-living bacteria were higher than apparent decay rates of particle-attached bacteria in all mesocosms.
- Apparent decay rates of total *E. coli* concentration in mesocosms left to deposit ranged from 1.43 ± 0.15 to 1.17 ± 0.13 day^{-1} when exposed to light and dark conditions, respectively. Apparent decay rates in mesocosms stirred prior to sampling ranged from 0.50 ± 0.15 to -0.14 ± 0.37 day^{-1} when exposed to light and dark conditions, respectively.

- Deposition accounted for an average of 92% of the estimated *E. coli* stock reduction in the water column, while 2% of the estimated *E. coli* stock reduction was due to the exposure to solar radiation.
- By resuspending the bottom sediment prior to sample collecting in RD mesocosms, we mobilized the deposited *E. coli* that showed stable concentration during the first 5 days of the experiment, suggesting a survival of bacterial population in bed sediments.

The improved understanding of factors controlling *E. coli* fate should be exploited to further develop practical strategies for a better management of natural ecosystems like wetlands. This work brings insights to improve modeling approaches in tropical contexts by providing a range of bacterial decay rates to parameterize hydrological and water quality models.

Chapter 5. Impact of hydropower dams on hydro-sedimentary and *Escherichia coli* dynamics on watershed-scale, case of Nam Khan river in the lower Mekong basin

Introduction to chapter 5

Given the importance of various environmental (TSS, hydrology) and anthropic factors (land use) in FIB dissemination reported in this thesis and in previous studies, it only seemed reasonable to investigate the impact of rapidly developing hydropower dam projects on FIB dynamics. Driven by the fast-paced development in Southeast Asia, rivers are being regulated and altered due to the boom in dam constructions. In the context of rapid global changes, assessment of such infrastructure on river ecosystem and public health are not well established before their operations. Therefore, very little knowledge exist on dam-induced impacts on FIB dynamics and the associated health risks. This chapter brings some insights on changes in the hydro-sedimentary and *E. coli* dynamics under dam impact at large watershed-scale, Nam Khan, Lao PDR. In addition to the dam retention potential of TSS and *E. coli*, the concerns about bacterial fate in dam reservoirs arise and deserve urgent further investigations.

This work was based on statistical analyses, coupled with a first exploratory modeling approach using SWAT tool and modified bacteria module at large watershed-scale. These preliminary results point out the need to improve the model performance, but also the new opportunities to explore this research field that could help stakeholders to better manage water resources.

Abstract

The Mekong River, well known for its rich aquatic ecosystem, sustains the livelihoods of over 60 million people who are highly vulnerable to changes in surface water quality. This study aims to assess the impact of a hydropower dams constructed in 2014 in the Nam Khan watershed, northern Lao PDR, on changes in discharge regime, and fluxes of total suspended sediment (TSS) and fecal bacteria like *Escherichia coli* (*E. coli) downstream the* reservoir. In this context, we aimed at first, to detect trends and change points in a 10-year record of pre and post-dam discharge, and TSS and *E. coli* concentrations, at two monitoring stations downstream, using Pettitt-test, Mann-Kendall and Double mass curve approaches. Significant change points were detected for measured discharge, and TSS and *E. coli* concentrations, in 2013, 2015 and 2016 respectively. The absence of significant precipitation trend between 2011 and 2020 and the presence of abrupt changes in time-series, likely reflects dam-induced hydrological disruptions in the Nam Khan watershed. Furthermore, we aimed to quantitatively estimate the dam impact on river discharge, and TSS and *E. coli* concentrations. To do so, we have used the Soil and Water Assessment Tool (SWAT) to simulate the discharge, sediments and bacteria, excluding the presence of dams, in order to compare unregulated simulated variables (no dam) with observed variables (with dam). Overall, mean river discharge observed between 2014 and 2019 were 42% below pre-dam mean and 54% below simulated unregulated discharge mean, which can suggest a strong dam effect on the hydrological regime of the Nam Khan watershed. The model performance in this first exploratory study was judged not satisfactory for TSS and *E. coli*, with NS of -0.10 and -0.15 respectively. Therefore, further improvements are still needed for sediment and bacterial fate and transport simulation at catchment-scale in order to optimize the model performance. Overall, the findings of this work knowledge can help improve our understanding of dam impact on water quality, which is important in the development of effective strategies for water resource management.

5.1 Introduction

Water quality is the key factor in determining environmental health (WHO, 2016b). Many vulnerable communities worldwide rely on unimproved surface water for their daily domestic uses, due to inadequate sanitation facilities and low access to safe water resources (Prüss-Ustün et al., 2019). This is, for instance, the case of the Mekong basin where main livelihoods of rural

populations are highly vulnerable to changes in surface water quality. Fecal contamination of surface water is one of the major water quality issues in the developing countries of Southeast Asia (SEA), which is expected to be exacerbated by various anthropogenic pressures and rapid global changes (e.g. deforestation, hydropower development, climate change, etc.) (UNEP, 2016). The probable presence of fecal pathogens in water bodies can be detected using low-cost reliable proxies, namely Fecal Indicator Bacteria (FIB) such as *Escherichia coli* (*E. coli*) (WHO, 2011b). Many waterborne diseases like diarrhea, can be caused by fecal pathogens , are still, up to this day, a leading cause of mortality, especially among children under five years old in the tropical SEA countries (Boithias et al., 2016; GBD LRI Collaborators, 2017).

Several studies have improved our understanding of the fate and transport of FIB in SEA tropical watersheds (Rochelle-Newall et al., 2016), in Singapore (Ekklesia et al., 2015b), Vietnam (Isobe et al., 2004; Nguyen et al., 2016), Africa (Robert et al., 2021), and in Lao PDR (Boithias et al., 2021b; Causse et al., 2015; Nakhle et al., 2021c; O. Ribolzi et al., 2011; Ribolzi et al., 2016). Despite the increasing number of studies in the tropical area, many knowledge gaps remain on the anthropogenic impact on FIB fate at large tropical watershed-scale, due to limited data and to the absence of adequate structures for the long term monitoring of FIB dynamics (Rochelle-Newall et al., 2015). Considering the known risks for public health associated with such microbiological pollutants, it is necessary to further investigate the impact of fast-paced human activities like hydropower development on FIB spatio-temporal dynamics in tropical aquatic ecosystems.

With the rapid economic development of SEA and the intensifying pressure on water demand, Mekong is undergoing unprecedented extensive hydropower dam construction throughout its basin (Grumbine et al., 2012; MRC, 2011c). Despite the perceived benefits of the “clean renewable energy”, there is increasing evidence showing direct significant hydrological and ecological repercussions threatening the world’s most biodiverse rivers, including Mekong (Poff and Zimmerman, 2010; Winemiller et al., 2016). Multiple large hydropower dams have resulted in considerable discharge changes in the Mekong River associated to an attenuation of the seasonal variability downstream of the dams (Hecht et al., 2019b; Piman et al., 2013; Pokhrel et al., 2018; Räsänen et al., 2017). The disruption of the Mekong seasonal flood pulse governed by the monsoon climate (MRC, 2005), results in a disruption of sediments and nutrients transport to downstream environments and extensive floodplains inundation (Junk and Wantzen, 2007).

Several studies reported significant sediment retention in the dam reservoir (Gao et al., 2010; Vörösmarty et al., 2010), which creates sediment-starved or "hungry" water downstream with an increased erosive potential (Kondolf, 1997; Manh et al., 2015). Sediment particles and sediment transport processes in turn affect the transport of bacteria, including fecal pathogens which tend to be particle-attached in the water column (Malham et al., 2014; Oliver et al., 2007), especially in tropical aquatic systems (Byamukama et al., 2005; Nakhle et al., 2021c; Nguyen et al., 2016) where water is often more turbid (Milliman et al., 1983).Hydropower dams interrupt the river connectivity, which can result in not only sediment retention, but also FIB retention in the dam reservoir. Hence, it is possible that dams attenuate the contamination in downstream environment. Recent studies in n China, have stated dam impact on spatial isolation of sediment bacterial distributions (Chen et al., 2020, 2018). However, to our knowledge, no studies have investigated the changes in FIB dynamics induced by dam construction. On the other hand, given the potential FIB survival in sediments reported in various environments within the tropical context (Nakhle et al., 2021b; Pachepsky and Shelton, 2011; Rochelle-Newall et al., 2015), dams can also lead to serious consequences on the water quality and the implemented activities directly relying on untreated surface waters (fishing, irrigation or daily domestic uses),. . Therefore, understanding the impact of hydropower dams on water quality is crucial for the sustainability of river basins and for public health safety especially in Southeast Asia where access to clean water, sanitation and hygiene remains challenging.

Modeling is an interesting approach to assess global changes impact on dynamics of river discharge, suspended sediments, nutrients and pathogens at large watershed-scale. The mechanistic semi-distributed model Soil and Water Assessment Tool (SWAT) has been successfully applied to predict the impact of land use and climate change on sediment transport in Southeast Asia (Tan et al., 2019) and in the Mekong basin particularly (Shrestha et al., 2018, 2013; Sok et al., 2020). Recent advances have improved the ability of SWAT to simulate *E. coli* numbers in a small-scale tropical montane catchment after including bacteria resuspension process as well as hyporheic exchange, and regrowth processes (Kim et al., 2017).

To our knowledge, no information exists on hydropower-induced effects on FIB transport in the tropical context. Furthermore, impact assessments of hydropower dams on hydro-sedimentary and bacterial fluxes alteration, are limited in Mekong tributaries due to the relatively

restricted number of streamflow stations downstream of dams with long pre and post-dam water quality monitoring records (>10 years) (Lacombe et al., 2014; Lyon et al., 2017).

In this study, we hypothesized that hydropower dam induced changes in discharge regime, and reduced the transfer of sediments and bacteria to the downstream environment. Hence, our general objective here is to identify changes in discharge patterns as well as sedimentary and bacterial transfer patterns in a Mekong tributary, Nam Khan, under the impacts of a hydropower dam constructed in 2014. In this context, we aimed at first, to detect trends and change-points in a 10-year record of pre and post-dam discharge and total suspended sediments and *E. coli* concentrations, at a monitoring station downstream the dam, using change-point detection statistical approach. Furthermore, we aimed to quantitatively the dam impact on river discharge, and TSS and *E. coli* concentrations excluding the presence of a dam using SWAT, in order to compare it with the observed variables. Finally, we aimed to test the SWAT model performance in simulating *E. coli* numbers in the large-scale Nam Khan watershed, using the modified bacteria module developed by Kim et al., (2017).

5.2 Material and methods

5.2.1 Study area

The study area is the Nam Khan watershed in northern Lao PDR (Fig. 29). Nam Khan river is a first order tributary of the Mekong River, located on its left bank in the northern mountainous part of the Lao PDR within 101.916667-103.716667 and 19.366667-20.283333, and covers a total area of 7,448 km^2. The elevation ranges from 263 to 2,035 m above the mean sea level (m a.s.l). The average slope across the watershed is between 15% and 17.5%.

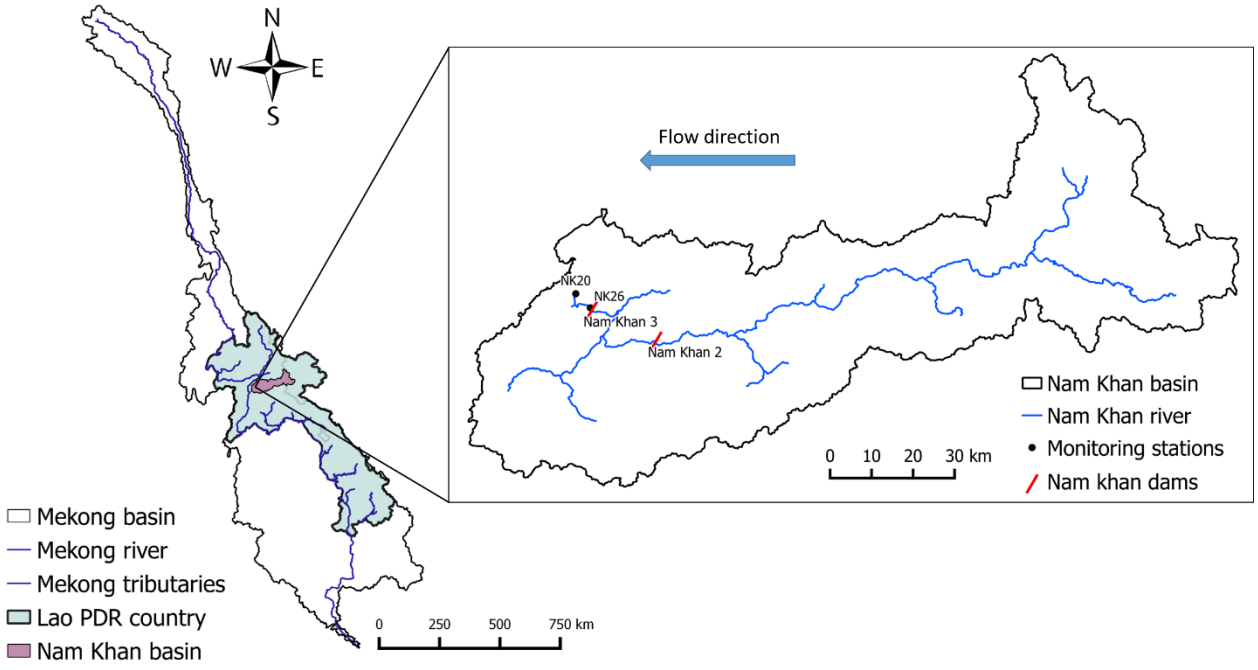

Figure 29: Location of the Nam Khan watershed in Lao PDR, of the two monitoring stations (NK26 and NK20) along the river, and of the two hydropower dams currently operated (Nam Khan 2 and 3).

The climate is characterized by two distinct seasons: a wet season from May to October, and a dry season from November to April. The mean annual temperature (2008-2020) ranges from 20 to 30 °C. The mean annual rainfall is about 1,495 mm (CV= 0.31), with an average of 83% occurring during the wet season (2008–2020). Major soil type in this river watershed is haplic acrisol, covering nearly 94 % of its total area. Land-use data from the Department of Agricultural Land Management (DALaM 2015) shows that the dominant land covers in the watershed are shrub-land and forests covering respectively around 56 % and 32 % of the total watershed area. Most of the cultivated area of the watershed is dominated by annual crops and commercial perennial monocultures, typical of the rural landscape in northern Lao PDR..

The Nam Khan River flows into the Mekong at Luang Prabang city, a major commercial, transport and touristic hub in the area with 431,889 habitants in 2015, 68% of which is rural (Lao Statistics Bureau, 2016). To meet the increasing need for electricity, the hydropower project developed in the Nam Khan watershed by Electricité du Laos (EDL) and the Chinese company Sinohydro, consisted in a cascade of two dams (Fig. 30). The Nam Khan 2 hydropower project construction began in 2011 and was operational in 2015, with a generating capacity of 130 MW and total storage area of 30.6 km^2 (19.685, 102.367). The construction of Nam Khan 3 hydropower

dam, located downstream of Nam Khan 2 dam, started in 2014 and was operational in 2016, with a generating capacity of 60 MW (19.749, 102.220) (WLE, 2020).

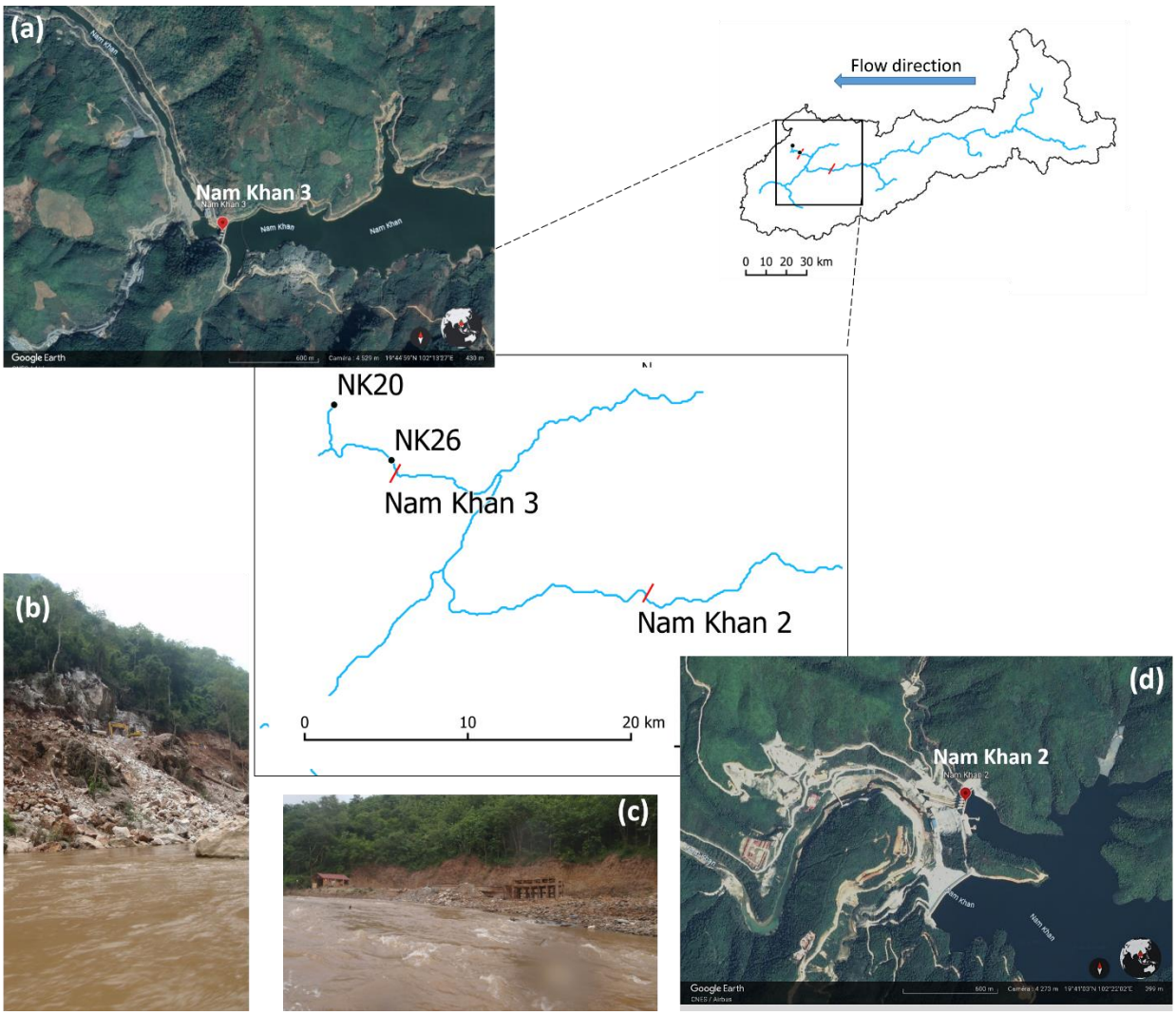

Figure 30: Location of the two monitoring stations (NK26 and NK20) along the Nam Khan river, and of the two hydropower dams currently operated (Nam Khan 2 and 3). (a, d): images taken from Google Earth of Nam Khan 3 and 2 respectively; (b,c): photos taken along the Nam Khan river in 2011 by Olivier RIBOLZI.

5.2.2 Monitoring data

The Nam Khan is monitored downstream of the dam at two monitoring stations NK26 (19.75536, 102.21755) located directly downstream of Nam Khan 3 dam, and NK20 (19.78602, 102.18336) located downstream of NK26 (Fig.30). Water heights are recorded twice per day between 2008 and 2019 at NK20 station by the National Meteorological and Hydrological Center of Lao PDR. A control-rating curve (water level-discharge relationship) was determined using the

velocity area method to calculate the daily discharge of the Nam Khan river.

The water quality measurements were taken from the dataset collected within the framework of the Critical Zone Observatories Multiscale TROPIcal CatchmentS (CZO M-TROPICS) (Ribolzi et al., 2021). The dataset comprised a set of physico-chemical parameters including temperature (T), pH, dissolved oxygen (DO), and electrical conductivity normalized to 25 °C (EC) measured *in situ* every 15 days between 2011 and 2016, and every 10 days between 2017 and 2020, using a Multi Probe System with a data logger (YSI 556 MPS). Concentrations of DO were transformed to oxygen saturations (%), using the Hua formula (Hua, 1990).

In addition to the previously mentioned variables, water turbidity was monitored regularly every 15 days, using a turbidity meter (EUTECH Instruments). Water samples of 500-mL were collected 10 cm beneath the water surface in sterile plastic containers and conserved them at a low temperature in the dark until laboratory analysis. A subsample of which was used to measure the Total Suspended Sediments concentrations ([TSS]) *in situ* starting 2013; therefore, we used the regular turbidity measurements to establish a linear regression (turbidity-total suspended sediments, 2013-2020) in order to determine [TSS] (TSS-NTU) at 15-day time interval between 2011 and 2020.

. Another subsample of the collected water was analyzed within 24 h for *E. coli* counts using the standardized microplate method (ISO 9308-3). This technique is based on a 48-hour incubation at 44 °C at four dilution rates (1:2, 1:20, 1:200, 1:2000) in a culture medium specific for *E. coli* on a 96-well microplate (MUG/EC, Biokar Diagnostics). The number of positive wells for each microplate after incubation (fluorescent under UV light) allows the concentrations of *E. coli* to be calculated using a statistical analysis based on Poisson's distribution. The concentration of *E. coli* ([*E. coli*]) is expressed in MPN 100 mL^{-1} and used as an indicator of the fecal contamination (Lebaron et al., 2005).

5.2.3 Statistical approach

In the present study, Pettitt test, with a statistical significance level of 5%, was used to assess the occurrence of change points in records of rainfall, river discharge at NK20, and [*E. coli*] and [TSS] at NK20 and NK26, downstream of the constructed dam. The daily rainfall data

(averaged over the watershed area) was obtained from Multi-Source Weighted-Ensemble Precipitation (MSWEP V2) (Beck et al., 2017) . The Pettitt nonparametric test proposed by Pettitt, (1979) is a rank-based test which has been widely adopted to identify changes in hydrological and climatic time series (Kundzewicz and Robson, 2000; Palaniswami and Muthiah, 2018; Zuo et al., 2014).

The Mann–Kendall test (MK test) was applied to detect the long-term trends of MSWEP rainfall, river discharge at NK20, as well as [*E. coli*] and [TSS] at two monitoring stations, NK20 and NK26, downstream of the constructed dam. The rank-based Mann–Kendall non-parametric test was originally proposed by Mann (1945) and later reformulated by Kendall (1975). This method has been widely applied for general use throughout the world, due to its robustness for non-normally distributed data. The Mann–Kendall Z statistic was used for significance testing. A positive value of Z represents an upward trend, while a negative Z value indicates a negative trend.

Double mass curves (DMC) is a graphical method based on a scatter plot of cumulated values of two parameters (i.e. rainfall and river discharge) over a defined time span (Searcy and Hardison, 1960). This method was initially developed to investigate the consistency of hydro-meteorological time series. Currently, DMC method is frequently applied to assess the responses of the river discharge to climate change and human disturbance (Gao et al., 2017; Huo et al., 2008). Theoretically, the ratio of the studied variables is a constant if both variables are equally affected by external disturbances. Slope breaks help us to determine the change point driven by the occurrence of various external factors (deforestation, dam construction, etc.). In the present study, DMC of rainfall with (i) river discharge, (ii) TSS load and (iii) *E. coli* load, was used as a supplementary confirmation of the detected change points induced by human activities, e.g. dam construction along the Nam Khan tributary. TSS load and *E. coli* load are calculated by multiplying the TSS and bacterial concentrations determined as described above, by the discharge measured at NK20 station per day.

5.2.4 Hydrological modeling

For this study, the Soil and Water Assessment Tool (SWAT) was used to simulate the hydrological response in the Nam Khan watershed over a 10-year period beginning in 2011. The modeling tool was used without introducing in the SWAT model the presence of a dam, in order

to simulate the hydro-sedimentary and microbiological dynamics excluding the dam impact. By comparing the simulated dynamics to the measured dynamics reflecting the dam presence, we can quantify the dam impact on the hydro-sedimentary and microbiological dynamics in the Nam Khan watershed.

5.2.4.1 SWAT model description

SWAT is a physically based watershed-scale agro-hydrological model developed by Arnold et al., 2012, (1998). In this study, SWAT operated at a daily time-step and its main objective is to predict the impact of land management practices on hydrology, sediment and water quality on watershed-scale. The watershed is divided into multiple sub-basins with both stream network and sub-basin outlets, based on the digital elevation model (DEM). Subsequently, each sub-basin is further subdivided into several Hydrologic Response Units (HRUs), composed of unique combinations of homogeneous soil, land use and slope. Subdividing the watershed into sub-basins allows the model to reflect the differences in hydrology according to diverse land uses and soils properties (Neitsch et al., 2011). SWAT model is made up of several modules linked together by the hydrological cycle. The hydrological cycle in SWAT can be separated into two major phases. The land phase controls the loading of water, sediments, nutrients and pesticides to the main channel per sub-basin, and the water or routing phase that controls the amount of water, sediments, nutrients and pesticides loading through the stream network. The runoff is simulated for each HRU and then summed together to get the total runoff from the sub-basin. The output of one sub-basin is the input of the following sub-basin.

SWAT has been applied in tropical Asian basins and performed well in various simulations (Bannwarth et al., 2014; Giang et al., 2014; Piman et al., 2013; Shrestha et al., 2018; Yaduvanshi et al., 2018). In Southeast Asia, SWAT was commonly applied to Mekong River basin (Arias et al., 2014b; Shrestha et al., 2018) and local small-scale basins (Kim et al., 2017; Marhaento et al., 2018).

5.2.4.2 SWAT setup and input data

In this study, we used SWAT2012 model (revision 637). The watershed was discretized

into 22 sub-basins (minimal drainage area of 239 km^2), and 817 HRUs after selecting 8 land use classes and 4 soil classes, and 5 slope classes (0–10, 10–25, 25–40, 40–60 and over 60 %). The simulation was done at the daily time step from January 2011 to December 2020 (excluding a 3-year warm-up from 2008 to 2010). SWAT uses spatial input data used to set up the model with the QSWAT (v_2012.10_1.5) (Fig. 31).

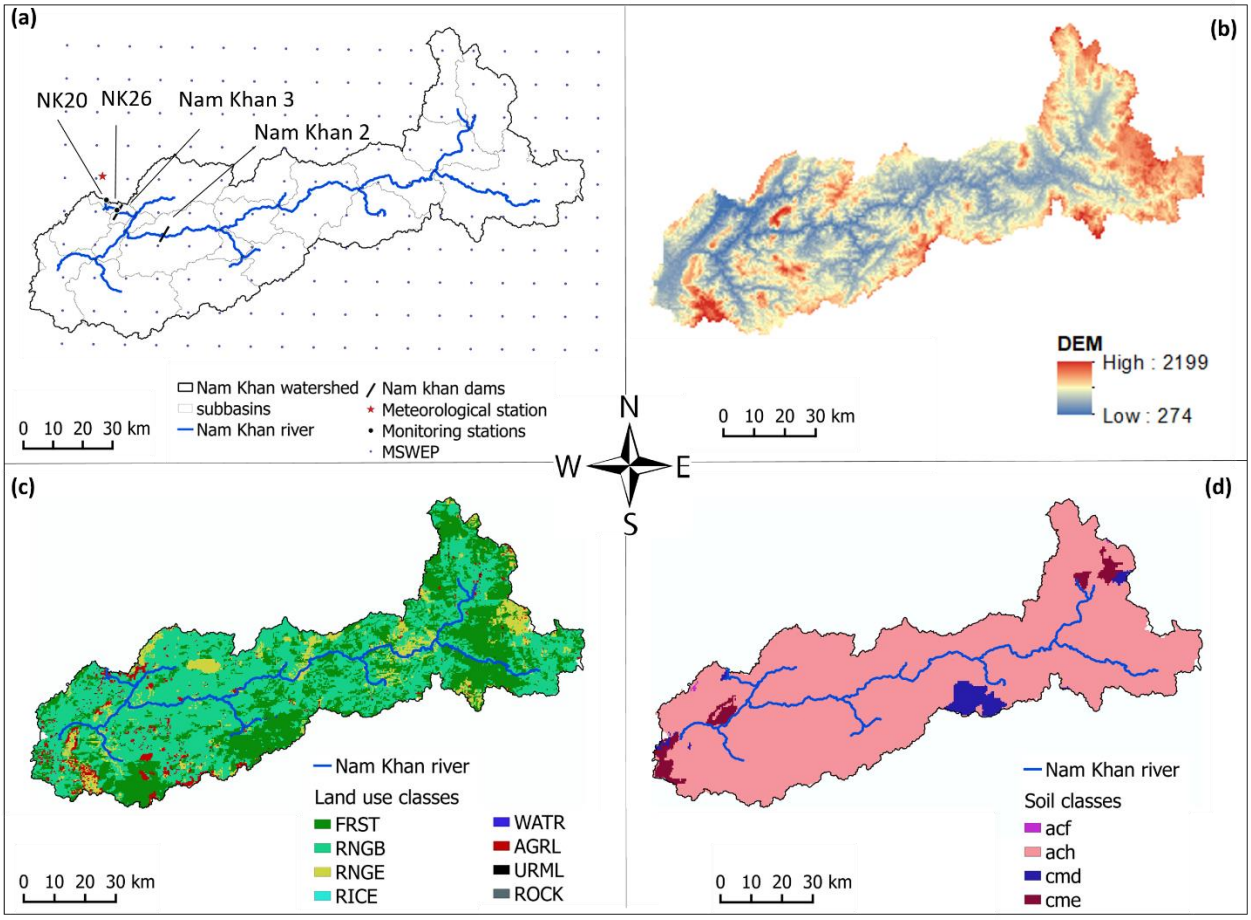

Figure 31: Geographical and meteorological characteristics of the and meteorological characteristics of the Nam Khan watersheds in Lao PDR: (a) meteorological stations in the Nam Khan watershed; (b) geomorphological features (Digital Elevation Model (DEM v4.1)); (c) land use map (DALaM); (d) soil map (MRC).

The spatial input data used to set up the model are the following:

- **Precipitation:** The daily precipitation data was obtained from Multi-Source Weighted-Ensemble Precipitation (MSWEP V2) (Beck et al., 2017) in order to have accurate, spatially distributed precipitation with a high temporal (daily) and spatial (0.1°) resolution over the

watershed (Fig 31a). MSWEP is a global precipitation product merged from gauge, satellite, and reanalysis data and has, which was evaluated and assessed on a global scale (Beck et al., 2019) and in Eastern Asia (Wu et al., 2018; Xu et al., 2019).

- **Climate data:** The climate data except for the precipitation was obtained from the climate station (19.853, 102.167) installed in the Houay Pano catchment and operated by the M-TROPICS CZO (Silvera et al., 2015) (Fig. 31a). Daily climate data (min and max temperature (°C), relative humidity (%), wind speed (km h^{-1}) and solar radiation (J cm^{-2}) was collected by an automatic climate station (Campbell BWS200).
- **Topography:** Digital Elevation Model (DEM v4.1), 90 m× 90 m resolution at the equator, was obtained from the NASA Shuttle Radar Topographic Mission (SRTM) (Jarvis et al., 2008) (Fig. 31b).
- **Soil map:** The soil map was provided by the MRC Secretariat, Phnom Penh, Cambodia in 2013 with associated soil properties (Shrestha et al., 2013) and included 4 categories: ferric acrisols (ACf), haplic acrisols (ACh), dystriccambiosols (CMd), eutric cambiosols (CMe) (Fig 31d).
- **Land use:** The land use map was provided by the Department of Agricultural Land Management (DALaM) of Lao PDR in 2013. The land use map included land cover classes, namely: rock, water, grassland, forest, and land use classes, namely: unstocked forest, paddy rice, other agriculture, and urban areas. The land use/land cover categories were classified respectively into 8 main classes in SWAT: rock (ROCK), water (WATR), range grasses (RNGE), mixed forest (FRST), range-brush (RNGB), paddy rice (RICE), generic agriculture (AGRL), and urban medium density (URML) (Fig 31c).

SWAT vegetation database was developed for temperate zones, thus, it was not suitable for tropical climates (Wagner 2011). Therefore, we adapted the SWAT vegetation parameter database (FRST, RNGB, and RNGE) to adjust leaf area index (LAI) and evapotranspiration (ET) to match the observed tropical dynamics found in the literature (Alemayehu et al., 2017; Zhu et al., 2016).

We modified the land use map by adding pixels attributed to the URML class based on village location according to the 2015 population and housing census (Lao Statistics Bureau Ministry of Planning and Investment, 2015), and 2010-2011 census of Agriculture (Department of Planning, Ministry of Agriculture and Forestry, 2012). For each sub-basin, we calculated the

number of humans and livestock taken from the census of population and agriculture, which was divided on different HRUs (Table 9). In order to introduce *E. coli* bacteria into the system, we added continuous fertilization operation in HRUs classified as URML, FRST, RNGE and RNGB. URML was attributed the total number of humans and half the number of livestock, while the other half was attributed to FRST, RNGE and RNGB. We calculated the total fecal production per type of animal in the HRUs of each sub-basin (g feces capita^{-1} day^{-1}) by multiplying the number of humans and livestock by the fecal production (g feces capita^{-1} day^{-1}) per type of animal taken from (Causse et al., 2015). Then for each type of animal, we calculated the total *E. coli* production per day (*E. coli day^{-1})* by multiplying the total fecal production per type of animal by the *E. coli* content (*E. coli g^{-1})* per type of animal taken from (Causse et al., 2015). To obtain the BACTPDB (*E. coli* g^{-1} manure) per HRU in each sub-basin, we divided the total *E. coli production* (*E. coli day^{-1})* by the total fecal production (g feces day^{-1}). To obtain the CFRT_KG (kg ha^{-1}) per HRU in each sub-basin, we divided the total fecal production (g feces day^{-1}) by the area of the HRU in each sub-basin. Management input data is summarized in Table 9 and detailed in Appendix III, table 17).

Table 9: Management input data

Land use class	**Management schedule (planting-harvesting)**	***E. coli* input (continuous fertilization)**
AGRL	15 May -15 October	No input
RICE	15 May -15 October	No input
FRST, RNGE and RNGB	No harvest	Half no. of goats, cattles and buffaloes
URML	No harvest	Other half no. of goats, cattles and buffaloes; Humans, pigs, ducks, chickens.
ROCK	-	-
WATR	-	-

5.2.4.3 SWAT modules (hydrology, sediments, bacteria)

The hydrological cycle in SWAT is composed of the landscape component and the channel component. In the landscape component, water quantity is calculated as follows:

$$SW_t = SW_0 + \sum_{i=1}^{t}(R_{day} - Q_{surf} - E_A - W_{seep} - Q_{gw}) \quad (5.1)$$

where SW_t is the final soil water content (mm H2O), SW_0 is the initial soil water content (mm

H2O), t is the time (days), R_{day} is the amount of precipitation on day i (mm H2O), Q_{surf} is the amount of surface water flow on day i (mm H2O), E_A is the amount of evaporation on day i (mm H2O), w_{seep} is the amount of percolation and bypass flow exiting the soil profile bottom on day i (mm H2O), Q_{gw} is the amount of return flow on day i (mm H2O).

The processes modeled are canopy storage, redistribution in the soil profile, evapotranspiration from the soil profile, surface runoff, subsurface runoff, and infiltration to the aquifer. Details of the equations can be found in **Chapter 2** and in the official theoretical documentation (Neitsch et al., 2011).

In the channel, water balance is estimated as follows:

$$V_{stored,2} = V_{stored,1} + V_{in} - V_{out} - \text{tloss} - E_{ch} + \text{div} + V_{bnk} \quad (5.2)$$

where $V_{stored,2}$ is the volume of water in the reach at the end of the day (m^3 H2O), $V_{stored,1}$ is the volume of water in the reach at the beginning of the day (m^3 H2O), V_{in} is the volume of water flowing into the channel during the time step (m^3 H2O), V_{out} is the volume of water flowing out of the channel during the time step (m^3 H2O), $tloss$ is the volume of water lost from the reach via transmission through the bed (m^3 H2O), E_{ch} is the evaporation form the reach for the day (m^3 H2O), div is the volume of water added or removed from the reach for the day through diversion (m^3 H2O), and V_{bnk} is the volume of water added to the reach via return flow from bank storage (m^3 H2O). Details of the equations can be found in **Chapter 2** and in the official theoretical documentation (Neitsch et al., 2011).

Sediment transport in SWAT is composed of the landscape component and the channel component. For the landscape component, SWAT uses the Modified version of the Universal Soil Losses Equation (MUSLE) to calculate the erosion and daily sediment yield within each HRU (Williams, 1975):

$$\text{Sed} = 11.8 \times \left(Q_{surf} \cdot q_{peak} \cdot area_{HRU}\right)^{0.56} \times USLE.K \times USLE.C \times USLE.P \times LS_{USLE} \times CFRG \quad (5.3)$$

where Sed is the sediment yield on a given day (tons), Q_{surf} is the surface runoff volume (mm ha^{-1}), q_{peak} is the peak runoff rate (m^3 s^{-1}), $area_{hru}$ is the HRU area (ha); USLE_K is the USLE soil erodibility factor, USLE_C is the USLE cover and management factor, USLE_P is the USLE

support practice factor, LS_{USLE} is the USLE topographic factor, and CFRG is the coarse fragment factor.

The sediment routing in the channel is a function of two processes: suspended sediment deposition and resuspension. The Simplified Bagnold equation (Bagnold, 1977) determines resuspension as a function of channel slope and flow velocity. Once in the tributary channel, the maximum amount of sediment that can be transported is a function of the peak channel velocity. If the latter is bigger than the concentration of sediment in the reach at the beginning of the time step, the dominant process in the reach segment will be deposition. In the opposite case, the available stream power is used to re-entrain loose and deposited material until all of the material is removed. Detailed description of all the equations can be found in Chapter 2 and in the official theoretical documentation (Neitsch et al., 2011).

The transport of bacteria in SWAT is described in the landscape component and the channel component. Bacteria is introduced in the system through manure and can be attached either to foliage or on the soil surface where they can die off. Bacteria is transferred via surface runoff during rain events to the river network or leached along the soil profile, depending on the hydrological conditions and on the free/attached bacteria partition. Bacteria can either die off or regrow (depending on the temperature of bacterial regrowth rate) in river, can settle with sediment deposition in streambed or be released from streambed with sediment resuspension events. In addition to the simulation using the original bacteria module of SWAT, we have tested the modified version of SWAT bacteria module developed by (Kim et al., 2017), where bacteria in-stream processes (resuspension, regrowth, hyporheic exchange) are taken into account. Detailed description of all the equations can be found in Chapter 2.

5.4.2.4. SWAT calibration

We have used a 3 years warm-up period from 2008 to 2010 and a 3-years calibration period from 2011 to 2013. After the parametrization of the model with the previously described inputs, we carried out model calibration both manually when *in-situ* data was available, and automatically. Automatic calibration was performed using the Sequential Uncertainty Fitting (SUFI-2) tool in the SWAT Calibration and Uncertainty Programs (SWAT-CUP) (Abbaspour, 2014; Abbaspour et al., 2004). The SUFI-2 algorithm was applied separately to discharge (n=1096), followed by suspended

sediments (n=61), and then bacteria (n=60), and provided the sensitivity of the 20 parameters governing discharge and of the 8 parameters governing suspended sediments and 4 parameters governing bacteria.

Hydrological parameters were calibrated to fit the observed discharge during both the dry season (baseflow) and wet season (high flow and discharge peaks). The calibration of parameters related to discharge was divided into two steps: manual and automatic calibration. Based on observations done in Houay Pano watershed, parameters like runoff curve number (CN2) (Vigiak et al., 2008) and saturated hydraulic conductivity (SOL_K) (*unpublished work*) were set for each land use and soil depth. CN2 was set to 80 for RNGB, AGRL, and RICE, 51 for RNGE, 60 for FRST, 90 for URML and 92 for WATR. Moreover, SOL_K was set for each land use category and for each soil depth (300-600-1000-2000 mm respectively): 52-22-3-1 for RNGB; 74-16-0.4-0.2 for RNGE; 63-38-4-0.7 for FRST; 23-4-0.7-0.3 for AGRL and RICE; 23-4-0.7-0.3 for RICE; 7-4-3-3 for URML and 0-0-0-0 for WATR. Subsequently, the automatic calibration was performed on the other 20 parameters related to hydrological processes (Table 10).

Following the calibration of hydrology, calibration of parameters related to sediments was also divided into two steps: manual and automatic calibration. The MUSLE approach was adopted to simulate total suspended sediment load at the catchment scale (eq. 6.1). The cover-management factor (USLE_C) plays a key role in determining the rate of sediments erosion in the RUSLE approach. Therefore, referring to the values in the literature adopted for tropical regions of Southeast Asia (Ranzi et al., 2011), USLE_C values were set in accordance with different land use categories to reflect water infiltration and erosion rates: 0.17 for RNGB, 0.54 for RNGE, 0.18 for FRST, 0.17 for AGRL, 0.41 for AGRL, 0 for WATR. Subsequently, the automatic calibration was performed on the 8 parameters related to sediments (Table 10).

After the discharge and sediments calibration, automatic calibration of the 6 bacteria-related parameters was performed and summarized in Table 12. In order to test the 3 modified bacteria modules, we considered the values of 6 bacteria parameters (CLAY, BSC1, BSC2, BSC3, BSC4, C_{T1}) related to resuspension, regrowth and hyporheic exchange taken from (Kim et al., 2017).

Tableau 10: Automatic calibration and sensitivity analysis for discharge, [TSS], and [E. coli] simulated by the SWAT model applied to the Nam Khan catchment, Lao P.D.R. Sensitive parameters (p-value ≤ 0.01) are highlighted in bold and sensitivity ranks are indicated from 1 the most sensitive to n the least sensitive.

Parameters	Description	Range of value for calibration	Calibrated value
Discharge			
ESCO.hru	Soil evaporation compensation factor (-)	0.5-0.9	0.77
EPCO.hru	Plant uptake compensation factor (-)	0.5-1	0.80
CANMX.hru	Canopy storage (mm)	0-100	83
OV_N.hru	Manning's roughness coefficient for overland flow ($m^{-1/3}$ s)	0.02-0.2	0.04
LAT_TIME.hru	Lateral flow travel time (days)	0-15	**13** [1]
SURLAG.hru	Surface runoff lag coefficient (-)	0.05-24	9.74
CH_N1.sub	Manning's "n" value for tributary channels ($m^{-1/3}$ s)	0.025-0.15	**0.08** [4]
CH_K1.sub	Effective hydraulic conductivity in tributary channels (mm h^{-1})	0-300	56
GW_DELAY.gw	Groundwater delay time (days)	30-500	270
ALPHA_BF.gw	Baseflow recession constant (-)	0.5-1	**0.62** [3]
GWQMN.gw	Threshold depth of water in the shallow aquifer required for return flow to occur (mm)	0-5000	1085
GW_REVAP.gw	Groundater "revap" coefficient	0.02-0.2	0.17
REVAPMN.gw	Threshold depth of water in the shallow aquifer required for "revap" or percolation to occur (mm)	0-500	343
RCHRG_DP.gw	Deep aquifer percolation fraction (-)	0-0.5	0.08
CH_N2.rte	Manning's "n" value for main channel ($m^{-1/3}$ s)	0.025-0.15	0.11
CH_K2.rte	Effective hydraulic conductivity in main channel (mm h^{-1})	0-500	120
SOL_AWC.sol	Available soil water capacity (mm H2O mm $soil^{-1}$)	±20%	-0.3%
SOL_CBN.sol	Organic carbon content (%)	±20%	17%
SOL_BD.sol	Moist bulk density (g cm^{-3})	±20%	**+19%** [2]
SOL_CLAY.sol	Clay content (%)	±20%	7%
Suspended sediments			

PRF_BSN.bsn	Peak rate adjustment factor for sediment routing in the main channel	0-2	0.68
ADJ_PKR.bsn	Peak rate adjustment factor for sediment routing in the tributary channels	0.5-2	**1.88** [2]
SPCON.bsn	Linear parameter for calculating the maximum sediment that can be reentrained during channel sediment routing	0.0001-0.01	0.02
SPEX.bsn	Exponent parameter for calculating sediment reentrained in channel sediment routing	1-2	1.57
USLE_K.sol	USLE equation soil erodibility factor	0-1	**0.22** [1]
USLE_P.mgt	USLE equation support practice factor	0-1	**0.25** [3]
CH_COV1.rte	Channel bank erodibility factor	-0.05-0.6	0.08
CH_COV2.rte	Channel bed erodibility factor	-0.01-1	0.30
Bacteria			
BACTKDQ.bsn	Bacteria partition coefficient in soil	150-200	**178** [1]
BACTMX.bsn	Bacteria percolation coefficient	7-20	18
BACTKDDB	Bacteria partition coefficient in manure	0-1	0.98
WOF_P.bsn	Wash-off fraction for persistent bacteria	0-1	0.02
BACT_SWF.bsn	Fraction of manure applied to land areas that has active colony forming units	0-1	**0.82** [2]
WDPRCH.bsn	Die-off factor for persistent bacteria in streams at 20 °C	0-1	0.5
CLAY	The percentage of clay in suspended sediment in stream water in the reach segment (%)	20-80	28.86*
BSC_1	The regression coefficients in streambed bacteria concentration equation	0-20	0.17*
BSC_2	The regression coefficients in streambed bacteria concentration equation	-	2.05*
BSC_3	The regression coefficients in streambed bacteria concentration equation	-	180*
BSC_4	The regression coefficients in streambed bacteria concentration equation	-	3.302*
C_{T1}	Growth temperature function shape parameter 1	-	0.035*

*indicates fitted values in (Kim et al., 2017) for the modified bacteria modules.

Metrics of model performance

Model output uncertainty was evaluated by using the standard statistical criteria provided by SUFI-2 algorithm. The p-factor is the percentage of observation covered by the 95% confidence band and the r-factor is the relative thickness of the 95% uncertainty band (Abbaspour et al., 2015, 2004). We evaluated the performances of the model using the Nash-Sutcliffe efficiency (NS) index, the coefficient of determination (R^2) and the percentage of bias (PBIAS). The NS ranges between $-\infty$ and 1. Typically, NS = 1 indicates a perfect match between observed and predicted values. 0 < NS < 1 generally indicate acceptable levels of performance. NS values above 0.5 are considered as satisfactory in hydrological modeling performance according to the guidelines by Moriasi et al., (2007). R^2 ranges between 0 and 1. Typically, $R^2 > 0.5$ is considered acceptable. Low PBIAS values indicate an accurate model simulation. Positive values indicate under-estimation bias, and negative values indicate over-estimation bias.

$$NS = 1 - \frac{\sum_i (O_i - S_i)^2}{\sum_i (O_i - \bar{O})^2} \quad (6.2)$$

$$R^2 = \frac{[\sum_i (O_i - \bar{O})(S_i - \bar{S})]^2}{\sum_i (O_i - \bar{O}) \sum_i (S_i - \bar{S})^2} \quad (6.3)$$

$$PBIAS = \left[\frac{\sum_{i=1}^{n} (O_i - P_i) * 100}{\sum_{i=1}^{n} (O_i)}\right] \quad (6.4)$$

where O_i and S_i represent the observed and simulated variables respectively, and $\bar{O}$ and $\bar{S}$ are the average values of the observed and simulated values, respectively.

5.3 Results

5.3.1 Statistical analyses

5.3.1.1 Hydrology

At NK20, discharge showed seasonal variations with peaks observed following rainfall events during rainy season (May-September) from 2010 to 2015 (Fig. 32a). It is worth noting that from 2015 to 2019, seasonal discharge peaks were not regularly occurring anymore, and only two discharge peaks were noted in September 2016 and August 2018. As the Mann–Kendall test showed a significant downward trend in discharge, the Pettitt test was further used to detect the change-points (Table 11, Fig. 32a). The Pettitt test was applied to daily discharge and detected the

change-point in December 2013 ($p<0.0001$). The average discharge decreased from 102 m^3 s^{-1} to 65 m^3 s^{-1} in the 2010-2013 and in the 2014-2019 periods, respectively (Fig. 32a). Pettitt test and Mann-Kendall performed on rainfall records did not show any significant trend and did not detect a change point (Table 11).

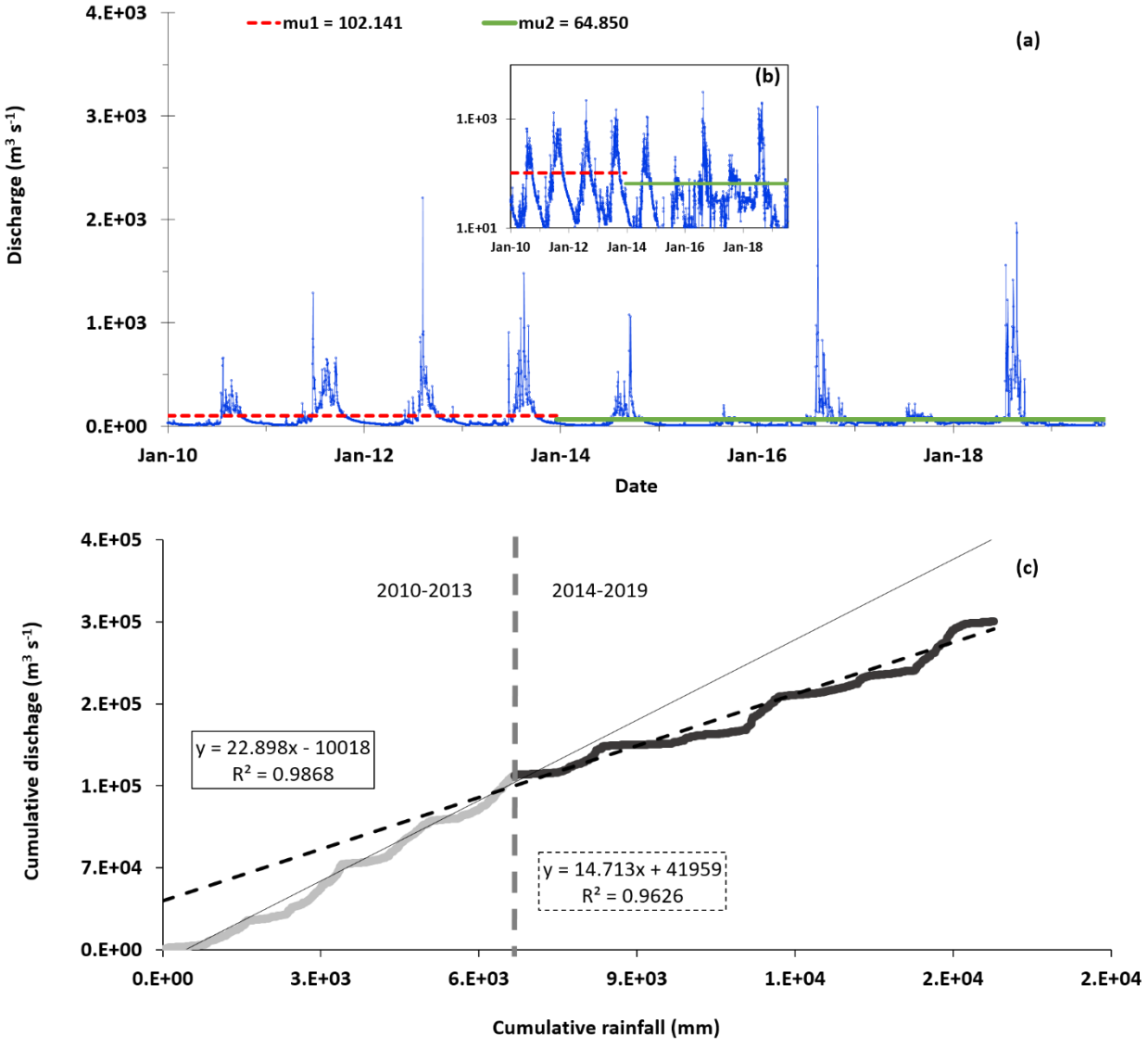

Figure 32: : (a) Temporal variations (Pettitt test) of daily discharge (m^3 s^{-1}) measured from January 2010 to July 2019; (b) log-transformed temporal variations (Pettitt test) of daily discharge (m^3 s^{-1}) measured from January 2010 to July 2019; (c) double mass curve analysis of cumulative rainfall (mm) and cumulative water discharge (m^3 s^{-1}) during 2010-2019 at NK20 station in the Nam Khan watershed, Lao PDR. The straight continuous line and the dotted line are the regression lines for the cumulative data before and after the change point respectively

As can be seen from (Fig. 32b), the double-mass curve representing the correlation between cumulative river discharge and cumulative rainfall (MSWEP averaged over the Nam Khan watershed), showed a change in the slope in 2014. According to the established linear regression

equations, the analysis results showed that the cumulative decrease of river discharge after the change-point was 20% when comparing theoretical cumulative discharge with the observed cumulative river discharge (Table 11).

Table 11: Linear regression Equation (1): Cumulative water discharge (Q) and cumulative precipitation (P) for period before transition years (ΣQ, cumulative water discharge; ΣP, cumulative precipitation; Q1, extrapolated cumulative water discharge until 2020; Q2, observed cumulative water discharge until 2020)

Regression equation	**ΣQ = 22.90 ΣP-10018 (R^2=0.97)**
Q1 (m^3 s^{-1})	351118
Q2 (m^3 s^{-1})	280593
(Q1-Q2)/Q1 *100 (%)	20%

5.3.1.2 Suspended sediment and bacteria concentrations

As the Mann–Kendall test showed a significant downward trend in [TSS] and [*E. coli*] at NK20 and NK26 stations (Table 12), the Pettitt test was adopted to detect the change-points (Table 12, Fig. 33). The Pettitt test results showed that for [*E. coli*], the change-point years were detected in 2016 and 2017 at NK20 and NK26 stations respectively. The average [*E. coli*] decreased from 3002 to 331 MPN 100 mL^{-1} at NK20 and from 1071 to 111 MPN 100 mL^{-1} at NK26 in the 2011-2016 and 2017-2020 periods, respectively (Fig. 33a, b).

Mean [*E. coli*] at NK26 station decreased from 434 ± 280 MPN mL^{-1} (dry seasons) and 1.251 ± 1,223 MPN mL^{-1} (wet seasons) over the pre-dam period, to 43 ± 98 MPN mL^{-1} (dry season) and 145 ± 161 MPN mL^{-1} (wet season) over the post-dam period. Further downstream at NK20 station, mean [*E. coli*] decreased from 577 ± 252 MPN mL^{-1} (dry seasons) and 1,772 ± 683 MPN mL^{-1} (wet seasons) over the pre-dam period, to 294 ± 90 MPN mL^{-1} (dry season) and 380 ± 124 MPN mL^{-1} (wet season) over the post-dam period.

The change-point years for the [TSS] were detected in 2015, at both NK20 and NK26. The average [TSS] decreased from 0.267 to 0.024 g L^{-1} at NK20 and from 0.183 to 0.015 g L^{-1} at NK26, in the 2011-2015 and 2016-2020 periods, respectively (Fig. 31c, d). Mean [TSS] at NK26 station decreased from 0.05 ± 0.03 (dry seasons) and 0.30 ± 0.20 g L^{-1} (wet seasons) over the pre-dam period, to 0.005 ± 0.004 g L^{-1} (dry season) and 0.02 ± 0.02 g L^{-1} (wet season) over the post-dam period. Further downstream at NK20 station, mean [TSS] decreased from 0.06 ± 0.05 (dry seasons) and 0.45 ± 0.32 g L^{-1} (wet seasons) over the pre-dam period, to 0.01 ± 0.01 g L^{-1} (dry season) and

0.03 ± 0.02 g L^{-1} (wet season) over the post-dam period (Fig. 33).

Table 12: Results of Pettitt tests and Mann-Kendall statistics at significance level of α = 0.05 evaluating changes in precipitation, TSS and E. coli concentrations, measured at the NK20 and NK26 stations downstream of the dam.

Station	Parameter	Mann-Kendall (Z)	Pettitt-test (T)	p-value
MSWEP	Precipitation	-1	-	0.29
NK20	Discharge	-7.55	12/20/2013	<0.0001
	[*E. coli*]	-4.80	11/11/2016	<0.0001
	[TSS]	-5.55	08/23/2015	<0.0001
NK26	[*E. coli*]	-7.48	07/06/2017	<0.0001
	[TSS]	-7.92	11/08/2015	<0.0001

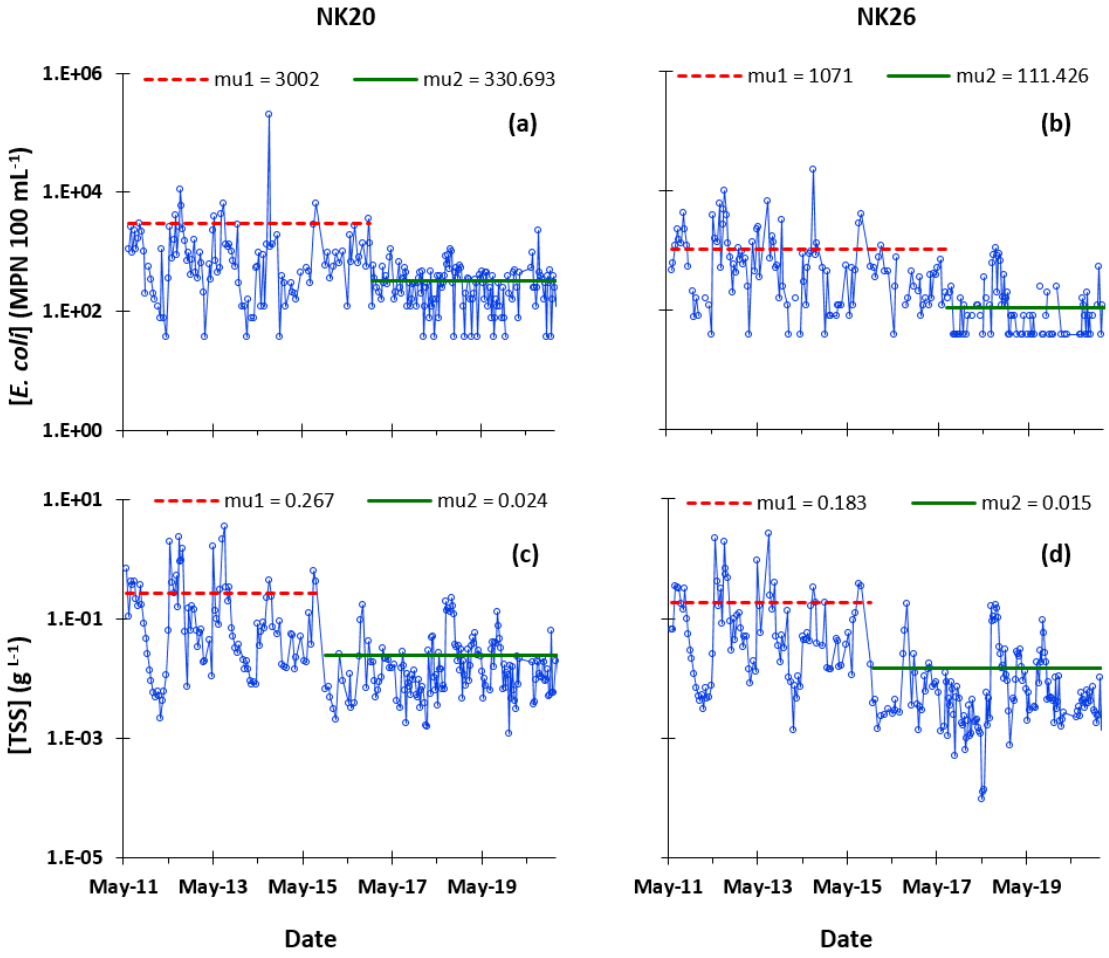

Figure 33: Temporal variations and change-point (Pettitt test) of parameters measured between May 2011 and December 2020. Left side panels are for NK20 station and Right side panels are for NK26 station. (a,b) [E. coli]: E. coli concentrations (MPN 100 mL^{-1}), (c,d) [TSS]: Total suspended sediment concentrations (g L^{-1}). Dotted lines are the mean before the detected change point and straight lines are the mean after the detected change-point.

The DMC between TSS load, *E. coli* load and precipitation (Fig. 34) provided a useful

method to detect the change-point year associated to the significant decrease in sediment and bacteria load. Unlike the Pettitt-test, which detected the change points in 2015 and 2016 for TSS and *E. coli* respectively (Table 12; Fig. 35), the DMC detected the change point in TSS and *E. coli* loads in 2013. The latter can be proven with the decrease of the regression coefficient between 2011-2013 and 2014-2020 periods, varying respectively from 6×10^{12} to 6×10^{11} for *E. coli* load, and from 172 to 11 for TSS load.

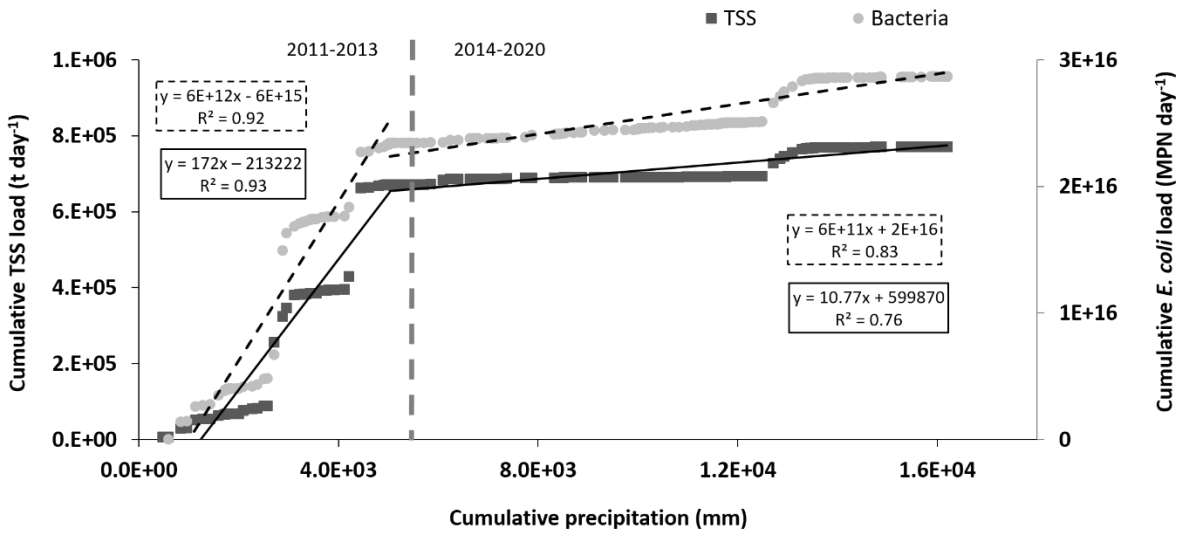

Figure 34: Double mass curve analyses of cumulative rainfall (mm) and cumulative TSS load (t day^{-1}) and E. coli load (MPN day^{-1}) measured between 2011 and 2020 at NK20 station in the Nam Khan watershed, Lao PDR. The straight continuous line and the dotted line are the regression lines and corresponding equations for the TSS and E. coli load, respectively.

5.3.2 Hydrological modeling

The model showed a good match with observed discharge data over the calibration period, following seasonal variations characterized with discharge high flow and peaks during wet season and low baseline flow during the dry season. The discharge calibration resulted in a p-factor and a r-factor of 0.70 and 0.62 respectively (Fig. 35a), thus both meeting the 'satisfactory' thresholds (Abbaspour et al., 2015, 2007). NS and R^2 were 0.70 and 0.71 respectively, and PBIAS was -13%. The mean simulated and observed discharge and their respective standard deviations were 121.81 ± 151.70 and 113.62 ± 177.82 m^3 s^{-1} respectively. The performances of the model at daily time-step were thus considered satisfactory over the 2011-2013 period according to the guidelines suggested by Moriasi et al., (2015) at daily time-step.

The relative difference between observed discharge and simulated discharge (Fig. 35b) during the calibration period (2011-2013) shows a slight over-estimation of simulated discharge compared to observed discharge during wet season (peak flow) and an underestimation during dry season (base flow). The relative difference between observed discharge and simulated discharge (without dam implementation) during the post-dam construction period showed an important increase in positive difference (over-estimation) during both wet and dry seasons but emphasized during peak flow. Overall, the model overestimated the discharge by an average of 34% during the calibration period (2011-2013) and 338% during the post-dam period (2014-2020).

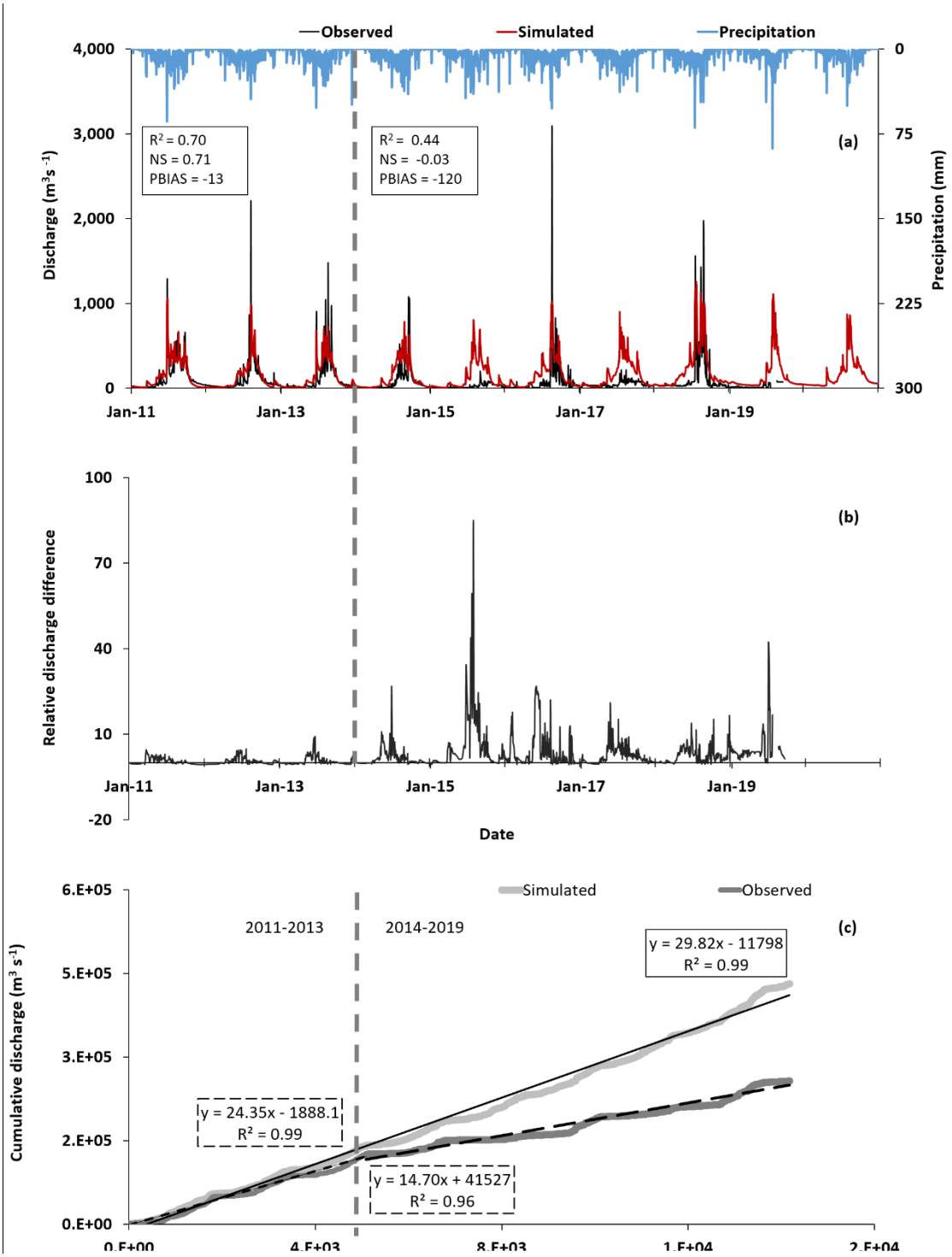

Figure 35: (a) Daily observed and simulated discharge ($m^3 s^{-1}$), and daily mean watershed precipitation (mm); (b) Relative discharge difference between daily simulated and observed discharge ($(Q_{sim} - Q_{obs})/ Q_{obs}$). The dotted vertical line separates the calibration period (2011-2013) and the post-dam construction period (2014-2020) at NK20 station in the Nam Khan watershed, Lao PDR;(c) Double mass curve analysis of cumulative rainfall (mm) and cumulative observed and simulated discharge ($m^3 s^{-1}$) during 2011-2019 at NK20 station in the Nam Khan watershed, Lao PDR. The straight continuous line and the dotted line are the regression lines and corresponding equations for the simulated (2011-2019) and observed pre-dam (2011-201) and post-dam (2014-2019) cumulative data respectively.

The current preliminary results of [TSS] and [*E. coli*] calibration did not show a good match with the observed data (Fig. 36). The model was only able to capture the high concentrations of sediment and bacteria during the first flood event of 2011, while simulated [TSS] and [*E. coli*] was under-estimated during the rest of wet seasons.

[TSS] calibration resulted in a p-factor and r-factor of 0.18 and 1.51 respectively (Fig. 36a). NS and R^2 were -0.10 and 0.07 respectively, and PBIAS was 68%. The mean simulated and observed sediments and their respective standard deviations were 108.80 ± 287.80 and 361.62 ± 662.41 mg L^{-1} respectively. Performance of the model were thus not considered satisfactory over the 2011-2013 period (Abbaspour et al., 2007, 2015). Likewise, bacteria calibration resulted in a p-factor and r-factor of 0.05 and 0.08 respectively (Fig. 36b). NS and R^2 were -0.15 and 0.17 respectively, and PBIAS was 72.1%. The mean simulated and observed bacteria and their respective standard deviations were 413.59 ± 756.23 and 1,482 ± 1,867 mg L^{-1} respectively. The performances of the model at the daily time-step were as well not considered satisfactory.

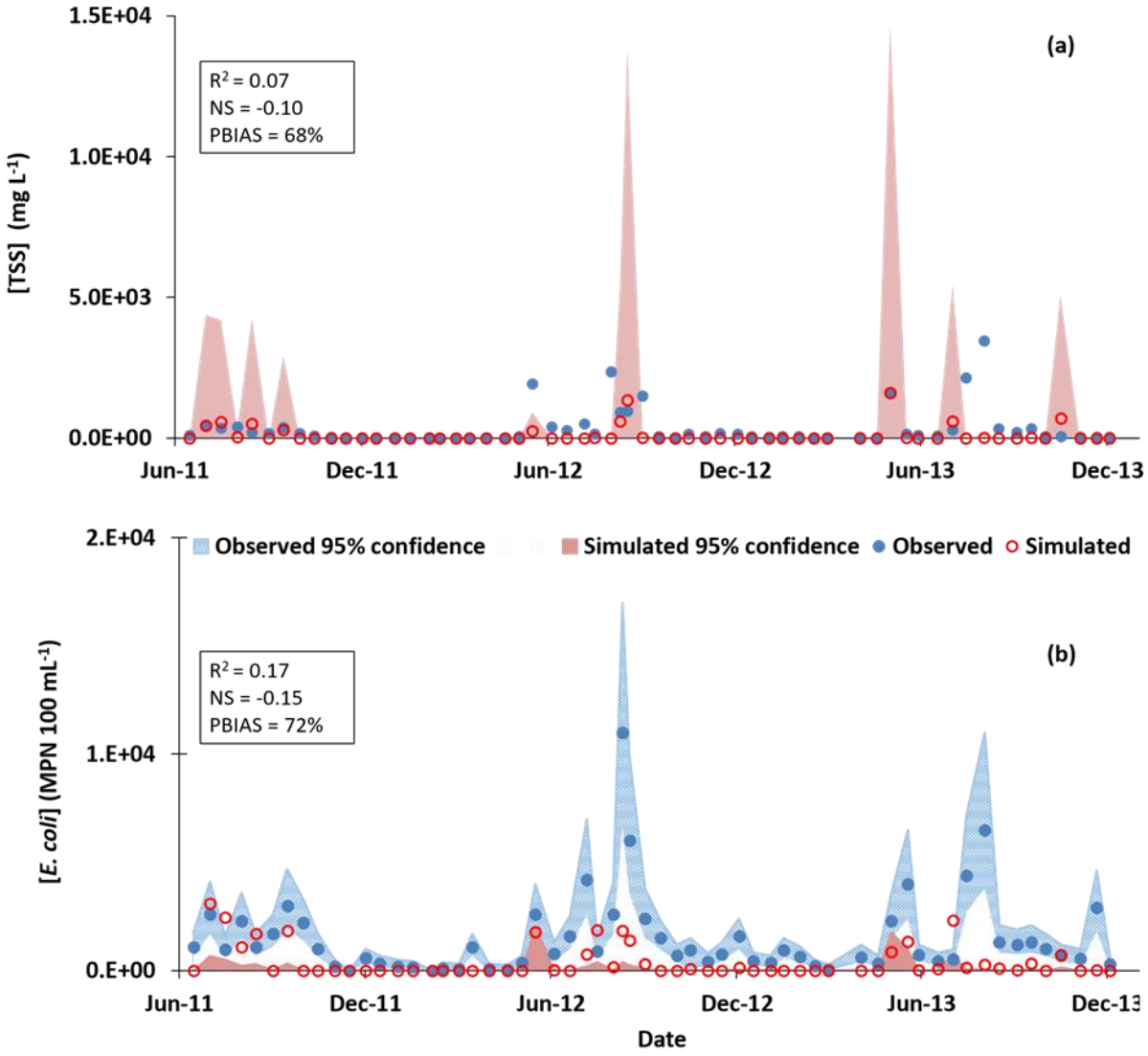

Figure 36: (a) Observed and simulated TSS concentrations ([TSS] MPN 100mL^{-1}); (b) observed and simulated E. coli concentrations ([E. coli] MPN 100mL^{-1}) during the calibration period (2011-2013) at NK20 station in the Nam Khan watershed, Lao PDR.

We proceeded by testing 3 modified bacteria modules of (Kim et al., 2017) at small-scale Houay Pano watershed, in order to assess the importance of newly added in-stream processes on bacteria simulation by SWAT and evaluate the model performance at large-scale Nam Khan watershed (Fig. 37). *E. coli* during low flow events were not well simulated, while simulated *E. coli* during wet season showed similar seasonal trends of those measured yet not well reproduced (Fig. 37a, b). The difference between the original module and the modified module including resuspension release is not important in terms of performance metrics (Table 13). The model

performance did not improve with the implementation of the regrowth process (Table 13), but overestimated the peaks during high flow periods (Fig. 37c). On the other hand, the performance was slightly yet insufficiently, improved when hyporheic exchange was implemented (Fig. 37d; Table 13).

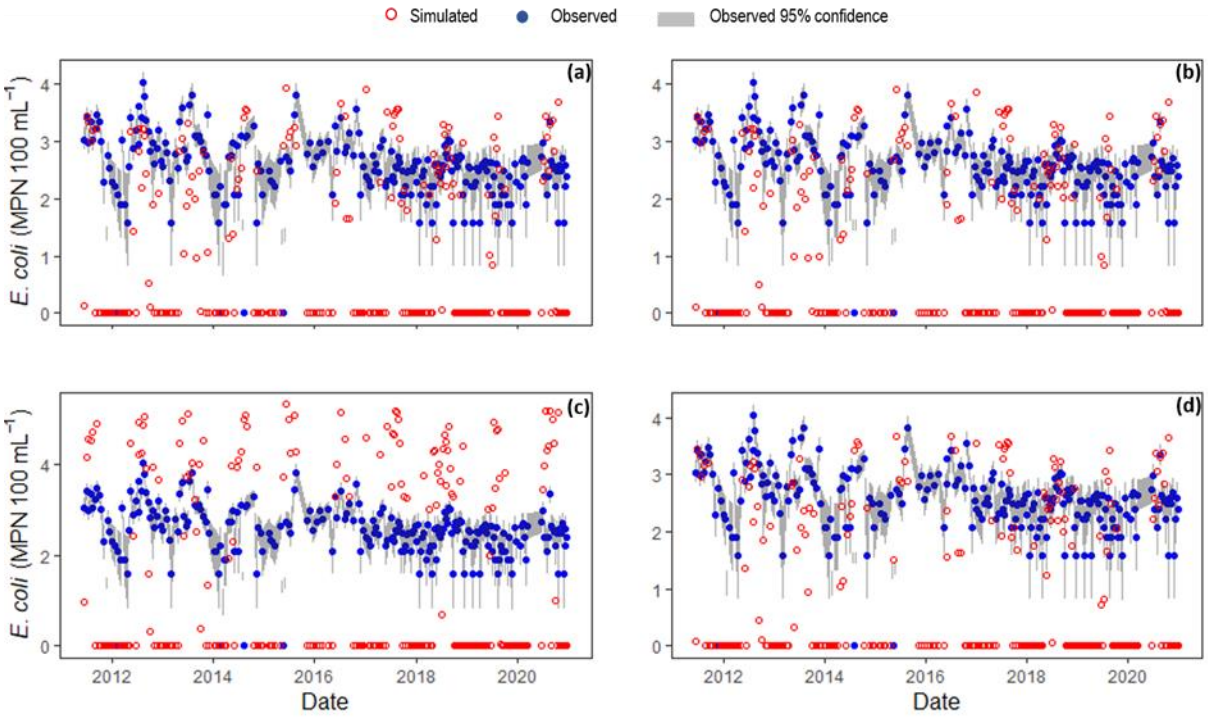

Figure 37: Observed and simulated [E. coli] (MPN 100 mL^{-1}) at the NK20 station from May 2011 to December 2020: Log-transformed comparison with (a) the original SWAT bacteria module; (b) the resuspension release processes; (c) the resuspension release processes and regrowth; (d) the resuspension release processes and hyporheic exchange.

Table 13: Model's performances of the original SWAT bacteria module and of 3 modified versions of the module including the resuspension release processes; the resuspension release processes and regrowth; the resuspension release processes and hyporheic exchange, during the before-dam period 2011-2013 (a), and the after dam period 2014-2020 (b).

Metrics	Original		Resuspension		+ Regrowth		+ Hyporheic exchange	
	a	b	a	b	a	b	a	b
NS	-0.15	-33	-0.18	-28	-290	-7,503	-0.20	-6
R^2	0.17	0.01	0.18	0.01	0.22	0.02	0.18	0.008
PBIAS	72	-75	76	-66	-903	-4,027	80	-19

5.4 Discussion

Many authors have already shown the hydrological changes induced by rapid hydropower development in Mekong basin (Hecht et al., 2019b; Piman et al., 2013; Soukhaphon et al., 2021). Relatively few streamflow stations downstream of tributary dams have pre- and post-dam flow and water quality records exceeding ten years (Lacombe et al., 2014a; Lyon et al., 2017), which limits assessments of dam impact. Hereafter we present our results of observed changes after dams cascade was implemented, most recently the Nam Khan 3 dam built in 2014 and commissioned in 2016 in the Nam Khan watershed upstream of the long-term monitoring stations NK26 and NK20.

5.4.1 Observed hydrological alterations

Our statistical analyses results shed the light on seasonality alterations observed in Nam khan river discharge when comparing pre and post-dam time series at the watershed's hydrological monitoring NK20 station (Fig. 32). Between 2010 and 2014 included, discharge was highly seasonal, with different patterns recorded during dry and wet seasons (Fig. 32a). Discharge peaks occurred during the wet season following intense rainfall events (May-Oct) ranging in average between 131 and 1,172 m3 s^{-1} from 2010 to 2014. However, after 2014, the year in which the dam construction started, seasonal variability of river discharge was less marked. Discharge peaks were not recorded during wet seasons (May-Oct) in 2015, 2017, and 2019, ranging in average only between 39 and 167 m3 s^{-1}. Nonetheless, in 2016 a high amplitude discharge peak, ranging from 671 to 3,088 m3 s^{-1} was recorded between 18 and 20 August, exceeding average peaks of previous years. In the current study, the absence of significant trend in rainfall records between 2010 and 2020, and the detected change point in 2015 in the discharge pattern (Fig. 32b), may suggest that noted changes are not directly linked to changes in rainfall, but to a significant impact of an external driving factor like the dam on the river's hydrological regime. Discharge alterations due to natural factors can be expected to progress gradually, but those due to anthropogenic factors are likely to occur abruptly after a change, as can be seen from the double mass curve approach (Fig. 32b).

As stated by numerous studies (Adamson, 2001; Pokhrel et al., 2018), dams can attenuate flow seasonality. Moreover, hydropower dams along the Mekong River and its tributaries are severely disrupting hydrological patterns. To meet electricity demands, water is stored during wet seasons in the reservoirs along the Mekong mainstream as well as its tributaries and released during dry seasons, resulting in dampening the annual flood pulse of the Mekong. However, the typical

seasonal hydrological patterns of Mekong are ecologically important for the sustainability of aquatic life that depend on seasonal water level fluctuation (Baird, 2011; Lamberts, 2008; MRC, 2010b). The construction of mainstream Mekong dams in the upper Mekong basin were attributed to the observed pronounced fluctuations to water levels throughout the basin (Pokhrel et al., 2018). Clear evidence of more recent projects is the LS2 dam constructed on the 3S system in 2014 (Sesan, Sekong, Srepok) which is the largest tributary to the Mekong River shared between Vietnam, Cambodia and Laos. LS2 dam have led to multiple serious basin-wide hydrological impacts resulting in decline in fish biomass (Arias et al., 2014b) and social impact on well beyond the immediate downstream communities near these dams e.g in the Tonle Sap Lake (IFReDI, 2012).

Overall, there is mounting evidence suggesting that dam-related disruptions to river hydrology, extreme and sudden releases or constraint of flow, and amplification of drought and run-off, have cumulative and large-scale impacts not only on aquatic habitat (Bunn and Arthington, 2002) and riparian habitats (Nilsson and Berggren, 2000), but also on river geomorphology instability (Brandt, 2000). The decreased amplitude of the flood pulse is expected to reduce the sediment and nutrient transport (Bunn and Arthington, 2002). As rivers approach large reservoirs, the flow velocity decreases and loses the potential to transport sediments, while low turbulence allows finer sediments to settle down in streambed (Donald et al., 2015; Garnier et al., 2005; Kunz et al., 2011).

5.4.2 Sediment trapping

The present study revealed that [TSS] showed a decreasing trend from 2011 to 2020, which was confirmed by Pettitt test that detected a change-point occurring in 2015 in both of the monitoring stations (Table 11, Fig. 33), and further proven in the double mass curve approach (Fig. 33). The mean [TSS] at NK26 station decreased by an average of 83% between the periods of 2011-2015 (0.183 ± 0.42 g L^{-1}) and 2015-2020 (0.031 ± 0.03 g L^{-1}). Further downstream at NK20 station, mean [TSS] decreased by an average of 90% between the periods of 2011-2015 (0.27 ± 0.56 g L^{-1}) and 2015-2020 (0.024 ± 0.07 g L^{-1}). Similarly to river discharge, [TSS] seasonal variations were less clear after the dam construction, although [TSS] in tropical regions generally follow distinctive seasonal fluctuations with higher values during wet season due to soil erosion by surface runoff and streambed resuspension in response to rainfall events (Isobe et al., 2004; Nakhle et al., 2021c;

Nguyen et al., 2016). In case of the Nam Khan river between 2011 and 2020, [TSS] high concentrations during wet seasons was reduced after dam construction (Fig. 33). The high [TSS] concentrations between 2011 and 2014 can be also attributed to the construction of the Nam Khan 2 dam that started in 2011 and operated in 2015. Hence, the [TSS] marked change point occurring in 2015 can be the result of cumulative impact of the dam cascade construction and operation on the Nam Khan river.

Our results are consistent with several studies indicating substantial reductions in sediment entering the Mekong mainstream system at regional scale (Kummu and Varis, 2007; Kunz et al., 2011). A study conducted in the Manwan reservoir in China revealed an important sediment trapping of around 60.5 % of the total sediment load transported between 1993 and 2003 (Fu et al., 2008). Recent studies assessed the basin-wide sediment trapping efficiency of existing reservoirs along the Mekong mainstream (Piman and Shrestha, 2017b) and estimated their potential to trap around 34 to 43 Mt (i.e. 15-18%) of sediment annually and around 95 to 100 Mt if all the planned dams were built. Consequently, sediment load reaching the Mekong delta in Vietnam may decrease by 50 %, which raises major concerns over a number of consequences. Reduced sediment loads is likely to be linked with decreased floodplain sedimentation, thus, loss of agricultural land (rice production) in inundated areas, riverbank gardens and floodplains. In consequence, the connectivity of sediment transport is interrupted by dams which release water with reduced sediment load, is known as “hungry water”, prone to erode riverbeds and banks due to its increased transport capacity (Kondolf, 1997; Kondolf et al., 2014). This process could potentially have widespread impacts on river habitats, food webs and fish bio-ecology adapted to the seasonal and inter-annual variations and composition of sediments in the river. In the Lower Mekong Basin, Cambodian communities downstream of Yali Falls on the Sesan River, have reported a dramatic decline in fish catches since the construction of the dam (Wyatt and Baird, 2007). Alternatively, during flood periods, when sudden and high discharge peaks occur, like the ones observed in August 2016 and 2018 (Fig. 32a), downstream environment will receive unnaturally high concentrations of sediment (MRC, 2011).

In addition to the dam impact on downstream ecosystem structure and sediment balance, it subsequently leads to reduction in available nutrient to the downstream environment (Lu and Siew, 2006; Morris and Fan, 1998). Given that in tropical context, populations often rely on untreated

surface water, which can be highly turbid and contaminated, it seems crucial to investigate dam impact on water microbiological quality as well (Winton et al., 2019).

5.4.3 Bacteria trapping

[*E. coli*] showed similar patterns as river discharge and [TSS], following distinct seasonal variations during the pre-dam period and a significant attenuation since the dam construction. Our results indicate a decreasing trend from 2011 to 2020, with an abrupt change point in [*E. coli*] records, occurring in 2016 and 2017 for NK20 and NK26 respectively (Table 11, Fig. 33). Mean [*E. coli*] decreased by an average of 89% in both monitoring stations between before and after detected change points. Similarly to river discharge and to [TSS], distinct seasonal variations of [*E.* coli] diminished after the dam construction, in contrast to the typical observed pattern of *E. coli* reported by previous studies in tropical watersheds (Boithias et al., 2020; Cho et al., 2016; Nguyen et al., 2016; Rochelle-Newall et al., 2016). The time difference between dam construction and detected change points in terms of [*E. coli*] can be due to the presence of workers along stream banks during the construction phase, adding diffuse sources of fecal contamination into the stream, in addition to sources delivered by Houay Khan river, a densely populated Nam Khan tributary debouching between NK20 and NK26 stations.

When present in secondary habitats (soil and water), FIB are highly dependent on environmental conditions (Nakhle et al., 2021b; Petersen and Hubbart, 2020c) and tend to be attached to suspended sediments as stated by several studies (Malham et al., 2014; Oliver et al., 2007). Therefore, it is expected that dam-induced changes can strongly impact microbial communities. We suspect that dams can lead to high FIB concentrations in the dam reservoir, and to reduced bacterial flow into downstream ecosystem. A recent study has reported a significant impact of the large three Gorges dam on the structural and functional patterns of microbial communities (Yan et al., 2015). In addition to the decreasing water level and flow velocity in the main channel, impacts on bacterial community composition was detected more than 30 km un the estuary of Xiangxi river (Yan et al., 2015). Moreover, a study conducted in Kenya investigating the fecal contamination in informal water resources (dams, rivers, springs, wells), have reported the highest concentrations of *E. coli* (3,800 ± 1,807 coliforms 100 mL^{-1}) in samples taken from dams (Opisa et al., 2012). Given the potential survival of FIB in sediments (Pachepsky and Shelton,

2011) and the associated health risks, it is important to investigate not only the contamination attenuation in downstream environments, but also the FIB retention and possible survival in dam reservoirs.

Major knowledge gaps remain present regarding rapid hydropower dams impact on the water's microbiological quality, which stresses the need to improve our understandings to achieve better water resource management.

5.4.4 Hydrological modeling

The modeling approach allows us to test the scenario of unregulated river discharge (no dam) in order to compare it with the actual situation (with dam) and to quantify the dam's impact on hydrology, and in-stream sediment and bacteria concentrations. In this first approach, SWAT was able to simulate daily river discharge in a large-scale watershed (7,448 km2) with satisfactory performance over the calibration period (Fig. 35). The simulated discharge shows an agreement with both the baseline flow and the peaks despite some magnitude underestimations. Although there is room for further improving the hydrological calibration, the performance of the model enabled us to study the dam impact on discharge by comparing the simulations of unregulated river discharge with the observed regulated river discharge after 2014. The modeling tool coupled with the double mass curve approach (Fig. 35c), shows that the simulation showed a good match during calibration period while the cumulative observed discharge started to shift downward after 2014, which is also reflected by the regression coefficient..Overall, mean river discharge between 2014 and 2019 were 42% below pre-dam mean and 54% below simulated unregulated discharge mean, which can suggest a strong dam effect on hydrological regime of the Nam Khan watershed.

A study using SWAT in the Red River (Wei et al., 2019), indicated a discharge decrease of 13% between 2000-2007 and 2008-2013, 9% of which were caused by climate variability and 4% caused by dams. Another study in Chi river basin in Thailand, used SWAT to investigate land use changes on water yield (Homdee et al., 2011). In our study, the detected change in discharge dynamics after 2014 was significant while no significant trend in rainfall records was noted between 2010 and 2019. In future studies it is important to take into account other factors related to climate change, e.g. increase in seasonal temperature and seasonal precipiatation, which is

projected to decrease the discharge of e.g. the Nam Ou river in northern Lao PDR(Shrestha et al., 2013). Moreover land-use changes in Lao PDR have also been proven to have effects on soil erosion and on hydrological response, thus impacting the water and sediment yield on watershed-scale (Mouche et al., 2014; Ribolzi et al., 2018).

This study shows the results of a first modeling application on Nam Khan watershed in northern Lao PDR that resulted in a satisfactory performance on hydrology, however the model could not simulate well sediments nor bacteria concentrations at catchment-scale and needs more improvements suggested in the following section 5.4.5.

5.4.5 Structural and parametric uncertainties

Most of the discharge simulations were within the 95% confidence band, however the simulated peaks at the beginning of each wet season between April and June are slightly over-estimated compared to the observed discharge. This can be due to reliability of the climate *in-situ* data (temperature, relative humidity, wind speed and solar radiation) having some gaps in the records or due to the MSWEP precipitation data during this period, leading to potential errors in evapotranspiration estimations. It can be also due to errors in the water level measurements and the corresponding rating curve used to estimate the daily discharge. Furthermore, the magnitudes of extreme peaks during the wet season were improved when we referred to the values of CN2 used to estimate surface runoff in different land use types estimated for the northern Lao PDR conditions (Vigiak et al., 2008). When we calibrated the 20 discharge-associated parameters, we have found 4 significantly sensitive parameters, soil moist bulk density (SOL_BD), Manning's roughness coefficient in tributary channels (CH_N1) and recession constant (ALPHA_BF), and the lateral flow travel time (LAT_TIME). The latter parameters can affect the flow velocity, soil saturation time, and the watershed response to recharge, thus leading to errors in estimating the baseline flow and the flood peaks during dry and wet seasons. In order to better account for different soil properties according to various land use types (Patin et al., 2012; Ribolzi et al., 2017; Ziegler et al., 2006), which up to now remained constant due to the model concept, it would be interesting in future studies to link soil and land use management parameters (Kim et al., 2018).

The underestimation of the maximum concentration of sediment that can be transported by the water during wet seasons might be related to underestimation in discharge peak magnitude

because both surface runoff and peak runoff rate determine the temporal variation in soil erosion in SWAT. In tropical regions, temporal trends of TSS were found to be following that of surface runoff (Nakhle et al., 2021c; Ribolzi et al., 2017).. Other studies have also reported that modeling might underestimate TSS during large floods and intensive precipitation events (Oeurng et al., 2011; Xu et al., 2009). This underestimation can come from the description of in-stream erosion processes in SWAT, may be from the landscape component using a runoff factor instead of rainfall energy factor, or from the channel component where particle size distribution of sediments particle-size are not well considered in the physical processes (Wei et al., 2019). In our preliminary study, peak rate adjustment factor for sediment routing in the tributary channel (ADJ_PKR) was the most sensitive parameter, which calculates the maximum amount of suspended solids transported in the channel. In addition, two MUSLE parameters (USLE_K and USLE_P) were significantly sensitive. It is necessary to further improve and better take into account more parameters related to the complex soil conditions of Nam Khan watershed. As mentioned earlier, uncertainties can also come from the analytical measurement errors or the sampling strategy and the sporadic frequency of *in-situ* data, which is not adequate to capture the entire TSS dynamics especially following rainfall events.

Consequently, bacteria simulation did not lead to satisfactory results neither, since the only source of bacteria to the stream is surface runoff and consequent land erosion. Only three high concentrations were simulated during the calibration period, however, the peaks magnitudes were not reached when compared to the observed data. Nevertheless, SWAT in its original bacteria module did not reproduce well *E. coli* dynamics in tropical watersheds like Houay Pano in Lao PDR, especially during dry seasons (Kim et al., 2017) . Therefore, we tested the modified bacteria module in SWAT (Kim et al., 2017) which takes into account in-stream processes, such as deposition and resuspension, regrowth and hyporheic exchange. Hydrological modeling in the small-scale watershed Houay Pano (Kim et al., 2017), has proven that the model performance improved when *E. coli* release with sediment resuspension was considered. Moreover, the implementation of hyporheic exchange of bacteria across the Sediment-Water Interface improved bacteria simulation only during the dry season. The implementation of the regrowth process improved the model during the dry season but also induced an overestimation during the wet season. The model performance for [*E. coli*] simulation in our study is considered not acceptable (NS<0) (Table 13). A recent study (Sowah et al., 2020) suggested a bacterial performance criterion

based on NS values reported in previous studies. Performance can be judged "satisfactory" when NS> 0.2, which is lower than those for discharge, nitrogen, and sediment developed by Moriasi et al., (2007). Sowah et al., (2020) attributed the uncertainties involved in modeling fecal bacteria at the watershed level to uncertainties in temporal and spatial distribution of fecal sources that influence model performance, which is cited in previous bacterial modeling studies as well (Cho et al., 2012; Coffey et al., 2013; Frey et al., 2013). In conclusion, the current study presents preliminary results of a first SWAT application on Nam Khan watershed, but major improvements for TSS and *E. coli* simulations are still needed to increase the model performance. Improvements in terms of particle size distribution from streambank and streambed erosion could be a way to simulate more reliable and accurate sediments loads. Moreover, we can improve the model's performance by calibrating parameters related to the concentration of bacteria in streambed (BSC1, BSC2, BSC3, and BSC4) and to bacterial regrowth (C_{T1}) that were taken from Kim et al., (2017).

5.5 Conclusion

This study contributes to the assessment of the impact of water resource management (dam construction) in a major Mekong tributary, the Nam Khan river. Relatively few streamflow stations downstream of tributary dams have pre- and post-dam water quality long-term records, which limits the assessments of dam impacts. In this study, we have taken a step further and investigated not only the corresponding hydrological alterations, but also the significant disruptions to water quality, in particular TSS and *E. coli* dynamics, based on both a statistical and a modeling approaches.

- Change points (Pettitt-test) detected in time-series of measured discharge, TSS, and *E. coli*, occurred in 2014, 2015 and 2016 respectively. These change points coincide well with the construction date in 2014 and commission date in 2016 of the Nam Khan 3 dam. The absence of significant precipitation trend between 2011 and 2020 and the presence of abrupt changes in time-series, likely reflects dam-induced disruptions in the Nam Khan watershed.

- The mean [TSS] at NK26 and NK20 stations decreased by over an average of 83% before and after the detected change points (2015), and mean [*E. coli*] at NK26 and

NK20 stations decreased by over 89% before and after the detected change points (2017 and 2016 respectively).

- Overall, observed mean river discharge between 2014 and 2019 were 42% below pre-dam mean and 54% below simulated unregulated discharge mean, which can be suggests a strong dam effect on hydrological regime of the Nam Khan watershed.

- Finally, in this study, model performance was satisfactory in terms of hydrology (NS>0.7), however, of the simulation of suspended sediment and bacteria (NS of -0.10 and -0.15 respectively) at catchment-scale needs major improvement in order to increase the model performance.

The survival or even growth of bacteria deposited in the sediments of reservoirs upstream of dams must be investigated by future studies in tropical environments. It is important to acquire *in-situ* monitoring on a fine temporal scale in order to capture the risks of highly contaminated flows, especially during the flushing periods of dams. Understanding dam-induced changes, especially large dams or cascade dams in Mekong basin, considered among the most severe human disturbance on the integrity of watersheds, is essential for anticipating and mitigating their yet underexplored negative impacts on river ecosystems and public health.

Chapter 6. Conclusion & perspectives

English version

The research work presented in this thesis aimed to improve our understanding of natural and anthropic key factors controlling fecal bacteria at various spatial-scales in the lower Mekong basin (Fig. 38). The motivation behind this work lies in the necessity to fill major knowledge gaps regarding water fecal contamination dynamics in tropical developing countries. Water availability and quality are crucial to the human-animal-ecosystem health. The Mekong river and its tributaries are an essential shared resource across six countries and main livelihoods for over 70 million people. The water pollution concern is a major problem with multiple facets. Recognizing and understanding the link between human activities, natural process and bacterial dynamics are prerequisites for reducing the risks to the exposed populations. Given the important contribution (35%) of the Mekong tributaries in Lao PDR to the annual discharge of the Mekong mainstream, this work is conducted at various spatial-scales across Lao PDR.

The first part of this thesis (Chapter 3) provided some of the first internationally published data on FIB numbers in major Mekong tributaries from northern to southern Lao PDR, covering a broad range of catchment sizes (239 km^2 to 25,946 km^2), and a large range of geographical, topographical, and land use features. The sampling was conducted at the outlet of 19 tributaries, once during dry season and once during wet season. The Partial Least Square (PLS) analysis mainly allowed us to identify during both seasons, positive correlations between *E. coli* concentrations and the percentage of unstocked forest area, while negative correlations were noted with the percentage of forest and grassland areas. During dry season, *E. coli* concentrations varied between 38 and 11,000 MPN 100 mL^{-1}, while during wet seasons it varied between 38 and 80,000 MPN 100 mL^{-1}. The highest *E. coli* concentrations occurred in watersheds located in steep mountainous areas of northern Lao PDR and in the Vientiane plain, whereas the lowest concentrations occurred in forested watersheds in southern Lao PDR during both seasons. This approach was completed by a close-up investigation at 10-day interval between July 2017 and December 2018, of water quality in the Mekong river and two of its major tributaries in northern Lao PDR. The latter revealed as well the strong seasonal variability of *E. coli* marked by higher concentrations during wet season, and strong correlation with TSS during both seasons. These findings suggest the importance of TSS as an important vector for bacterial transport, which is particularly to be taken into account when land management increase deforested areas exposed to soil erosion, thus to *E. coli* dissemination

during erosive rainfall events.

Most importantly, the present data showed a continuous in-stream presence of *E. coli* in all of the three catchments over the 2017-2018 period, exceeding the international thresholds accepted for drinking and recreational water. The highest range of *E. coli* was measured at the sampling site on the Mekong river (250-350,000 MPN 100 mL^{-1}), followed by the outlet of Nam Suang (78-39,000 MPN 100 mL^{-1}) and the outlet of Nam Ou (0-7,100 MPN 100 mL^{-1}). Likewise, the majority of sampled tributaries across Lao PDR presented very high *E. coli* concentrations during the rainy season, exceeding 500 colonies per 100 mL, the threshold above which the WHO considers a 10% risk of gastrointestinal illness after one single exposure.

It is well known that water microbiological quality can vary greatly across the river. Overall, it reflects the balance between the ecosystem self-cleaning potential and the pollution input. In tropical humid systems like the Mekong basin, land use features like wetlands are widespread and provide multiple ecosystem services including food production, flood control, habitat biodiversity, and water purification. Headwater wetlands, although representing a limited proportion of the drainage watershed area, are likely to play a key role in stream water purification of fecal pollutants. However, the FIB behavior in tropical mountainous headwater wetlands are poorly documented, hence still poorly understood.

Therefore, in the second part of the thesis (Chapter 4), we adopted an experimental approach, in which we evaluated *E. coli* decay/survival under the impact of two key factors, i.e. solar radiation exposition and suspended particles deposition. In order to obtain decay rates (k) estimates as realistic as possible, we conducted the experiments in a semi-controlled environment, so we installed and monitored 12 mesocosms for 8 days in the water column of the main headwater wetland of the Houay Pano catchment in northern Lao PDR. The mesocosms were divided into four treatments with triplicates as follows: sediment deposition-light (DL); sediment deposition-dark (DD); sediment resuspension-light (RL); and sediment resuspension-dark (RD). Over 91% of total *E. coli* were attached to particles over the incubation period, and showed lower decay rates than those of free-living *E. coli* in all treatments. These results further highlights the role of TSS in *E. coli* dynamics, suggesting a key role in protecting bacteria from various stressors such as predation and sunlight. These findings point out as well the role of TSS as vectors for vertical migration of FIB within the water column settling in bottom sediment, thereby providing a new

environment for the cells. While deposition process was the main factor responsible for an average of 92% of the estimated *E. coli* stock reduction in the water column, only 2% was due to the exposure to solar radiation. The apparent decay rates of total *E. coli* concentration for mesocosms left to deposit ($k = 1.43\ day^{-1}$ in DL and 1.17 day−1 in DD) were higher than in mesocosms subject to resuspension ($k = 0.50\ day^{-1}$ in RL and $-0.14\ day^{-1}$ in RD). Overall, the time required to achieve T_{50}, i.e. 50% reduction, of particle-attached *E. coli*, was the longest in RD followed by RL ranging respectively between 117.8 and 33.4 hours, and the shortest for DL followed by DD ranging respectively between 11.6 and 14.2 hours. On the other hand, the T_{50} in RD and RL is divided by two for free-living *E. coli* ranging respectively between 59.4 and 13.9 hours, whereas in DL and DD, the T_{50} is similar to the particle-attached *E. coli* ranging respectively between 10.9 and 12.2 hours. The artificial resuspension process, prior to each sample collection allowed us to access the dynamics of deposited bacteria in the bottom sediment, which suggested a potential *E. coli* survival, or even a regrowth in the sediment under tropical conditions. Therefore, it is imperative to consider key factors like TSS dynamics as well as deposition and resuspension processes when investigating fecal contamination in tropical wetlands and riparian areas used for rice cultivation, in the perspective of the effective conservation of the valuable ecosystem services that they deliver.

Given the importance of hydro-sedimentary dynamics on *E. coli* fate and transport at watershed-scale, there is great need to assess dam impact widely known for important hydrological alterations and sediments retention. The hydrological connectivity in the river network plays a critical role in the hydrological cycle, processing and transporting sediments, and associated nutrients and contaminants like *E. coli* to oceans. The exerted disturbance in the upstream basin can affect significantly the water availability and the water quality downstream.

In the last part of this thesis work (Chapter 5), we aimed to detect and quantify the dam induced changes on downstream river discharge, TSS and *E. coli* concentrations in the Nam Khan tributary. To do so, we used at first statistical analysis, i.e. Pettitt-test, Mann-Kendall and double mass curves, to detect trends and change points in a 10-year record of pre and post-dam discharge, and TSS and *E. coli* concentrations. Significant change points were detected for measured discharge, and TSS and *E. coli* concentrations, in 2013, 2015 and 2016 respectively, which are likely to reflect the impact of the dam constructed in 2014. Discharge alterations due to natural factors can be expected to progress gradually, but those due to anthropogenic factors are likely to

occur abruptly after a change, as can be seen from the double mass curve approach. Similarly to river discharge, TSS seasonal variations were less clear after the dam construction, decreased by an average of 83% between the periods of pre-dam (0.183 ± 0.42 g L^{-1}) and post-dam (0.031 ± 0.03 g L^{-1}). *E. coli* showed similar patterns as river discharge and TSS, following distinct seasonal variations during the pre-dam period and a significant attenuation by an average of 89 % since the dam construction.

Subsequently, in a first exploratory modelling work, we tested the ability of the modelling tool SWAT, at large watershed-scale (7,448 km^2), in order to quantitatively estimate the dam impact on river discharge, and TSS and *E. coli* concentrations. Several studies have investigated the impact on hydro-sedimentary dynamics but up to our knowledge, no study have used SWAT to quantify the dam impact on fecal bacteria dynamics. In this first approach, SWAT was able to simulate daily river discharge in a large-scale watershed with satisfactory performance over the calibration period, with a p-factor and r-factor of 0.70 and 0.62 respectively, and NS and R^2 of 0.70 and 0.71 respectively. Overall, mean river post-dam discharge were 42% below pre-dam mean and 54% below simulated unregulated discharge mean, which suggests a strong dam effect on hydrological regime of the Nam Khan watershed. However, the simulation of TSS and *E. coli* at catchment-scale needs major improvement in order to increase the model performance. In future studies, SWAT can be used as a predictive tool that might help to establish sustainable and reasonable water resources management.

In view of the elements discussed during this thesis and by other studies, the question of the survival or even growth of bacteria deposited in the sediments of reservoirs upstream of dams must investigated by future studies in tropical environments. It is important to acquire *in-situ* monitoring on a fine temporal scale in order to capture the risks of highly contaminated flows, especially during the flushing periods of dams.

Driving forces:

- Humid tropical climate variability
- Steep montane landscape
- Transboundary river
- Population growth
- Regional development
- Economic constraints

Policies & management

Regulation & development

Pressure:

- Land and water resources
- Hydropower dams
- Deforestation
- Inadequate sanitary infrastructure
- Low access to safe resources
- Human behavior

Responses:

- Regular monitoring at adequate spatio-temporal scales
- Impact assessment (modeling tools…)
- Wetland conservation
- Integrated resource management
- Sustainable development

Impacts:

- Floods and droughts
- Hydrological disruptions
- Soil surface infilitrability
- Surface runoff
- Sediment and bacteria export
- Bacterial resuspension
- Loss of ecosystem services
- High FIB concentrations
- Public health risk

Mitigation strategies

Monitoring & prevention

State of the environment:

- Monoculture plantations
- Low understory cover
- Annual cash crops
- Rapid dam construction
- Wetland ecosystems disruption
- Use of unimproved water resources
- Diffuse pollution increase

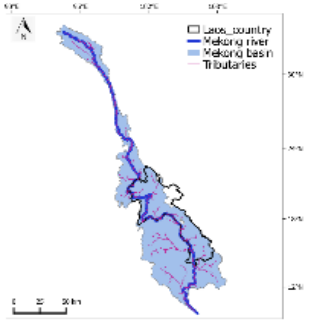

SWAT

SDG goals

One-health

Figure 38: The Driving force-Pressure-State-Exposure-Effect-Action framework applied to the fecal contamination of tropical hydrosystems in the Mekong watershed, Lao PDR.

Version française

Le travail de recherche présenté dans cette thèse vise à améliorer notre compréhension des facteurs clés environnementaux et anthropiques contrôlant les bactéries fécales à différentes échelles spatiales dans le bassin inférieur du Mékong (Fig. 38). La motivation de ce travail réside dans la nécessité de combler les lacunes majeures en termes de connaissances sur la dynamique de la contamination fécale de l'eau dans les pays tropicaux en développement. La disponibilité et la qualité de l'eau sont cruciales pour la santé de l'homme, de l'animal et de l'écosystème. Le fleuve Mékong et ses affluents sont une ressource essentielle partagée par six pays et les principaux moyens de subsistance de plus de 70 millions de personnes. La pollution de l'eau est un problème majeur aux multiples facettes. Reconnaître et comprendre le lien entre les activités humaines, les processus naturels et la dynamique bactérienne sont des conditions préalables à la réduction des risques pour les populations exposées. Etant donné la contribution importante (35%) des tributaires du Mékong au Laos, au débit annuel du Mékong principal, ce travail est mené à différentes échelles spatiales au Laos.

La première partie de cette thèse (Chapitre 3) a fourni certaines des premières données publiées au niveau international sur le nombre de FIB dans les principaux affluents du Mékong du nord au sud du Laos, couvrant une large gamme de tailles de bassins versants (239 km^2 à 25 946 km^2), et une grande variété de caractéristiques géographiques, topographiques et d'utilisation des terres. L'échantillonnage a été réalisé à la sortie de 19 affluents, une fois pendant la saison sèche et une fois pendant la saison humide. L'analyse des moindres carrés partiels (PLS) a principalement permis d'identifier, au cours des deux saisons, des corrélations positives entre les concentrations d'*E. coli* et le pourcentage de zone forestière non exploitée, tandis que des corrélations négatives ont été notées avec le pourcentage de zones forestières et de prairies. Pendant la saison sèche, les concentrations d'*E. coli* ont varié entre 38 et 11,000 NPP 100 mL^{-1}, tandis que pendant les saisons humides, elles ont varié entre 38 et 80,000 NPP 100 mL^{-1}. Les concentrations d'*E. coli* les plus élevées ont été observées dans les bassins versants situés dans les zones montagneuses escarpées du nord du Laos et dans la plaine de Vientiane, tandis que les concentrations les plus faibles ont été observées dans les bassins versants forestiers du sud du Laos pendant les deux saisons. Cette approche a été complétée par une étude rapprochée à 10 jours d'intervalle entre juillet 2017 et décembre 2018, de la qualité de l'eau du Mékong et de deux de ses principaux affluents dans le

nord du Laos. Cette dernière a révélé également la forte variabilité saisonnière d'*E. coli* marquée par des concentrations plus élevées pendant la saison humide, et une forte corrélation avec les MES pendant les deux saisons. Ces résultats suggèrent l'importance des MES en tant que vecteur important du transport bactérien, ce qui est particulièrement à prendre en compte lorsque la gestion des terres augmente les zones déboisées exposées à l'érosion du sol, donc à la dissémination d'*E. coli* lors d'événements pluvieux érosifs.

Plus important encore, les présentes données ont montré une présence continue d'*E. coli* dans les cours d'eau dans les trois bassins versants au cours de la période 2017-2018, dépassant les seuils internationaux acceptés pour l'eau potable et récréative. La gamme la plus élevée d'*E. coli* a été mesurée sur le site d'échantillonnage du Mékong (250-350,000 NPP 100 mL^{-1}), suivi par la sortie de Nam Suang (78-39,000 NPP 100 mL^{-1}) et la sortie de Nam Ou (0-7,100 NPP 100 mL^{-1}). De même, la majorité des affluents échantillonnés au Laos présentaient des concentrations très élevées d'E. coli pendant la saison des pluies, dépassant 500 colonies par 100 mL, seuil au-delà duquel l'OMS considère qu'il existe un risque de 10 % de maladie gastro-intestinale après une seule exposition.

Il est bien connu que la qualité microbiologique de l'eau peut varier considérablement d'un cours d'eau à l'autre. Globalement, elle reflète l'équilibre entre le potentiel d'auto-nettoyage de l'écosystème et l'apport de pollution. Dans les systèmes tropicaux humides comme le bassin du Mékong, les caractéristiques de l'utilisation des terres, comme les zones humides, sont très répandues et fournissent de multiples services écosystémiques, notamment la production alimentaire, le contrôle des inondations, la biodiversité des habitats et la purification de l'eau. Les zones humides d'amont, bien que représentant une proportion limitée de la superficie du bassin versant, sont susceptibles de jouer un rôle clé dans l'épuration des polluants fécaux dans les cours d'eau. Cependant, le comportement des FIB dans les zones humides de tête des montagnes tropicales est peu documenté et donc encore mal compris.

Par conséquent, dans la deuxième partie de la thèse (Chapitre 4), nous avons adopté une approche expérimentale, dans laquelle nous avons évalué la mortalité/survie d'*E. coli* sous l'impact de deux facteurs clés, à savoir l'exposition au rayonnement solaire et le dépôt de particules en suspension. Afin d'obtenir des estimations de taux de décomposition (k) les plus réalistes possible, nous avons mené les expériences dans un environnement semi-contrôlé, nous avons donc installé

et échantillonné l'eau dans 12 mésocosmes pendant 8 jours dans la colonne d'eau de la principale zone humide d'amont du bassin versant de Houay Pano dans le nord du Laos. Les mésocosmes ont été divisés en quatre traitements avec des triplicats comme suit : dépôt de sédiments - lumière (DL) ; dépôt de sédiments - obscurité (DD) ; remise en suspension de sédiments - lumière (RL) ; et remise en suspension de sédiments - obscurité (RD). Plus de 91% des *E. coli* totaux étaient attachés aux particules pendant la période d'incubation, et ont montré des taux de décomposition plus faibles que ceux des *E. coli* libres dans tous les traitements. Ces résultats mettent en évidence le rôle des MES dans la dynamique d'*E. coli*, suggérant un rôle clé dans la protection des bactéries contre divers facteurs de stress tels que la prédation et la lumière du soleil. Ces résultats soulignent également le rôle des MES en tant que vecteurs de la migration verticale des agents pathogènes dans la colonne d'eau, qui se déposent dans les sédiments de fond, offrant ainsi un nouvel environnement aux cellules. Alors que le processus de dépôt était le principal facteur responsable d'une moyenne de 92% de la réduction estimée du stock d'*E. coli* dans la colonne d'eau, seulement 2% était dû à l'exposition au rayonnement solaire. Les taux de mortalité apparents de la concentration totale d'*E. coli* pour les mésocosmes laissés au dépôt ($k = 1{,}43$ jour^{-1} dans DL et 1,17 jour-1 dans DD) étaient plus élevés que dans les mésocosmes soumis à une remise en suspension ($k = 0{,}50$ jour^{-1} dans RL et -0,14 jour^{-1} dans RD). Dans l'ensemble, le temps nécessaire pour atteindre la T_{50}, c'est-à-dire une réduction de 50 % des *E. coli* fixés sur les particules, a été le plus long dans le cas de RD, suivi de RL, variant respectivement entre 117,8 et 33,4 heures, et le plus court dans le cas de DL, suivi de DD, variant respectivement entre 11,6 et 14,2 heures. D'autre part, le T_{50} dans RD et RL est divisé par deux pour les *E. coli* libres, variant respectivement entre 59,4 et 13,9 heures, alors que dans DL et DD, le T_{50} est similaire aux *E. coli* attachés aux particules, variant respectivement entre 10,9 et 12,2 heures. Le processus de remise en suspension artificielle, avant chaque collecte d'échantillons, nous a permis d'accéder à la dynamique des bactéries déposées dans le sédiment de fond, ce qui suggère une survie potentielle d'*E. coli* ou même une recroissance dans le sédiment dans des conditions tropicales. Par conséquent, il est impératif de prendre en compte des facteurs clés comme la dynamique des MES ainsi que les processus de dépôt et de remise en suspension lors de l'étude de la contamination fécale dans les zones humides tropicales et les zones riveraines utilisées pour la riziculture, dans la perspective d'une conservation efficace des précieux services écosystémiques qu'elles fournissent.

Compte tenu de l'importance de la dynamique hydro-sédimentaire sur le devenir et le

transport d'*E. coli* à l'échelle du bassin versant, il est indispensable d'évaluer l'impact des barrages, largement connus pour leurs importantes modifications hydrologiques et la rétention des sédiments. La connectivité hydrologique dans le réseau fluvial joue un rôle essentiel dans le cycle hydrologique, transportant les sédiments, ainsi que les nutriments et les contaminants associés comme *E. coli*. La perturbation exercée dans le bassin amont peut affecter de manière significative la disponibilité et la qualité de l'eau en aval.

Dans la dernière partie de ce travail de thèse (Chapitre 5), nous avons cherché à détecter et à quantifier les changements induits par le barrage sur le débit de la rivière en aval, les concentrations de MES et d'*E. coli* dans le tributaire de la Nam Khan. Pour ce faire, nous avons d'abord utilisé une analyse statistique, basée sur le test de Pettitt, les courbes de Mann-Kendall et de double masse, pour détecter les tendances et les points de rupture dans un enregistrement de 10 ans du débit avant et après barrage, et des concentrations en MES et *E. coli*. Des points de rupture significatifs ont été détectés pour le débit mesuré et les concentrations de MES et d'*E. coli*, en 2013, 2015 et 2016 respectivement, qui sont susceptibles de refléter l'impact du barrage construit en 2014. On peut s'attendre à ce que les modifications du débit dues à des facteurs naturels progressent progressivement, mais celles dues à des facteurs anthropiques sont susceptibles de se produire brusquement après un changement, comme le montre l'approche de la double courbe de masse. De même que pour le débit de la rivière, les variations saisonnières des MES étaient moins claires après la construction du barrage, diminuant en moyenne de 83% entre les périodes avant barrage (0,183 ± 0,42 g L^{-1}) et après barrage (0,031 ± 0,03 g L^{-1}). *E. coli* a montré des schémas similaires à ceux du débit de la rivière et des TSS, suivant des variations saisonnières distinctes pendant la période avant barrage et une atténuation significative de 89 % en moyenne depuis la construction du barrage.

Par la suite, dans un premier travail de modélisation exploratoire, nous avons testé la capacité de l'outil de modélisation SWAT, à l'échelle d'un grand bassin versant (7,448 km^2), afin d'estimer quantitativement l'impact du barrage sur le débit des rivières et les concentrations de MES et d'*E. coli*. Plusieurs études ont étudié l'impact sur la dynamique hydro-sédimentaire mais à notre connaissance, aucune étude n'a utilisé SWAT pour quantifier l'impact du barrage sur la dynamique des bactéries fécales. Dans cette première approche, SWAT a été capable de simuler le débit journalier de la rivière dans un bassin versant à grande échelle avec des performances satisfaisantes

sur la période de calibration, montrant un facteur p et un facteur r de 0,70 et 0,62 respectivement, ainsi qu'un NS et un R^2 de 0,70 et 0,71 respectivement. Dans l'ensemble, le débit moyen de la rivière après le barrage était de 42 % inférieur au débit moyen avant barrage et de 54 % inférieur au débit moyen non régulé simulé, ce qui suggère un effet important du barrage sur le régime hydrologique du bassin versant de la Nam Khan. Cependant, la simulation des MES et des *E. coli* à l'échelle du bassin versant doit être considérablement améliorée afin d'accroître les performances du modèle. Dans les études futures, SWAT peut être utilisé comme un outil de prédiction qui pourrait aider à établir une gestion durable et raisonnable des ressources en eau.

En vue des éléments discutés au cours de cette thèse et par d'autres études, la question sur la survie voire croissance des bactéries déposées dans les sédiments des réservoirs en amont des barrages, doit faire l'objet de futures investigations en milieu tropical. Il est urgent d'étudier cette problématique à une échelle temporelle fine afin de capter les variabilités susceptibles de générer des flux fortement contaminés, notamment lors des périodes de chasse des barrages.

References

Abbas, A., Baek, S., Silvera, N., Soulileuth, B., Pachepsky, Y., Ribolzi, O., Boithias, L., Cho, K.H., 2021. In-stream Escherichia Coli Modeling Using high-temporal-resolution data with deep learning and process-based models. Hydrol. Earth Syst. Sci. Discuss. [preprint] 1–55. https://doi.org/10.5194/HESS-2021-98

Abbaspour, K.C., 2014. SWAT Calibration and Uncertainty Programs - A User Manual. Swiss Fed. Inst. Aquat. Sci. Technol. Fed. Inst. Aquat. Sci. Technol. 106.

Abbaspour, K.C., Johnson, C.A., van Genuchten, M.T., 2004. Estimating Uncertain Flow and Transport Parameters Using a Sequential Uncertainty Fitting Procedure. Vadose Zo. J. 3, 1340–1352. https://doi.org/10.2113/3.4.1340

Abbaspour, K.C., Rouholahnejad, E., Vaghefi, S., Srinivasan, R., Yang, H., Kløve, B., 2015. A continental-scale hydrology and water quality model for Europe: Calibration and uncertainty of a high-resolution large-scale SWAT model. J. Hydrol. 524, 733–752. https://doi.org/10.1016/J.JHYDROL.2015.03.027

Abbaspour, K.C., Yang, J., Maximov, I., Siber, R., Bogner, K., Mieleitner, J., Zobrist, J., Srinivasan, R., 2007. Modelling hydrology and water quality in the pre-alpine/alpine Thur watershed using SWAT. J. Hydrol. 333, 413–430. https://doi.org/10.1016/j.jhydrol.2006.09.014

Adamson, P., 2001. Hydrological perspectives of the Lower Mekong. Int. Water Power Dam Constr. 3, 16–17, 19–21.

Ahmed, W., Zhang, Q., Lobos, A., Senkbeil, J., Sadowsky, M.J., Harwood, V.J., Saeidi, N., Marinoni, O., Ishii, S., 2018. Precipitation influences pathogenic bacteria and antibiotic resistance gene abundance in storm drain outfalls in coastal sub-tropical waters. Environ. Int. 116, 308–318. https://doi.org/10.1016/J.ENVINT.2018.04.005

Alemayehu, T., Van Griensven, A., Bauwens, W., 2017. An improved SWAT vegetation growth module and its evaluation for four tropical ecosystems. Hydrol. Earth Syst. Sci. https://doi.org/10.5194/hess-2017-104

Alexander, R.B., Boyer, E.W., Smith, R.A., Schwarz, G.E., Moore, R.B., 2007. The Role of Headwater Streams in Downstream Water Quality1. JAWRA J. Am. Water Resour. Assoc. 43, 41–59. https://doi.org/10.1111/j.1752-1688.2007.00005.x

Almuktar, S.A.A.A.N., Abed, S.N., Scholz, M., 2018. Wetlands for wastewater treatment and subsequent recycling of treated effluent: a review. Environ. Sci. Pollut. Res. 25, 23595–23623. https://doi.org/10.1007/s11356-018-2629-3

Amalfitano, S., Corno, G., Eckert, E., Fazi, S., Ninio, S., Callieri, C., Grossart, H.-P., Eckert, W.,

2017. Tracing particulate matter and associated microorganisms in freshwaters. Hydrobiol. 2017 8001 800, 145–154. https://doi.org/10.1007/S10750-017-3260-X

Anderson, K.L., Whitlock, J.E., Harwood, V.J., 2005. Persistence and differential survival of fecal indicator bacteria in subtropical waters and sediments. Appl. Environ. Microbiol. 71, 3041–3048. https://doi.org/10.1128/AEM.71.6.3041-3048.2005

Arias, C., Sala, M.R., Domonguez, A., Bartolome, R., Benavente, A., Veciana, P., Pedrol, A., Hoyo, G., 2006. Waterborne epidemic outbreak of Shigella sonnei gastroenteritis in Santa Maria de Palautordera, Catalonia, Spain. Epidemiol. Infect. 134, 598–604. https://doi.org/10.1017/S0950268805005121

Arias, M.E., Holtgrieve, G.W., Ngor, P.B., Dang, T.D., Piman, T., 2019. Maintaining perspective of ongoing environmental change in the Mekong floodplains. Curr. Opin. Environ. Sustain. 37, 1–7. https://doi.org/10.1016/j.cosust.2019.01.002

Arias, M.E., Piman, T., Lauri, H., Cochrane, T.A., Kummu, M., 2014a. Dams on Mekong tributaries as significant contributors of hydrological alterations to the Tonle Sap Floodplain in Cambodia. Hydrol. Earth Syst. Sci. 18, 5303–5315. https://doi.org/10.5194/hess-18-5303-2014

Arias, M.E., Piman, T., Lauri, H., Cochrane, T.A., Kummu, M., 2014b. Dams on Mekong tributaries as significant contributors of hydrological alterations to the Tonle Sap Floodplain in Cambodia. Hydrol. Earth Syst. Sci. 18, 5303–5315. https://doi.org/10.5194/hess-18-5303-2014

Arnold, J.G., Moriasi, D.N., Gassman, P.W., Abbaspour, K.C., White, M.J., Srinivasan, R., Santhi, C., Harmel, R.D., Van Griensven, A., Liew, M W Van, Kannan, N., Jha, M.K., Harmel, D., Member, A., Liew, Michael W Van, Arnold, J.-F.G., 2012. SWAT: MODEL USE, CALIBRATION, AND VALIDATION. Trans. ASABE 55, 1491–1508.

Arnold, J.G., Srinivasan, R., Muttiah, R.S., Williams J.R., 1998. Large area hydrological modeling and assessment part 1: model development. JAWRA J. Am. Water Resour. Assoc. 34, 73–89.

Bagnold, R.A., 1977. Bed load transport by natural rivers. Water Resour. Res. 13, 303–312. https://doi.org/10.1029/WR013I002P00303

Bain, R., Cronk, R., Hossain, R., Bonjour, S., Onda, K., Wright, J., Yang, H., Slaymaker, T., Hunter, P., Prüss-Ustün, A., Bartram, J., 2014. Global assessment of exposure to faecal contamination through drinking water based on a systematic review. Trop. Med. Int. Heal. 19, 917–927. https://doi.org/10.1111/tmi.12334

Baird, I.G., 2011. The Don Sahong Dam: Potential Impacts on Regional Fish Migrations, Livelihoods, and Human Health 43, 211–235. https://doi.org/10.1080/14672715.2011.570567

Bannwarth, M.A., Sangchan, W., Hugenschmidt, C., Lamers, M., Ingwersen, J., Ziegler, A.D.,

Streck, T., 2014. Pesticide transport simulation in a tropical catchment by SWAT. https://doi.org/10.1016/j.envpol.2014.04.011

Beck, H.E., van Dijk, A.I.J.M., Levizzani, V., Schellekens, J., Miralles, D.G., Martens, B., de Roo, A., 2017. MSWEP : 3-hourly 0.25° global gridded precipitation (1979-2015) by merging gauge, satellite, and reanalysis data. Hydrol. Earth Syst. Sci. 21, 589–615. https://doi.org/10.5194/hess-21-589-2017

Beck, H.E., Wood, E.F., Pan, M., Fisher, C.K., Miralles, D.G., Van Dijk, A.I.J.M., McVicar, T.R., Adler, R.F., 2019. MSWep v2 Global 3-hourly 0.1° precipitation: Methodology and quantitative assessment. Bull. Am. Meteorol. Soc. 100, 473–500. https://doi.org/10.1175/BAMS-D-17-0138.1

Berg, H., Ekman Söderholm, A., Söderström, A.S., Tam, N.T., 2017. Recognizing wetland ecosystem services for sustainable rice farming in the Mekong Delta, Vietnam. Sustain. Sci. 12, 137–154. https://doi.org/10.1007/s11625-016-0409-x

Billen, G., Garnier, J., Hanset, P., 1994. Modelling phytoplankton development in whole drainage networks: the RIVERSTRAHLER Model applied to the Seine river system. Hydrobiol. 1994 2891 289, 119–137. https://doi.org/10.1007/BF00007414

Blaustein, R.A., Pachepsky, Y., Hill, R.L., Shelton, D.R., Whelan, G., 2013. Escherichia coli survival in waters: Temperature dependence. Water Res. 47, 569–578. https://doi.org/10.1016/j.watres.2012.10.027

Blumberg, A.F., Mellor, G.L., 2012. A Description of a Three-Dimensional Coastal Ocean Circulation Model 1–16. https://doi.org/10.1029/CO004P0001

Boaretti, M., Lleò, M., Bonato, B., Signoretto, C., Canepari, P., 2003. Involvement of rpoS in the survival of Escherichia coli in the viable but non-culturable state. Environ. Microbiol. 5, 986–996. https://doi.org/10.1046/J.1462-2920.2003.00497.X

Boithias, L., Auda, Y., Audry, S., Bricquet, J., Chanhphengxay, A., Chaplot, V., Rouw, A., Tureaux, T.H., Huon, S., Janeau, J., Latsachack, K., Le Troquer, Y., Lestrelin, G., Maeght, J., Marchand, P., Moreau, P., Noble, A., Pando-Bahuon, A., Phachomphon, K., Phanthavong, K., Pierret, A., Ribolzi, O., Riotte, J., Robain, H., Rochelle-Newall, E., Sayavong, S., Sengtaheuanghoung, O., Silvera, N., Sipaseuth, N., Soulileuth, B., Souliyavongsa, X., Sounyaphong, P., Tasaketh, S., Thammahacksa, C., Thiebaux, J., Valentin, C., Vigiak, O., Viguier, M., Xayyathip, K., 2021a. The Multiscale TROPIcal CatchmentS critical zone observatory M-TROPICS dataset II: land use, hydrology and sediment production monitoring in Houay Pano, northern Lao PDR. Hydrol. Process. e14126. https://doi.org/10.1002/hyp.14126

Boithias, L., Choisy, M., Souliyaseng, N., Jourdren, M., Quet, F., Buisson, Y., Thammahacksa, C., Silvera, N., Latsachack, K., Sengtaheuanghoung, O., Pierret, A., Rochelle-Newall, E., Becerra, S., Ribolzi, O., 2016. Hydrological Regime and Water Shortage as Drivers of the Seasonal Incidence of Diarrheal Diseases in a Tropical Montane Environment. PLoS Negl. Trop. Dis. 10, e0005195. https://doi.org/10.1371/journal.pntd.0005195

Boithias, L., Ribolzi, O., Lacombe, G., Thammahacksa, C., Silvera, N., Latsachack, K., Soulileuth, B., Viguier, M., Auda, Y., Robert, E., Evrard, O., Huon, S., Pommier, T., Zouiten, C., Sengtaheuanghoung, O., Rochelle-Newall, E., 2021b. Quantifying the effect of overland flow on Escherichia coli pulses during floods: use of a tracer-based approach in an erosion-prone tropical catchment. J. Hydrol. 594, 125935. https://doi.org/10.1016/j.jhydrol.2020.125935

Bordalo, A.A., Onrassami, R., Dechsakulwatana, C., 2002. Survival of faecal indicator bacteria in tropical estuarine waters (Bangpakong River, Thailand). J. Appl. Microbiol. 93, 864–871. https://doi.org/10.1046/j.1365-2672.2002.01760.x

Boutilier, L., Jamieson, R., Gordon, R., Lake, C., Hart, W., 2009. Adsorption, sedimentation, and inactivation of E. coli within wastewater treatment wetlands. Water Res. 43, 4370–4380. https://doi.org/10.1016/j.watres.2009.06.039

Bouvy, M., Briand, E., Boup, M.M., Got, P., Leboulanger, C., Bettarel, Y., Arfi, R., Bouvy, M., Briand, E., Boup, M.M., Got, P., Leboulanger, C., Bettarel, Y., Arfi, R., 2008. Effects of sewage discharges on microbial components in tropical coastal waters (Senegal, West Africa). Mar. Freshw. Res. 59, 614–626. https://doi.org/10.1071/MF07244

Brandt, S.A., 2000. Classification of geomorphological effects downstream of dams. CATENA 40, 375–401. https://doi.org/10.1016/S0341-8162(00)00093-X

Brauman, K.A., Daily, G.C., Duarte, T.K. eo, Mooney, H.A., 2007. The nature and value of ecosystem services: An overview highlighting hydrologic services. Annu. Rev. Environ. Resour. 32, 67–98. https://doi.org/10.1146/annurev.energy.32.031306.102758

Brendel, C., Soupir, M.L., 2017. Relating watershed characteristics to elevated stream Escherichia coli levels in agriculturally dominated landscapes: An Iowa case study. Water (Switzerland) 9. https://doi.org/10.3390/w9030154

Brettar, I., Hoflet, M.G., 1992. Influence of Ecosystematic Factors on Survival of Escherichia coli after Large-Scale Release into Lake Water Mesocosms. Appl. Environ. Microbiol. 58, 2201–2210. https://doi.org/0099-2240/92/072201-10$02.00/0

Brown, S.B., Ikenberry, C.D., Soupir, M.L., Bisinger, J., Russell, J.R., 2014. Predicting Time Cattle Spend in Streams to Quantify Direct Deposition of Manure. Appl. Eng. Agric. 30, 187–195. https://doi.org/10.13031/AEA.30.10393

Buckley, R., Clough, E., Warnken, W., Wild, C., 1998. Coliform bacteria in streambed sediments in a subtropical rainforest conservation reserve. Water Res. 32, 1852–1856. https://doi.org/10.1016/S0043-1354(97)00414-4

Bunn, S.E., Arthington, A.H., 2002. Basic Principles and Ecological Consequences of Altered Flow Regimes for Aquatic Biodiversity. Environ. Manag. 2002 304 30, 492–507. https://doi.org/10.1007/S00267-002-2737-0

Burton, G.A., Gunnison, D., Lanzal, G.R., 1987. Survival of Pathogenic Bacteria in Various

Freshwater Sediments. Appl. Environ. Microbiol. 53, 633–638.

Byamukama, D., Mach, R.L., Kansiime, F., Manafi, M., Farnleitner, A.H., 2005. Discrimination efficacy of fecal pollution detection in different aquatic habitats of a high-altitude tropical country, using presumptive coliforms, Escherichia coli, and Clostridium perfringens spores. Appl. Environ. Microbiol. 71, 65–71. https://doi.org/10.1128/AEM.71.1.65-71.2005

Byappanahalli, M.., Fujioka, R., 2004. Indigenous soil bacteria and low moisture may limit but allow faecal bacteria to multiply and become a minor population in tropical soils. Water Sci. Technol. A J. Int. Assoc. Water Pollut. Res. 50, 27–32.

Byappanahalli, M.N., Fujioka, R.S., 1998. EVIDENCE THAT TROPICAL SOIL ENVIRONMENT CAN SUPPORT THE GROWTH OF ESCHERICHIA COLI, Pergamon Wal. SeL Tech. https://doi.org/10.1016/S0273-1223(98)00820-8

Byappanahalli, M.N., Nevers, M.B., Korajkic, A., Staley, Z.R., Harwood, V.J., 2012a. Enterococci in the Environment. https://doi.org/10.1128/MMBR.00023-12

Byappanahalli, M.N., Shively, D.A., Nevers, M.B., Sadowsky, M.J., Whitman, R.L., 2003. Growth and survival of Escherichia coli and enterococci populations in the macro-alga Cladophora (Chlorophyta). FEMS Microbiol. Ecol. 46, 203–211. https://doi.org/10.1016/S0168-6496(03)00214-9

Byappanahalli, M.N., Yan, T., Hamilton, M.J., Ishii, S., Fujioka, R.S., Whitman, R.L., Sadowsky, M.J., 2012b. The population structure of Escherichia coli isolated from subtropical and temperate soils. https://doi.org/10.1016/j.scitotenv.2011.12.041

Cabelli, V.J., 1989. Swimming-Associated Illness and Recreational Water Quality Criteria. Water Sci. Technol. 21, 13–21. https://doi.org/10.2166/WST.1989.0022

Cabral, J.P., Marques, C., 2006. Faecal coliform bacteria in febros river (Northwest Portugal): Temporal variation, correlation with water parameters, and species identification. Environ. Monit. Assess. 118, 21–36. https://doi.org/10.1007/S10661-006-0771-8

Cano-Paoli, K., Chiogna, G., Bellin, A., 2019. Convenient use of electrical conductivity measurements to investigate hydrological processes in Alpine headwaters. Sci. Total Environ. 685, 37–49. https://doi.org/10.1016/j.scitotenv.2019.05.166

Causse, J., Billen, G., Garnier, J., Henri-des-Tureaux, T., Olasa, X., Thammahacksa, C., Latsachak, K.O., Soulileuth, B., Sengtaheuanghoung, O., Rochelle-Newall, E., Ribolzi, O., 2015. Field and modelling studies of Escherichia coli loads in tropical streams of montane agro-ecosystems. J. Hydro-Environment Res. 9, 496–507. https://doi.org/10.1016/j.jher.2015.03.003

Chahinian, N., Bancon-Montigny, C., Caro, A., Got, P., Perrin, J.L., Rosain, D., Rodier, C., Picot, B., Tournoud, M.G., 2012. The role of river sediments in contamination storage downstream of a waste water treatment plant in low flow conditions: Organotins, faecal indicator bacteria and nutrients. Estuar. Coast. Shelf Sci. 114, 70–81.

https://doi.org/10.1016/j.ecss.2011.09.007

Chan, Y.M., Thoe, W., Lee, J.H.W., 2015. Field and laboratory studies of Escherichia coli decay rate in subtropical coastal water. J. Hydro-Environment Res. 9, 1–14. https://doi.org/10.1016/j.jher.2014.08.002

Chao, W., Sha-sha, Z., Pei-fang, W., Jun, H., 2015. Interactions between vegetation, water flow and sediment transport: A review * 27, 24–37. https://doi.org/10.1016/S1001-6058(15)60453-X

Charriere, G., Mossel, D.A.A., Beaudeau, P., Leclerc, H., 1994. Assessment of the marker value of various components of the coli-aerogenes group of Enterobacteriaceae and of a selection of Enterococcus spp. for the official monitoring of drinking water supplies. J. Appl. Bacteriol. 76, 336–344. https://doi.org/10.1111/J.1365-2672.1994.TB01637.X

Chea, R., Grenouillet, G., Lek, S., 2016. Evidence of Water Quality Degradation in Lower Mekong Basin Revealed by Self-Organizing Map. PLoS One 11, e0145527. https://doi.org/10.1371/journal.pone.0145527

Chen, J., Wang, P., Wang, C., Wang, X., Miao, L., Liu, S., Yuan, Q., Key, 2018. Bacterial Communities in Riparian Sediments: A Large-Scale Longitudinal Distribution Pattern and Response to Dam Construction. Front. Microbiol. 9. https://doi.org/10.3389/fmicb.2018.00999

Chen, J., Wang, P., Wang, C., Wang, X., Miao, L., Liu, S., Yuan, Q., Sun, S., 2020. Fungal community demonstrates stronger dispersal limitation and less network connectivity than bacterial community in sediments along a large river. Environ. Microbiol. 22, 832–849. https://doi.org/10.1111/1462-2920.14795

Chick, H., 1908. An investigation of the laws of disinfection. J. Hyg. (Lond). 8, 92–158. https://doi.org/10.1017/S0022172400006987

Chin, D.A., Sakura-Lemessy, D., Bosch, D.D., Gay, P.A., 2009. WATERSHED-SCALE FATE AND TRANSPORT OF BACTERIA. Trans. ASABE 52, 145–154.

Cho, K., Pachepsky, Y., Kim, JH, Kim, JW, Park, M., 2012. The modified SWAT model for predicting fecal coliforms in the Wachusett Reservoir Watershed, USA. Water Res. 46, 4750–4760. https://doi.org/10.1016/J.WATRES.2012.05.057

Cho, K.H.., Cha, M., S.., Kang, J.-H.., Lee, S.W.., Park, Y.., Kim, J.-W.., Kim, J.H., 2010a. Meteorological effects on the levels of fecal indicator bacteria in an urban stream: A modeling approach. Water Res. 44, 2189–2202. https://doi.org/10.1016/j.watres.2009.12.051

Cho, K.H.., Pachepsky, Y.A., Kim, J.H., Guber, A.K., Shelton, D.R., Rowland, R., 2010b. Release of Escherichia coli from the bottom sediment in a first-order creek: Experiment and reach-specific modeling. J. Hydrol. 391, 322–332. https://doi.org/10.1016/j.jhydrol.2010.07.033

Cho, K.H., Pachepsky, Y.A., Kim, M., Pyo, J.C., Park, M.H., Kim, Y.M., Kim, J.W., Kim, J.H.,

2016. Modeling seasonal variability of fecal coliform in natural surface waters using the modified SWAT. J. Hydrol. 535, 377–385. https://doi.org/10.1016/j.jhydrol.2016.01.084

Christian, L., Epps, T., Diab, G., Hathaway, J., 2020. Pollutant Concentration Patterns of In-Stream Urban Stormwater Runoff. Water 2020, Vol. 12, Page 2534 12, 2534. https://doi.org/10.3390/W12092534

Chu, Y., Salles, C., Tournoud, M.G., Got, P., Troussellier, M., Rodier, C., Caro, A., 2011. Faecal bacterial loads during flood events in Northwestern Mediterranean coastal rivers. J. Hydrol. 405, 501–511. https://doi.org/10.1016/j.jhydrol.2011.05.047

Coffey, R., Cummins, E., Flaherty, V.O., Cormican, M., 2010. Pathogen Sources Estimation and Scenario Analysis Using the Soil and Water Assessment Tool (SWAT). Hum. Ecol. Risk Assess. An Int. J. 16, 913–933. https://doi.org/10.1080/10807039.2010.502051

Coffey, R., Dorai-Raj, S., O'Flaherty, V., Cormican, M., Cummins, E., 2013. Modeling of Pathogen Indicator Organisms in a Small-Scale Agricultural Catchment Using SWAT. Hum. Ecol. Risk Assess. 19, 232–253. https://doi.org/10.1080/10807039.2012.701983

Colvin, S.A.R., Sullivan, S.M.P., Shirey, P.D., Colvin, R.W., Winemiller, K.O., Hughes, R.M., Fausch, K.D., Infante, D.M., Olden, J.D., Bestgen, K.R., Danehy, R.J., Eby, L., 2019. Headwater Streams and Wetlands are Critical for Sustaining Fish, Fisheries, and Ecosystem Services. Fisheries 44, 73–91. https://doi.org/10.1002/fsh.10229

Conan, P., Joux, F., Torréton, J.-P., Pujo-Pay, M., Douki, T., Rochelle-Newall, E., Mari, X., 2008. Effect of solar ultraviolet radiation on bacterio- and phytoplankton activity in a large coral reef lagoon (southwest New Caledonia). Aquat. Microb. Ecol. 52, 83–98. https://doi.org/10.3354/AME01204

Crabill, C., Donald, R., Snelling, J., Foust, R., Southam, G., 1999. The impact of sediment fecal coliform reservoirs on seasonal waterquality in Oak Creek, Arizona. Water Res. 33, 2163–2171. https://doi.org/10.1016/S0043-1354(98)00437-0

Craig, D.L., Fallowfield, H.J., Cromar, N.J., 2004. Use of microcosms to determine persistence of Escherichia coli in recreational coastal water and sediment and validation with in situ measurements. J. Appl. Microbiol. 96, 922–930. https://doi.org/10.1111/j.1365-2672.2004.02243.x

Crump, B.C., Baross, J.A., Simenstad, C.A., 1998. Dominance of particle-attached bacteria in the Columbia River estuary, USA. Aquat. Microb. Ecol. 14, 7–18. https://doi.org/10.3354/AME014007

Davies-Colley, R.J., Donnison, A.M., Speed, D.J., Ross, C.M., Nagels, J.W., 1999. Inactivation of faecal indicator micro-organisms in waste stabilisation ponds: Interactions of environmental factors with sunlight. Water Res. 33, 1220–1230. https://doi.org/10.1016/S0043-1354(98)00321-2

Davies, C.M., Bavor, H.J., 2000. The fate of stormwater-associated bacteria in constructed

wetland and water pollution control pond systems. J. Appl. Microbiol. 89, 349–360. https://doi.org/10.1046/j.1365-2672.2000.01118.x

Davies, C.M., Long, J.A.H., Donald, M., Ashbolt, N.J., 1995. Survival of Fecal Microorganisms in Marine and Freshwater Sediments. Appl. Environ. Microbiol. 61, 1888–1896.

De Wit, R., Bouvier, T., 2006. "Everything is everywhere, but, the environment selects"; what did Baas Becking and Beijerinck really say? Environ. Microbiol. 8, 755–758. https://doi.org/10.1111/J.1462-2920.2006.01017.X

Delahoy, M.J., Wodnik, B., McAliley, L., Penakalapati, G., Swarthout, J., Freeman, M.C., Levy, K., 2018. Pathogens transmitted in animal feces in low- and middle-income countries. Int. J. Hyg. Environ. Health 221, 661. https://doi.org/10.1016/J.IJHEH.2018.03.005

Department of Planning, Ministry of Agriculture and Forestry, L.P., 2012. Lao Census of Agriculture 2010/11: Highlights.

Derose, K.L., Roche, L.M., Lile, D.F., Eastburn, D.J., Tate, K.W., 2020. Microbial Water Quality Conditions Associated with Livestock Grazing, Recreation, and Rural Residences in Mixed-Use Landscapes. Sustain. 2020, Vol. 12, Page 5207 12, 5207. https://doi.org/10.3390/SU12125207

Destoumieux-Garzón, D., Mavingui, P., Boetsch, G., Boissier, J., Darriet, F., Duboz, P., Fritsch, C., Giraudoux, P., Le Roux, F., Morand, S., Paillard, C., Pontier, D., Sueur, C., Voituron, Y., 2018. The One Health Concept: 10 Years Old and a Long Road Ahead. Front. Vet. Sci. 0, 14. https://doi.org/10.3389/FVETS.2018.00014

DHI, 2011. MIKE 21 & MIKE 3 FLOW MODEL FM Hydrodynamic Module-Short Description. Horsholm, Denmark, MIKE by DHI.

Ding, J., Jiang, Y., Liu, Q., Hou, Z., Liao, J., Fu, L., Peng, Q., 2016. Influences of the land use pattern on water quality in low-order streams of the Dongjiang River basin, China: A multi-scale analysis. Sci. Total Environ. 551–552, 205–216. https://doi.org/10.1016/j.scitotenv.2016.01.162

Donald, D.B., Parker, B.R., Davies, J.M., Leavitt, P.R., 2015. Nutrient sequestration in the Lake Winnipeg watershed. J. Great Lakes Res. 41, 630–642. https://doi.org/10.1016/J.JGLR.2015.03.007

Dorner, S.M., Anderson, W.B., Slawson, R.M., Kouwen, N., 2006. Hydrologic Modeling of Pathogen Fate and Transport. Environ. Sci. Technol. 40, 4746–4753. https://doi.org/10.1021/ES060426Z

Droppo, I.G., Liss, S.N., Williams, D., Nelson, T., Jaskot, C., Trapp, B., 2009. Dynamic existence of waterborne pathogens within river sediment compartments. Implications for water quality regulatory affairs. Environ. Sci. Technol. 43, 1737–1743. https://doi.org/10.1021/es802321w

Ducharne, A., 2007. HAL Id: hal-00330807 https://hal.archives-ouvertes.fr/hal-00330807

Importance of stream temperature to climate change impact on water quality. Eur. Geosci. Union 4, 2425–2460.

Dufour, A., Ballentine, R., 1986. Ambient water quality criteria for bacteria. U.S Environ. Prot. Agency.

EC, 2006. Directive 2006/7/EC of the European Parliament and of the Council of 15 February 2006 concerning the management of bathing water quality and repealing Directive 76/160/EE. Off. J. Eur. Union.

Edokpayi, J.N., Odiyo, J.O., Durowoju, O.S., 2017. Impact of Wastewater on Surface Water Quality in Developing Countries: A Case Study of South Africa. Water Qual. https://doi.org/10.5772/66561

Edokpayi, J.N., Odiyo, J.O., Durowoju, O.S., 2016. Impact of Wastewater on Surface Water Quality in Developing Countries: A Case Study of South Africa Provisional chapter Household Hazardous Waste Management in sub-Saharan Africa. https://doi.org/10.5772/66561

EIA, 2016. World Energy Outlook 2016 with projections to 2040. U.S. Energy Information Administration (EIA).

Eisenstark, A., 1971. Mutagenic and Lethal Effects of Visible and Near-Ultraviolet Light on Bacterial Cells. Adv. Genet. 16, 167–198. https://doi.org/10.1016/S0065-2660(08)60358-2

Ekklesia, E., Shanahan, P., Chua, L.H.C., Eikaas, H.S., 2015a. Associations of chemical tracers and faecal indicator bacteria in a tropical urban catchment. Water Res. 75, 270–281. https://doi.org/10.1016/J.WATRES.2015.02.037

Ekklesia, E., Shanahan, P., Chua, L.H.C., Eikaas, H.S., 2015b. Temporal variation of faecal indicator bacteria in tropical urban storm drains. Water Res. 68, 171–181. https://doi.org/10.1016/j.watres.2014.09.049

EPA, 2012. Recreational Water Quality Criteria. U S Environmental Protection Agency: Washington.

Evrard, O., Némery, J., Gratiot, N., Duvert, C., Ayrault, S., Lefèvre, I., Poulenard, J., Prat, C., Bonté, P., Esteves, M., 2010. Sediment dynamics during the rainy season in tropical highland catchments of central Mexico using fallout radionuclides. Geomorphology 124, 42–54. https://doi.org/10.1016/j.geomorph.2010.08.007

FAO, 2011. AQUASTAT Transboundary River Basin – Mekong River Basin. Food and Agriculture Organization of the United Nations (FAO). Rome, Italy.

Farrell, C., Hassard, F., Jefferson, B., Leziart, T., Nocker, A., Jarvis, P., 2018. Turbidity composition and the relationship with microbial attachment and UV inactivation efficacy. Sci. Total Environ. 624, 638–647. https://doi.org/10.1016/j.scitotenv.2017.12.173

Ferguson, C., De Roda Husman, A.M., Altavilla, N., Deere, D., Ashbolt, N., 2003. Fate and

transport of surface water pathogens in watersheds. Crit. Rev. Environ. Sci. Technol. 33, 299–361. https://doi.org/10.1080/10643380390814497

Ferguson, C.M., Coote, B.G., Ashbolt, N.J., Stevenson, I.M., 1996. Relationships between indicators, pathogens and water quality in an estuarine system. Water Res. 30, 2045–2054. https://doi.org/10.1016/0043-1354(96)00079-6

Ferguson, D., Signoretto, C., 2011. Environmental Persistence and Naturalization of Fecal Indicator Organisms, in: Microbial Source Tracking: Methods, Applications, and Case Studies. Springer, New York, NY., pp. 379–397.

Flint, K.P., 1987. The long-term survival of *Escherichia coli* in river water. J. Appl. Bacteriol. 63, 261–270. https://doi.org/10.1111/j.1365-2672.1987.tb04945.x

Flotemersch, J.E., Leibowitz, S.G., Hill, R.A., Stoddard, J.L., Thoms, M.C., Tharme, R.E., 2016. A Watershed Integrity Definition and Assessment Approach to Support Strategic Management of Watersheds. River Res. Appl. 32, 1654–1671. https://doi.org/10.1002/RRA.2978

Food and Agricutlure Organization of the United Nations, 2011. AQUASTAT Transboundary River Basins –Mekong RiverBasin.

Forestry Department Food and Agriculture Organization of the United Nations, 2010. Global forest resources assassment, 2010 country report Lao PDR. Rome.

Frémion, F., Bordas, F., Mourier, B., Lenain, J.F., Kestens, T., Courtin-Nomade, A., 2016. Influence of dams on sediment continuity: A study case of a natural metallic contamination. Sci. Total Environ. 547, 282–294. https://doi.org/10.1016/J.SCITOTENV.2016.01.023

Frey, S., Topp, E., Edge, T., Fall, C., Gannon, V., Jokinen, C., R, M., N, N., Ruecker, N., Wilkes, G., DR, L., 2013. Using SWAT, Bacteroidales microbial source tracking markers, and fecal indicator bacteria to predict waterborne pathogen occurrence in an agricultural watershed. Water Res. 47, 6326–6337. https://doi.org/10.1016/J.WATRES.2013.08.010

Fries, J.S., Characklis, G.W., Noble, R.T., 2008. Sediment-water exchange of Vibrio sp. and fecal indicator bacteria: Implications for persistence and transport in the Neuse River Estuary, North Carolina, USA. Water Res. 42, 941–950. https://doi.org/10.1016/j.watres.2007.09.006

Fu, K.D., He, D.M., Lu, X.X., 2008. Sedimentation in the Manwan reservoir in the Upper Mekong and its downstream impacts. Quat. Int. 186, 91–99. https://doi.org/10.1016/J.QUAINT.2007.09.041

Fujioka, R.S., Byappanahalli, M.N., 2001. Microbial ecology controls the establishment of fecal bacteria in tropical soil environment. Adv. Water Wastewater Treat. Technol. 273–283. https://doi.org/10.1016/B978-044450563-7/50211-0

Fujioka, R.S., Hashimoto, H.H., Siwak, E.B., Young', R.H.F., 1981. Effect of Sunlight on Survival of Indicator Bacteria in Seawater. Appl. Environ. Microbiol. 41, 690–696. https://doi.org/10.1128/aem.41.3.690-696.1981

Fujiokal, R.S., Narikawa, O.T., 1982. Effect of Sunlight on Enumeration of Indicator Bacteria Under Field Conditions. Appl. Environ. Microbiol. 44, 395–401. https://doi.org/0066-4804/82/080395-07$02.00/0

Gaillardet, J., Braud, I., Hankard, F., Anquetin, S., Zitouna, R., et al., 2018. OZCAR: The French Network of Critical Zone Observatories. Vadose Zo. J. 17, 180067. https://doi.org/10.2136/vzj2018.04.0067

Gannon, V., Duke, G., Thomas, J., Vanleeuwen, J., Byrne, J., Johnson, D., 2005. Use of in-stream reservoirs to reduce bacterial contamination of rural watersheds. Sci. Total Environ. 348, 19–31. https://doi.org/10.1016/J.SCITOTENV.2004.12.076

Gao, P., Li, P., Zhao, B., Xu, R., Zhao, G., Sun, W., Mu, X., 2017. Use of double mass curves in hydrologic benefit evaluations. Hydrol. Process. 31, 4639–4646. https://doi.org/10.1002/hyp.11377

Gao, P., Zhang, Xunchang, Mu, X., Wang, F., Li, R., Zhang, Xiaoping, 2010. Trend and change-point analyses of streamflow and sediment discharge in the Yellow River during 1950–2005. https://doi.org/10.1080/02626660903546191 55, 275–285. https://doi.org/10.1080/02626660903546191

Gardner, R.A.M., Gerrard, A.J., 2003. Runoff and soil erosion on cultivated rainfed terraces in the Middle Hills of Nepal. Appl. Geogr. 23, 23–45. https://doi.org/10.1016/S0143-6228(02)00069-3

Garnier, J., Némery, J., Billen, G., Théry, S., 2005. Nutrient dynamics and control of eutrophication in the Marne River system: modelling the role of exchangeable phosphorus. J. Hydrol. 304, 397–412. https://doi.org/10.1016/J.JHYDROL.2004.07.040

Garzio-Hadzick, A., Shelton, D.R., Hill, R.L., Pachepsky, Y.A., Guber, A.K., Rowland, R., 2010. Survival of manure-borne E. coli in streambed sediment: Effects of temperature and sediment properties. Water Res. 44, 2753–2762. https://doi.org/10.1016/j.watres.2010.02.011

GBD LRI Collaborators, 2017. Estimates of the global, regional, and national morbidity, mortality, and aetiologies of lower respiratory tract infections in 195 countries: a systematic analysis for the Global Burden of Disease Study 2015. Lancet Infect. Dis. 17, 1133–1161. https://doi.org/10.1016/S1473-3099(17)30396-1

Geladi, P., Kowalski, B.R., 1986. Partial least-squares regression: a tutorial. Anal. Chim. Acta 185, 1–17. https://doi.org/10.1016/0003-2670(86)80028-9

Geldreich, E.E., 1970. APPLYING BACTERIOLOGICAL PARAMETERS TO RECREATIONAL WATER QUALITY, Journal (American Water Works Association).

Giang, P.Q., Toshiki, K., Sakata, M., Kunikane, S., Vinh, T.Q., 2014. Modelling climate change impacts on the seasonality of water resources in the upper Ca river watershed in Southeast Asia. Sci. World J. 2014. https://doi.org/10.1155/2014/279135

Gonzalez, J.M., Iriberri, J., Egea, L., Barcina, I., 1992. Characterization of Culturability, Protistan Grazing, and Death of Enteric Bacteria in Aquatic Ecosystems. Appl. Environ. Microbiol. 998–1004.

Gonzalez, J.M., Iriberri, J., Egea, L., Barcina, I., 1990. Differential Rates of Digestion of Bacteria by Freshwater and Marine Phagotrophic Protozoa. Appl. Environ. Microbiol. 56, 1851–1857.

Gourdin, E., Evrard, O., Huon, S., Lefèvre, I., Ribolzi, O., Reyss, J.L., Sengtaheuanghoung, O., Ayrault, S., 2014. Suspended sediment dynamics in a Southeast Asian mountainous catchment: Combining river monitoring and fallout radionuclide tracers. J. Hydrol. 519, 1811–1823. https://doi.org/10.1016/J.JHYDROL.2014.09.056

Gourmelon, M., Caprais, M.P., Mieszkin, S., Marti, R., Wéry, N., Jardé, E., Derrien, M., Jadas-Hécart, A., Communal, P.Y., Jaffrezic, A., Pourcher, A.M., 2010. Development of microbial and chemical MST tools to identify the origin of the faecal pollution in bathing and shellfish harvesting waters in France. Water Res. 44, 4812–4824. https://doi.org/10.1016/J.WATRES.2010.07.061

Grant, S.B., Litton-Mueller, R.M., Ahn, J.H., Grant, S.B., Litton-Mueller, R.M., Ahn, J.H., 2011. Measuring and modeling the flux of fecal bacteria across the sediment-water interface in a turbulent stream. WRR 47, W05517. https://doi.org/10.1029/2010WR009460

Gregory, L.F., Karthikeyan, R., Aitkenhead-Peterson, J.A., Gentry, T.J., Wagner, K.L., Harmel, R.D., 2017. Nutrient loading impacts on culturable E. coli and other heterotrophic bacteria fate in simulated stream mesocosms. Water Res. 126, 442–449. https://doi.org/10.1016/j.watres.2017.09.043

Grumbine, R.E., Dore, J., Xu, J., 2012. Mekong hydropower: drivers of change and governance challenges. Front. Ecol. Environ. 10, 91–98. https://doi.org/10.1890/110146

Grundy-Warr, C., Andrews, R.H., Sithithaworn, P., Petney, T.N., Sripa, B., Laithavewat, L., Ziegler, A.D., 2012. Raw attitudes, wetland cultures, life-cycles: Socio-cultural dynamics relating to Opisthorchis viverrini in the Mekong Basin. Parasitol. Int. 61, 65–70. https://doi.org/10.1016/j.parint.2011.06.015

Guzman, A. De, Reyes, V.C. de los, Sucaldito, M.N., Tayag, E., 2015. Availability of safe drinking-water: the answer to cholera outbreak?Nabua, Camarines Sur, Philippines, 2012. West. Pacific Surveill. Response J. WPSAR 6, 12. https://doi.org/10.5365/WPSAR.2015.6.1.005

Haller, L., Amedegnato, E., Poté, J., Wildi, W., 2009. Influence of Freshwater Sediment Characteristics on Persistence of Fecal Indicator Bacteria. Water. Air. Soil Pollut. 203, 217–227. https://doi.org/10.1007/s11270-009-0005-0

Harwood, V., Staley, C., Badgley, B., Borges, K., Korajkic, A., 2014. Microbial source tracking markers for detection of fecal contamination in environmental waters: relationships between pathogens and human health outcomes. FEMS Microbiol. Rev. 38, 1–40.

https://doi.org/10.1111/1574-6976.12031

Hathaway, J.M., Hunt, W.F., SimmonsIII, O.D., 2010. Statistical Evaluation of Factors Affecting Indicator Bacteria in Urban Storm-Water Runoff. J. Environ. Eng. 136, 1360–1368. https://doi.org/10.1061/(ASCE)EE.1943-7870.0000278

Hecht, J.S., Lacombe, G., Arias, M.E., Dang, T.D., Piman, T., 2019a. Hydropower dams of the Mekong River basin: A review of their hydrological impacts. J. Hydrol. https://doi.org/10.1016/j.jhydrol.2018.10.045

Hecht, J.S., Lacombe, G., Arias, M.E., Dang, T.D., Piman, T., 2019b. Hydropower dams of the Mekong River basin: A review of their hydrological impacts. J. Hydrol. 568, 285–300. https://doi.org/10.1016/j.jhydrol.2018.10.045

Henry, R., Schang, C., Kolotelo, P., Coleman, R., Rooney, G., Schmidt, J., Deletic, A., McCarthy, D.T., 2016. Effect of environmental parameters on pathogen and faecal indicator organism concentrations within an urban estuary. Estuar. Coast. Shelf Sci. 174, 18–26. https://doi.org/10.1016/J.ECSS.2016.03.012

Herrera, D., Ellis, A., Fisher, B., Golden, C.D., Johnson, K., Mulligan, M., Pfaff, A., Treuer, T., Ricketts, T.H., 2017. Upstream watershed condition predicts rural children's health across 35 developing countries. Nat. Commun. 8. https://doi.org/10.1038/s41467-017-00775-2

Herrig, I., Seis, W., Fischer, H., Regnery, J., Manz, W., Reifferscheid, G., Böer, S., 2019. Prediction of fecal indicator organism concentrations in rivers: the shifting role of environmental factors under varying flow conditions. Environ. Sci. Eur. 2019 311 31, 1–16. https://doi.org/10.1186/S12302-019-0250-9

Hipsey, M.R., Antenucci, J.P., Brookes, J.D., 2008. A generic, process-based model of microbial pollution in aquatic systems. Water Resour. Res. 44, 7408. https://doi.org/10.1029/2007WR006395

Hjulstrom, F., 1935. Studies of the morphological activity of rivers as illustrated by the river fyris, bulletin. Geol. Inst. Upsalsa 25, 221--527.

Hlavsa, M.C.., Roberts, V.A.;, Anderson, A.R.., 2011. Surveillance for Waterborne Disease Outbreaks and Other Health Events Associated with Recreational Water --- United States, 2007--2008 [WWW Document]. MMWR Surveill Summ. URL https://www.cdc.gov/Mmwr/preview/mmwrhtml/ss6012a1.htm (accessed 9.22.21).

Hofstra, N., 2011. Quantifying the impact of climate change on enteric waterborne pathogen concentrations in surface water. Curr. Opin. Environ. Sustain. 3, 471–479. https://doi.org/10.1016/J.COSUST.2011.10.006

Homdee, T., Pongput, K., Kanae, S., 2011. Impacts of Land Cover Changes on Hydrologic Responses: A Case Study of Chi River Basin, Thailand. J. Japan Soc. Civ. Eng. Ser. B1 (Hydraulic Eng. 67, I_31-I_36. https://doi.org/10.2208/JSCEJHE.67.I_31

Hortle, K.., 2007. Consumption and the yield of fish and other aquatic animals from the Lower

Mekong Basin. MRC Technical Paper No. 16.

Howard, G., 2021. The future of water and sanitation: global challenges and the need for greater ambition. J. Water Supply Res. Technol. https://doi.org/10.2166/aqua.2021.127

Howell, J.M., Coyne, M.S., Cornelius, P.L., 1996. Effect of Sediment Particle Size and Temperature on Fecal Bacteria Mortality Rates and the Fecal Coliform/Fecal Streptococci Ratio. J. Environ. Qual. 25, 1216–1220. https://doi.org/10.2134/jeq1996.00472425002500060007x

Hrdinka, T., Novický, O., Hanslík, E., Rieder, M., 2012. Possible impacts of floods and droughts on water quality. J. Hydro-environment Res. 6, 145–150. https://doi.org/10.1016/J.JHER.2012.01.008

Hua, H., 1990. Accurate Method for Calculation of Saturation DO. J. Environ. Eng. 116, 988–990. https://doi.org/10.1061/(ASCE)0733-9372(1990)116:5(988)

Huo, Z., Feng, S., Kang, S., Li, W., Chen, S., 2008. Effect of climate changes and water-related human activities on annual stream flows of the Shiyang river basin in arid north-west China. Hydrol. Process. 22, 3155–3167. https://doi.org/10.1002/HYP.6900

Huon, S., de Rouw, A., Bonté, P., Robain, H., Valentin, C., Lefèvre, I., Girardin, C., Le Troquer, Y., Podwojewski, P., Sengtaheuanghoung, O., 2013. Long-term soil carbon loss and accumulation in a catchment following the conversion of forest to arable land in northern Laos. Agric. Ecosyst. Environ. 169, 43–57. https://doi.org/10.1016/j.agee.2013.02.007

Huon, S., Evrard, O., Gourdin, E., Lefèvre, I., Bariac, T., Reyss, J.L., Henry des Tureaux, T., Sengtaheuanghoung, O., Ayrault, S., Ribolzi, O., 2017. Suspended sediment source and propagation during monsoon events across nested sub-catchments with contrasted land uses in Laos. J. Hydrol. Reg. Stud. 9, 69–84. https://doi.org/10.1016/j.ejrh.2016.11.018

Huon, S., Ribolzi, O., Aubry, E., Soulileuth, B., Longchamp, M., Angeli, O., Sengtaheuanghoung, N., 2008. Iron and manganese concentration levels in watercress cultivated within the main stream of the Houay Pano catchment, Northern Lao PDR. Lao J. Agric. For. 17, 113–128. https://doi.org/bioemco-00397021

Huong, T. Le, Rochelle-Newall, E., Auda, Y., Ribolzi, O., Sengtaheuanghoung, O., Thébault, E., Soulileuth, B., Pommier, T., 2018. Vicinal land use change strongly drives stream bacterial community in a tropical montane catchment. FEMS Microbiol. Ecol. 94, 1–16. https://doi.org/10.1093/femsec/fiy155

IFReDI, 2012. Food and nutrition security vulnerability to mainstream hydropower dam development in Cambodia. Fisheries Administration, Phnom Penh, Cambodia.

Iriberri, J., Ayo, B., Artolozaga, I., Barcina, I., 1994. Grazing on allochthonous vs autochthonous bacteria in river water. Lett. Appl. Microbiol. 18, 12–14. https://doi.org/10.1111/J.1472-765X.1994.TB00786.X

Ishii, S., Ksoll, W.B., Hicks, R.E., Sadowsky, J., M., 2006. Presence and Growth of Naturalized

Escherichia coli in Temperate Soils from Lake Superior Watersheds. Appl. Environ. Microbiol. 72, 612. https://doi.org/10.1128/AEM.72.1.612-621.2006

Ishii, S., Sadowsky, M.J., 2008. Escherichia coli in the environment: Implications for water quality and human health. Microbes Environ. 23, 101–108. https://doi.org/10.1264/jsme2.23.101

Islam, M.M.M., Hofstra, N., Islam, M.A., 2017. The Impact of Environmental Variables on Faecal Indicator Bacteria in the Betna River Basin, Bangladesh. Environ. Process. 2017 42 4, 319–332. https://doi.org/10.1007/S40710-017-0239-6

Islam, M.M.M., Iqbal, M.S., D'Souza, N., Islam, M.A., 2021. A review on present and future microbial surface water quality worldwide. Environ. Nanotechnology, Monit. Manag. 16, 2215–1532. https://doi.org/10.1016/J.ENMM.2021.100523

Isobe, K.O., Tarao, M., Chiem, N.H., Minh, L.Y., Takada, H., 2004. Effect of Environmental Factors on the Relationship between Concentrations of Coprostanol and Fecal Indicator Bacteria in Tropical (Mekong Delta) and Temperate (Tokyo) Freshwaters. Appl. Environ. Microbiol. 70, 814–821. https://doi.org/10.1128/AEM.70.2.814-821.2004

Jagai, J.S., Castronovo, D.A., Monchak, J., Naumova, E.N., 2009. Seasonality of cryptosporidiosis: A meta-analysis approach. Environ. Res. 109, 465–478. https://doi.org/10.1016/J.ENVRES.2009.02.008

Jamieson, R.C., Joy, D.M., Lee, H., Kostaschuk, R., Gordon, R.J., 2005. Resuspension of Sediment-Associated Escherichia coli in a Natural Stream . J. Environ. Qual. 34, 581–589. https://doi.org/10.2134/jeq2005.0581

Janeau, J.L., Gillard, L.C., Grellier, S., Jouquet, P., Le, T.P.Q., Luu, T.N.M., Ngo, Q.A., Orange, D., Pham, D.R., Tran, D.T., Tran, S.H., Trinh, A.D., Valentin, C., Rochelle-Newall, E., 2014. Soil erosion, dissolved organic carbon and nutrient losses under different land use systems in a small catchment in northern Vietnam. Agric. Water Manag. 146, 314–323. https://doi.org/10.1016/j.agwat.2014.09.006

Jarvis, A., Guevara, E., Reuter, H.I., Nelson, A.D., 2008. Hole-filled SRTM for the globe : version 4 : data grid.

Jeanneau, L., Solecki, O., Wéry, N., Jardé, E., Gourmelon, M., Communal, P.-Y., Jadas-Hécart, A., Caprais, M.-P., Gruau, G., Pourcher, A.-M., 2012. Relative Decay of Fecal Indicator Bacteria and Human-Associated Markers: A Microcosm Study Simulating Wastewater Input into Seawater and Freshwater. Environ. Sci. Technol. 46, 2375–2382. https://doi.org/10.1021/ES203019Y

Johnston, C.A., 1991. Sediment and nutrient retention by freshwater wetlands: Effects on surface water quality. Crit. Rev. Environ. Control 21, 491–565. https://doi.org/10.1080/10643389109388425

Jones, E.R., Van Vliet, M.T.H., Qadir, M., Bierkens, M.F.P., 2021. Country-level and gridded

estimates of wastewater production, collection, treatment and reuse. Earth Syst. Sci. Data 13, 237–254. https://doi.org/10.5194/ESSD-13-237-2021

Jozić, S., Morović, M., Šolić, M., Krstulović, N., Ordulj, M., 2014. Effect of solar radiation, temperature and salinity on the survival of two different strains of Escherichia coli. Fresenius Environ. Bull. 23, 1852--1859.

Junk, W.J., Wantzen, K.M., 2007. Flood Pulsing and the Development and Maintenance of Biodiversity in Floodplains Construction and analysis of a geohistorical database of the Rhine with a view to the functional restoration of the river hydrosystem View project Tropical Riparian Zones Vie. https://doi.org/10.1525/california/9780520247772.003.0011

Kapuscinski, R.B., Mitchell, R., 1983. Sunlight-Induced Mortality of Viruses and Escherichia Coli in Coastal Seawater. Environ. Sci. Technol. 17, 1–6. https://doi.org/10.1021/es00107a003

Karim, M.R., Manshadi, F.D., Karpiscak, M.M., Gerba, C.P., 2004. The persistence and removal of enteric pathogens in constructed wetlands. Water Res. 38, 1831–1837. https://doi.org/10.1016/j.watres.2003.12.029

Kashefipour, S., Lin, B., Harris, E., Falconer, R., 2002. Hydro-environmental modelling for bathing water compliance of an estuarine basin. Water Res. 36, 1854–1868. https://doi.org/10.1016/S0043-1354(01)00396-7

Kay, D., Stapleton, C.M., Wyer, M.D., McDonald, A.T., Crowther, J., Paul, N., Jones, K., Francis, C., Watkins, J., Wilkinson, J., Humphrey, N., Lin, B., Yang, L., Falconer, R.A., Gardner, S., 2005. Decay of intestinal enterococci concentrations in high-energy estuarine and coastal waters: Towards real-time T90 values for modelling faecal indicators in recreational waters. Water Res. 39, 655–667. https://doi.org/10.1016/j.watres.2004.11.014

Kelly-Hope, L.A.., Alonso, W.J.., Thiem, V.Di., Anh, D.D., 2007. Geographical Distribution And Risk Factors Associated With Enteric Diseases In Vietnam. Am. J. Trop. Med. Hyg. 76, 706–712. https://doi.org/10.4269/AJTMH.2007.76.706

Kim, J.W., Pachepsky, Y.A., Shelton, D.R., Coppock, C., 2010. Effect of streambed bacteria release on E. coli concentrations: Monitoring and modeling with the modified SWAT. Ecol. Modell. 221, 1592–1604. https://doi.org/10.1016/J.ECOLMODEL.2010.03.005

Kim, M., Boithias, L., Cho, K.H., Sengtaheuanghoung, O., Ribolzi, O., 2018. Modeling the Impact of Land Use Change on Basin-scale Transfer of Fecal Indicator Bacteria: SWAT Model Performance. J. Environ. Qual. 47, 1115–1122. https://doi.org/10.2134/jeq2017.11.0456

Kim, M., Boithias, L., Cho, K.H., Silvera, N., Thammahacksa, C., Latsachack, K., Rochelle-Newall, E., Sengtaheuanghoung, O., Pierret, A., Pachepsky, Y.A., Ribolzi, O., 2017. Hydrological modeling of Fecal Indicator Bacteria in a tropical mountain catchment. Water Res. 119, 102–113. https://doi.org/10.1016/j.watres.2017.04.038

Kirchner, J.W., 2003. A double paradox in catchment hydrology and geochemistry. Hydrol. Process. 17, 871–874. https://doi.org/10.1002/HYP.5108

Kloot, R., 2007. Locating Escherichia coli contamination in a rural South Carolina watershed. J. Environ. Manage. 83, 402–408. https://doi.org/10.1016/J.JENVMAN.2006.03.008

Knox, A.K., Dahlgren, R.A., Tate, K.W., Atwill, E.R., 2008. Efficacy of Natural Wetlands to Retain Nutrient, Sediment and Microbial Pollutants. J. Environ. Qual. 37, 1837–1846. https://doi.org/10.2134/jeq2007.0067

Koirala, S.R., Gentry, R.W., Perfect, E., Schwartz, J.S., Sayler, G.S., 2008. Temporal Variation and Persistence of Bacteria in Streams. J. Environ. Qual. 37, 1559–1566. https://doi.org/10.2134/JEQ2007.0310

Kondolf, G.M., 1997. Hungry water: Effects of dams and gravel mining on river channels. Environ. Manage. 21, 533–551. https://doi.org/10.1007/s002679900048

Kondolf, G.M., Rubin, Z.K., Minear, J.T., 2014. Dams on the Mekong: Cumulative sediment starvation. Water Resour. Res. 50, 5158–5169. https://doi.org/10.1002/2013WR014651

Korajkic, A., Wanjugi, P., Harwood, V.J., 2013. Indigenous Microbiota and Habitat Influence Escherichia coli Survival More than Sunlight in Simulated Aquatic Environments. Number 17 Appl. Environ. Microbiol. 79, 5329–5337. https://doi.org/10.1128/AEM.01362-13

Krecek, J., Haigh, M., 2006. Environmental Role of Wetlands in Headwaters. Springer Science & Business Media, Dordrecht, Netherlands.

Kummu, M., Lu, X.X., Wang, J.J., Varis, O., 2010. Basin-wide sediment trapping efficiency of emerging reservoirs along the Mekong. Geomorphology 119, 181–197. https://doi.org/10.1016/J.GEOMORPH.2010.03.018

Kummu, M., Sarkkula, J., 2008. Impact of the Mekong River Flow Alteration on the Tonle Sap Flood Pulse. R. Swedish Acad. Sci. 37.

Kummu, M., Sarkkula, J., Koponen, J., Nikula, J., 2006. Ecosystem Management of the Tonle Sap Lake: An Integrated Modelling Approach. Int. J. Water Resour. Dev. 22, 497–519. https://doi.org/10.1080/07900620500482915

Kummu, M., Varis, O., 2007. Sediment-related impacts due to upstream reservoir trapping, the Lower Mekong River. Geomorphology, Monsoon Rivers of Asia 85, 275–293. https://doi.org/10.1016/j.geomorph.2006.03.024

Kundzewicz, Z.W., Robson, A., 2000. Detecting Trend and Other Changes in Hydrological Data, World Climate Programme - Water.

Kunz, M.J., Wüest, A., Wehrli, B., Landert, J., Senn, D.B., 2011. Impact of a large tropical reservoir on riverine transport of sediment, carbon, and nutrients to downstream wetlands. Water Resour. Res. 47. https://doi.org/10.1029/2011WR010996

Zhu, L., Torres, M., Betancourt, W. Q., Sharma, M., Micallef, S. A., Gerba, C., Sapkota, A. R., Sapkota, A., Parveen, S., Hashem, F., May, E., Kniel, K., Pop, M., Ravishankar, S., 2019. Incidence of fecal indicator and pathogenic bacteria in reclaimed and return flow waters in Arizona, USA. Environ. Res. 170, 122–127. https://doi.org/10.1016/J.ENVRES.2018.11.048

Lacombe, G., Douangsavanh, S., Baker, J., Hoanh, C.T., Bartlett, R., Jeuland, M., Phongpachith, C., 2014. Are hydropower and irrigation development complements or substitutes? The example of the Nam Ngum River in the Mekong Basin. Water Int. 39, 649–670. https://doi.org/10.1080/02508060.2014.956205

Lacombe, G., Valentin, C., Sounyafong, P., de Rouw, A., Soulileuth, B., Silvera, N., Pierret, A., Sengtaheuanghoung, O., Ribolzi, O., 2018. Linking crop structure, throughfall, soil surface conditions, runoff and soil detachment: 10 land uses analyzed in Northern Laos. Sci. Total Environ. 616–617, 1330–1338. https://doi.org/10.1016/j.scitotenv.2017.10.185

Lal, R., 1983. Soil Erosion in the Humid Tropics with Particular Reference to Agricultural Land Development and Soil Management. Proceeding Symp. Hydrol. Humid Trop. Reg. with Part. Ref. to Hydrol. Eff. Agric. For. Pract. 221–240.

Lamberts, D., 2008. Little impact, much damage: the consequences of Mekong river flow alterations for the tonle sap ecosystem.

Lamberts, D., 2006. The Tonle Sap Lake as a Productive Ecosystem. Int. J. Water Resour. Dev. 22, 481–495. https://doi.org/10.1080/07900620500482592

Lamberts, D., Koponen, J., 2008. Flood Pulse Alterations and Productivity of the Tonle Sap Ecosystem: A Model for Impact Assessment.

Lane, C.R., Leibowitz, S.G., Autrey, B.C., LeDuc, S.D., Alexander, L.C., 2018. Hydrological, Physical, and Chemical Functions and Connectivity of Non-Floodplain Wetlands to Downstream Waters: A Review. J. Am. Water Resour. Assoc. 54, 346–371. https://doi.org/10.1111/1752-1688.12633

Lao Statistics Bureau, 2016. Result of population and housing census 2015. Lao Stat. Bur. 282.

Lao Statistics Bureau Ministry of Planning and Investment, 2015. The 4th Population and Housing Census (PHC) 2015.

Larsson, C., Andersson, Y., Allestam, G., Lindqvist, A., Nenonen, N., Bergstedt, O., 2014. Epidemiology and estimated costs of a large waterborne outbreak of norovirus infection in Sweden. Epidemiol. Infect. 142, 592–600. https://doi.org/10.1017/S0950268813001209

Le, H.A., Gratiot, N., Santini, W., Ribolzi, O., Tran, D., Meriaux, X., Deleersnijder, E., Soares-Frazão, S., 2020. Suspended sediment properties in the Lower Mekong River, from fluvial to estuarine environments. Estuar. Coast. Shelf Sci. 233, 106522. https://doi.org/10.1016/j.ecss.2019.106522

Le Meur, M., Phu, V. Le, Gratiot, N., 2021. What Is the Future of the Lower Mekong Basin Struggling against Human Activities? A Review. River Deltas - Recent Adv. [Working Title]. https://doi.org/10.5772/INTECHOPEN.95010

Le, T.P.Q., Billen, G., Garnier, J., Thery, S., Fezard, C., Minh, C. V., 2005. Nutrient (N, P) budgets for the Red River basin (Vietnam and China). Global Biogeochem. Cycles 19, 1–16. https://doi.org/10.1029/2004GB002405

Lebaron, P., Henry, A., Lepeuple, A.S., Pena, G., Servais, P., 2005. An operational method for the real-time monitoring of E. coli numbers in bathing waters. Mar. Pollut. Bull. 50, 652–659. https://doi.org/10.1016/j.marpolbul.2005.01.016

Lemée, R., Rochelle-Newall, E., Wambeke, F. Van, Pizay, M.-D., Rinaldi, P., Gattuso, J.-P., 2002. Seasonal variation of bacterial production, respiration and growth efficiency in the open NW Mediterranean Sea. Aquat. Microb. Ecol. 29, 227–237. https://doi.org/10.3354/AME029227

Lerner, H., Berg, C., 2015. The concept of health in One Health and some practical implications for research and education: what is One Health? https://doi.org/10.3402/iee.v5.25300 5, 25300. https://doi.org/10.3402/IEE.V5.25300

Lestrelin, G., Trockenbrodt, M., Phanvilay, K., Thongmanivong, S., Vongvisouk, T., Pham Thu Thuy, Castella, J.-C., Center for International Forestry Research, 2013. The context of REDD+ in the Lao People's Democratic Republic : drivers, agents and institutions.

Liang, Z., He, Z., Zhou, X., Powell, C.A., Yang, Y., He, L.M., Stoffella, P.J., 2013. Impact of mixed land-use practices on the microbial water quality in a subtropical coastal watershed. Sci. Total Environ. 449, 426–433. https://doi.org/10.1016/j.scitotenv.2013.01.087

Loucks, D.P., Beek, E. van, 2017. Water Resources Planning and Management: An Overview. Water Resour. Syst. Plan. Manag. 1–49. https://doi.org/10.1007/978-3-319-44234-1_1

Lu, X.X., Siew, R.Y., 2006. Water discharge and sediment flux changes over the past decades in the Lower Mekong River: Possible impacts of the Chinese dams. Hydrol. Earth Syst. Sci. 10, 181–195. https://doi.org/10.5194/HESS-10-181-2006

Luu, T.N.M., Garnier, J., Billen, G., Orange, D., Némery, J., Le, T.P.Q., Tran, H.T., Le, L.A., 2010. Hydrological regime and water budget of the Red River Delta (Northern Vietnam). J. Asian Earth Sci. 37, 219–228. https://doi.org/10.1016/J.JSEAES.2009.08.004

Ly, K., Metternicht, G., Marshall, L., 2020. Linking changes in land cover and land use of the lower mekong basin to instream nitrate and total suspended solids variations. Sustain. 12. https://doi.org/10.3390/su12072992

Lyon, S.W., King, K., Polpanich, O. uma, Lacombe, G., 2017. Assessing hydrologic changes across the Lower Mekong Basin. J. Hydrol. Reg. Stud. 12, 303–314. https://doi.org/10.1016/J.EJRH.2017.06.007

MacAlister, C., Mahaxay, M., 2009. Mapping wetlands in the Lower Mekong Basin for wetland

resource and conservation management using Landsat ETM images and field survey data. J. Environ. Manage. 90, 2130–2137. https://doi.org/10.1016/j.jenvman.2007.06.031

Mackenzie, J.S., Jeggo, M., 2019. The One Health Approach—Why Is It So Important? Trop. Med. Infect. Dis. 2019, Vol. 4, Page 88 4, 88. https://doi.org/10.3390/TROPICALMED4020088

Madge, B.A., Jensen, J.N., 2006. Ultraviolet Disinfection of Fecal Coliform in Municipal Wastewater: Effects of Particle Size. Water Environ. Res. 78, 294–304. https://doi.org/10.2175/106143005x94385

Magdoff, F., Weil, R.R., 2004. Soil Organic Matter in Sustainable Agriculture. Soil Org. Matter Sustain. Agric. https://doi.org/10.1201/9780203496374

Mahloch, J.L., 1974. Comparative Analysis of Modeling Techniques for Coliform Organisms in Streams. Appl. Microbiol. 27, 340–345. https://doi.org/10.1128/AM.27.2.340-345.1974

Malham, S.K., Rajko-Nenow, P., Howlett, E., Tuson, K.E., Perkins, T.L., Pallett, D.W., Wang, H., Jago, C.F., Jones, D.L., McDonald, J.E., 2014. The interaction of human microbial pathogens, particulate material and nutrients in estuarine environments and their impacts on recreational and shellfish waters. Environ. Sci. Process. Impacts 16, 2145–2155. https://doi.org/10.1039/c4em00031e

Mander, Ü., Mitsch, W.J., 2009. Pollution control by wetlands. Ecol. Eng. 35, 153–158. https://doi.org/10.1016/j.ecoleng.2008.10.005

Manh, N. Van, Dung, N.V., Hung, N.N., Kummu, M., Merz, B., Apel, H., 2015. Future sediment dynamics in the Mekong Delta floodplains: Impacts of hydropower development, climate change and sea level rise. Glob. Planet. Change 127, 22–33. https://doi.org/10.1016/J.GLOPLACHA.2015.01.001

Mannschatz, T., Wolf, T., Hülsmann, S., 2016. Nexus Tools Platform: Web-based comparison of modelling tools for analysis of water-soil-waste nexus. Environ. Model. Softw. 76, 137–153. https://doi.org/10.1016/J.ENVSOFT.2015.10.031

Maraccini, P.A., Mattioli, M.C.M., Sassoubre, L.M., Cao, Y., Griffith, J.F., Ervin, J.S., Van De Werfhorst, L.C., Boehm, A.B., 2016. Solar Inactivation of Enterococci and Escherichia coli in Natural Waters: Effects of Water Absorbance and Depth. Environ. Sci. Technol. 50, 5068–5076. https://doi.org/10.1021/acs.est.6b00505

Marhaento, H., Booij, M.J., Hoekstra, A.Y., 2018. Hydrological response to future land-use change and climate change in a tropical catchment. https://doi.org/10.1080/02626667.2018.1511054 63, 1368–1385. https://doi.org/10.1080/02626667.2018.1511054

Mateo-Sagasta, J., Raschid-Sally, L., Thebo, A., 2015. Global wastewater and sludge production, treatment and use, in: Wastewater: Economic Asset in an Urbanizing World. Springer Netherlands, pp. 15–38. https://doi.org/10.1007/978-94-017-9545-6_2

Meals, D.W., Braun, D.C., 2006. Demonstration of Methods to Reduce E. coli Runoff from Dairy Manure Application Sites. J. Environ. Qual. 35, 1088–1100. https://doi.org/10.2134/JEQ2005.0380

Millennium Ecosystem Assessment, 2005. Ecosystems and human well-being: Synthesis. Island Press, Washington, DC, USA.

Miller, C.T., Dawson, C.N., Farthing, M.W., Hou, T.Y., Huang, J., Kees, C.E., Kelley, C.T., Langtangen, H.P., 2013. Numerical simulation of water resources problems: Models, methods, and trends. Adv. Water Resour. 51, 405–437. https://doi.org/10.1016/j.advwatres.2012.05.008

Milliman, J.D.., Syvitski, J.P.M., 1991. Geomorphic/Tectonic Control of Sediment Discharge to the Ocean: The Importance of Small Mountainous Rivers. J. Geol. 100, 525–544. https://doi.org/10.1086/629606

Milliman, J.D., 1995. Sediment discharge to the ocean from small mountainous rivers: The New Guinea example. Geo-Marine Lett. 15, 127–133. https://doi.org/10.1007/BF01204453

Milliman, J.D., Meade, R.H., Milliman2, J.D., 1983. World-Wide Delivery of River Sediment to the Oceans. Source J. Geol. 91, 1–21.

Milne, D.P., Curran, J.C., Findlay, J.S., Crowther, J.M., Bennett, J., Wood, B.J.B., 1991. The Effect of Dissolved Nutrients and Inorganic Suspended Solids on the Survival of E. coli in Seawater. Water Sci. Technol. 24, 133–136. https://doi.org/10.2166/WST.1991.0044

Mitch, A., Gasner, K., Mitch, W., 2010. Fecal coliform accumulation within a river subject to seasonally-disinfected wastewater discharges. Water Res. 44, 4776–4782. https://doi.org/10.1016/J.WATRES.2010.05.060

Miura, S., Yoshinaga, S., Yamada, T., 2003. Protective effect of floor cover against soil erosion on steep slopes forested with Chamaecyparis obtusa (hinoki) and other species. J. For. Res. 8, 27–35. https://doi.org/10.1007/s103100300003

Monaghan, R.M., Carey, P.L., Wilcock, R.J., Drewry, J.J., Houlbrooke, D.J., Quinn, J.M., Thorrold, B.S., 2009. Linkages between land management activities and stream water quality in a border dyke-irrigated pastoral catchment. Agric. Ecosyst. Environ. 129, 201–211. https://doi.org/10.1016/J.AGEE.2008.08.017

Monteith, J.L., 1965. Evaporation and the environment: in the state and movement of water in living organisms. Cambridge Univ. Press 205–234.

Moreira, N.A., Bondelind, M., 2017. Safe drinking water and waterborne outbreaks. J. Water Health 15, 83–96. https://doi.org/10.2166/WH.2016.103

Morgan, J.A., Hoet, A.E., Wittum, T.E., Monahan, C.M., Martin, J.F., 2008. Reduction of Pathogen Indicator Organisms in Dairy Wastewater Using an Ecological Treatment System. J. Environ. Qual. 37, 272–279. https://doi.org/10.2134/jeq2007.0120

Moriasi, D.N., Arnold, J.G., Liew Van, M.W., Bingner, R.L., Harmel, R.D., Veith, T.L., 2007. Model Evaluation Guidelines for Systematic Quantification of Accuracy in Watershed Simulations. Trans. ASABE 50, 885–900. https://doi.org/10.13031/2013.23153

Moriasi, D.N., Gitau, M.W., Pai, N., Daggupati, P., 2015. Hydrologic and water quality models: Performance measures and evaluation criteria. Trans. ASABE 58, 1763–1785. https://doi.org/10.13031/TRANS.58.10715

Morris, G.L., Fan, J., 1998. Reservoir Sedimentation Handbook.

Mouche, E., Moussu, F., Mügler, C., Ribolzi, O., Valentin, C., Sengtahevanghoung, O., Lacombe, G., 2014. Impact of land-use change on the hydrology of North Lao PDR watersheds. IAHS Publ.

MRC, 2021. The integrated water resources management–based Basin Development Strategy for the Lower Mekong Basin 2021–2030 and the MRC Strategic Plan 2021–2025, MRC Strategic Plan. Vientiane: MRC Secretariat.

MRC, 2011a. Planing Altas of the Lower Mekong River Basin, Mekong River Commission For Sustainable Development.

MRC, 2011b. Resilience To Climate Change-Induced Challenges In The Mekong River Basin: The Role of the MRC.

MRC, 2011c. Assessment of Basin-wide Development Scenarios: Main Report, Basin Development Plan Programme. Vientiane, Lao PDR.

MRC, 2010a. State of the Basin Report 2010.

MRC, 2010b. Assessment of Basin-wide Development Scenarios.

MRC, 2005. Overview of the Hydrology of the Mekong Basin. Mekong River Commission, Vientiane.

MRC, 2003a. State of the Basin Report 2003 . Mekong River Commission, Phnom Penh.

MRC, 2003b. Social Atlas of the Lower Mekong Basin Atlas prepared by the MRC Basin Development Plan.

Mthembu, M., Odinga, C., Swalaha, F.M., Bux, F., 2013. Constructed wetlands: A future alternative wastewater treatment technology. African J. Biotechnol. 12, 4542–4553. https://doi.org/10.5897/AJB2013.12978

Mügler, C., Ribolzi, O., Janeau, J.-L., Rochelle-Newall, E., Latsachack, K., Thammahacksa, C., Viguier, M., Jardé, E., Henri-Des-Tureaux, T., Sengtaheuanghoung, O., Valentin, C., n. d., 2020. Experimental and modelling evidence of short-term effect of raindrop impact on hydraulic conductivity and overland flow intensity. Environ. Sci. Pollut. Res. In review.

Mügler, C., Ribolzi, O., Viguier, M., Janeau, J.-L., Jardé, E., Latsachack, K., Henry-Des-

Tureaux, T., Thammahacksa, C., Valentin, C., Sengtaheuanghoung, O., Rochelle-Newall, E., 2021. Experimental and modelling evidence of splash effects on manure borne Escherichia coli washoff. Environ. Sci. Pollut. Res. https://doi.org/10.1007/s11356-021-13011-8

Müller, A., Österlund, H., Marsalek, J., Viklander, M., 2020. The pollution conveyed by urban runoff: A review of sources. Sci. Total Environ. 709, 136125. https://doi.org/10.1016/J.SCITOTENV.2019.136125

Naganandhini, S., Kennedy, Z.J., Uyttendaele, M., Balachandar, D., 2015. Persistence of pathogenic and non-pathogenic Escherichia coli strains in various tropical agricultural soils of India. PLoS One 10. https://doi.org/10.1371/journal.pone.0130038

Nakhle, P., Boithias, L., Pando-Bahuon, A., Thammahacksa, C., Gallion, N., Sounyafong, P., Silvera, N., Latsachack, K., Soulileuth, B., Rochelle-Newall, E., Marcangeli, Y., Pierret, A., Ribolzi, O., 2021a. Concentrations of Escherichia coli, total suspended sediment, and dissolved organic carbon, turbidity, and environmental variables measured in 2019 in a headwater wetland in the Houay Pano catchment, northern Lao PDR [WWW Document]. DataSuds. https://doi.org/https://doi.org/10.23708/E52ZTX

Nakhle, P., Boithias, L., Pando-Bahuon, A., Thammahacksa, C., Gallion, N., Sounyafong, P., Silvera, N., Latsachack, K., Soulileuth, B., Rochelle-Newall, E.J., Marcangeli, Y., Pierret, A., Ribolzi, O., 2021b. Decay Rate of Escherichia coli in a Mountainous Tropical Headwater Wetland. Water 2021, Vol. 13, Page 2068 13, 2068. https://doi.org/10.3390/W13152068

Nakhle, P., Ribolzi, O., Boithias, L., Rattanavong, S., Auda, Y., Sayavong, S., Zimmermann, R., Soulileuth, B., Pando, A., Thammahacksa, C., Rochelle-Newall, E.J., Santini, W., Martinez, J.M., Gratiot, N., Pierret, A., 2021c. Effects of hydrological regime and land use on in-stream Escherichia coli concentration in the Mekong basin, Lao PDR. Sci. Rep. 11, 3460. https://doi.org/10.1038/s41598-021-82891-0

Navratil, O., Legout, C., Gateuille, D., Esteves, M., Liebault, F., 2010. Assessment of intermediate fine sediment storage in a braided river reach (southern French Prealps). Hydrol. Process. 24, 1318–1332. https://doi.org/10.1002/hyp.7594

Neitsch, S.L., Arnold, J.G., Kiniry, J.R., Williams, J.R., 2011. Soil and Water Assessment Tool Theoretical Documentation-Version 2009. Coll. Agric. life Sci.

Nelson, K.L., Boehm, A.B., Davies-Colley, R.J., Dodd, M.C., Kohn, T., Linden, K.G., Liu, Y., Maraccini, P.A., McNeill, K., Mitch, W.A., Nguyen, T.H., Parker, K.M., Rodriguez, R.A., Sassoubre, L.M., Silverman, A.I., Wigginton, K.R., Zepp, R.G., 2018. Sunlight-mediated inactivation of health-relevant microorganisms in water: a review of mechanisms and modeling approaches. Environ. Sci. Process. Impacts 20, 1089–1122. https://doi.org/10.1039/c8em00047f

Neyret, M., Robain, H., de Rouw, A., Janeau, J.L., Durand, T., Kaewthip, J., Trisophon, K., Valentin, C., 2020. Higher runoff and soil detachment in rubber tree plantations compared to annual cultivation is mitigated by ground cover in steep mountainous Thailand. Catena 189, 104472. https://doi.org/10.1016/j.catena.2020.104472

Nguyen, H.T.M., Le, Q.T.P., Garnier, J., Janeau, J.L., Rochelle-Newall, E., 2016. Seasonal variability of faecal indicator bacteria numbers and die-off rates in the Red River basin, North Viet Nam. Sci. Rep. 6, 21644. https://doi.org/10.1038/srep21644

Niazi, M., Obropta, C., Miskewitz, R., 2015. Pathogen transport and fate modeling in the Upper Salem River Watershed using SWAT model. J. Environ. Manage. 151, 167–177. https://doi.org/10.1016/J.JENVMAN.2014.12.042

Nichols, G., Lane, C., Asgari, N., Verlander, N.Q., Charlett, A., 2009. Rainfall and outbreaks of drinking water related disease and in England and Wales. J. Water Health 7, 1–8. https://doi.org/10.2166/WH.2009.143

Nilsson, C., Berggren, K., 2000. Alterations of riparian ecosystems caused by river regulation. Bioscience 5, 783–792.

Nilsson, C., Reidy, C.A., Dynesius, M., Revenga, C., 2005. Fragmentation and Flow Regulation of the World's Large River Systems. Science (80-.). 308, 405–408. https://doi.org/10.1126/SCIENCE.1107887

Noble, R.., Lee, I.., Schiff, K., 2004a. Inactivation of indicator micro-organisms from various sources of faecal contamination in seawater and freshwater. J. Appl. Microbiol. 96, 464–472. https://doi.org/10.1111/j.1365-2672.2004.02155.x

Noble, R.., MK, L., CD, M., SB, W., K;, R., 2004b. Comparison of bacterial indicator analysis methods in stormwater-affected coastal waters. Water Res. 38, 1183–1188. https://doi.org/10.1016/J.WATRES.2003.11.038

Nowicki, S., DeLaurent, Z.R., de Villiers, E.P., Githinji, G., Charles, K.J., 2021. The utility of Escherichia coli as a contamination indicator for rural drinking water: Evidence from whole genome sequencing. PLoS One 16, e0245910. https://doi.org/10.1371/journal.pone.0245910

Ntajal, J., Falkenberg, T., Kistemann, T., Evers, M., 2020. Influences of Land-Use Dynamics and Surface Water Systems Interactions on Water-Related Infectious Diseases—A Systematic Review. Water 12, 631. https://doi.org/10.3390/w12030631

O'Geen, A.T., Bianchi, M.L., 2015. Using Wetlands to Remove Microbial Pollutants from Farm Discharge Water. Agric. Nat. Resour. Publ. 1–11. https://doi.org/https://doi.org/10.3733/ucanr.8512

Odagiri, M., Schriewer, A., Daniels, M.E., Wuertz, S., Smith, W.A., Clasen, T., Schmidt, W.P., Jin, Y., Torondel, B., Misra, P.R., Panigrahi, P., Jenkins, M.W., 2016. Human fecal and pathogen exposure pathways in rural Indian villages and the effect of increased latrine coverage. Water Res. 100, 232–244. https://doi.org/10.1016/J.WATRES.2016.05.015

Odonkor, S.T., Ampofo, J.K., 2013. Escherichia coli as An Indicator of Bacteriological Quality of Water: An Overview. Microbiol. Res. 2013, Vol. 4, Pages 5-11 4, 5–11. https://doi.org/10.4081/MR.2013.E2

OECD, 2017. Diffuse Pollution, Degraded Water: Emerging Policy Solutions.

Oeurng, C., Sauvage, S., Sánchez-Pérez, J.M., 2011. Assessment of hydrology, sediment and particulate organic carbon yield in a large agricultural catchment using the SWAT model. J. Hydrol. 401, 145–153. https://doi.org/10.1016/J.JHYDROL.2011.02.017

Oliver, D.M., Clegg, C.D., Heathwaite, A.L., Haygarth, P.M., 2007. Preferential attachment of Escherichia coli to different particle size fractions of an agricultural grassland soil. Water. Air. Soil Pollut. 185, 369–375. https://doi.org/10.1007/s11270-007-9451-8

Olsen, C.R., Cutshall, N.H., Larsen, I.L., 1982. Pollutant—particle associations and dynamics in coastal marine environments: a review. Mar. Chem. 11, 501–533. https://doi.org/10.1016/0304-4203(82)90001-9

OMS/UNICEF, 2017. Progrès en matières d'eau, d'assainissment, et d'hygiène: mise à jour 2017 et estimation des ODD. OMS et UNICEF Genève.

ONU, 2021. Rapport mondial des Nations Unies sur la mise en valeur des ressources en eau 2021 : la valeur de l'eau.

ONU, 2020. Rapport sur les objectifs de développement durable 2020.

Opisa, S., Odiere, M.R., Jura, W.G.Z.O., Karanja, D.M.S., Mwinzi, P.N.M., 2012. Faecal contamination of public water sources in informal settlements of Kisumu City, western Kenya. Water Sci. Technol. 66, 2674–2681. https://doi.org/10.2166/wst.2012.503

Pachepsky, Y., Shelton, D., Dorner, S., Whelan, G., 2016. Can E. Coli or thermotolerant coliform concentrations predict pathogen presence or prevalence in irrigation waters? Crit. Rev. Microbiol. 42, 384–393. https://doi.org/10.3109/1040841X.2014.954524

Pachepsky, Y., Shelton, D.R., McLain, J.E.T., Patel, J., Mandrell, R.E., 2011. Irrigation Waters as a Source of Pathogenic Microorganisms in Produce. A Review, 1st ed, Advances in Agronomy. Elsevier Inc. https://doi.org/10.1016/B978-0-12-386473-4.00007-5

Pachepsky, Y., Stocker, M., Saldaña, M.O., Shelton, D., 2017. Enrichment of stream water with fecal indicator organisms during baseflow periods. Environ. Monit. Assess. 189, 1–10. https://doi.org/10.1007/s10661-016-5763-8

Pachepsky, Y.A., Allende, A., Boithias, L., Cho, K., Jamieson, R., Hofstra, N., Molina, M., 2018. Microbial Water Quality: Monitoring and Modeling. J. Environ. Qual. 47, 931–938. https://doi.org/10.2134/JEQ2018.07.0277

Pachepsky, Y.A., Shelton, D.R., 2011. Escherichia coli and fecal coliforms in freshwater and estuarine sediments. Crit. Rev. Environ. Sci. Technol. 41, 1067–1110. https://doi.org/10.1080/10643380903392718

Paing, J., Guilbert, A., Gagnon, V., Chazarenc, F., 2015. Effect of climate, wastewater composition, loading rates, system age and design on performances of French vertical flow constructed wetlands: A survey based on 169 full scale systems. Ecol. Eng. 80, 46–52. https://doi.org/10.1016/j.ecoleng.2014.10.029

Palaniswami, S., Muthiah, K., 2018. Change point detection and trend analysis of rainfall and temperature series over the vellar river basin. Polish J. Environ. Stud. 27, 1673–1682. https://doi.org/10.15244/pjoes/77080

Palmer, J., Flint, S., Brooks, J., 2007. Bacterial cell attachment, the beginning of a biofilm. J. Ind. Microbiol. Biotechnol. 34, 577–588. https://doi.org/10.1007/s10295-007-0234-4

Palmer, M.A., Liermann, C.A.R., Nilsson, C., Flörke, M., Alcamo, J., Lake, P.S., Bond, N., 2008. Climate change and the world's river basins: anticipating management options. Front. Ecol. Environ. 6, 81–89. https://doi.org/10.1890/060148

Pandey, P.K., Kass, P.H., Soupir, M.L., Biswas, S., Singh, V.P., 2014. Contamination of water resources by pathogenic bacteria. AMB Express 2014 41 4, 1–16. https://doi.org/10.1186/S13568-014-0051-X

Pandey, P.K., Soupir, M.L., Haddad, M., Rothwell, J.J., 2012. Assessing the impacts of watershed indexes and precipitation on spatial in-stream E. coli concentrations. Ecol. Indic. 23, 641–652. https://doi.org/10.1016/J.ECOLIND.2012.05.023

Pandey, P.K., Soupir, M.L., Ikenberry, C.D., Rehmann, C.R., 2016. Predicting Streambed Sediment and Water Column Escherichia coli Levels at Watershed Scale. JAWRA J. Am. Water Resour. Assoc. 52, 184–197. https://doi.org/10.1111/1752-1688.12373

Passerat, J., Ouattara, N.K., Mouchel, J.M., Vincent Rocher, Servais, P., 2011. Impact of an intense combined sewer overflow event on the microbiological water quality of the Seine River. Water Res. 45, 893–903. https://doi.org/10.1016/J.WATRES.2010.09.024

Patin, J., Mouche, E., Ribolzi, O., Chaplot, V., Sengtahevanghoung, O., Latsachak, K.O., Soulileuth, B., Valentin, C., 2012. Analysis of runoff production at the plot scale during a long-term survey of a small agricultural catchment in Lao PDR. J. Hydrol. 426–427, 79–92. https://doi.org/10.1016/j.jhydrol.2012.01.015

Pellerin, B.A., Wollheim, W.M., Feng, X., Vörörsmarty, C.J., 2008. The application of electrical conductivity as a tracer for hydrograph separation in urban catchments. Hydrol. Process. 22, 1810–1818. https://doi.org/10.1002/hyp.6786

Perkins, T.L., Perrow, K., Rajko-Nenow, P., Jago, C.F., Jones, D.L., Malham, S.K., McDonald, J.E., 2016. Decay rates of faecal indicator bacteria from sewage and ovine faeces in brackish and freshwater microcosms with contrasting suspended particulate matter concentrations. Sci. Total Environ. 572, 1645–1652. https://doi.org/10.1016/j.scitotenv.2016.03.076

Petersen, F., Hubbart, J.A., 2020a. Quantifying escherichia coli and suspended particulate matter concentrations in a mixed-land use appalachian watershed. Water 12, 532. https://doi.org/10.3390/w12020532

Petersen, F., Hubbart, J.A., 2020b. Advancing Understanding of Land Use and Physicochemical Impacts on Fecal Contamination in Mixed - Land - Use Watersheds. Water (Switzerland) 12, 1094. https://doi.org/10.3390/W12041094

Petersen, F., Hubbart, J.A., 2020c. Physical Factors Impacting the Survival and Occurrence of Escherichia coli in Secondary Habitats. Water 12, 1796. https://doi.org/10.3390/w12061796

Pettitt, A.N., 1979. A Non-Parametric Approach to the Change-Point Problem. Source J. R. Stat. Soc. Ser. C (Applied Stat. 28, 126–135.

Philipsborn, R., Ahmed, S.M., Brosi, B.J., Levy, K., 2016. Climatic Drivers of Diarrheagenic Escherichia coli Incidence: A Systematic Review and Meta-analysis. J. Infect. Dis. 214, 6–15. https://doi.org/10.1093/INFDIS/JIW081

Pienaar, J.A., Singh, A., Barnard, T.G., 2016. The viable but non-culturable state in pathogenic Escherichia coli: A general review. Afr. J. Lab. Med. 5, 2225–2002. https://doi.org/10.4102/ajlm.v5i1.368

Piman, T., Lennaerts, T., Southalack, P., 2013. Assessment of hydrological changes in the lower Mekong Basin from Basin-Wide development scenarios. Hydrol. Process. 27, 2115–2125. https://doi.org/10.1002/HYP.9764

Piman, T., Shrestha, M., 2017a. Case study on sediment in the Mekong River Basin: Current state and future trends. UNESCO and Stockholm Environment Institute (SEI).

Piman, T., Shrestha, M., 2017b. Stockholm Environment Institute, Project Report 2017-03 Case study on sediment in the Mekong River Basin: Current state and future trends.

Piman, T., Shrestha, M., 2008. Case study on sediment in the Mekong River Basin: current state and future trends; 2017. Ambio.

Pirouz, D.M., 2010. An Overview of Partial Least Squares. SSRN Electron. J. 1–16. https://doi.org/10.2139/ssrn.1631359

Podwojewski, P., Orange, D., Jouquet, P., Valentin, C., Nguyen, V.T., Janeau, J.L., Tran, D.T., 2008. Land-use impacts on surface runoff and soil detachment within agricultural sloping lands in Northern Vietnam. CATENA 74, 109–118. https://doi.org/10.1016/J.CATENA.2008.03.013

Poff, N.L., Zimmerman, J.K.H., 2010. Ecological responses to altered flow regimes: a literature review to inform the science and management of environmental flows. Freshw. Biol. 55, 194–205. https://doi.org/10.1111/J.1365-2427.2009.02272.X

Pokhrel, Y., Burbano, M., Roush, J., Kang, H., Sridhar, V., Hyndman, D.W., 2018. A review of the integrated effects of changing climate, land use, and dams on Mekong river hydrology. Water (Switzerland) 10, 1–25. https://doi.org/10.3390/w10030266

Pringle, C., 2003. What is hydrologic connectivity and why is it ecologically important? Hydrol. Process. 17, 2685–2689. https://doi.org/10.1002/HYP.5145

Prüss-Ustün, A., Wolf, J., Bartram, J., Clasen, T., Cumming, O., Freeman, M.C., Gordon, B., Hunter, P.R., Medlicott, K., Johnston, R., 2019. Burden of disease from inadequate water, sanitation and hygiene for selected adverse health outcomes: An updated analysis with a

focus on low- and middle-income countries. Int. J. Hyg. Environ. Health 222, 765–777. https://doi.org/10.1016/j.ijheh.2019.05.004

Qiu, Z., Giri, S., Wang, L., Luo, B., 2018. SWAT modeling of fecal indicator bacteria fate and transport in a suburban watershed with mixed land uses. Proc. Int. Acad. Ecol. Environ. Sci. 8, 28–46.

Quin, A., Jaramillo, F., Destouni, G., 2015. Dissecting the ecosystem service of large-scale pollutant retention: The role of wetlands and other landscape features. Ambio 44, 127–137. https://doi.org/10.1007/s13280-014-0594-8

Ranzi, R., Le, T.H., Rulli, M.C., 2011. A RUSLE approach to model suspended sediment load in the Lo river (Vietnam): Effects of reservoirs and land use changes [WWW Document]. J. Hydrol.

Räsänen, T.A., Someth, P., Lauri, H., Koponen, J., Sarkkula, J., Kummu, M., 2017. Observed river discharge changes due to hydropower operations in the Upper Mekong Basin. J. Hydrol. 545, 28–41. https://doi.org/10.1016/J.JHYDROL.2016.12.023

Ribolzi, O., Andrieux, P., Valles, V., Bouzigues, R., Bariac, T., Voltz, M., 2000. Contribution of groundwater and overland flows to storm flow generation in a cultivated Mediterranean catchment. Quantification by natural chemical tracing. J. Hydrol. 233, 241–257. https://doi.org/10.1016/S0022-1694(00)00238-9

Ribolzi, O., Boithias, L., Thammahacksa, C., Silvera, N., Pando-Bahuon, A., Sengtaheuanghoung, Oloth and Sipaseuth, N., Latsachack, K., Soulileuth, B., Sounyafong, P., Xayyathip, K., Pierret, A., 2021. Escherichia coli concentrations and physico-chemical measurements (2011-2021) at the outlet of six catchments of the Mekong river basin, northern Lao PDR [WWW Document]. DataSuds. URL https://doi.org/10.23708/1YZQHH

Ribolzi, O., Cuny, J., Sengsoulichanh, P., Mousquès, C., Soulileuth, B., Pierret, A., Huon, S., Sengtaheuanghoung, O., 2011. Land use and water quality along a mekong tributary in Northern Lao P.D.R. Environ. Manage. 47, 291–302. https://doi.org/10.1007/s00267-010-9593-0

Ribolzi, Olivier, Cuny, J., Sengsoulichanh, P., Mousquès, C., Soulileuth, B., Pierret, A., Huon, S., Sengtaheuanghoung, O., 2011. Land use and water quality along a mekong tributary in Northern Lao P.D.R. Environ. Manage. 47, 291–302. https://doi.org/10.1007/s00267-010-9593-0

Ribolzi, O., Evrard, O., Huon, S., De Rouw, A., Silvera, N., Latsachack, K.O., Soulileuth, B., Lefèvre, I., Pierret, A., Lacombe, G., Sengtaheuanghoung, O., Valentin, C., 2017. From shifting cultivation to teak plantation: Effect on overland flow and sediment yield in a montane tropical catchment. Sci. Rep. 7, 1–12. https://doi.org/10.1038/s41598-017-04385-2

Ribolzi, O., Evrard, O., Huon, S., Rochelle-Newall, E., Henri-des-Tureaux, T., Silvera, N., Thammahacksac, C., Sengtaheuanghoung, O., 2016. Use of fallout radionuclides (7Be, 210Pb) to estimate resuspension of Escherichia coli from streambed sediments during floods

in a tropical montane catchment. Environ. Sci. Pollut. Res. 23, 3427–3435. https://doi.org/10.1007/s11356-015-5595-z

Ribolzi, O., Lacombe, G., Pierret, A., Robain, H., Sounyafong, P., de Rouw, A., Soulileuth, B., Mouche, E., Huon, S., Silvera, N., Latxachak, K.O., Sengtaheuanghoung, O., Valentin, C., 2018. Interacting land use and soil surface dynamics control groundwater outflow in a montane catchment of the lower Mekong basin. Agric. Ecosyst. Environ. 268, 90–102. https://doi.org/10.1016/j.agee.2018.09.005

Ribolzi, Olivier;, Patin, J.., Bresson, L.-M., Latsachack, K.O., Mouche, E.., Sengtaheuanghoung, O.., Silvera, N., Thiébaux, J.-P., Valentin., C., 2011. Impact of slope gradient on soil surface features and infiltration on steep slopes in northern Laos. Geomorphology 127, 53–63. https://doi.org/10.1016/j.geomorph.2010.12.004

Robert, E., Grippa, M., Nikiema, D.E., Kergoat, L., Koudougou, H., Auda, Y., Rochelle-Newall, E., 2021. Environmental determinants of E. coli, link with the diarrheal diseases, and indication of vulnerability criteria in tropical West Africa (Kapore, Burkina Faso). PLoS Negl. Trop. Dis. 15, e0009634. https://doi.org/10.1371/JOURNAL.PNTD.0009634

Rochelle-Newall, E., Nguyen, T.M.H., Le, T.P.Q., Sengtaheuanghoung, O., Ribolzi, O., 2015. A short review of fecal indicator bacteria in tropical aquatic ecosystems: Knowledge gaps and future directions. Front. Microbiol. 6, 308. https://doi.org/10.3389/fmicb.2015.00308

Rochelle-Newall, E.J., Ribolzi, O., Viguier, M., Thammahacksa, C., Silvera, N., Latsachack, K., Dinh, R.P., Naporn, P., Sy, H.T., Soulileuth, B., Hmaimum, N., Sisouvanh, P., Robain, H., Janeau, J.L., Valentin, C., Boithias, L., Pierret, A., 2016. Effect of land use and hydrological processes on Escherichia coli concentrations in streams of tropical, humid headwater catchments. Sci. Rep. 6, 1–12. https://doi.org/10.1038/srep32974

Røstum, J., Aasen, A., Eikebrokk, B., 2009. Risk and Vulnerability Assessment ("Ros-Analysis") of the Bergen Water Supply System – A Source to Tap Approach 73–83. https://doi.org/10.1007/978-90-481-2365-0_8

Sagir Ahmed, M., Raknuzzaman, M., Akther, H., Ahmed, S., 2007. The role of cyanobacteria blooms in cholera epidemic in Bangladesh. J. Appl. Sci. 7, 1785–1789. https://doi.org/10.3923/JAS.2007.1785.1789

Sani, A., Scholz, M., Bouillon, L., 2013. Seasonal assessment of experimental vertical-flow constructed wetlands treating domestic wastewater. Bioresour. Technol. 147, 585–596. https://doi.org/10.1016/j.biortech.2013.08.076

Scarcella, C., Carasi, S., Cadoria, F., Macchi, L., Pavan, A., Salamana, M., Alborali, G.L., Losio, M.N., Boni, P., Lavazza, A., Seyler, T., 2009. An outbreak of viral gastroenteritis linked to municipal water supply, Lombardy, Italy, June 2009. Eurosurveillance 14, 19274. https://doi.org/10.2807/ESE.14.29.19274-EN

Scholz, M., 2010. Wetland Systems: Storm water management control, Green Energy and Technology. Springer Science & Business Media.

Schwarzenbach, R.P., Egli, T., Hofstetter, T.B., von Gunten, U., Wehrli, B., 2010. Global Water Pollution and Human Health. Annu. Rev. Environ. Resour. 35, 109–136. https://doi.org/10.1146/annurev-environ-100809-125342

Searcy, J.K., Hardison, C.H., 1960. Double-mass curves, Manual of hydrology: Part 1. General Surface-Water Techniques. US Government Printing Office.

September, S.M., Els, F.A., Venter, S.N., Brözel, V.S., 2007. Prevalence of bacterial pathogens in biofilms of drinking water distribution systems. J. Water Health 5, 219–227. https://doi.org/10.2166/WH.2007.004B

Shelton, D.R., Pachepsky, Y.A., Kiefer, L.A., Blaustein, R.A., McCarty, G.W., Dao, T.H., 2014. Response of coliform populations in streambed sediment and water column to changes in nutrient concentrations in water. Water Res. 59, 316–324. https://doi.org/10.1016/j.watres.2014.04.019

Shiklomanov, I.A., 1993. Water in crisis: A Guide to the World's Fresh Water Resources. Pacific Inst. Stud. Dev., Environ. Secur. Stock. Env. Institute, Oxford Univ. Press. 9, 1051–0761. https://doi.org/10.1016/B978-0-323-60984-5.00062-7

Shrestha, B., Babel, M.S., Maskey, S., Griensven, A. van, Uhlenbrook, S., Green, A., Akkharath, I., 2013. Impact of climate change on sediment yield in the Mekong River basin: a case study of the Nam Ou basin, Lao PDR. Hydrol. Earth Syst. Sci. 17, 1–20. https://doi.org/10.5194/hess-17-1-2013

Shrestha, B., Maskey, S., Babel, M.S., van Griensven, A., Uhlenbrook, S., 2018. Sediment related impacts of climate change and reservoir development in the Lower Mekong River Basin: a case study of the Nam Ou Basin, Lao PDR. Clim. Change 149, 13–27. https://doi.org/10.1007/s10584-016-1874-z

Sidhu, J.P.S., Ahmed, W., Gernjak, W., Aryal, R., McCarthy, D., Palmer, A., Kolotelo, P., Toze, S., 2013. Sewage pollution in urban stormwater runoff as evident from the widespread presence of multiple microbial and chemical source tracking markers. Sci. Total Environ. 463–464, 488–496. https://doi.org/10.1016/J.SCITOTENV.2013.06.020

Sidle, R.C., Ziegler, A.D., Negishi, J.N., Nik, A.R., Siew, R., Turkelboom, F., 2006. Erosion processes in steep terrain - Truths, myths, and uncertainties related to forest management in Southeast Asia. For. Ecol. Manage. 224, 199–225. https://doi.org/10.1016/j.foreco.2005.12.019

Silvera, N., Ribolzi, O., Boithias, L., Rochelle-Newall, E., Riotte, J., Audry, S., Sipaseut, N., Al, E., 2015. Weather station data, Houay Pano, Laos. Theia.

Sinclair, A., Hebb, D., Jamieson, R., Gordon, R., Benedict, K., Fuller, K., Stratton, G.W., Madani, A., 2009. Growing season surface water loading of fecal indicator organisms within a rural watershed. Water Res. 43, 1199–1206. https://doi.org/10.1016/J.WATRES.2008.12.006

Sinton, L.W., Hall, C.H., Lynch, P.A., Davies-Colley, R.J., 2002. Sunlight inactivation of fecal indicator bacteria and bacteriophages from waste stabilization pond effluent in fresh and saline waters. Appl. Environ. Microbiol. 68, 1122–1131. https://doi.org/10.1128/AEM.68.3.1122-1131.2002

Smith, J., Edwards, J., Hilger, H., Steck, T.R., 2008. Sediment can be a reservoir for coliform bacteria released into streams. J. Gen. Appl. Microbiol. 54, 173–179. https://doi.org/10.2323/jgam.54.173

Smith, J.E., Stocker, M.D., Hill, R.L., Pachepsky, Y.A., 2019. The Effect of Temperature Oscillations and Sediment Texture on Fecal Indicator Bacteria Survival in Sediments. Water. Air. Soil Pollut. 230. https://doi.org/10.1007/s11270-019-4278-7

Sok, T., Oeurng, C., Ich, I., Sauvage, S., Sánchez-Pérez, J.M., 2020. Assessment of hydrology and sediment yield in the mekong river basin using swat model. Water (Switzerland) 12, 1–26. https://doi.org/10.3390/w12123503

Solo-Gabriele, H.M., Wolfert, M.A., Desmarais, T.R., Palmer, C.J., 2000. Sources of Escherichia coli in a Coastal Subtropical Environment. Appl. Environ. Microbiol. 66, 230–237. https://doi.org/10.1128/AEM.66.1.230-237.2000

Song, L., Boithias, L., Sengtaheuanghoung, O., Oeurng, C., Valentin, C., Souksavath, B., Sounyafong, P., Rouw, A. De, Soulileuth, B., Silvera, N., Lattanavongkot, B., Pierret, A., Ribolzi, O., 2020. Understory Limits Surface Runoff and Soil Loss in Teak Tree Plantations of Northern Lao PDR 1–23.

Sor, R., Ngor, P.B., Soum, S., Chandra, S., Hogan, Z.S., Null, S.E., 2021. Water quality degradation in the lower mekong basin. Water (Switzerland) 13, 1–18. https://doi.org/10.3390/w13111555

Soukhaphon, A., Baird, I.G., Hogan, Z.S., 2021. The Impacts of Hydropower Dams in the Mekong River Basin: A Review. Water 2021, Vol. 13, Page 265 13, 265. https://doi.org/10.3390/W13030265

Soupir, M.L., Mostaghimi, S., 2011. Escherichia coli and enterococci attachment to particles in runoff from highly and sparsely vegetated grassland. Water. Air. Soil Pollut. 216, 167–178. https://doi.org/10.1007/s11270-010-0524-8

Soupir, M.L., Mostaghimi, S., Yagow, E.R., Hagedorn, C., Vaughan, D.H., 2006. Transport of fecal bacteria from poultry litter and cattle manures applied to pastureland. Water. Air. Soil Pollut. 169, 125–136. https://doi.org/10.1007/S11270-006-1808-X

Sowah, R.A., Bradshaw, K., Snyder, B., Spidle, D., Molina, M., 2020. Evaluation of the soil and water assessment tool (SWAT) for simulating E. coli concentrations at the watershed-scale. Sci. Total Environ. 746, 140669. https://doi.org/10.1016/j.scitotenv.2020.140669

Staley, C., Reckhow, K.H., Lukasik, J., Harwood, V.J., 2012. Assessment of sources of human pathogens and fecal contamination in a Florida freshwater lake. Water Res. 46, 5799–5812.

https://doi.org/10.1016/J.WATRES.2012.08.012

Strauch, A.M., Mackenzie, R.A., Bruland, G.L., Tingley, R., Giardina, C.P., 2014. Climate Change and Land Use Drivers of Fecal Bacteria in Tropical Hawaiian Rivers. J. Environ. Qual. 43, 1475–1483. https://doi.org/10.2134/JEQ2014.01.0025

Stumpf, C., Piehler, M., Thompson, S., Noble, R., 2010. Loading of fecal indicator bacteria in North Carolina tidal creek headwaters: hydrographic patterns and terrestrial runoff relationships. Water Res. 44, 4704–4715. https://doi.org/10.1016/J.WATRES.2010.07.004

Suif, Z., Fleifle, A., Yoshimura, C., Saavedra, O., 2016. Spatio-temporal patterns of soil erosion and suspended sediment dynamics in the Mekong River Basin. Sci. Total Environ. 568, 933–945. https://doi.org/10.1016/j.scitotenv.2015.12.134

Suter, E., Juhl, A.R., O'Mullan, G.D., 2011. Particle Association of Enterococcus and Total Bacteria in the Lower Hudson River Estuary, USA. J. Water Resour. Prot. 3, 715–725. https://doi.org/10.4236/jwarp.2011.310082

Szogi, A.A., Vanotti, M.B., Ro, K.S., 2015. Methods for Treatment of Animal Manures to Reduce Nutrient Pollution Prior to Soil Application. Curr. Pollut. Reports 2015 11 1, 47–56. https://doi.org/10.1007/S40726-015-0005-1

Tan, M.L., Gassman, P.W., Srinivasan, R., Arnold, J.G., Yang, X.Y., 2019. A review of SWAT studies in Southeast Asia: Applications, challenges and future directions. Water (Switzerland). https://doi.org/10.3390/w11050914

Tang, Q., He, X., Bao, Y., Zhang, X., Guo, F., Zhu, H., 2013. Determining the relative contributions of climate change and multiple human activities to variations of sediment regime in the Minjiang River, China. Hydrol. Process. 27, 3547–3559. https://doi.org/10.1002/HYP.9472

Tavares Carneiro, M., Bandeira Vianna Cortes, M., Cesar Wasserman, J., 2018. Critical evaluation of the factors affecting Escherichia coli environmental decay for outfall plume models. Rev. Ambient. Água 13. https://doi.org/10.4136/1980-993X

Teeter, A.M., Johnson, B.H., Berger, C., Stelling, G., Scheffner, N.W., Garcia, M.H., Parchure, T.M., 2001. Hydrodynamic and sediment transport modeling with emphasis on shallow-water, vegetated areas (lakes, reservoirs, estuaries and lagoons). Hydrobiologia 444, 1–23. https://doi.org/https://doi.org/10.1023/A:1017524430610

Thi Ha, D., Ouillon, S., Van Vinh, G., 2018. Water and Suspended Sediment Budgets in the Lower Mekong from High-Frequency Measurements (2009–2016). Water 10, 846. https://doi.org/10.3390/w10070846

Thoe, W., Wong, S.H.C., Choi, K.W., Lee, J.H.W., 2012. Daily prediction of marine beach water quality in Hong Kong. J. Hydro-environment Res. 6, 164–180. https://doi.org/10.1016/J.JHER.2012.05.003

Thongmanivong, S., Fujita, Y., 2006. Recent Land Use and Livelihood Transitions in Northern

Laos. Mt. Res. Dev. 26 26, 237–244. https://doi.org/10.1659/0276-4741(2006)26[237:RLUALT]2.0.CO;2

Thornton, C.I., Abt, S.R., Clary, W.P., 2007. VEGETATION INFLUENCE ON SMALL STREAM SILTATION. J. Am. Water Resour. Assoc. 33, 1279–1288. https://doi.org/10.1111/j.1752-1688.1997.tb03552.x

Topp, E., Welsh, M., Tien, Y.-C., Dang, A., Lazarovits, G., Conn, K., Zhu, H., 2003. Strain-dependent variability in growth and survival of Escherichia coli in agricultural soil. FEMS Microbiol. Ecol. 44, 303–308. https://doi.org/10.1016/S0168-6496(03)00055-2

Trevisan, D., Vansteelant, J.Y., Dorioz, J.M., 2002. Survival and leaching of fecal bacteria after slurry spreading on mountain hay meadows: consequences for the management of water contamination risk. Water Res. 36, 275–283. https://doi.org/10.1016/S0043-1354(01)00184-1

Troeger, C., Forouzanfar, M., Rao, P.C., Khalil, I., Mokdad, A.H., et al., 2017. Estimates of the global, regional, and national morbidity, mortality, and aetiologies of lower respiratory tract infections in 195 countries: a systematic analysis for the Global Burden of Disease Study 2015. Lancet Infect. Dis. 17, 1133–1161. https://doi.org/10.1016/S1473-3099(17)30396-1

Turkelboom, F., Poesen, J., Trébuil, G., 2008. The multiple land degradation effects caused by land-use intensification in tropical steeplands: A catchment study from northern Thailand. Catena 75, 102–116. https://doi.org/10.1016/j.catena.2008.04.012

UN-Water, 2018. Sustainable Development Goal 6 Synthesis Report 2018 on Water and Sanitation, United Nations. United Nations Organization, New York.

UN, 2021. The United Nations World Water Development Report 2021: Valuing water. Water Polit. 206.

UN, 2019. World Population Prospects 2019: Highlights. United Nations, Department of economic and social affairs, population division, USA.

UNEP, 2002. Vital Water Graphics: An Overview of the State of the World's Fresh and Marine Waters, United Nations Environment Progamme Nairobi, Kenya.

UNEP, A., 2016. A Snapshot of the World's Water Quality: Towards a global assessment, Nairobi, United Nations Environment Programme. United Nations Environment Programme, Nairobi, Kenya.

UNESCO, UN-Water, 2020. Rapport mondial des Nations Unies sur la mise en valeur des ressources en eau 2020 : L'eau et les changements climatiques. Paris, UNESCO.

USDA-SCS, 1972. National Engineering Handbook, Section 4 Hydrology. United States Department of Agriculture – Soil Con- servation Service: Washington, USA.

USEPA, 2013. Literature review of contaminants in livestock and poultry manure and implications for water quality. EPA Office of Water: Washington, DC.

USEPA (U.S. Environmental Protection Agency), 2015. Connectivity of Streams and Wetlands to Downstream Waters: A Review and Synthesis of the Scientific Evidence. US Environmental Protection Agency Washington, DC, USA.

Valentin, C., Agus, F., Alamban, R., Boosaner, A., Bricquet, J.P., Chaplot, V., de Guzman, T., de Rouw, A., Janeau, J.L., Orange, D., Phachomphonh, K., Do Duy Phai, Podwojewski, P., Ribolzi, O., Silvera, N., Subagyono, K., Thiébaux, J.P., Tran Duc Toan, Vadari, T., 2008a. Runoff and sediment losses from 27 upland catchments in Southeast Asia: Impact of rapid land use changes and conservation practices. Agric. Ecosyst. Environ. 128, 225–238. https://doi.org/10.1016/j.agee.2008.06.004

Valentin, C., Lestrelin, G., Chanthavongsa, A., Phachomphon, K., De Rouw, A., Chanhphengxay, A., Chaplot, V., Bourdon, E., Bricquet, J.P., Marchand, P., Pierret, A., 2008b. The MSEC project in the Lao PDR at a glance : biophysical and socio-economic background and project experimental set up.

Van Elsas, J.D., Semenov, A. V., Costa, R., Trevors, J.T., 2011. Survival of Escherichia coli in the environment: Fundamental and public health aspects. ISME J. 5, 173–183. https://doi.org/10.1038/ismej.2010.80

Vermeulen, L.C., Hofstra, N., 2014. Influence of climate variables on the concentration of Escherichia coli in the Rhine, Meuse, and Drentse Aa during 1985-2010. Reg. Environ. Chang. 14, 307–319. https://doi.org/10.1007/S10113-013-0492-9

Vidon, P., Tedesco, L.P., Wilson, J., Campbell, M.A., Casey, L.R., Gray, M., 2008. Direct and Indirect Hydrological Controls on E. coli Concentration and Loading in Midwestern Streams. J. Environ. Qual. 37, 1761–1768. https://doi.org/10.2134/JEQ2007.0311

Vigiak, O., Ribolzi, O., Pierret, A., Sengtaheuanghoung, O., Chaplot, V., Valentin, C., 2008. Estimation of runoff curve number (CN) of some Laotian land use types.

Vijayavel, K., Sadowsky, M.J., Ferguson, J.A., Kashian, D.R., 2013. The establishment of the nuisance cyanobacteria Lyngbya wollei in Lake St. Clair and its potential to harbor fecal indicator bacteria. J. Great Lakes Res. 39, 560–568. https://doi.org/10.1016/J.JGLR.2013.09.018

Vörösmarty, C.J., McIntyre, P.B., Gessner, M.O., Dudgeon, D., Prusevich, A., Green, P., Glidden, S., Bunn, S.E., Sullivan, C.A., Liermann, C.R., Davies, P.M., 2010. Global threats to human water security and river biodiversity. Nature 467, 555–561. https://doi.org/10.1038/nature09440

Vorosmarty, C.J., Sahagian, D., 2000. Anthropogenic disturbance of the terrestrial water cycle. Bioscience 50, 753–765. https://doi.org/10.1641/0006-3568(2000)050[0753:ADOTTW]2.0.CO;2

Wade, T.J., Calderon, R.L., Sams, E., Beach, M., Brenner, K.P., Williams, A.H., Dufour, A.P., 2006. Rapidly Measured Indicators of Recreational Water Quality Are Predictive of Swimming-Associated Gastrointestinal Illness. Environ. Health Perspect. 114, 24–28.

https://doi.org/10.1289/EHP.8273

Walters, E., Graml, M., Behle, C., Horn, H., Müller, E., Schwarzwälder, K., Rutschmann, P., Müller, E., Horn, H., 2014. Influence of Particle Association and Suspended Solids on UV Inactivation of Fecal Indicator Bacteria in an Urban River. Water Air Soil Pollut 225, 1822. https://doi.org/10.1007/s11270-013-1822-8

Walters, S.P., Thebo, A.L., Boehm, A.B., 2011. Impact of urbanization and agriculture on the occurrence of bacterial pathogens and stx genes in coastal waterbodies of central California. Water Res. 45, 1752–1762. https://doi.org/10.1016/J.WATRES.2010.11.032

Wang, S., Yan, Y., Yan, M., Zhao, X., 2012. Quantitative estimation of the impact of precipitation and human activities on runoff change of the Huangfuchuan River Basin. J. Geogr. Sci. 2012 225 22, 906–918. https://doi.org/10.1007/S11442-012-0972-8

Wang, Y., Pandey, P., Zheng, Y., Atwill, E.R., Pasternack, G., 2018. Particle attached and free floating pathogens survival kinetics under typical stream and thermal spring temperature conditions. AMB Express 8. https://doi.org/10.1186/s13568-018-0626-z

Wanjugi, P., Harwood, V.J., 2013. The influence of predation and competition on the survival of commensal and pathogenic fecal bacteria in aquatic habitats. Environ. Microbiol. 15, 517–526. https://doi.org/10.1111/j.1462-2920.2012.02877.x

Ward, J. V., TOCKNER, K., ARSCOTT, D.B., CLARET, C., 2002. Riverine landscape diversity. Freshw. Biol. 47, 517–539. https://doi.org/10.1046/J.1365-2427.2002.00893.X

Wardrop, N.A., Hill, A.G., Dzodzomenyo, M., Aryeetey, G., Wright, J.A., 2018. Livestock ownership and microbial contamination of drinking-water: Evidence from nationally representative household surveys in Ghana, Nepal and Bangladesh. Int. J. Hyg. Environ. Health 221, 33–40. https://doi.org/10.1016/J.IJHEH.2017.09.014

Wei, X., Sauvage, S., Le, T.P.Q., Ouillon, S., Orange, D., Vinh, V.D., Sanchez-Perez, J.M., 2019. A modeling approach to diagnose the impacts of global changes on discharge and suspended sediment concentration within the Red River Basin. Water (Switzerland) 11, 958. https://doi.org/10.3390/w11050958

Whitman, R.L., Nevers, M.B., Korinek, G.C., Byappanahalli, M.N., 2004. Solar and Temporal Effects on Escherichia coli Concentration at a Lake Michigan Swimming Beach. Appl. Environ. Microbiol. 70, 4276--4285. https://doi.org/10.1128/AEM.70.7.4276-4285.2004

WHO/UNICEF, 2020. Progress on drinking water, sanitation and hygiene in school: special focus on COVID-19. UNICEF.

WHO/UNICEF, 2019. Progress on household drinking water, sanitation and hygiene I 2000-2017: special focus on inequalities. UNIICEF and WHO: New York.

WHO/UNICEF, 2015. Progress on sanitation and drinking water: 2015 update and MDG Assessment. World Health Organization, Geneva, Switzerland.

WHO/UNICEF, 2013. Progress on sanitation and drinking-water 2013 update: Joint Monitoring Programme for Water Supply and Sanitation.

WHO, 2020. WHO global water, sanitation and hygiene: annual report 2019.

WHO, 2018. WHO recommendations on scientific, analytical and epidemiological developments relevant to the parameters for bathing water quality in the bathing water directive (2006/7/EC).

WHO, 2017. Inheriting a sustainable world? Atlas on children's health and the environment. World Health Organization, Geneva, Switzerland.

WHO, 2016a. Mortality rate attributed to exposure to unsafe WASH services (SDG 3.9.2), WHO. World Health Organization.

WHO, 2016b. Protecting surface water for health: Identifying, assessing and managing drinking-water quality risks in surface-water catchments. WHO geneva.

WHO, 2015. Lao People's Democratic Republic: WHO statistical profile.

WHO, 2011a. Faecal pollution and water quality.

WHO, 2011b. Guidelines for drinking-water quality, fourth edition. WHO chronicle.

WHO, 2003. Guidelines for Safe RecreationalWater Environments, chapter 4: faecal pollution and water quality. Wolrd Health Organization: Geneva Switzerland.

WHO, 1993. Guidelines for Drinking-water Quality: second edition. World Health Organization, Geneva.

WHO and OECD, 2003. Assessing Microbial Safety of Drinking Water: Improving Approaches and Methods - Google Books. IWA Publishing: London, UK.

Wilkes, G., Edge, T., Gannon, V., Jokinen, C., Lyautey, E., Medeiros, D., Neumann, N., Ruecker, N., Topp, E., Lapen, D.R., 2009. Seasonal relationships among indicator bacteria, pathogenic bacteria, Cryptosporidium oocysts, Giardia cysts, and hydrological indices for surface waters within an agricultural landscape. Water Res. 43, 2209–2223. https://doi.org/10.1016/J.WATRES.2009.01.033

Wilkinson, J., Jenkins, A., Wyer, M., Kay, D., 1995. Modelling faecal coliform dynamics in streams and rivers. Water Res. 29, 847–855. https://doi.org/10.1016/0043-1354(94)00211-O

Williams, J.R., 1975. Sediment-yield prediction with Universal Equation using runoff energy factor. undefined.

Winemiller, K.O., McIntyre, P.B., Castello, L., Fluet-Chouinard, E., Giarrizzo, T., Nam, S., Baird, I.G., Darwall, W., Lujan, N.K., Harrison, I., Stiassny, M.L.J., Silvano, R.A.M., 2016. Balancing hydropower and biodiversity in the Amazon, Congo, and Mekong. Science (80-.). 351, 128–129. https://doi.org/10.1126/science.aac7082

Winfield, M., Groisman, E., 2003. Role of nonhost environments in the lifestyles of Salmonella and Escherichia coli. Appl. Environ. Microbiol. 69, 3687–3694. https://doi.org/10.1128/AEM.69.7.3687-3694.2003

Wingender, J., Flemming, H., 2011. Biofilms in drinking water and their role as reservoir for pathogens. Int. J. Hyg. Environ. Health 214, 417–423. https://doi.org/10.1016/J.IJHEH.2011.05.009

Winton, R.S., Calamita, E., Wehrli, B., 2019. Reviews and syntheses: Dams, water quality and tropical reservoir stratification. Biogeosciences 16, 1657–1671. https://doi.org/10.5194/bg-16-1657-2019

WLE, 2020. Dataset on the Dams of the Greater Mekong.

Wu, J., SC, L., D, D., SM, D., 2011. Are microbial indicators and pathogens correlated? A statistical analysis of 40 years of research. J. Water Health 9, 265–278. https://doi.org/10.2166/WH.2011.117

Wu, Z., Xu, Z., Wang, F., He, H., Zhou, J., Wu, X., Liu, Z., 2018. Hydrologic Evaluation of Multi-Source Satellite Precipitation Products for the Upper Huaihe River Basin, China. Remote Sens. 10, 840. https://doi.org/10.3390/rs10060840

WWAP, 2017. Rapport mondial des Nations Unies sur la mise en valeur des ressources en eau 2017: Les eaux usées, une ressource inexploitée. Paris, UNESCO.

WWF, 2013. Ecosystems in the Greater Mekong: past trends, current status, possible futures. World Wide Fund For Nature (Formerly World Wildlife Fund), Greater Mekon.

Wyatt, A.B., Baird, I.G., 2007. Transboundary Impact Assessment in the Sesan River Basin: The Case of the Yali Falls Dam. http://dx.doi.org/10.1080/07900620701400443 23, 427–442. https://doi.org/10.1080/07900620701400443

Xu, Z., Wu, Z., He, H., Wu, X., Zhou, J., Zhang, Y., Guo, X., 2019. Evaluating the accuracy of MSWEP V2.1 and its performance for drought monitoring over mainland China. Atmos. Res. 226, 17–31. https://doi.org/10.1016/j.atmosres.2019.04.008

Xu, Z.X., Pang, J.P., Liu, C.M., Li, J.Y., 2009. Assessment of runoff and sediment yield in the miyun reservoir catchment by using SWAT model. Hydrol. Process. 23, 3619–3630. https://doi.org/10.1002/HYP.7475

Yaduvanshi, A., Sharma, R.K., Kar, S.C., Sinha, A.K., 2018. Rainfall–runoff simulations of extreme monsoon rainfall events in a tropical river basin of India. Nat. Hazards 90, 843–861. https://doi.org/10.1007/S11069-017-3075-0

Yajima, A., Kurokura, H., 2008. Microbial risk assessment of livestock-integrated aquaculture and fish handling in Vietnam. Fish. Sci. 2008 745 74, 1062–1068. https://doi.org/10.1111/J.1444-2906.2008.01625.X

Yan, Q., Bi, Y., Deng, Y., He, Z., Wu, L., Van Nostrand, J.D., Shi, Z., Li, J., Wang, X., Hu, Z.,

Yu, Y., Zhou, J., 2015. Impacts of the Three Gorges Dam on microbial structure and potential function. Sci. Reports 2015 51 5, 1–9. https://doi.org/10.1038/srep08605

Yong, S.T.Y., Chen, W., 2002. Modeling the relationship between land use and surface water quality. J. Environ. Manage. 66, 377–393. https://doi.org/10.1006/jema.2002.0593

Zarfl, C., Lumsdon, A.E., Berlekamp, J., Tydecks, L., Tockner, K., 2015. A global boom in hydropower dam construction. Aquat. Sci. 77, 161–170. https://doi.org/10.1007/s00027-014-0377-0

Zedler, J.B., Kercher, S., 2005. WETLAND RESOURCES: Status, Trends, Ecosystem Services, and Restorability. Annu. Rev. Environ. Resour. 30, 39–74. https://doi.org/10.1146/annurev.energy.30.050504.144248

Zhang, Y., Huang, C., Zhang, W., Chen, J., Wang, L., 2021. The concept, approach, and future research of hydrological connectivity and its assessment at multiscales. Environ. Sci. Pollut. Res. 2021 1–20. https://doi.org/10.1007/S11356-021-16148-8

Zhu, W., Xiang, W., Pan, Q., Zeng, Y., Ouyang, S., Lei, P., Deng, X., Fang, X., Peng, C., 2016. Spatial and seasonal variations of leaf area index (LAI) in subtropical secondary forests related to floristic composition and stand characters. Biogeosciences 13, 3819–3831. https://doi.org/10.5194/bg-13-3819-2016

Ziegelhoffer, E.C., Donohue, T.J., 2009. Bacterial responses to photo-oxidative stress. Nat. Rev. Microbiol. 7, 856–863. https://doi.org/10.1038/nrmicro2237

Ziegler, A.D., Bruun, T.B., Guardiola-Claramonte, M., Giambelluca, T.W., Lawrence, D., Thanh Lam, N., 2006. Environmental consequences of the demise in swidden cultivation in montane mainland southeast asia: Hydrology and geomorphology. Hum. Ecol. 37, 361–373. https://doi.org/10.1007/s10745-009-9258-x

Zuazo, V.H.D., Pleguezuelo, C.R.R., 2008. Soil-erosion and runoff prevention by plant covers. A review. Agron. Sustain. Dev. https://doi.org/10.1051/agro:2007062

Zuo, D., Xu, Z., Wu, W., Zhao, J., Zhao, F., 2014. Identification of streamflow response to climate change and human activities in the wei river Basin, China. Water Resour. Manag. 28, 833–851. https://doi.org/10.1007/s11269-014-0519-0

Appendices

Appendix I: Supplementary information of chapter 3

Table 14: Summary of geographical and meteorological characteristics per group of sampled watersheds in Lao PDR. Altitude (m a.m.s.l.), slope (%), areal percentages of: forest (%), unstocked forest (%), paddy rice (%), other agriculture (OA, %), grassland (%), water (%), and urban (%), dams' reservoir area (Dams, ha), human density (HD, people ha^{-1}), livestock density (LD, animal ha^{-1}), rainfall during rainy season (mm week^{-1}) one week preceding the sampling in July 2016.

Sampling sites	Altitude	Slope	Forest	Unstocked forest	Paddy rice	OA	Grass-land	Water	Urban	Dams	HD	LD	Rainfall rainy season
	(m a.m.s.l.)	(%)	(%)	(%)	(%)	(%)	(%)	(%)	(%)	(ha)	(people ha^{-1})	(animal ha^{-1})	(mm week $^{-1}$)
Nou	887	30	30.7	56.6	0.1	2.9	2.7	1.4	0	1,570	0.2	0.4	108
Nsu	839	32.7	21.9	72.9	0	1.5	3.3	0.2	0	0	0.1	0.5	88
Npa	900	33.9	13.9	78.9	0.1	3.6	3.6	0	0	0	0.2	0.6	107
Nk20	950	31.6	31.8	56.3	0	3.3	8.4	0.1	0	3,056	0.2	0.5	124
A6	820	30.3	18.8	74	0.6	4.4	2.2	0	0	0	0.3	0.8	128
Nmi	345	13.9	31	47.1	4.8	16.6	0.3	0	0	0	0.2	0.6	128
Nsa	325	13.5	33.3	56.7	1.8	8	0	0.1	0	0	0.4	0.9	175
Ntho	235	5.62	25.6	60.1	9.5	4.7	0	0.2	0	0	0.3	1.5	206
Nlik	522	24.1	51.5	33.8	2.3	6.7	4.6	1.1	0	24,40	0.2	0.7	175
Nng_1	631	18.3	33	41.6	5.2	7.8	6.9	5.1	0.3	37,000	0.4	1.5	161
Nma	596	14.2	49.9	41.4	1.1	1.4	3.5	1.8	0.1	1,720	0.1	0.9	203
Ngn	990	25.4	31.8	51.5	0.6	4.1	7.6	4.4	0	0	0.1	0.7	117
Nxa	373	21.5	55.6	39	2.2	1.8	0.8	6.5	0	12,300	0.2	0.6	143
Nka	707	24.2	60.2	28	0.5	1	2.9	0.5	0	0	0.1	0.3	69
Nhi	310	16	31.1	27.6	5.3	1.1	2.7	1.7	0	0	0.2	0.4	83
Xbi	246	8.6	44	32.1	5.5	1.7	3.4	0.3	0	0	0.2	0.4	97
Xbg	237	4.7	44.9	36.8	9	1.9	2.3	1.2	0	0	0.3	0.5	126
Xbn	278	5.4	70.2	23.5	3	1.1	1.6	0.5	0	0	0.1	0.7	152
SR	244	3.4	44.9	17.2	16.9	19.5	0.9	0.3	0.2	55	0.7	0.9	172

Table 15: Model quality by number of components, the first component (Comp1) and the second component (Comp2) of the PLS analyses for dry and rainy seasons. The Q^2 cumulated (Q^2 cum) index measures the global contribution of the first two components to the predictive quality of the model. The R^2Y cumulated (R^2Y cum) index represents the sum of the coefficients of determination between the dependent variables and the two first components. The R^2X cumulated (R^2X cum) index is the sum of the coefficients of determination between the explanatory variables and the two first components.

Dry season		
Statistics	**Comp1**	**Comp2**
Q^2 cum	0.290	-0.297
R^2Y cum	0.568	0.787
R^2X cum	0.208	0.291
Rainy season		
Statistics	**Comp1**	**Comp2**
Q^2 cum	0.481	0.477
R^2Y cum	0.657	0.841
R^2X cum	0.178	0.292

Table 16: Spearman correlation coefficients between E. coli concentration ([E. coli], MPN 100 mL^{-1}), total suspended sediment concentration ([TSS], g L^{-1}), electrical conductivity (EC, µS cm^{-1}), water level (m), and rainfall (Rainfall, mm day^{-1}), measured from July 2017 to December 2018 at the outlet of three watersheds in northern Lao PDR: Nam Ou (Nou), Nam Suang (Nsu), and Mekong (MK_17). Values in bold letters indicate significant correlation ($p < 0.05$).

Nou				
	[*E. coli*]	[TSS]	EC	Water level
[TSS]	**0.45**	-		
EC	**-0.55**	**-0.76**	-	
Water level	**0.52**	**0.86**	**-0.82**	-
Rainfall	0.24	0.25	-0.17	0.25
Nsu				
	[*E. coli*]	[TSS]	EC	Water level
[TSS]	**0.66**	-		
EC	**-0.72**	**-0.68**	-	
Water level	**0.72**	**0.77**	**-0.85**	-
Rainfall	**0.62**	**0.51**	**-0.50**	**0.49**
MK_17				
	[*E. coli*]	[TSS]	EC	Water level
[TSS]	**0.44**	-		
EC	**-0.30**	**-0.60**	-	
Water level	**0.48**	**0.71**	**-0.79**	-
Rainfall	**0.31**	**0.41**	**-0.33**	**0.36**

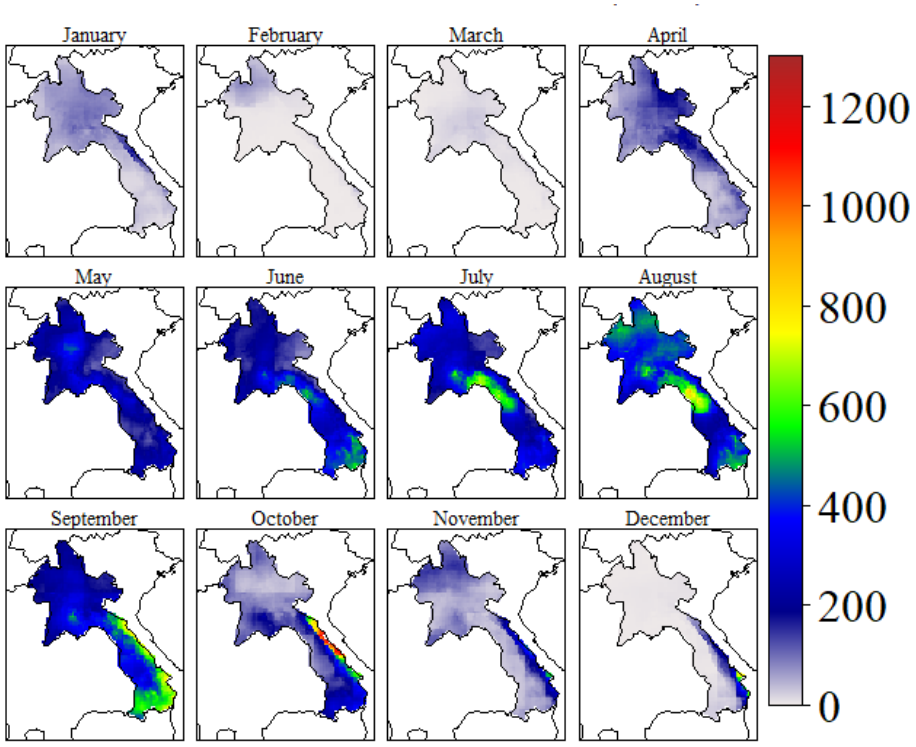

Figure 39: Spatial distribution of the cumulated rainfall (mm month-1) during 2016 over Lao PDR, obtained from the Multi-Source Weighted-Ensemble Precipitation (MSWEP V2) data.

Appendix II: Supplementary information of chapter 4

Calculation of *E. coli* stock variations

Estimate of bacterial decay due to solar radiation and to particle deposition

We applied a balance method to estimate the respective contributions of solar radiation and particle deposition to bacterial apparent decay during the experiment. In this approach, initial and final stocks of *E. coli* in the water column were compared between the treatments DL and DD, and sediment resuspension from the bottom deposit of the mesocosms was thus not considered. The control treatment was used to verify the absence of atmospherics deposits, which were considered to be negligible and were therefore also excluded. Only solar radiation-related decay and solid particle deposition were assumed to be involved in this balance. After a period of time (Δt) after the start of the experiment, the total number of decayed *E. coli* in the water column (N_t) was calculated as follows:

$$N_t = n_t^L + n_t^D \quad \text{(S1)}$$

where n_t^L and n_t^D are the number of bacteria decayed due to solar radiation and to particle deposition, respectively. Considering that treatment DL cumulates the decay effects of both solar radiation and solid particle deposition, N_t was defined as the difference between the *E. coli* stock at the start of the experiment (S_o) and after Δt for treatment DL (S_t^{DL}):

$$N_t = S_o - S_t^{DL} \quad \text{(S2)}$$

S_o was calculated by multiplying a normalized initial concentration (C_o = 500,000 MPN 100 mL^{-1}) by the volume of water at the beginning of the experiment (V_o = 4,500 mL), while S_t^{DL} was estimated by multiplying the remaining volume of water (V_t^{DL}) by the final *E. coli* concentration (C_f^{DL}) in treatment DL. C_f^{DL} was obtained using equation (1) considering the fitted value of the apparent decay rate (Table 7) for treatment DL (k^{DL}). As a result, equation (S2) can be written:

$$N_t = C_o \left(V_o - V_t^{DL} e^{-k^{DL} t} \right) \quad \text{(S3)}$$

Similarly, n_t^D was deduced from the difference between S_o and *E. coli* stock after Δt for treatment DD (S_t^{DD}):

$$n_t^D = S_o - S_t^{DD} \quad \text{(S4)}$$

S_t^{DD} was calculated by multiplying the remaining volume of water (V_t^{DD}) by the final *E. coli* concentration

(C_f^{DD}) of treatment DD, and C_f^{DD} was obtained using equation (1) considering the fitted value of the apparent decay rate (Table 7) for treatment DD (k^{DD}). As a result, equation (S4) can be written:

$$n_t^D = C_o\ (V_o\ -\ V_t^{DD}\ e^{-k^{DD}\ t}) \tag{S5}$$

n_t^L was then obtained from the combination of equations (S1), (S3) and (S5):

$$n_t^L = C_o\left(V_t^{DD}\ e^{k^{DD}\ t} - V_t^{DL}\ e^{k^{DL}\ t}\right) \tag{S6}$$

Finally, we deduced the respective fractional contributions (expressed in percentage) of solar radiation (F_L) and solid particle deposition (F_D) in the total bacterial decay as follows:

$$F_L = \frac{n_t^L}{N_t}\ 100 \tag{S7}$$

$$F_D = 100 - F_L \tag{S8}$$

Uncertainty estimation of bacterial decay due to solar radiation and particle deposition

We used a Monte Carlo approach to quantify the uncertainty in n_t^D and n_t^L calculations. With the exception of t and C_o, each known parameter of equations (S5) and (S6) was assigned an estimated expectation and an estimated standard deviation. The fitted values (Fig. 42) were assigned to k^{DD} and k^{DL} as mathematical expectation, whereas their respective errors were used as standard deviations (see Table 8). For V_o, the expectation corresponded to the initial volume using a 1-litre measuring cylinder, whereas the standard deviation corresponded to the cumulated inaccuracy of the measurement. Finally, for V_t^{DD} and V_t^{DL}, at each sampling time of the experiment, the mathematical expectation is considered to be equivalent to the theoretical residual volume obtained after subtracting from V_o the successive volumes of sampled water and a volume of evaporated water. An average 45% accuracy of the residual volume was used to estimate the standard deviation.

For each parameter, and at each sampling time, 10,000 random samples were taken in accordance with the normal distribution defined by the estimated expectation and the estimated standard deviation. At each random draw, n_t^D and n_t^L were calculated using equations (S5) and (S6). The 10,000 values obtained for each decay number were used to calculate the statistic descriptive parameters (i.e., mean, median, first and third quartiles and standard deviation, minimum and maximum) of n_t^D and n_t^L shown in Fig. 28.

Supplementary figures

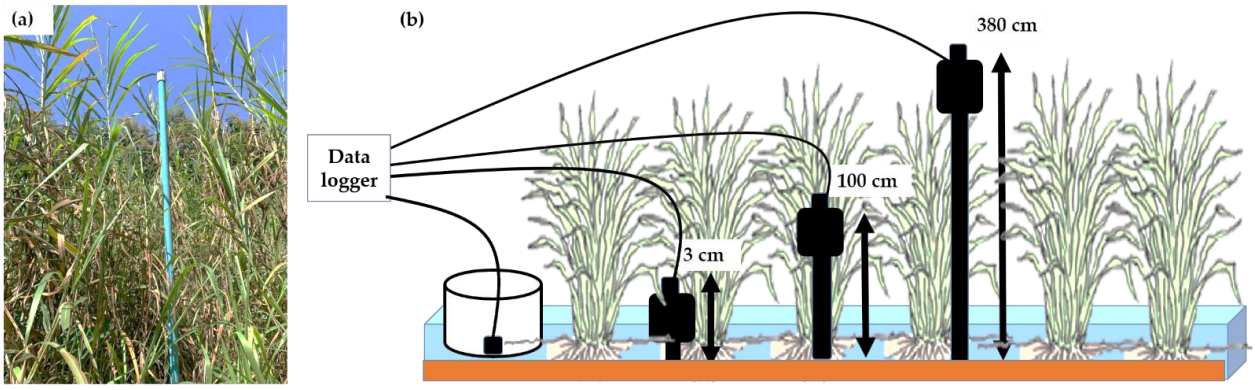

Figure 40:((a) Photo of the Napier grass and solar sensor installed in the wetland of Houay Pano catchment, northern Lao PDR; (b) diagram of the solar sensors installed at different heights (380 cm, 100 cm, 3 cm, and inside the mesocosm) to measure the solar radiation attenuation by Napier grass during two days (24 and 25 October 2020) in the wetland of the Houay Pano catchment. The pyranometers used to measure solar radiation at 380 cm height: SP110 (Campbell CS300); at 100 cm height: RG100 Solems; at 3 cm height: Li200X (LI-COR PY34392); and inside covered top mesocosm: RG100 Solems.

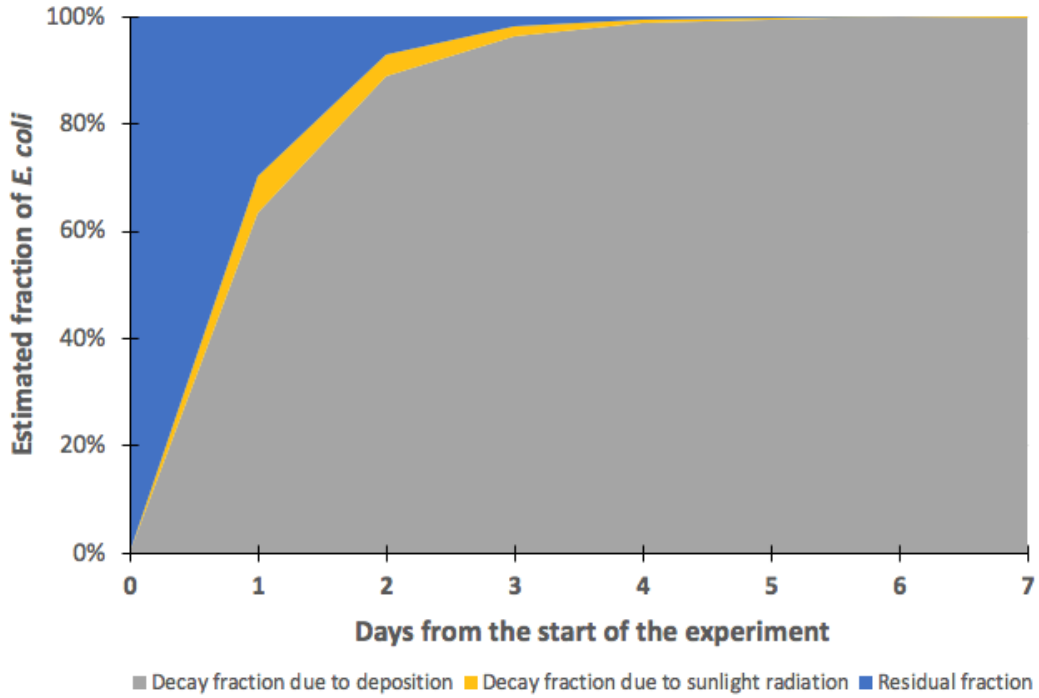

Figure 41: Stacked area graph showing the average percentage of the estimated fraction of decayed E. coli at daily time steps during the experiment: the grey area corresponds to the decay fraction due to particle deposition, the yellow area corresponds to the decay fraction due to solar radiation, and the blue area is the residual fraction of decayed E. coli.

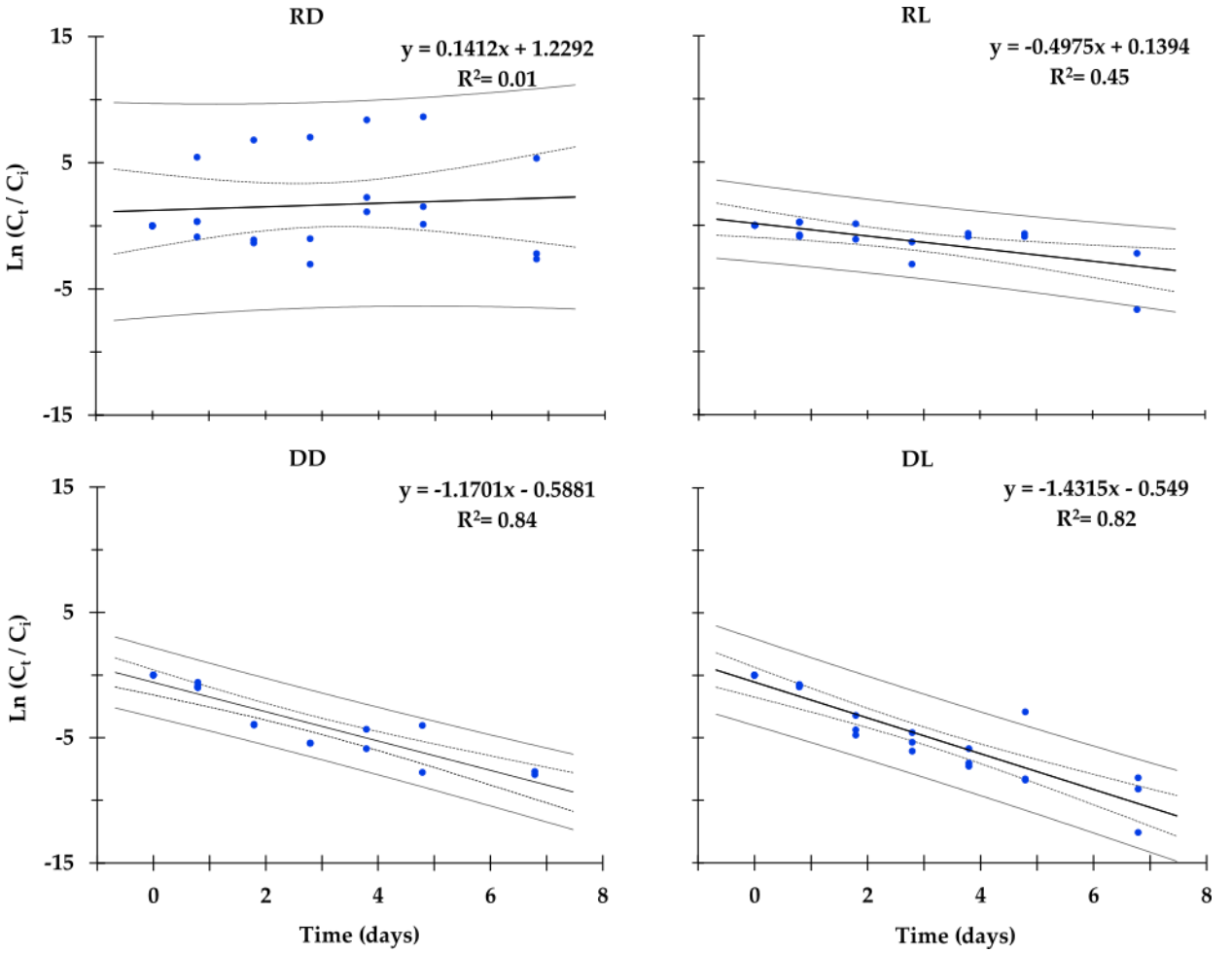

Figure 42: Plot of Ln(Ct/Ci) versus time in days where Ct is the measured concentration of total E. coli at time t in MPN 100 mL-1, Ci is the measured initial concentration of total E. coli in MPN 100 mL-1 for the mesocosms installed in the headwater wetland of the Houay Pano catchment, northern Lao PDR, from August 9 to August 16, 2019. (a) Resuspension-Dark (RD); (b) Resuspension-Light (RL); (c) Deposition-Dark (DD); (d) Deposition-Light (DL). Dotted lines represent 95% confidence interval and continuous lines represent 95% prediction interval

Appendix III: Supplementary information of chapter 5

Table 17: E. coli input data introduced in SWAT model: concentrations of persistent bacteria in manure (BACTPDB, E. coli g^{-1}) and amount of manure applied to ground in each application (CFRT_KG, kg ha^{-1}).

Sub-baisn	Area (ha)	BACTPDB (*E. coli* g $^{-1}$ maure)		CFRT_KG (kg manure ha^{-1})	
		URML	FRST, RNGB, RNGE	URML	FRST, RNGB, RNGE
1	30,505	1.25×10^{7}	1.50×10^{6}	1.40×10^{2}	4.7×10^{-2}
2	43,178	1.13×10^{7}	1.49×10^{6}	1.22×10^{2}	3.31×10^{-1}
3	25,790	7.18×10^{6}	1.49×10^{6}	5.49×10^{2}	6.48×10^{-1}
4	45,434	8.99×10^{6}	1.25×10^{7}	1.48×10^{2}	2.10×10^{-1}
5	98,446	9.56×10^{6}	1.25×10^{7}	1.26×10^{2}	9.42×10^{-2}
6	24,355	1.25×10^{7}	1.25×10^{7}	1.80×10^{2}	6.11×10^{-1}
7	42,257	8.87×10^{6}	1.25×10^{7}	2.50×10^{2}	1.14×10^{-1}
8	25,927	1.25×10^{7}	1.25×10^{7}	1.97×10^{2}	1.14×10^{-1}
9	39,917	1.06×10^{7}	1.25×10^{7}	3.73×10^{2}	8.99×10^{-1}
10	38,062	8.36×10^{6}	1.25×10^{7}	3.46×10^{2}	9.86×10^{-1}
11	65,685	7.24×10^{6}	1.25×10^{7}	2.74×10^{2}	3.11×10^{-1}
12	8,788	9.78×10^{6}	1.25×10^{7}	4.34×10^{2}	2.28×10^{-1}
13	37,612	5.55×10^{6}	1.25×10^{7}	1.34×10^{2}	9.44×10^{-2}
14	9,038	1.86×10^{7}	1.25×10^{7}	1.01×10^{1}	1.48
15	41,859	6.7×10^{6}	1.25×10^{7}	4.02×10^{2}	3.98×10^{-4}
16	50,620	9.18×10^{6}	1.25×10^{7}	3.02×10^{2}	1.18×10^{-1}
17	25,091	5.75×10^{6}	1.25×10^{7}	2.34×10^{2}	5.84×10^{-2}
18	58,432	1.16×10^{7}	1.25×10^{7}	2.28×10^{2}	2.09×10^{-1}
19	3,933	1.01×10^{7}	1.25×10^{7}	3.69×10^{-1}	7.19×10^{-2}
20	4,329	1.48×10^{7}	1.25×10^{7}	1.23×10^{2}	1.73×10^{-1}
21	1,103	1.68×10^{7}	1.25×10^{7}	3.26×10^{2}	4.27×10^{-1}
22	1,824	4.78×10^{7}	1.25×10^{7}	8.46×10^{1}	2.94×10^{-1}